

Springer Theses

Recognizing Outstanding Ph.D. Research

Marc Hutchby

Novel Synthetic Chemistry of Ureas and Amides



Springer

Springer Theses

Recognizing Outstanding Ph.D. Research

For further volumes:
<http://www.springer.com/series/8790>

Aims and Scope

The series “Springer Theses” brings together a selection of the very best Ph.D. theses from around the world and across the physical sciences. Nominated and endorsed by two recognized specialists, each published volume has been selected for its scientific excellence and the high impact of its contents for the pertinent field of research. For greater accessibility to non-specialists, the published versions include an extended introduction, as well as a foreword by the student’s supervisor explaining the special relevance of the work for the field. As a whole, the series will provide a valuable resource both for newcomers to the research fields described, and for other scientists seeking detailed background information on special questions. Finally, it provides an accredited documentation of the valuable contributions made by today’s younger generation of scientists.

Theses are accepted into the series by invited nomination only and must fulfill all of the following criteria

- They must be written in good English.
- The topic should fall within the confines of Chemistry, Physics, Earth Sciences, Engineering and related interdisciplinary fields such as Materials, Nanoscience, Chemical Engineering, Complex Systems and Biophysics.
- The work reported in the thesis must represent a significant scientific advance.
- If the thesis includes previously published material, permission to reproduce this must be gained from the respective copyright holder.
- They must have been examined and passed during the 12 months prior to nomination.
- Each thesis should include a foreword by the supervisor outlining the significance of its content.
- The theses should have a clearly defined structure including an introduction accessible to scientists not expert in that particular field.

Marc Hutchby

Novel Synthetic Chemistry of Ureas and Amides

Doctoral Thesis accepted by
the University of Bristol, UK

 Springer

Author

Dr. Marc Hutchby
The Royal Society of Chemistry
Thomas Graham House
Cambridge
UK

Supervisor

Prof. Dr. Kevin Booker-Milburn
School of Chemistry
University of Bristol
Bristol Avon
UK

ISSN 2190-5053

ISBN 978-3-642-32050-7

DOI 10.1007/978-3-642-32051-4

Springer Heidelberg New York Dordrecht London

ISSN 2190-5061 (electronic)

ISBN 978-3-642-32051-4 (eBook)

Library of Congress Control Number: 2012943625

© Springer-Verlag Berlin Heidelberg 2013

This work is subject to copyright. All rights are reserved by the Publisher, whether the whole or part of the material is concerned, specifically the rights of translation, reprinting, reuse of illustrations, recitation, broadcasting, reproduction on microfilms or in any other physical way, and transmission or information storage and retrieval, electronic adaptation, computer software, or by similar or dissimilar methodology now known or hereafter developed. Exempted from this legal reservation are brief excerpts in connection with reviews or scholarly analysis or material supplied specifically for the purpose of being entered and executed on a computer system, for exclusive use by the purchaser of the work. Duplication of this publication or parts thereof is permitted only under the provisions of the Copyright Law of the Publisher's location, in its current version, and permission for use must always be obtained from Springer. Permissions for use may be obtained through RightsLink at the Copyright Clearance Center. Violations are liable to prosecution under the respective Copyright Law.

The use of general descriptive names, registered names, trademarks, service marks, etc. in this publication does not imply, even in the absence of a specific statement, that such names are exempt from the relevant protective laws and regulations and therefore free for general use.

While the advice and information in this book are believed to be true and accurate at the date of publication, neither the authors nor the editors nor the publisher can accept any legal responsibility for any errors or omissions that may be made. The publisher makes no warranty, express or implied, with respect to the material contained herein.

Printed on acid-free paper

Springer is part of Springer Science+Business Media (www.springer.com)

Parts of this thesis have been published in the following journal articles:

Houlden, C. E.; Hutchby, M.; Bailey, C. D.; Ford, J. G.; Tyler, S. N. G.; Gagné, M. R.; Lloyd-Jones, G. C.; Booker-Milburn, K. I. *Angew. Chem. Int. Ed.* 2009, **48**, 1830–1833.

Hutchby, M.; Houlden, C. E.; Ford, J. G.; Tyler, S. N. G.; Gagné, M. R.; Lloyd-Jones, G. C.; Booker-Milburn, K. I. *Angew. Chem. Int. Ed.* 2009, **48**, 8721–8724.

Hutchby, M.; Houlden, C. E.; M. F. Haddow; Tyler, S. N. G.; Lloyd-Jones, G. C.; Booker-Milburn, K. I. *Angew. Chem. Int. Ed.* 2012, **51**, 548–551.

Supervisor's Foreword

Dr. Marc Hutchby's thesis was concerned with an investigation into the chemistry and application of molecules containing urea and amide bonds. These bonds are some of the strongest known and are fundamental to biological processes. For example the very strength of the amide (peptide) bond is core to the stability and function of proteins, without which life on earth could not exist. Marc initially studied the use of ureas as C–H activating groups in palladium-catalysed reactions of aromatic systems. C–H activation is currently a very important topic in chemistry as it avoids the need to use halogenated starting materials which means a significant reduction in toxic waste. Marc showed that aryl ureas were highly effective C–H activating groups and was able to report the first room-temperature examples of such a process.

During the course of this study Marc made the discovery that sterically hindered ureas undergo solvolysis (bond breaking) reactions at room temperature under neutral conditions. This is a remarkable observation since ureas are generally inert under these conditions and a general rule of chemistry is that hindered substrates are less reactive.

Even more incredibly, Marc was able to translate these findings into the corresponding sterically hindered amides, some of which underwent room temperature cleavage with half-lives of just minutes at neutral pH. Compare this to standard peptides which have solvolysis half-lives of 150–600 years under the same conditions!

Marc's thesis resulted in three publications in the top international chemistry journal *Angewandte Chemie*. Two of these papers were selected by the Editor as 'Hot Papers'. His groundbreaking amide paper has generated huge interest as evidenced by three news highlights in Chemical & Engineering News, *Angewandte Chemie* and most recently Nature.

Bristol Avon, UK, August 2012

Kevin Booker-Milburn

Acknowledgments

This page will no doubt be the most read in this thesis and the people mentioned will always have my greatest respect and thanks.

First, I would like to thank Kev. He has been a fantastic supervisor and allowed me to follow the natural flow of some interesting, unusual and groundbreaking chemistry. This freedom was not without support however and his enthusiasm and love of chemistry made my Ph.D. a success, it will always be greatly appreciated.

Dr. Simon Tyler has provided me with amazing support and guidance throughout all of our meetings and during my stay at AZ. I wish you luck in the new business. I would also like to thank Prof. Guy Lloyd-Jones for all of the help in Team Pd meetings and with all of the physorg that made good papers, exceptional ones.

In no particular order I would like to thank all past and present members of the KBM group, you made it a pleasure to come to work everyday. Piers, Paul and Mike showed me that a 'positive work environment' was as important as the chemistry. Chris Bailey showed me how easy chemistry can be (well it seemed that way when he did it) and for all the practical tips, passed on knowledge and good friendship, I am always grateful. I would also like to thank Chris Houlden, his knowledge and enthusiasm for chemistry was fantastic and without his help my Ph.D. would be nowhere near as successful. Joe deserves a special mention for his relentless humour, drive and work ethic, something everyone should aspire to (well maybe not the humour). Kara sailed with me from the start and we shared the Ph.D. growing pains together, I thank you for all the good times we had. Rickki, Luke, Claudio (good, good people) have also made these last few years unforgettable.

Parts of the last few years have been hard, very hard. Chemistry has a knack of raising your hopes and then knocking you down—then kicking you when you are there. Having said this, I have been very lucky and have experienced the highs as well as the lows. All of this would not have been possible without the staff that keeps this department running. To Adrian, Tony, Paul, Rose, Mairi, the secretaries, the cleaners and stores personnel, a big thank you.

Ruth has been a constant source of support, humour, and above all friendship. I will never forget these four years and all the adventures we have had—I can't wait for the many more in the years to come.

Lastly and most importantly I want to thank and dedicate this thesis to my family. I have received nothing but support at every hard decision I have taken and I hope this makes you proud. My grandparents are a true inspiration and have taught me so much. The love and support from my mum and sister is boundless and lastly to my dad—thank you.

Contents

1	Introduction	1
1.1	Transition Metal Catalysis	1
1.2	Palladium Catalysis	1
1.2.1	Non-Oxidative Palladium Catalysis	2
1.2.2	Oxidative Palladium Catalysis	3
1.2.3	Alkene Functionalisation by Pd(II)/Pd(0) Manifolds	4
1.2.4	Carbonylation of Pd(II) Complexes	7
1.3	Palladium Catalysed C–H Activation	9
1.3.1	Overview	9
1.3.2	Directing Groups in C–H Activation	11
1.3.3	Mechanistic Aspects	12
1.3.4	Carbonylation and C–H Activation	14
1.4	The Urea Functional Group	15
1.4.1	Enzymatic Deprotection	16
1.4.2	Metal Catalysed Deprotection	17
1.4.3	Alternative Methods	19
1.5	Twisted Amides	20
1.5.1	Lactams	21
1.5.2	Alternative Twisted Amides	23
1.6	Ketenes	26
1.6.1	Structure, Spectroscopy and Physical Properties	26
1.6.2	Preparation of Ketenes	27
1.6.3	Reactivity of Ketenes	29
1.7	Project Aims	31
	References	31
2	Pd(II) Catalysed Aminocarbonylation of Alkenes	37
2.1	Background	37
2.2	Results and Discussion	38
2.2.1	Attempted β -Amino Acid Synthesis	38

2.2.2	Pyrimidione Formation	41
References	44
3	Carbonylation of Aryl Ureas	45
3.1	Background	45
3.2	Results and Discussion	46
3.2.1	Stoichiometric Reactions	46
3.2.2	Catalytic Reactions: Ortho-Esterification	47
3.2.3	Cyclic Imidate Formation	51
3.2.4	Mechanism of Action	52
3.2.5	Alternative Conditions	53
3.2.6	Quinazolinone Formation	54
3.2.7	Urea Removal	54
References	55
4	Urea Hydrolysis	57
4.1	Background	57
4.2	Results and Discussion	58
4.2.1	Mechanism	58
4.2.2	Alternative Nucleophiles	66
References	70
5	Amide Hydrolysis	71
5.1	Background	71
5.2	Results and Discussion	72
5.2.1	Substrate Exploration	72
5.2.2	Mechanistic Studies	80
5.2.3	Synthetic Uses	86
References	88
6	Conclusions and Future Work	89
6.1	Conclusions	89
6.1.1	Pd(II) Catalysed Aminocarbonylations of Alkenes	89
6.1.2	Carbonylation of Aryl Ureas	89
6.1.3	Urea Hydrolysis	90
6.1.4	Amide Hydrolysis	90
6.2	Future Work	91
6.2.1	Polymerisation of Hindered Tri-Substituted Ureas	91
6.2.2	Amide Hydrolysis: Direct Evidence of Ketene Formation	92
6.2.3	Amide Hydrolysis: Manipulations of Reactivity	92
6.2.4	Alternative Rotamides	94
References	94

7 Experimental	95
7.1 General Experimental Detail	95
7.2 Pd(II) Catalysed Aminocarbonylation of Alkenes	96
7.3 Carbonylation of Aryl Ureas	97
7.3.1 Preparation of Ureas	97
7.3.2 Preparation of Pd(OTs) ₂ (MeCN) ₂	105
7.3.3 Procedure for the Preparation of Ortho-Ester Aryl Ureas	105
7.3.4 Procedure for the Preparation of Cyclic Imidates	111
7.3.5 Use of Pd(OAc) ₂	113
7.3.6 Use of PdCl ₂	114
7.3.7 Procedure for the Preparation of Quinazolinediones	115
7.3.8 Procedure for the Preparation of Methyl 2-aminobenzoate	117
7.3.9 Procedure for the Preparation of 2-Aminobenzoic Acid	118
7.4 Urea Hydrolysis	118
7.4.1 Preparation of Ureas	118
7.4.2 Preparation of Unreactive Analogues	122
7.4.3 Procedure for the Methanolysis of Hindered Tri-Substituted Ureas	123
7.4.4 Procedure for Isocyanate Crossover Experiment	123
7.4.5 Partitioning of In Situ Generated N-Phenylisocyanate by Meoh, Etoh and Nproh	124
7.4.6 Kinetics of the Methanolysis of Hindered Tri-Substituted Ureas	124
7.4.7 Procedure for the Preparation of Carbamate Derivatives	126
7.5 Amide Hydrolysis	129
7.5.1 Procedure for the Preparation of Diphenylacetamides	129
7.5.2 Procedure for the Preparation of Hindered Amides	130
7.5.3 Procedure for the Preparation of Amides 172–174	147
7.5.4 Linear Free Energy Relationship for Methanolysis of Arylacetamides	148
7.5.5 Kinetics of α -CH/D Exchange	149
7.5.6 Procedure for the Preparation of Methyl Ester Derivatives	151
7.5.7 Procedure for the Preparation of Carboxylic Acid Derivatives	157
References	159
Appendix: X-Ray Crystal Structures Publications	161

Abbreviations

General Terms

app.	Apparent
aq	Aqueous
atm	Atmosphere(s)
br	Broad (spectral)
CI	Chemical ionisation
δ	Chemical shift
J	Coupling constant
d	Doublet (spectral)
eq	Equivalent(s)
ESI	Electrospray ionisation
FVT	Flash vacuum thermolysis
M	Generic metal
B	Generic base
g	Gram(s)
$t_{1/2}$	Half-life
hrs	Hours
Hz	Hertz
HMBC	Heteronuclear multiple bond correlation
HRMS	High-resolution mass spectrometry
HOMO	Highest occupied molecular orbital
IR	Infrared
LUMO	Lowest unoccupied molecular orbital
m	Multiplet (spectral)
M	Molar (moles per liter)
m/z	Mass-to-charge ratio
μL	Microlitre(s)
mg	Milligram(s)
MHz	Megahertz

min	Minute(s)
mL	Millilitre
mmol	Millimole(s)
mp	Melting point
NMR	Nuclear magnetic resonance
ppm	Part(s) per million
M ⁺	Parent molecular ion
χ_N	Pyramidalisation of nitrogen
χ_C	Pyramidalisation of carbon
q	Quartet (spectral)
rt	Room temperature
R_f	Retardation factor (for tlc)
sec	Second(s)
s	Singlet (spectral)
t	Triplet (spectral)
Temp	Temperature
tlc	Thin layer chromatography
τ	Twist angle
ν	Wavenumber

Reagents and Solvents

BQ	1,4-Benzoquinone
CO	Carbon monoxide
DCC	<i>N,N'</i> -Dicyclohexylcarbodiimide
DCE	1,2-dichloroethane
DMAP	4-(<i>N,N</i> -dimethylamino)pyridine
DME	1,2-dimethoxyethane
DMF	<i>N,N</i> -Dimethylformamide
DMSO	Dimethyl sulfoxide
DIBAL	Diisobutylaluminium hydride
dppb	Diphenylphosphino butane
<i>m</i> CPBA	<i>m</i> -Chloroperoxybenzoic acid
MeCN	Acetonitrile
NMP	<i>N</i> -Methyl-2-pyrrolidinone
PEG	Polyethylene glycol
PE	Petroleum Ether 40/60
TFA	Trifluoroacetic acid
TFE	Trifluoroethanol
THF	Tetrahydrofuran
TMS	Tetramethylsilane

Substituents and Protecting Groups

Ac	Acetyl
Ar	Aryl
Bn	Benzyl
Boc	<i>tert</i> -butoxycarbonyl
<i>t</i> Bu	<i>tert</i> -butyl
<i>n</i> Bu	<i>n</i> -Butyl
Cbz	Benzyloxycarbonyl
Cy	Cyclohexyl
Et	Ethyl
EWG	Electron withdrawing group
Fmoc	9-Fluorenylmethoxycarbonyl
<i>L</i> <i>n</i>	Generic ligand
Me	Methyl
MPC	Methyl phenylcarbamate
Nu	Generic nucleophile
Ph	Phenyl
^{<i>i</i>} Pr	Isopropyl
^{<i>n</i>} Pr	<i>n</i> -Propyl
py	2-Pyridyl
R	Generic aliphatic/aromatic group
TMP	2,2,6,6-tetramethylpiperidyl
Ts	Tosyl/ <i>p</i> -toluenesulfonyl

Chapter 1

Introduction

1.1 Transition Metal Catalysis

The field of catalysis is of great importance not only to chemists but to society in general. Ranging from enzymes in biological systems to the catalytic converters in the automobile industry, reactions occurring through catalytic procedures are ubiquitous.

Transition metals are often used as stoichiometric reagents in synthesis. These reagents however can suffer from extensive problems such as toxicity (chromium oxidants generating Cr(IV) are known carcinogens) or cost (OsO_4 , 1 g = £256) [1]. Developing catalytic procedures that are sub-stoichiometric in metal can reduce these problems and thereby can increase the impact of the synthetic transformations they allow.

There are many hundreds of catalytic procedures spanning the transition metal elements, for the purposes of this thesis, only palladium catalysis will be discussed.

1.2 Palladium Catalysis

Palladium is perhaps the most commonly used transition metal in catalytic synthetic procedures. It has many advantages over other catalytically useful metals.

Whilst exposure to the atmosphere may be unwise, palladium reagents are on the whole stable to the environment and tolerate moisture to such an extent that water can even be used as solvent [2, 3]. Other functional groups that may be present including the widely present and often reactive carbonyl group are generally untouched by palladium chemistry.

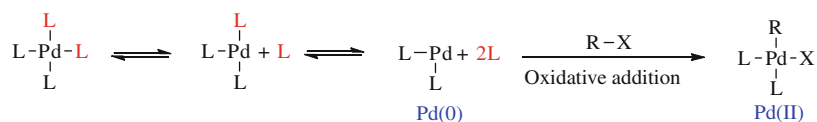
Industrial applications of palladium are also possible (and many are in use today) [4] due to the comparatively reduced costs against other noble metals such as platinum. Toxicity also poses less problems unlike some metals i.e. the use of tin in the Stille coupling [5].

1.2.1 Non-Oxidative Palladium Catalysis

In the broad sense of palladium catalysis, a reaction can be classified into one of two categories. The first, discussed herein, is the more widely applicable non-oxidative transformation (non-oxidative meaning no added external oxidant is required). These palladium (pd) (0) catalysed processes are responsible for some of the most efficient C–C and C-heteroatom bond forming reactions [6–9]. The other, requiring oxidation in order to regenerate the active palladium species will be discussed later (Sect. 1.2.2).

Pd(0) is (nominally) electron rich and can undergo oxidative addition to substrates such as halides and pseudo-halides (e.g. triflates). The result of this is a palladium species in the +2 oxidation state (Scheme 1.1).

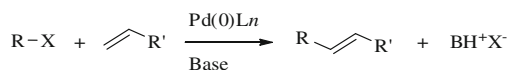
This new σ -alkyl Pd(II) intermediate is the key species for the following prominent non-oxidative palladium catalysed reactions.



Scheme 1.1 Oxidative addition of a Pd(0) species

The Mizoroki–Heck reaction (first discovered by Mizoroki [10] and subsequently improved by Heck [11]) is a carbon–carbon bond forming reaction between an alkyl, alkenyl or aryl halide/pseudohalide and an alkene via palladium catalysis (Scheme 1.2).

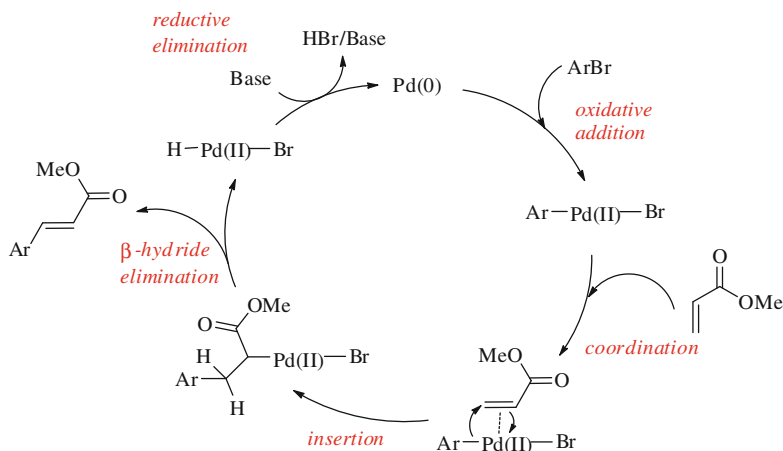
Scheme 1.2 Simplified Mizoroki–Heck reaction



Following oxidative addition and coordination to the alkene, migratory insertion into the Pd–C bond occurs (carbopalladation). β -hydride elimination then furnishes the target alkene, while reductive elimination of HX from the metal centre allows Pd(0) regeneration (Scheme 1.3).

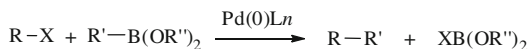
The Suzuki reaction differs slightly from the mechanism described above. Following oxidative addition, transmetalation transfers the coupling partner (e.g. aryl, alkenyl, alkyl) from the boron species to the palladium centre. Reductive elimination releases the desired product and regenerates the active palladium species (Scheme 1.4).

There are many variations on the cross-coupling reaction. All follow a similar mechanism to that described for the Suzuki reaction but differ in the nature of the cross-coupling partner. Hiyama (organosilanes) [12], Negishi (organozincs) [13], Sonogashira (alkynylcuprates) [14] and Stille cross-couplings (organostannanes) [15] are a few select examples.



Scheme 1.3 Mizoroki–Heck catalytic cycle

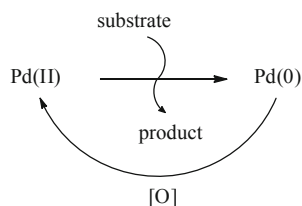
Scheme 1.4 Simplified Suzuki reaction



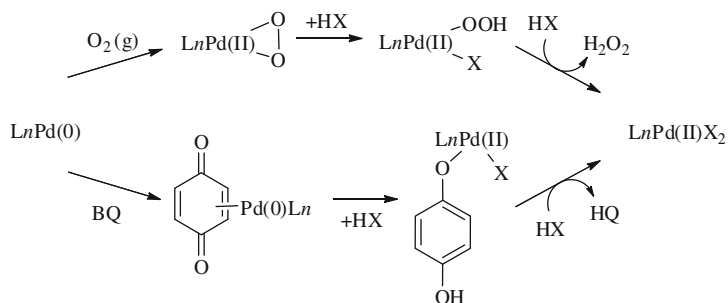
1.2.2 Oxidative Palladium Catalysis

The successes of C–C and C-heteroatom cross couplings has not been replicated in oxidative palladium catalysis. Here it is necessary to re-oxidise the palladium after the completion of every catalytic cycle (Scheme 1.5). For the purposes of this thesis only external oxidants will be discussed.

Scheme 1.5 Simplified oxidative palladium catalysis



Oxidation by air itself is an inefficient process, but the addition of copper (II) chloride (CuCl_2) along with molecular oxygen has been used to good effect in the re-oxidation of Pd(0) to Pd(II) [16]. Whilst there may be a problem associated with the solubility of O_2 , CuCl_2 can be used to oxidise Pd(0) to Pd(II) and is itself oxidised back to Cu(II) by oxygen. Stoichiometric levels of reliable and cheap chemical oxidants such as 1,4-benzoquinone (BQ) can also be exploited to generate very efficient catalytic systems (Scheme 1.6) [17]. These oxidants should not interfere with the reactions or products. One such example of this problem was the use of BQ in the presence of a diene reagent [18]. This resulted in unwanted Diels–Alder side reactions which consumed both the oxidant and one of the starting



Scheme 1.6 Mechanistic relationship between the oxidation of Pd(0) by molecular oxygen and benzoquinone [17]

materials. Many other oxidants have been used to good effect, these include; sodium persulfate [19], silver salts [20] and peroxides [21, 22].

If an oxidation pathway is not found that can oxidise palladium rapidly enough, a high concentration of Pd(0) can build up; aggregation follows causing the bulk metal to precipitate. This is then difficult to re-oxidise back to the active catalyst. A critical factor in the success of the non-oxidative palladium catalysed cross-couplings was the discovery of soft donor ligands which stabilise the metal centre. Due to the oxidising nature of these types of transformations, many soft ligands (i.e. phosphine ligands) are unsuitable under the reaction conditions and readily decompose. For these reasons the catalyst is normally introduced as a simple, stable salt i.e. PdCl₂ and Pd(OAc)₂. The insolubility of these compounds in organic solvents is well known however, as a consequence they are regularly complexed with coordinating solvents to aid solvation (i.e. Pd(MeCN)₂Cl₂).

The work presented here focuses on oxidative palladium catalysis, in particular the Pd(II)/Pd(0) manifold. The group of reactions exploiting the Pd(II)/Pd(IV) catalytic system will not be covered, although they can be extremely efficient systems in the area of C–H activation/functionalisation. These reactions often use hypervalent iodine reagents in a dual role. Along with oxidising Pd(II) intermediates to Pd(IV) they are also the coupling partner, transferring an organic fragment (e.g. aryl, acetate, oxime) to the palladium centre. Reductive elimination furnishes the product and regenerates the Pd(II) catalyst. This work has been pioneered by Sanford [23–28] and utilised by many others [29–31].

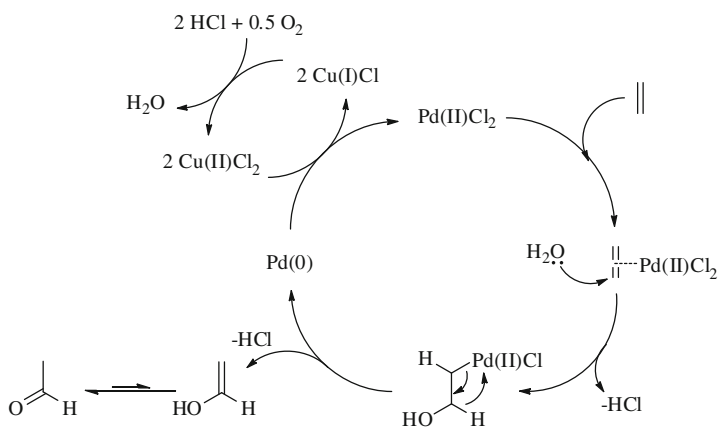
1.2.3 Alkene Functionalisation by Pd(II)/Pd(0) Manifolds

Pd(II) has a distinctly electron poor centre rendering it more electrophilic than Pd(0), this allows for coordination to alkenes to form Pd- π -complexes. The alkenes then become electron deficient and are susceptible to nucleophilic attack; a reversal in the reactivity normally associated with unactivated alkenes which

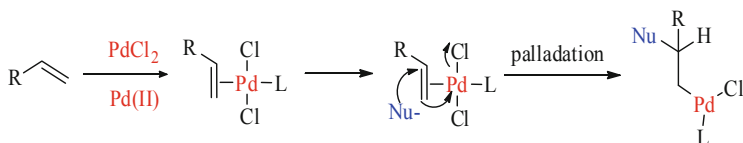
generally undergo electrophilic attack. One such case, the oxidation of ethylene to acetaldehyde catalysed by PdCl_2 , is known as the Wacker process [32] and is perhaps the most well-known Pd(II) catalysed reaction. This was the first example of a palladium catalysed process performed on an industrial scale and is named after the German company that implemented it. Whilst the mechanism has been studied widely [33–36] a simple representation is shown (Scheme 1.7).

The reaction proceeds through a Pd(II)/Pd(0) catalytic cycle with palladium being re-oxidised in situ by CuCl_2 and oxygen. Oxygen is the most environmentally friendly oxidant for such processes but without a co-catalyst it often fails to achieve complete oxidation of palladium due to the competing formation of inactive bulk metal. Copper salts are therefore often used which can provide a more expedient oxidation. The reduced copper species can then be oxidised by the oxygen atmosphere allowing for its use in catalytic quantities.

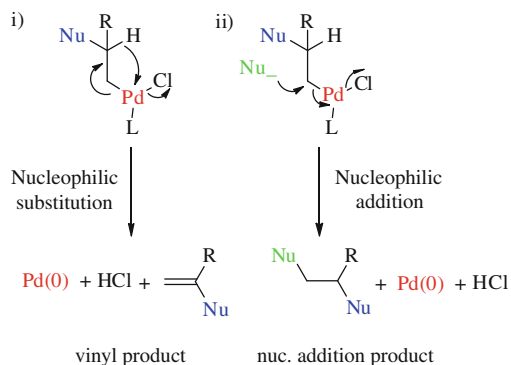
After coordination of Pd(II) to an alkene, a carbon-palladium σ -bond is formed through a process known as palladation (Scheme 1.8). Depending on the nucleophile present, palladation is named accordingly, i.e. aminopalladation when nitrogen containing reagents are used and oxy- (Wacker oxidation) or carbopalladation [37, 38] for when the nucleophile is oxygen and carbon respectively. The palladated species can then react in two distinct ways; (i) β -hydride elimination of



Scheme 1.7 Simplified Wacker mechanism



Scheme 1.8 Nucleophilic attack on a coordinated alkene–palladation



Scheme 1.9 Reactions of the intermediate palladated alkene

H–Pd–X to give the nucleophilic substitution vinyl product; (ii) attack by another nucleophile gives the nucleophilic addition product (Scheme 1.9).

Aminopalladation represents one of the key intermediates in the formation of many nitrogen containing species. Recent work from Senanayake [39] and Larock [40] has shown that different indoles can be synthesised in one-pot reactions by Pd catalysed aminopalladation. However, the reactivity of the nucleophile differs greatly according to the type of nitrogen source. For example, primary amines (which would give enamide products) can strongly coordinate to palladium and can cause catalytic death—that is an inability to displace the coordinated species from the metal, causing a shutdown of reactivity.

Figure 1.1 demonstrates some of the reactions available following aminopalladation. Tertiary amines (**a**) are available from secondary amines by reducing the corresponding palladated complex with a simple hydrogenation [41]. The same aminopalladated intermediate can be converted to the β -acetoxyalkyl amine derivative (**b**) with oxidation by lead acetate [42] and an in situ oxidation by *m*-CPBA can be used to generate 1,2 diaminoalkanes (**c**) [43]. Aziridine products (**d**) can be formed by bromination of the aminopalladate (**e**) [44] whilst a stable, chelated acylpalladium complex (**g**) can be obtained from the carbonylation of (**f**) [45].

The intramolecular versions of the above reactions occur much more readily [46]. This is primarily due a significantly lower entropic penalty, with both functional groups tethered together allowing for a more favourable and easier interaction. Stahl and co-workers have contributed significantly to developing intramolecular Pd(II) aminations [47]. Focusing on the development of aerobic oxidation methods, several efficient intramolecular pathways to *N*-heterocycles, including indoles (Scheme 1.10) and pyrrolidines (Scheme 1.11) were developed.

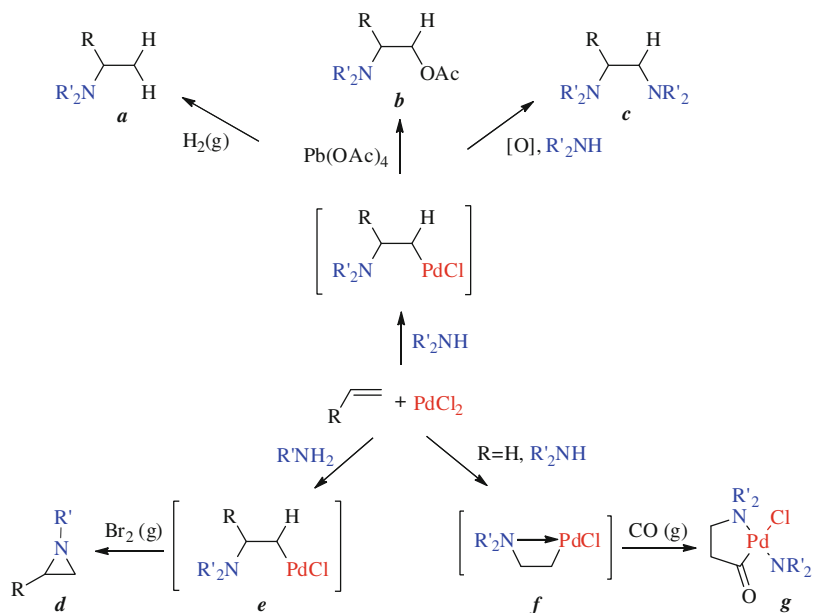
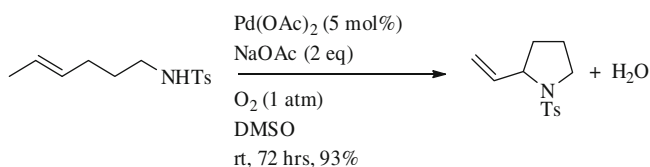
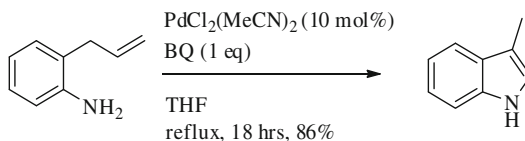


Fig. 1.1 Some possible transformations post-aminopalladation

Scheme 1.10 Intramolecular Pd(II) catalysed indole formation

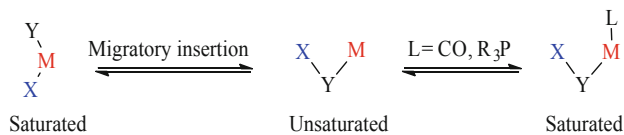


Scheme 1.11 Intramolecular Pd(II) catalysed pyrrolidine formation

1.2.4 Carbonylation of Pd(II) Complexes

It is well known that two ligands present on coordinated palladium can react together to produce a new complex that still has the composite ligand attached ready for further modification. This process of migratory insertion occurs when one of the ligands attached to the metal migrates onto another. This is then

followed by insertion of one of the ligands into the other metal–ligand bond (Scheme 1.12). It is a reversible process and, as the metal effectively loses a ligand in the process, the overall insertion may be driven by the addition of extra external ligands to produce a coordinatively saturated complex.

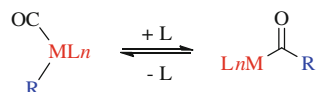


Scheme 1.12 Migratory insertion; X migrates from M to Y

In a similar way to reductive elimination, a *cis* arrangement of the ligands is required and the migrating group retains its stereochemistry (if any) during the migration. The ligand to be inserted must be unsaturated to accommodate the additional bonds that will be formed and examples of such ligands include carbon monoxide, alkenes and alkyl phosphanes. Theoretically, migratory insertion and chain extension can be maintained indefinitely, as seen with the much investigated palladium catalysed CO/vinyl polyketone synthesis [48].

Carbonylation (Scheme 1.13) is the addition of carbon monoxide to organic molecules and is an extremely important industrial process. The cheap and readily available gas is an excellent one-carbon feedstock and the resulting metal-acyl complexes can be converted into aldehydes, acids and their derivatives.

Scheme 1.13 Carbonylation

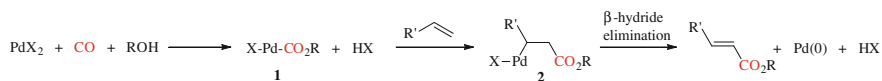
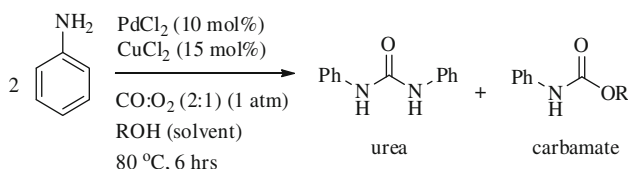
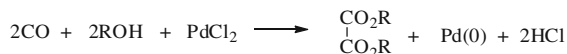


Due to the gaseous nature of the reagent, the insertion process can be driven effectively by increasing the pressure of CO, forcing external ligands onto the metal. Maintaining CO pressure is also advantageous in arresting the reverse carbonylation process—decarbonylation.

Oxidative carbonylation of alkenes is a unique reaction that occurs through the use of Pd(II) salts. When performed in alcoholic solvents it can be thought of as proceeding through the formation of an alkoxy-carbo palladate species **1** (Scheme 1.14). Carbopalladation of an alkene with **1** gives **2**. β -hydride elimination of this intermediate then yields the α , β -unsaturated ester.

In 1964 Tsuji [49] reported the first instance of oxidative carbonylation and following this initial discovery the scope of the reaction has been studied widely [50–52]

Oxidative carbonylation of alcohols (Scheme 1.15) is another extremely important example of the use of carbon monoxide as a convenient method of introducing carbonyl functionality. Selectivity between mono- and di-carbonylation is dependent on CO pressure and reaction conditions, in one particular case the reaction is rendered catalytic with Cu(II) and Fe(III) salts as external oxidants [53].

**Scheme 1.14** Oxidative carbonylation of alkenes**Scheme 1.15** Oxidative carbonylation of alcohols**Scheme 1.16** Oxidative carbonylation of amines

Analogous to the reaction above, ureas can be formed by oxidative carbonylation of amines under an atmosphere of CO. Again, these can be performed under mild conditions of 1 atm and at room temperature (Scheme 1.16) [54]. It was found that CuCl₂ influenced the catalytic nature of the reaction, and altering reaction conditions (30 bar, 110–150 °C) the proportion of carbamate esters could be increased.

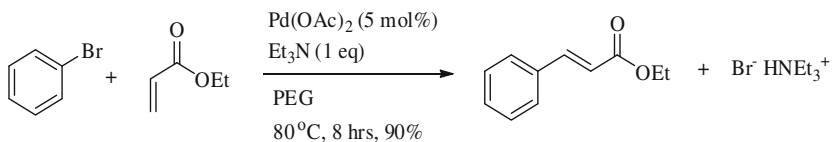
Anhydrides, diesters, carbamates and ureas are all important feedstocks for the pharmaceutical/fine chemical industries which, through the use of Pd(II) catalysis, can be synthesised with lower environmental impact than traditional methods.

1.3 Palladium Catalysed C–H Activation

1.3.1 Overview

The process of inserting a transition metal complex into a C–H bond allowing for further functionalisation is known as C–H activation. Through this direct process, the need for a pre-functionalised starting material is negated and as a consequence, waste can be reduced.

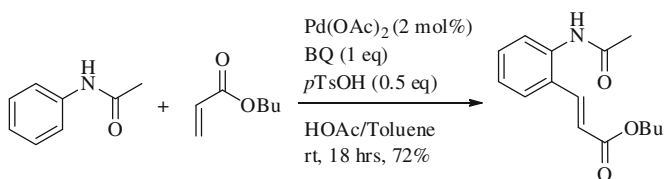
The Mizoroki–Heck reaction (Scheme 1.17) for example allows for selective functionalisation [55]. The π -electron system has been activated under ‘mild’ conditions and coupled to form a new C–C bond. Atom economy has been neglected with halogenation of the desired coupling position necessary. This extra



Scheme 1.17 A standard Mizoroki–Heck reaction

functionalisation will also use additional resources, cost more and generate significant amounts of salt waste.

In 2002, de Vries and co-workers demonstrated a Mizoroki–Heck type reaction which allowed direct insertion into an aryl C–H bond eliminating the need for organic halides (Scheme 1.18) [56].

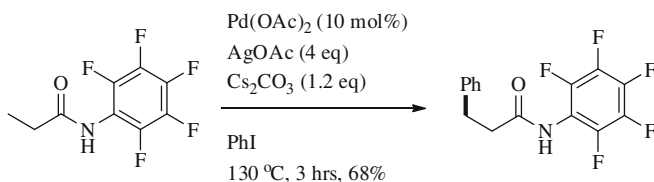


Scheme 1.18 Selective Pd-catalysed oxidative coupling of anilides with alkenes

A wide range of transition metal complexes have been at the forefront of such developments [57–59]. The ability to tune reactions electronically and sterically by varying the metal and/or ligands has led to wide interest. The ability to render these systems catalytic is extremely beneficial, not only lowering costs but also reducing the waste generated. C–H activation is one of the most active fields of research in organic chemistry and the already vast area is expanding rapidly [60–62]. For these reasons an extensive review will not be shown here, Pd(II) catalysis will be focused upon.

Palladium catalysed C–H activation reactions now populate the literature. They include oxidative (Pd(II)/Pd(0) [63] and Pd(II)/Pd(IV) [64]) and non-oxidative transformations [65] and span alkyl [66], allylic [67], aromatic [68] and hetero-aromatic [69] C–H bonds.

The difficulties associated with activating an sp^3 C–H bond are revealed in an example from Yu and co-workers (Scheme 1.19) [70]. Selectivity is a problem,



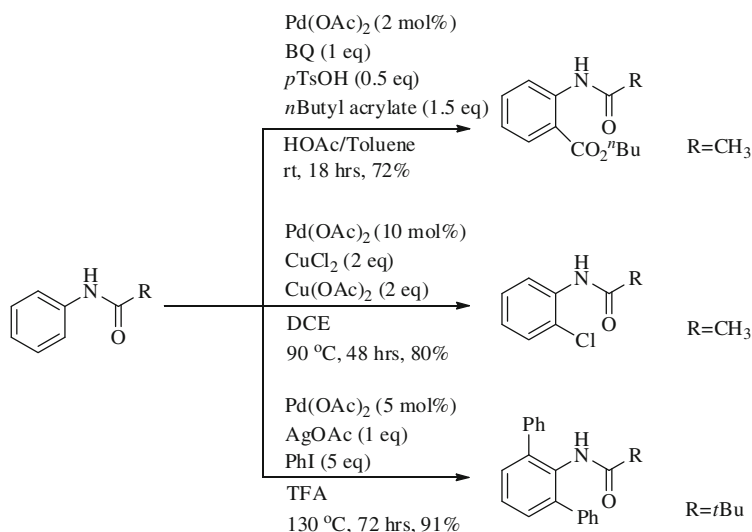
Scheme 1.19 Amide-directed arylation of sp^3 C–H bonds

with multiple C–H bonds leading to di- and tri-arylation. Reactions can also be very inefficient, with Yu utilising phenyl iodide as solvent, 4 equivalents of silver acetate and heating to high temperatures.

1.3.2 Directing Groups in C–H Activation

The challenge of selecting one particular C–H bond in a molecule where there can be multiple choices is a persistent problem within the field. To a large extent, directing groups have been successfully employed to overcome these issues.

This is particularly true in the *ortho*-functionalisation of aromatic rings where a myriad of examples are now present in the literature. Aldehydes [71], carbamates [30] and amides have all proved powerful directing groups with the latter providing a range of diverse examples (Scheme 1.20) [29, 56, 72].

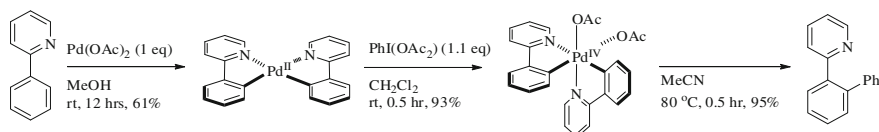
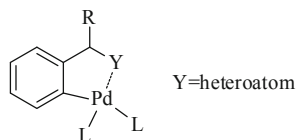


Scheme 1.20 *ortho*-Functionalisation of anilide derivatives

In these examples it is important to note the presence of a heteroatom in close proximity to the reaction site of interest. It is this heteroatom that is responsible for ‘trapping’ or holding the transition metal in place in the form of a metallacycle. The selectivity imparted through this process allows for the *ortho*-substitution reactions presented so far (Fig. 1.2).

Aside from the carbonyl functional group, pyridine has commonly been used to obtain selectivity. This work has been pioneered by Sanford and co-workers publishing not only synthetically useful procedures [73] but also elegant mechanistic investigations (Scheme 1.21) [74].

Fig. 1.2 Stabilisation of a palladium complex by a heteroatom



Scheme 1.21 Mechanistic studies on pyridine directed C–H activation

1.3.3 Mechanistic Aspects

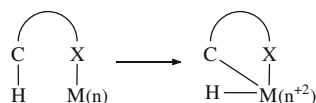
The rapid growth of this field has been stimulated by the desire to understand the subtle underlying processes behind such transformations [75, 76]. It is vital in order to predict and design new reactions such information is available.

‘True’ activation of a C–H bond encompasses the group of reactions in which an organometallic (σ -organyl) derivative is formed as an intermediate or a final product. The σ -bond that is created links together the metal centre with an organic fragment (alkyl, aryl etc.) via a carbon atom. In catalytic systems the breaking of this bond is required to complete the desired reaction through the transfer of a new functional group onto the carbon atom. There are several proposed mechanisms for C–H activation, some more related to specific reactions than others. These mechanisms will be discussed briefly.

1.3.3.1 Oxidative Addition

For the facile reaction shown in Scheme 1.22, the reactive palladium complex may have a high or low oxidation state and must have an empty σ -type molecular orbital to accommodate the incoming species. It must also have a high energy molecular orbital containing a lone pair of electrons which will be transferred into the σ^* orbital of the C–H bond. Overall the oxidation state of the metal increases by two and the C–H bond receives two electrons from the metal complex forming a new metal–carbon and metal–hydrogen bond.

Scheme 1.22 Oxidative addition by a metal species into a C–H bond

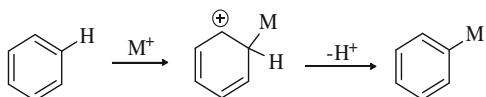


where X = O, N, P etc.

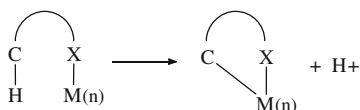
1.3.3.2 Electrophilic Addition

Metals with high oxidation states take part in electrophilic substitutions. For example electrophilic addition into an aromatic C–H bond proceeds in two stages (Scheme 1.23).

Scheme 1.23 Electrophilic substitution of a benzene ring by an electron deficient metal species (M^+)



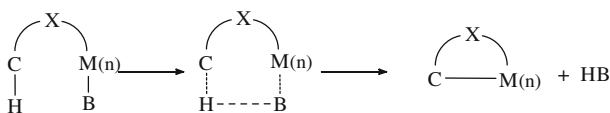
The central atom does not change oxidation number throughout the electrophilic mechanism. Such processes do not form metal hydrides, the proton simply dissociates as a free or bound species (Scheme 1.24).



where $X = O, N, P$ etc.

Scheme 1.24 Electrophilic addition resulting in dissociation of a free proton

In cases such as the one presented, nucleophilic assistance may be required to accept the leaving proton. This may be in the form of a coordinated or free base (Scheme 1.25).



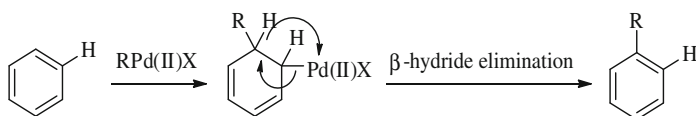
where $X = O, N, P$ etc.

Scheme 1.25 Coordinated base assisted electrophilic addition

1.3.3.3 Carbometallation

A Heck-like process could occur if the palladium centre already bears the cross-coupling partner (Scheme 1.26).

Although insertion into a C–H bond does not occur and the C–H bond ultimately broken is not the one bearing the palladium, we can still view this mechanism in the context of C–H activation, especially when selectivity is achieved through a directing group.

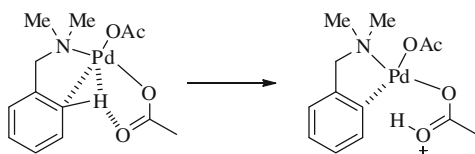


Scheme 1.26 Carbopalladation/Heck type C–H activation

1.3.3.4 Concerted Metalation/Deprotonation

In 2005 Davis and co-workers investigated the cyclometalation of dimethylbenzylamine through computational measurements [77]. In contrast to the original mechanistic studies (which proposed a Wheland intermediate) [78] the group suggested the formation of an agostic complex and subsequent deprotonation to be rate determining. The presence of an acetate ligand to act as an intramolecular base through a 6-membered transition state allows for this deprotonation with little distortion in the system (Scheme 1.27). This work was also pioneered by Fagnou and is the topic of many reviews [79].

Scheme 1.27 Acetate assisted deprotonation of an agostic intermediate



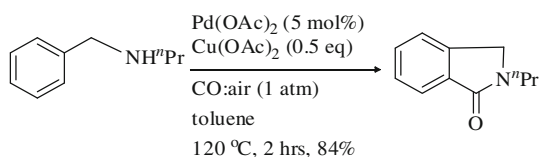
1.3.4 Carbonylation and C–H Activation

Once a formal C–H insertion has taken place, further functionalisation can occur in several ways. The introduction of carbon monoxide (Sect. 1.2.4) can lead to acyl palladium complexes and from this a wide range of derivatives, for example aldehydes, esters, amides etc.

Orito and co-workers reported a Pd(II) catalysed formation of benzolactams via aromatic carbonylation [80]. This was accomplished through the activation of the *ortho*-C–H bond, directed by a tethered amino group (Scheme 1.28).

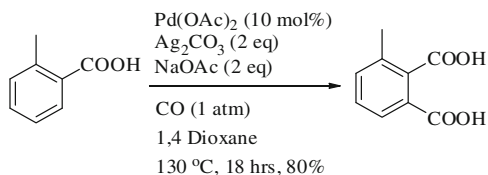
In 2008 Yu and co-workers developed a useful synthesis of dicarboxylic acids from both aryl and vinyl substrates [81]. Using the carboxylic acid motif to direct the palladium catalyst to the *ortho*-position, CO insertion and subsequent

Scheme 1.28 Benzolactam synthesis via Pd(II) catalysed C–H activation/carbonylative insertion



hydrolysis furnished the desired product (Scheme 1.29). It should be noted the above reaction is complementary to the *ortho*-lithiation/ CO_2 insertion process directed by amide groups [82].

Scheme 1.29 Synthesis of 1,2-carboxylic acids via Pd(II)-catalysed carboxylation



The previous two carbonylative insertion reactions demonstrate the potential for this chemistry. Unfortunately the high temperatures, high catalyst loading and expensive reagents reduce the applicability, especially in the fine chemical industry where maintaining high temperatures is difficult and expensive. It would therefore be advantageous to develop chemistry which can be performed at ambient temperatures.

1.4 The Urea Functional Group

A directing group, post C–H activation/functionalisation may be superfluous to the requirements of the researcher. It is therefore advantageous to be able to remove/transform such a group with the greatest of ease (akin to classic protecting group chemistry). The urea moiety has been shown to be an effective directing group in C–H activation [83] but the difficulty in its removal, subsequently limits its synthetic use.

The urea moiety can be thought of as a robust protecting group for aromatic and aliphatic amine groups. Inertness to nucleophilic attack comes through its resonance structure, providing stability in all but the most extreme reaction conditions (high temperatures, pH, high pressures etc.) (Fig. 1.3).

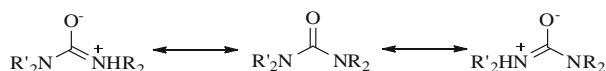
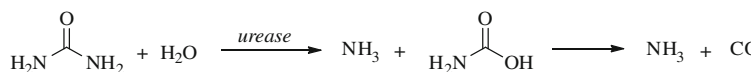


Fig. 1.3 Urea resonance forms

This resistance to nucleophilic attack can also limit their utility as a protecting group because they are difficult to remove. Current methods of urea ‘deprotection’ are limited to reactions involving metal or enzymatic catalysis, high temperatures and/or hydrolysis at extreme of pH.

1.4.1 Enzymatic Deprotection

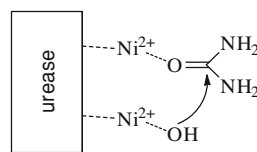
The enzyme urease catalyses the hydrolysis of urea into ammonia and carbamic acid (which then spontaneously decarboxylates to another molecule of ammonia and carbon dioxide) (Scheme 1.30).



Scheme 1.30 Urease catalysed hydrolysis of urea

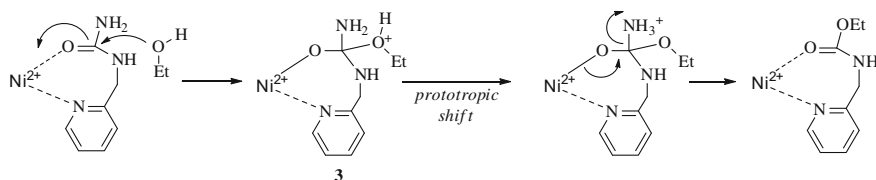
This is a well studied process with nickel (Ni) (II) present in the enzyme which catalyses the process [84]. Further elucidation of the crystal structure by Karplus and co-workers showed two Ni(II) atoms on the active site [85]. It is theorised that the oxygen of urea coordinates to one of the nickel atoms facilitating nucleophilic attack by a hydroxyl group ligated to the other metal centre (Fig. 1.4).

Fig. 1.4 Possible mechanism of action for urease catalysed hydrolysis of urea



There are some reports of urea coordination to a metal complex through nitrogen followed by decomposition to ammonia and carbon dioxide [86, 87]. These systems are not thought to be representative of the urease mode of action due to the differences in reaction conditions.

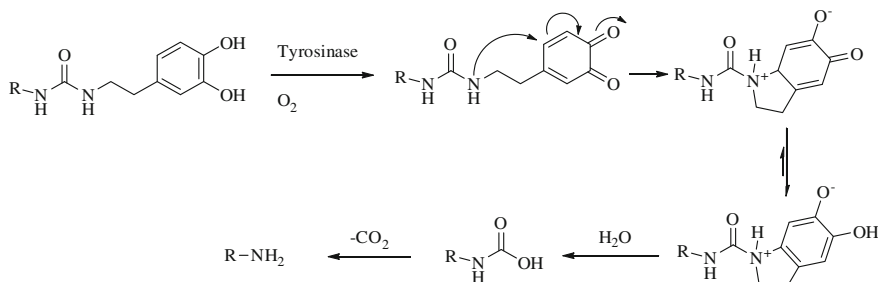
Zerner and co-workers were successfully able to mimic elements of the enzyme-catalysed reaction by employing excess NiCl₂ and *N*-(2-pyridylmethyl)urea in an aqueous ethanol system [88]. Through kinetic measurements and absorption spectroscopy they were able to conclude oxygen coordination of the urea promoted nucleophilic attack to form tetrahedral intermediate **3**. Following a prototropic shift, ammonia is ejected leaving the nickel bound to the hydrolysed product (Scheme 1.31).



Scheme 1.31 Model system for the urease catalysed hydrolysis of ureas

The effect urease has on hydrolysis is striking. Uncatalysed hydrolysis of urea in aqueous media has never been reported whereas best estimations have the enzymatic rate enhancement at least 10^{14} at biological pH (7) and temperature (37 °C) [89].

Mushroom tyrosinase was successfully used in the deprotection of ureas as reported by Osborn and Williams [90]. Building upon tyrosinase oxidations of phenols and catechols, the group cleverly exploited the enzymatic pathway that led to unstable urea intermediates. With the resonance stability disrupted, facile hydrolysis furnished the unprotected amine (Scheme 1.32).



Scheme 1.32 Mushroom tyrosinase catalysed deprotection of ureas

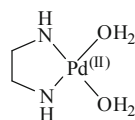
While the reaction uses a commercially available enzyme and can achieve high levels of chemoselectivity, the initial pre-functionalisation involving triphosgene and amine coupling partner may prove difficult in more complex molecules.

1.4.2 Metal Catalysed Deprotection

Knowing that Ni(II) plays a key role in urease catalysed hydrolysis of urea, a large variety of alternative metal species have been screened in an effort to find synthetic equivalents, these included rhodium (III) [91], platinum (II) [92] and cobalt (III) [93] complexes. Many of these systems showed modest to good activity but few were catalytic with respect to the metal.

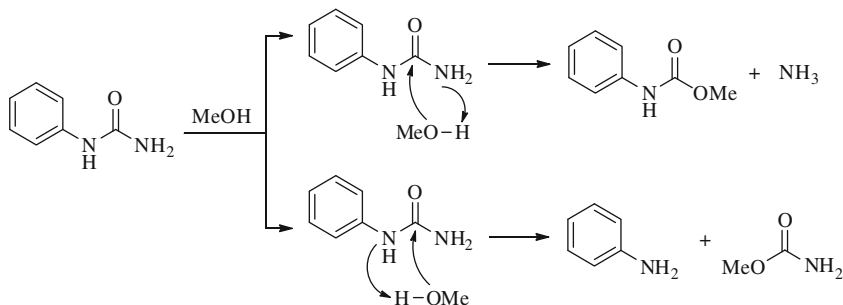
Kostić and co-workers found Pd(II) aqua complexes (Fig. 1.5) were active in catalysing the hydrolysis [94] and alcoholysis [95] of urea in aqueous media. They studied the roles of acid and base along with several inhibitors of the reaction (thiourea and ammonia). Using ^{13}C and ^{15}N enriched urea, NMR studies were successfully employed in producing a comprehensive kinetic profile. Both oxygen

Fig. 1.5 $cis\text{-}[\text{Pd}(\text{en})\text{-(H}_2\text{O)}_2]^{2+}$



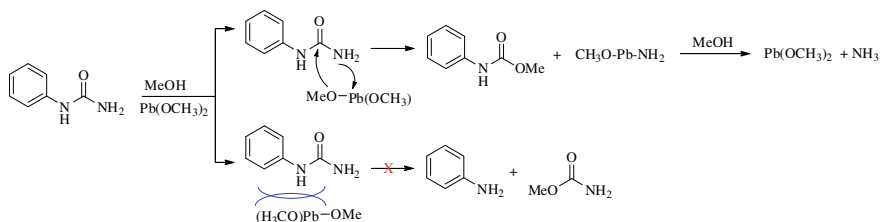
and nitrogen-bound Pd-urea species were observed to evolve CO_2 with the nitrogen-bound Pd-carbamic acid identified as a key intermediate.

Phenyl urea can be converted into methyl phenylcarbamate (MPC) in the presence of catalytic $\text{Pb}(\text{OCH}_3)_2$ in methanol [96]. Without the catalyst, selectivity and yield of MPC were modest (64 and 45 % respectively) with the formation of aniline, ammonia and methyl carbamate as by-products. It was speculated that a reaction between phenyl urea and methanol occurs via an addition–elimination mechanism resulting in two contrasting pathways dependent on the orientation of methanol (Scheme 1.33).



Scheme 1.33 MPC formation in the absence of $\text{Pb}(\text{OCH}_3)_2$

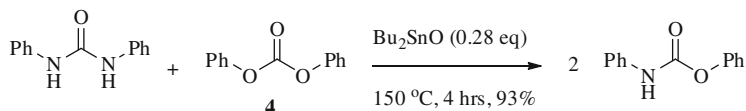
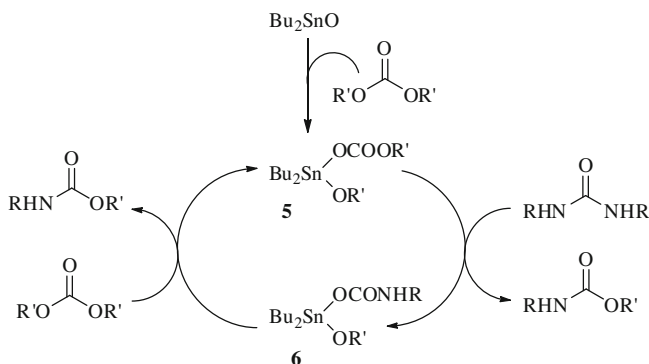
In the presence of $\text{Pb}(\text{OCH}_3)_2$, MPC selectivity increased (80 %) as did isolated yield (86 %). A similar addition/elimination pathway was proposed with aniline formation suppressed due to the size of $\text{Pb}(\text{OCH}_3)_2$ and the phenyl ring (Scheme 1.34).



Scheme 1.34 MPC formation in the presence of $\text{Pb}(\text{OCH}_3)_2$

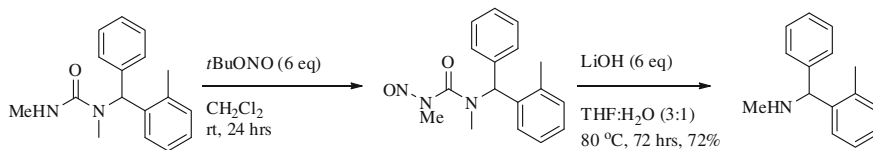
The conversion of ureas to carbamates has also been shown by Shivarkar et. al. using a tin based catalyst ($n\text{Bu}_2\text{SnO}$) and a carbonate coupling partner (**4**) (Scheme 1.35) [97].

The reaction is formally a tandem ester aminolysis of carbonate and alcoholysis of urea, proceeding via a nucleophilic attack by the tin catalyst on the carbonate carbonyl (Scheme 1.36). This leaves the key intermediate **5** which can then interact with the substituted urea to eliminate one molecule of carbamate. The resulting tin species **6** can then react with another molecule of carbonate, releasing the second carbamate and regenerating **5**.

**Scheme 1.35** Tin catalysed carbamate formation**Scheme 1.36** Catalytic cycle for tin mediated carbamate formation

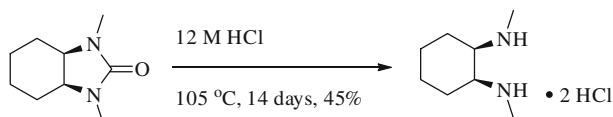
1.4.3 Alternative Methods

Clayden et. al. were able to use lithiated ureas to effect a stereospecific intramolecular electrophilic arylation [98]. Substituted diarylmethylamines were ultimately synthesised through the removal of the superfluous urea group, post-lithiation. This was achieved through either DIBAL reduction (refluxing toluene, 48 h) or nitroso derivatisation and subsequent base catalysed hydrolysis (Scheme 1.37).

**Scheme 1.37** Urea cleavage of nitroso urea derivatives

The need for two additional synthetic steps to remove the urea group is far from ideal. The conditions presented are also unsuitable for functionalities sensitive to nitration and/or strong base.

The synthesis of vicinal diamines has also been achieved through the removal of the urea functionality [99]. The procedure required prolonged reaction times, high temperatures and acidic conditions (Scheme 1.38).



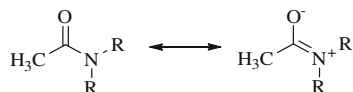
Scheme 1.38 Diamine synthesis requiring harsh reaction conditions

As the authors acknowledge, this methodology cannot be applied to molecules which have unprotected acid sensitive functionalities. Reaction times of 2 weeks are also impractical in all but the most extreme cases, especially for yields as modest as 45 %. This reaction highlights the difficulties in removing the urea group and the advantages that would be gained in the development of a high yielding, mild, expedient deprotection strategy.

1.5 Twisted Amides

The amide functional group can be considered one of the most fundamental and important motifs in both chemistry and biology. Akin to ureas (Sect. 1.4) the lone pair of electrons on nitrogen can be delocalised onto the carbonyl, forming a partial double bond (Fig. 1.6).

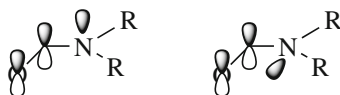
Fig. 1.6 Amide resonance



As a consequence, most non-cyclic amide bonds are planar. If conformational restrictions force the lone pair of electrons out of the plane, disrupting resonance, the amide can be considered to be ‘twisted’.

First proposed in 1938, [100] twisted amides can display dramatic differences in stability and reactivity, acting more like amines than standard amides due to the increased basicity of nitrogen. (Fig. 1.7).

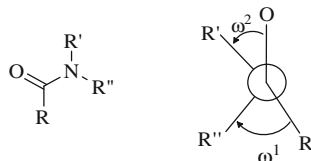
Fig. 1.7 Planar amide (*left*).
Twisted amide (*right*)



Whilst there are no minimum criteria to qualify as a twisted amide, there are several key features that are common throughout. The carbonyl infrared absorption band often lies within the ketone range ($\sim 1700\text{--}1800\text{ cm}^{-1}$ as opposed to $\sim 1650\text{ cm}^{-1}$ for amides) and ^{13}C NMR carbonyl shifts also see a significant change from standard amide values ($\sim 180\text{ ppm}$ for twisted amides vs. $\sim 165\text{ ppm}$ for planar amides) [101]. X-Ray crystallography is also highly diagnostic, enabling

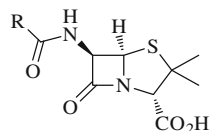
precise measurements of angles and bond lengths with Dunitz and Winkler reporting three independent values to quantitatively evaluate the extent an amide is twisted [102]. These parameters describe pyramidalisation of the nitrogen (χ_N) and carbon (χ_C) and the torsion angle about the C–N bond (τ) (Fig. 1.8).

Fig. 1.8 Dihedral angles used for determining torsion angle. $(\tau) = (\omega_1 + \omega_2)/2$



Twisted amides can exhibit unusual reactivity including facile hydrolysis in water [103, 104]. This is in contrast to planar amides where delocalisation effects provide stability against nucleophilic attack. Before the structure of penicillin was determined by X-Ray crystallography it was widely agreed that it could not contain an amide bond due to the speed of hydrolysis in water [105]. Woodward (correctly) postulated that a β -lactam ring in which ring strain forces the amide to adopt a non-planar conformation was responsible for activity (Fig. 1.9) [106].

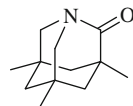
Fig. 1.9 General structure of penicillins



1.5.1 Lactams

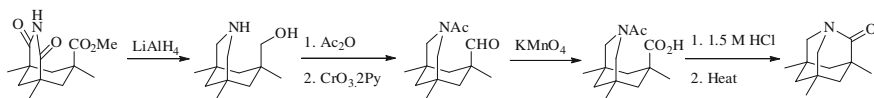
Many amides situated within lactams can become twisted, with rigid geometrical restraints forcing the non-planar conformation. Kirby et. al. reported the preparation, crystal structure, and reactivity of one such example; 1-aza-2-adamantanone (Fig. 1.10) [107].

Fig. 1.10 1-aza-2-adamantanone



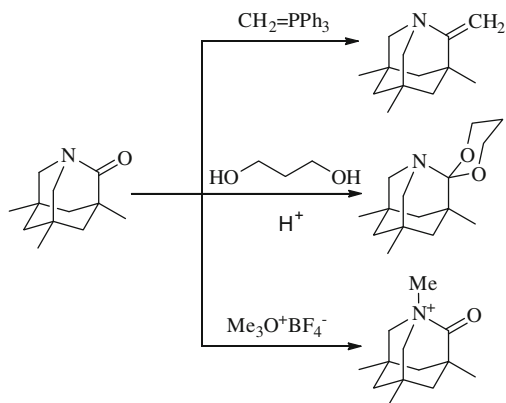
As expected, the structural data is unlike that for a regular amide bond (IR $C=O$, 1732 cm^{-1} , ^{13}C NMR $C=O$, 200 ppm) and the crystal structure shows a twist angle of $\tau = 90.5^\circ$. The amide was synthesised from a known ester imide in four steps (Scheme 1.39).

The ketone-like reactivity of this remarkable molecule further demonstrated its unusual features. Enamine formation occurred when reacted with a phosphorus ylid under standard Wittig conditions whilst acetal formation occurred in the



Scheme 1.39 Synthesis of 1-aza-adamantanone

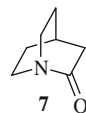
Scheme 1.40 Ketone like reactivity



presence of a diol under acid catalysis. Methylation also occurs on nitrogen with Meerwein's reagent (Scheme 1.40).

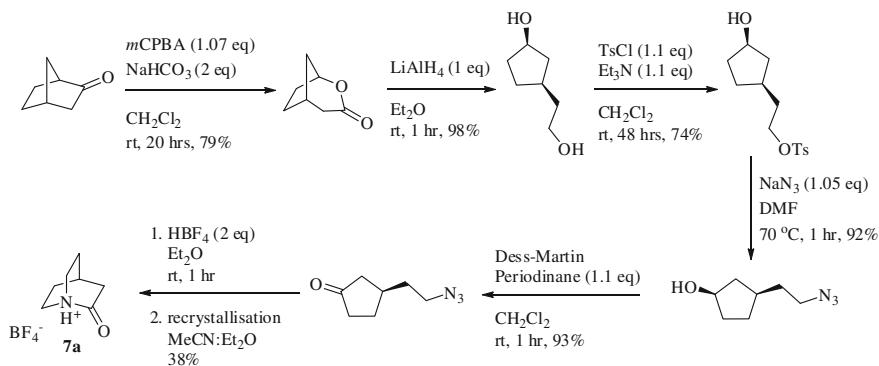
Amides of bicyclic bridgehead lactams are also highly twisted. In this emerging area there are now many examples of this class of molecule over a range of ring sizes [108–112]. Perhaps the most prominent example of these ‘anti Bredt’ [113] molecules is the widely targeted 2-quinuclidone **7** (Fig. 1.11).

Fig. 1.11 2-Quinuclidone



Originally proposed by Lukeš as a model system to examine twisted amides [100], the molecule remained ‘theoretical’ for over 60 years, despite many attempted syntheses [114–116]. Many routes to **7** focused on standard amide forming techniques (peptide coupling reagents etc.) and it became apparent that with a high susceptibility to hydrolysis, an alternate strategy was needed. By focussing on expulsion of N_2 as the driving force for the construction of the strained bicyclic core, Stoltz and Tani reported the first synthesis of 2-quinuclidone as the tetrafluoroborate salt (Scheme 1.41) [117].

As expected, the crystal structure of the BF_4^- salt of **7** (**7a**) showed a large twist angle ($\tau = 90.9^\circ$) and a carbonyl infrared absorption band of 1822 cm^{-1} . The need to trap **7** as the protonated salt is revealed upon investigations into its chemical reactivity. Instantaneous hydrolysis is observed when dissolved in D_2O



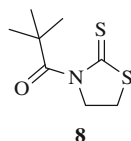
Scheme 1.41 Stoltz and Tani synthesis of 2-quinuclidone tetrafluoroborate

($t_{1/2}$ of <15 s) and all attempts to isolate the free-base resulted mainly in polymeric material.

1.5.2 Alternative Twisted Amides

Examples of twisted amides that are not geometrically restricted (either at a bridgehead or in strained lactam) are scarce. One such example from Yamada details the remarkable reactivity of a hindered thiocarbonyl moiety **8** (Fig. 1.12) [118]. These molecules can perhaps be thought of more accurately as thioimides rather than classical amides however.

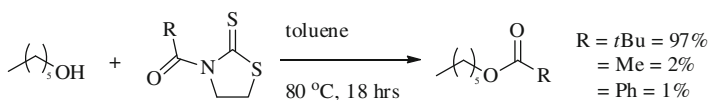
Fig. 1.12 Sterically encumbered twisted amide



It was found that **8** was able to acetylate alcohols under neutral conditions, whereas less sterically demanding analogues proved unreactive (Scheme 1.42) [119].

This disparity was investigated by examining the physical properties of a series of increasingly bulky substituents. (Table 1.1).

The carbonyl infrared absorption band shows more of a shift towards the ketone region in **8** than the less sterically demanding analogues, suggesting poorer overlap of the nitrogen lone-pair. A significantly more electron poor carbonyl also suggests electron donation is reduced. X-Ray crystallographic analysis finally revealed the extent to which the amide bond was twisted. The 1,3-thiazolidine-2-thione ring and the carbonyl group are nearly orthogonal, presumably from the steric repulsion



Scheme 1.42 Acylation of 1-hexanol

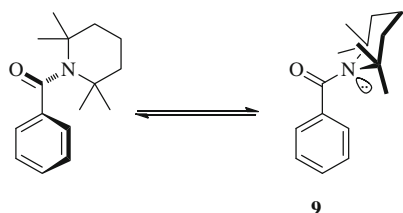
Table 1.1 Spectroscopic properties of increasingly hindered amides

Entry	IR (cm ⁻¹) (C = O)	δ (¹³ C C = O)
	1697	170.6
	1702	175.6
	1701	178.7
	1726	187.8

Fig. 1.13 Orthogonal conformation, disrupted overlap (*left*). Planar conformation, good overlap (*right*)



Fig. 1.14 Conformation and reactivity

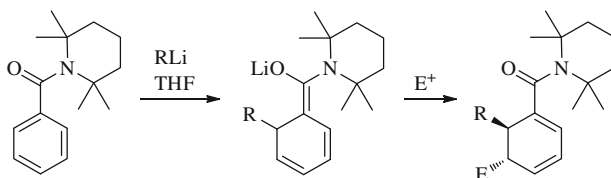


between the *tert*-butyl group and the thione. X-ray analysis of the methyl analogue shows the carbonyl and thione ring to be almost planar allowing for strong overlap between the nitrogen lone-pair and the carbonyl π -system (Fig. 1.13).

In 2002, Clayden et. al reported the unusual dearomatization of aryl 2,2,6,6-tetramethylpiperidine (TMP) amide derivatives through what was postulated to be a twisted, de-conjugated conformation **9** (Fig. 1.14) [120]. The barrier to C–N

rotation of these TMP amides (28 kJ mol^{-1}) [121] is substantially lower than that of smaller, less sterically demanding amides (e.g. 65 kJ mol^{-1} for the dimethyl analogue) [122], allowing for a greater proportion of **9**, the species thought to be susceptible to nucleophilic attack and dearomatisation.

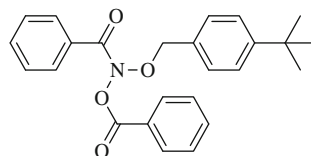
Treatment of these amides with organolithium reagents and then an electrophile furnished cyclohexadiene derivatives. This occurred through nucleophilic attack at the *ortho* position in a Michael-type addition and then subsequent electrophilic quench of the resultant enolate (Scheme 1.43). This unusual reactivity was thought to be due to the conjugation of the phenyl ring with the carbonyl π -bond, activating the ring towards nucleophilic attack while the four methyl groups on the TMP block the carbonyl from attack.



Scheme 1.43 Cyclohexadiene formation

Amides possessing two electronegative heteroatoms on nitrogen have also been shown to display twisted amide characteristics [123]. During their investigations into direct-acting mutagens [124] Glover and co-workers found that *N*-acetoxy-*N*-alkoxybenzamides (*ONO*) displayed vastly different properties when compared to normal amides. (Fig. 1.15).

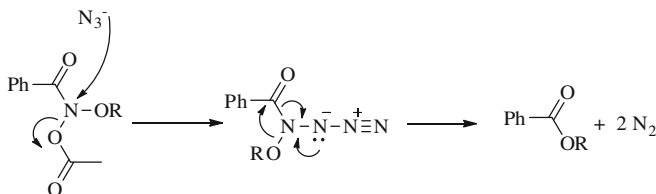
Fig. 1.15 *N*-Acetoxy-*N*-alkoxyamides



The nitrogen atom of such species was found to display a high level of pyramidalisation in order to maximise electron density distribution near the electronegative atoms. This tetrahedral shape allows for very little lone pair delocalisation onto the neighbouring carbonyl resulting in high $\text{C}=\text{O}$ stretch frequencies ($1730\text{--}1750$). Hydrazine derivatives (*NNO*) [125], chloro (*ONCl*) [126] and sulfonyl (*ONS*) [127] bis-heteroatom amides have also been synthesised, all exhibiting strong pyramidalisation at nitrogen.

The unusual reactivity of these compounds was exploited through the addition of sodium azide in an $\text{S}_{\text{N}}2$ displacement, followed by Heteroatom Rearrangement on Nitrogen (HERON), liberating N_2 and forming an ester (Scheme 1.44).

Twist angles for this class of compounds are moderate in comparison to those incorporated into a lactam bridgehead ($14\text{--}15^\circ$).

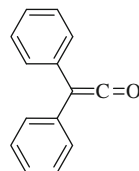


Scheme 1.44 Acetate displacement by azide followed by HERON

1.6 Ketenes

Since Staudinger first prepared and characterised diphenylketene (Fig. 1.16), ketenes have attracted organic chemist's attention for more than a century [128]. No less than 20 Nobel laureates (including Staudinger) have studied these fascinating molecules while research into their properties, structure and reactivity are still an active area of research.

Fig. 1.16 Diphenylketene

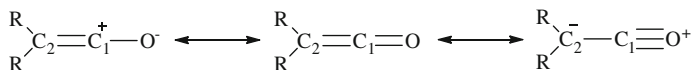


1.6.1 Structure, Spectroscopy and Physical Properties

The unique properties of ketenes are derived from their cumulene structure, with the highest occupied molecular orbital (HOMO) perpendicular to the ketene plane and the lowest unoccupied molecular orbital (LUMO) in the ketene plane (Fig. 1.17) [129].

A substantial negative charge on oxygen and C_2 can be seen, while there is a positive charge on C_1 in the ketene plane. Nucleophiles are therefore expected to attack the C_1 position while electrophiles should approach perpendicular to the plane at C_2 or at oxygen (Scheme 1.45) [130].

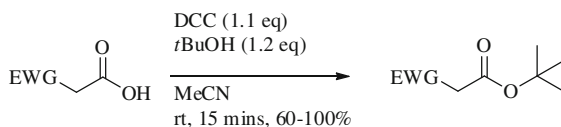
The simplest ketene, ($CH_2 = C = O$) first synthesised from the pyrolysis of acetic anhydride or acetone using a hot platinum wire [131], shows a remarkable 1H chemical shift at 2.32–2.46 ppm. For an alkene-type proton this value is unusually high and can be attributed to the high electron density at C_2 [132]. Similarly, ^{13}C shifts are affected with values in the range of 178–203 ppm for C_1 and 33–48 ppm for C_2 . Unsurprisingly, ketene IR absorption is very characteristic and show very strong bands between 2020 and 2200 cm^{-1} [133].

Fig. 1.17 Ketene orbital structures**Scheme 1.45** Ketene resonance forms

1.6.2 Preparation of Ketenes

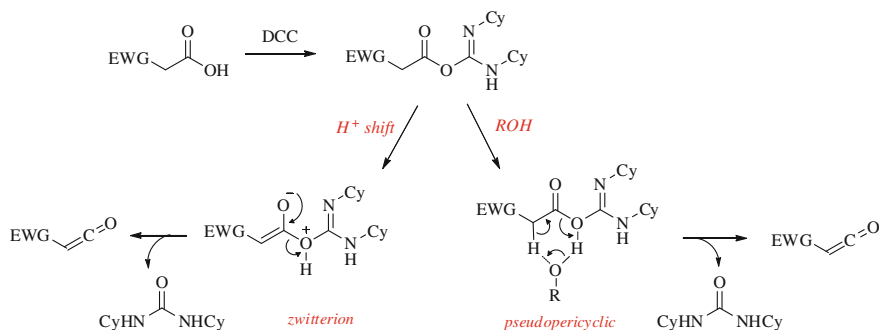
The preparation of ketenes has been widely studied [133–136]. Methods include pyrolysis of ketene dimers, Wolff rearrangements of diazo ketones, photolysis and the release from metal carbene complexes. Only a select few examples will be discussed here.

Carboxylic acids and their derivatives can offer simple and convenient routes to ketene formation in both industrial [137] and laboratory [138] environments. Reactions of carboxylic acids with strongly electron-withdrawing α -substituents with dicyclohexyl carbodiimide (DCC) led to rapid and high yielding ketene formation which ultimately produced esters in the presence of alcohols (Scheme 1.46) [139].

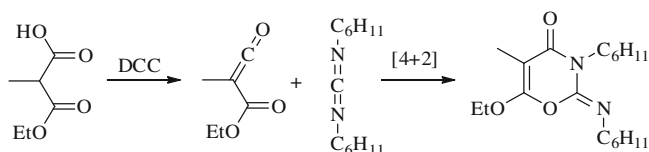
**Scheme 1.46** Ester formation from acid dehydration

The authors proposed two competing transition states for the formation of the ketene intermediate, one through a pseudopericyclic transition state and the other through a zwitterionic pathway. The presence of a strongly electron-withdrawing group should stabilise the zwitterionic intermediate, favouring this pathway, however for malonate derivatives it was proposed the pseudopericyclic intermediate may dominate. Despite numerous investigations the authors were unable to distinguish between the two (Scheme 1.47).

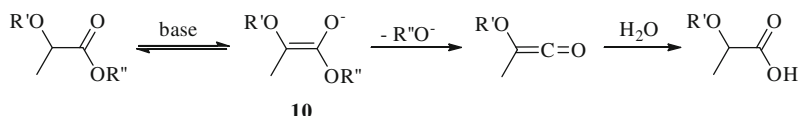
The formation of ketenes was explicitly implicated through the mono-incorporation of deuterium when *t*BuOD was used and through the formation of an oxazine in a [4 + 2] cycloaddition when an extra equivalent of DCC was used as a keteneophile (Scheme 1.48).



Scheme 1.47 Competing pathways to ketene formation



Scheme 1.48 Oxazine formation from 2 eq of DCC

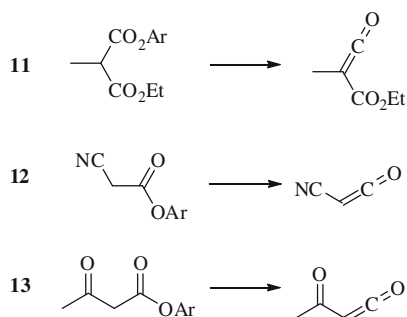


Scheme 1.49 Base catalysed ketene formation

The base catalysed hydrolysis of esters via an E1cB mechanism is another well documented case involving ketene intermediates [140]. Deprotonation next to the ester carbonyl leads to enolate **10**. Extrusion of a good alkoxy or aryloxy leaving group generates the ketene which in the presence of water leads to the carboxylic acid (Scheme 1.49).

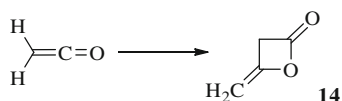
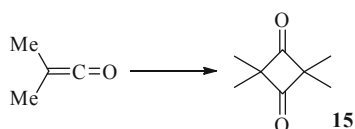
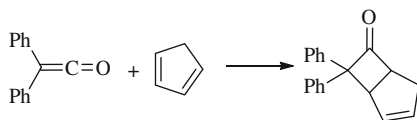
Evidence for this mechanism is revealed when examining the hydrolysis of aryl ethyl malonates (**11**), *o*-nitrophenyl cyanoacetate (**12**) and aryl acetoacetates (**13**) [141] which form carboethoxy-, cyano- and acetylketenes respectively (Fig. 1.18) [142]. The rate of hydrolysis is enhanced when increasing the bulk on the aryl leaving group, an opposite trend would be expected if the B_{AC}2 mechanism of base attack on the carbonyl was in operation. A linear correlation of log *k* for hydrolysis of **13** with the *pK_a* of the phenolate leaving group was also found.

Flash vacuum thermolysis (FVT) is a technique often used to form ketenes, a demonstration of the extreme conditions sometimes required for their generation. Temperatures in excess of 700 °C are not uncommon, limiting the use of this method to mechanistic investigations into simple molecules.

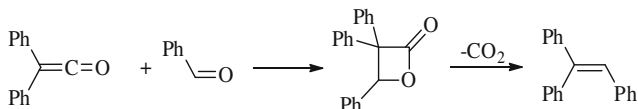
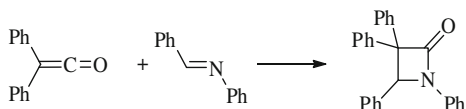
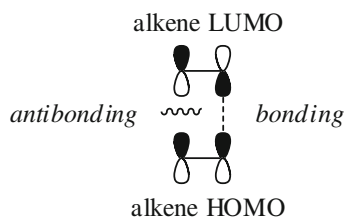
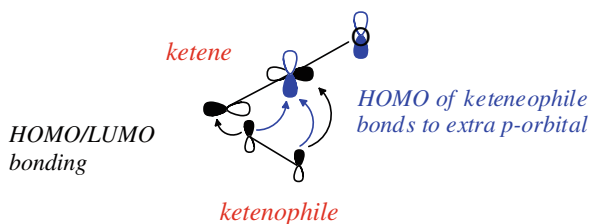
Fig. 1.18 Ketenes from ester enolates

1.6.3 Reactivity of Ketenes

Cycloaddition reactions have become synonymous with ketene chemistry and have become one of the most intellectually challenging reactions in the field. After the isolation of methylene- β -lactone (**14**) from ketene (Scheme 1.50) [143] and the formation of symmetrical dimer **15** from dimethylketene (Scheme 1.51) [144], a wide variety of cycloaddition reactions were soon discovered. These include the formation of cyclobutanones from cyclopentadiene (Scheme 1.52) [145], formation of β -lactams from imines (Scheme 1.53) and β -lactones from reactions with aldehydes (Scheme 1.54) [146].

Scheme 1.50 Lactone formation via ketene dimerisation**Scheme 1.51** Symmetrical dimerisation**Scheme 1.52** [2 + 2] Cycloaddition with cyclopentadiene

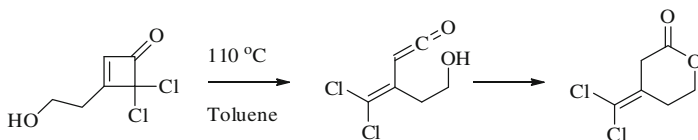
The unique propensity for ketenes to undergo facile [2 + 2] cycloadditions has led to many studies and reviews on the subject [147]. Alkenes do not normally undergo thermal [2 + 2] cycloadditions as the HOMO/LUMO combination is antibonding at one terminus (Fig. 1.19).

Scheme 1.53 β -Lactam formation**Scheme 1.54** β -Lactone formation and subsequent decarboxylation**Fig. 1.19** Disallowed thermal [2 + 2] cycloaddition**Fig. 1.20** Facile [2 + 2] cycloaddition of ketenes

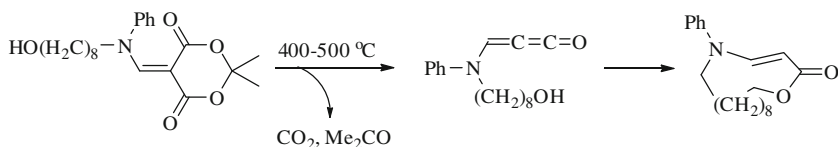
The orthogonal π -bond at the central ketene carbon enables the orbitals of the HOMO of the incoming keteneophile to bond to an extra p-orbital. This generates 4 bonding interactions and only two antibonding interactions allowing for favourable bond formation (Fig. 1.20).

The low energy LUMO of ketenes also makes them potent electrophiles, a feature exploited through the addition wide-range of nucleophiles. Carbon [148], silicon [149] and amine nucleophiles [150] have all been successfully employed and ketenes can even be reduced by hydrides [151]. Addition of oxygen nucleophiles is also common and the installation of an intramolecular hydroxyl group has provided routes to a variety of lactones (Scheme 1.55) [152].

Pommelet and co-workers also employed an intramolecular hydroxyl trap in the synthesis of macrocycles [153]. This work demonstrates some of the forcing conditions required in the generation of ketenes (in this case through the extrusion of CO_2 and acetone) (Scheme 1.56).



Scheme 1.55 Intramolecular lactonisation of a ketene



Scheme 1.56 Macrocyclisation through the generation of a ketene

1.7 Project Aims

This thesis and the projects described herein aimed to address several fundamental challenges facing synthetic chemists.

The development of a mild C–H activation/*ortho*-functionalisation process would provide a useful alternative to the sometimes harsh (pH, time, temperatures) protocols that can impede implementation on an industrial scale. Building upon the previous use of the urea functionality as a directing group would also complement the plethora of options currently available.

Methods to remove the urea moiety are limited. This robust functional group is generally inert to all but the extremes of hydrolysis and a few enzymatic or metal catalysed processes. The development of a mild, expedient and neutral removal procedure would allow chemists to utilise this group in a greater range of scenarios.

Nature's ability to manipulate amides under neutral, physiological conditions has challenged both chemists and biologists for decades. The implication of twisted amides has previously only been examined in conformationally locked lactams where the nitrogen is located at a bridgehead forcing the *N*-lone pair out of plane. The study of acyclic, linear amides that undergo facile hydrolysis under neutral conditions may be more suitable to biological systems and would contribute to the ongoing debate regarding peptide lysase.

References

1. Sigma Aldrich 2011
2. Li S, Lin Y, Cao J, Zhang SJ (2007) *Org Chem* 72:4067–4072
3. Nishikata T, Abela AR, Lipshutz BH (2010) *Angew Chem Int Ed* 49:781–784
4. Bullock KM, Mitchell MB, Toczko JF (2008) *Org Process Res Dev* 12:896–899

5. Mee SPH, Lee V, Baldwin JE (2004) *Angew Chem Int Ed* 43:1132–1136
6. So CM, Yeung CC, Lau CP, Kwong FYJ (2008) *Org Chem* 73:7803–7806
7. Shen Q, Hartwig JF (2008) *Org Lett* 10:4109–4112
8. Kantam ML, Srinivas P, Yadav J, Likhari PR, Bhargava SJ (2009) *Org Chem* 74:4882–4885
9. Cui X, Li J, Zhang Z-P, Fu Y, Liu L, Guo Q-XJ (2007) *Org Chem* 72:9342–9345
10. Mizoroki T, Mori K, Ozaki AB (1971) *Chem Soc Jpn* 44:581
11. Heck RF, Nolley JJP (1972) *Org Chem* 37:2320–2322
12. Powell DA, Fu GCJ (2004) *Am Chem Soc* 126:7788–7789
13. Milne JE, Buchwald SLJ (2004) *Am Chem Soc* 126:13028–13032
14. Li P, Wang L, Li H (2005) *Tetrahedron* 61:8633–8640
15. Li J-H, Liang Y, Wang D-P, Liu W-J, Xie Y-X, Yin D-LJ (2005) *Org Chem* 70:2832–2834
16. Meulemans TM, Kiers NH, Feringa BL, van Leeuwen PWNM (1994) *Tetrahedron Lett* 35:455–458
17. Popp BV, Thorman JL, Stahl SSJ (2006) *Mol Catal A-Chem* 251:2–7
18. Bar GLJ, Lloyd-Jones GC, Booker-Milburn KIJ (2005) *Am Chem Soc* 127:7308–7309
19. Itahara TJ (1985) *Org Chem* 50:5546–5550
20. Tanaka D, Romeril SP, Myers AGJ (2005) *Am Chem Soc* 127:10323–10333
21. Grimster NP, Gauntlett C, Godfrey CRA, Gaunt MJ (2005) *Angew Chem Int Ed* 44:3125–3129
22. Åakermark B, Larsson EM, Oslob JDJ (1994) *Org Chem* 59:5729–5733
23. Dick AR, Hull KL, Sanford MSJ (2004) *Am Chem Soc* 126:2300–2301
24. Desai LV, Hull KL, Sanford MSJ (2004) *Am Chem Soc* 126:9542–9543
25. Deprez NR, Kalyani D, Krause A, Sanford MSJ (2006) *Am Chem Soc* 128:4972–4973
26. Deprez NR, Sanford MS (2007) *Inorg Chem* 46:1924–1935
27. Desai LV, Sanford MS (2007) *Angew Chem Int Ed* 46:5737–5740
28. Neufeldt SR, Sanford MS (2009) *Org Lett* 12:532–535
29. Daugulis O, Zaitsev VG (2005) *Angew Chem Int Ed* 44:4046–4048
30. Bedford RB, Webster RL, Mitchell CJ (2009) *Org Biomol Chem* 7:4853–4857
31. Alexanian EJ, Lee C, Sorensen EJJ (2005) *Am Chem Soc* 127:7690–7691
32. Smidt J, Hafner W, Jira R, Sieber R, Sedlmeier J, Sabel A (1962) *Angew Chem Int Ed* 1:80–88
33. Keith JA, Nielsen RJ, Oxgaard J, Goddard WAJ (2007) *Am Chem Soc* 129:12342–12343
34. Anderson BJ, Keith JA, Sigman MSJ (2010) *Am Chem Soc* 132:11872–11874
35. Mitsudome T, Mizumoto K, Mizugaki T, Jitsukawa K, Kaneda K (2010) *Angew Chem Int Ed* 49:1238–1240
36. Keith JA, Henry PM (2009) *Angew Chem Int Ed* 48:9038–9049
37. Ito Y, Aoyama H, Hirao T, Mochizuki A, Saegusa TJ (1979) *Am Chem Soc* 101:494–496
38. Pei T, Wang X, Widenhoefer RAJ (2002) *Am Chem Soc* 125:648–649
39. Lu BZ, Zhao W, Wei H-X, Dufour M, Farina V, Senanayake CH (2006) *Org Lett* 8:3271–3274
40. Yue D, Yao T, Larock RCJ (2005) *Org Chem* 71:62–69
41. Åkermark B, Bäckvall JE, Hegedus LS, Zetterberg K, Siirala-Hansén K, Sjöberg KJ (1974) *Organomet Chem* 72:127–138
42. Bäckvall J-E (1975) *Tetrahedron Lett* 16:2225–2228
43. Bäckvall J-E (1978) *Tetrahedron Lett* 19:163–166
44. Bäckvall J-E (1977) *J Chem Soc Chem Comm* 27:413–414
45. Hegedus LS, Siirala-Hansen KJ (1975) *Am Chem Soc* 97:1184–1188
46. Tsuji J (1997) *Palladium reagents and catalysts*. Wiley, Chichester, p 301
47. Kotov V, Scarborough CC, Stahl SS (2007) *Inorg Chem* 46:1910–1923
48. Barsacchi M, Consiglio G, Medici L, Petrucci G, Suter UW (1991) *Angew Chem Int Ed* 30:989–991
49. Tsuji J, Morikawa M, Kiji JJ (1964) *Am Chem Soc* 86:4851–4853
50. Stille JK, James DEJ (1976) *Organomet Chem* 108:401–408
51. Stille JK, Divakaruni RJ (1979) *Org Chem* 44:3474–3482

52. McCormick M, Monahan R, Soria J, Goldsmith D, Liotta DJ (1989) *Org Chem* 54:4485–4487
53. Fenton DM, Steinwand PJJ (1974) *Org Chem* 39:701–704
54. Giannoccaro PJ (1987) *Organomet Chem* 336:271–278
55. Chandrasekhar S, Narsihmulu C, Sultana SS, Reddy NR (2002) *Org Lett* 4:4399–4401
56. Boele MDK, van Strijdonck GPF, de Vries AHM, Kamer PCJ, de Vries JG, van Leeuwen PWNM (2002) *J Am Chem Soc* 124:1586–1587
57. Fujita K-I, Nonogawa M, Yamaguchi R (2004) *Chem Commun* 1926–1927
58. Oi S, Aizawa E, Ogino Y, Inoue YJ (2005) *Org Chem* 70:3113–3119
59. Alberico D, Scott ME, Lautens M (2007) *Chem Rev* 107:174–238
60. Haffemayer B, Gulias M, Gaunt MJ (2010) *Chem Sci* 2:312–315
61. Kalyani D, Satterfield AD, Sanford MSJ (2010) *Am Chem Soc* 132:8419–8427
62. Vermeulen NA, Delcamp JH, White MCJ (2010) *Am Chem Soc* 132:11323–11328
63. Iida H, Yuasa Y, Kibayashi CJ (1980) *Org Chem* 45:2938–2942
64. Dick AR, Kampf JW, Sanford MSJ (2005) *Am Chem Soc* 127:12790–12791
65. Kametani Y, Satoh T, Miura M, Nomura M (2000) *Tetrahedron Lett* 41:2655–2658
66. Neumann JJ, Rakshit S, Dröge T, Glorius F (2009) *Angew Chem Int Ed* 48:6892–6895
67. Chen MS, Prabakaran N, Labenz NA, White MCJ (2005) *Am Chem Soc* 127:6970–6971
68. Mukhopadhyay S, Rothenberg G, Gitis D, Sasson YJ (2000) *Org Chem* 65:3107–3110
69. Satoh T, Miura M (2007) *Chem Lett* 36:200–205
70. Wasa M, Yu J-Q (2010) *Tetrahedron* 66:4811–4815
71. Gürbüz N, Özdemir I, Çetinkaya B (2005) *Tetrahedron Lett* 46:2273–2277
72. Wan X, Ma Z, Li B, Zhang K, Cao S, Zhang S, Shi ZJ (2006) *Am Chem Soc* 128:7416–7417
73. Kalyani D, Deprez NR, Desai LV, Sanford MSJ (2005) *Am Chem Soc* 127:7330–7331
74. Racowski JM, Dick AR, Sanford MSJ (2009) *Am Chem Soc* 131:10974–10983
75. Ryabov AD (1990) *Chem Rev* 90:403–424
76. Shilov AE, Shul'pin GB (1997) *Chem Rev* 97:2879–2932
77. Davies DL, Donald SMA, MacGregor SAJ (2005) *Am Chem Soc* 127:13754–13755
78. Ryabov AD, Sakodinskaya IK, Yatsimirsky AK (1985) *J Chem Soc Dalton* 12:2629–2638
79. Lapointe D, Fagnou K (2010) *Chem Lett* 39:1118–1126
80. Orito K, Horibata A, Nakamura T, Ushito H, Nagasaki H, Yuguchi M, Yamashita S, Tokuda MJ (2004) *Am Chem Soc* 126:14342–14343
81. Giri R, Yu JQJ (2008) *Am Chem Soc* 130:14082–14084
82. Whisler MC, MacNeil S, Snieckus V, Beak P (2004) *Angew Chem Int Ed* 43:2206–2225
83. Houlden CE, Bailey CD, Ford JG, Gagné MR, Lloyd-Jones GC, Booker-Milburn KI (2008) *J Am Chem Soc* 130:10066–10067
84. Dixon NE, Gazzola C, Blakeley RL, Zerner BJ (1975) *Am Chem Soc* 97:4131–4133
85. Jabri E, Carr MB, Hausinger RP, Karplus PA (1995) *Science* 268:998–1004
86. Maslak P, Szczepanski JJ, Parvez MJ (1991) *Am Chem Soc* 113:1062–1063
87. Fairlie DP, Jackson WG, McLaughlin GM (1989) *Inorg Chem* 28:1983–1989
88. Blakeley RL, Treston A, Andrews RK, Zerner BJ (1982) *Am Chem Soc* 104:612–614
89. Kolodziej AF (1991) *Prog Inorg Chem* 41:493
90. Osborn HMI, Williams NAO (2004) *Org Lett* 6:3111–3113
91. Curtis NJ, Dixon NE, Sargeson AMJ (1983) *Am Chem Soc* 105:5347–5353
92. Watson AA, Fairlie DP (1995) *Inorg Chem* 34:3087–3092
93. Dixon NE, Fairlie DP, Jackson WG, Sargeson AM (1983) *Inorg Chem* 22:4038–4046
94. Kaminskaia NV, Kostic NM (1997) *Inorg Chem* 36:5917–5926
95. Kaminskaia NV, Kostic NM (1998) *Inorg Chem* 37:4302–4312
96. Wang J, Li Q, Dong W, Kang M, Wang X, Peng S (2004) *Appl Catal A-Gen* 261:191–197
97. Shivarkar AB, Gupte SP, Chaudhari RVJ (2004) *Mol Catal A-Chem* 223:85–92
98. Clayden J, Dufour J, Grainger DM, Helliwell MJ (2007) *Am Chem Soc* 129:7488–7489
99. Akester J, Cui J, Fraenkel GJ (1997) *Org Chem* 62:431–434
100. Lukeš R (1938) *Collect Czech Chem C* 10:148–152

101. Szostak M (2009) *Aubé. J Org Lett* 11:3878–3881
102. Dunitz JD, Winkler FK (1975) *Acta Crystallogr B* 31:251–263
103. Kirby AJ, Komarov IV, Feeder NJ (2001) *Chem Soc Perkin Trans* 2:522–529
104. Kirby AJ, Komarov IV, Feeder NJ (1998) *Am Chem Soc* 120:7101–7102
105. Bennet AJ, Wang QP, Slebockatilk H, Somayaji V, Brown RS, Santarsiero BDJ (1990) *Am Chem Soc* 112:6383–6385
106. Clayden J, Moran WJ (2006) *Angew Chem Int Ed* 45:7118–7120
107. Kirby AJ, Komarov IV, Wothers PD, Feeder N (1998) *Angew Chem Int Ed* 37:785–786
108. Szostak M, Yao L, Aubé J (2009) *J Org Chem* 74:1869–1875
109. Lei Y, Wroblewski AD, Golden JE, Powell DR, Aubé JJ (2005) *Am Chem Soc* 127:4552–4553
110. Yao L, Aubé JJ (2007) *Am Chem Soc* 129:2766–2767
111. Szostak M, Aubé J (2009) *Chem Commun* 14:7122–7124
112. Szostak M, Aubé J (2010) *Org Biomol Chem* 9:27–35
113. Shea KJ (1980) *Tetrahedron* 36:1683–1715
114. Yakhontov LN, Rubsitov MV (1957) *J Gen Chem USSR* 27:83–87
115. von Pracejus H, Kehlen M, Kehlen H, Matschiner H (1965) *Tetrahedron* 21:2257–2270
116. Somayaji V, Brown RSJ (1986) *Org Chem* 51:2676–2686
117. Tani K, Stoltz BM (2006) *Nature* 441:731–734
118. Yamada S (1993) *Angew Chem Int Ed* 32:1083–1085
119. Yamada S (1992) *Tetrahedron Lett* 33:2171–2174
120. Clayden J, Foricher YJY, Lam HK (2002) *Chem Commun* 2138–2139
121. Lunazzi L, Macciantelli D, Tassi D, Dondoni AJ (1980) *Chem Soc Perkin Trans* 2:717–723
122. Stewart WE, Siddall TH (1970) *Chem Rev* 70:517–551
123. Gillson A-ME, Glover SA, Tucker DJ, Turner P (2003) *Org Biomol Chem* 1:3430–3437
124. Campbell JJ, Glover SA, Hammond GP, Rowbottom CAJ (1991) *Chem Soc Perkin Trans* 2:2067–2079
125. Glover SA, Mo G, Rauk A, Tucker DJ, Turner P (1999) *J Chem Soc Perkin Trans* 2:2053–2058
126. Glover SA, Mo GJ (2002) *Chem Soc Perkin Trans* 2:1728–1739
127. Adams M, Glover SA, Tucker DJ (2001) Unpublished Results
128. Staudinger H (1905) *Chem Ber* 38:1735–1739
129. Cossio FP, Ugalde JM, Lopez X, Lecea B, Palomo CJ (1993) *Am Chem Soc* 115:995–1004
130. Walsh ADJ (1946) *Am Chem Soc* 68:2408–2409
131. Wilshire NTM (1907) *J Chem Soc Perkin Trans* 91:1938–1941
132. Allred EL, Grant DM, Goodlett WJ (1965) *Am Chem Soc* 87:673–674
133. Tidwell TT (2005) *Ketenes II*. Wiley, Hoboken
134. Clemens RJ (1986) *Chem Rev* 86:241–318
135. Barteau MA (1996) *Chem Rev* 96:1413–1430
136. Williams A, Douglas KT (1975) *Chem Rev* 75:627–649
137. Aibaerli C, Miller RJ (1995) *Encyclopedia of chemical technology*. Wiley, New York
138. Krishnaswamy D, Bhawal BM, Deshmukh ARAS (2000) *Tetrahedron Lett* 41:417–419
139. Nahmany M, Melman A (2001) *Org Lett* 3:3733–3735
140. Inoue M, Bruice TCJ (1983) *Org Chem* 48:3559–3561
141. Holmquist B, Bruice TCJ (1969) *Am Chem Soc* 91:3003–3009
142. Pratt RF, Bruice TCJ (1970) *Am Chem Soc* 92:5956–5964
143. Wilshire NTMJ (1907) *Chem Soc* 91:1938–1941
144. Staudinger H, Klever HW (1906) *Chem Ber* 39:946–950
145. Staudinger H (1907) *Chem Ber* 40:115–118
146. Staudinger H (1907) *Liebigs Ann* 356:51–123
147. Snider BB (1988) *Chem Rev* 88:793–811
148. Baigrie LM, Lenoir D, Seikaly HR, Tidwell TTTJ (1985) *Org Chem* 50:2105–2109
149. Dalgard JE, Rychnovsky SDJ (2004) *Am Chem Soc* 126:15662–15663
150. de Lucas NC, Netto-Ferreira JC, Andraos J, Scaiano JCJ (2001) *Org Chem* 66:5016–5021

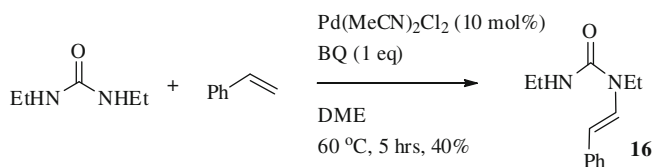
151. Frey J, Rappoport ZJ (1997) *Org Chem* 62:8372–8386
152. Dillon JL, Gao Q, Dillon EA, Adams N (1997) *Tetrahedron Lett* 38:2231–2234
153. Jourdain F, Pommelet JC (1994) *Tetrahedron Lett* 35:1545–1548

Chapter 2

Pd(II) Catalysed Aminocarbonylation of Alkenes

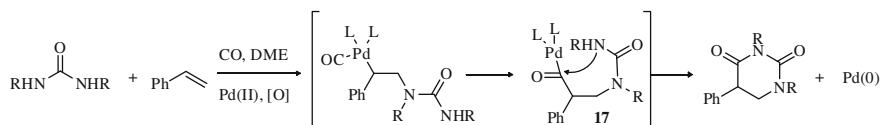
2.1 Background

Following on from the work of Bar on the diamination of conjugated dienes [18], a study of the diamination of simple alkenes revealed modest yields of enamide **16** (Scheme 2.1).



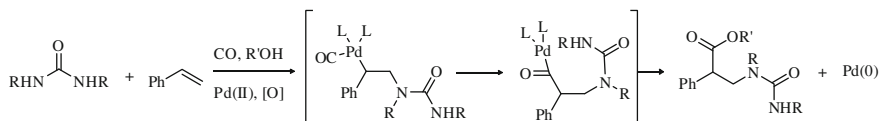
Scheme 2.1 Palladium (II) catalysed diamination of styrene

It was thought possible to affect a novel heterocycle synthesis of pyrimidiones through a similar process in the presence of carbon monoxide. The interception of palladate **17** via the terminal urea nitrogen would lead to cyclisation (Scheme 2.2). If successful, such a sequence could have wide synthetic applications and potential for functionality via different alkenes and ureas.

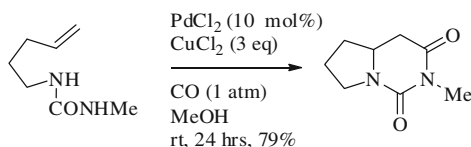


Scheme 2.2 Palladium (II) catalysed, three component pyrimidione formation

When performing this reaction in alcoholic solvents it may also be possible to synthesise β -amino acid derivatives (Scheme 2.3).

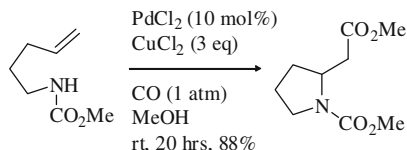


Scheme 2.3 Carbonylation— β -amino acid synthesis



Scheme 2.4 Pd(II) catalysed intramolecular aminocarbonylation of exo-ureas

Scheme 2.5 Pd(II) catalysed intramolecular aminocarbonylation of exo-carbamates



In 1988 Tamaru et al. published an intramolecular cyclisation utilising mild conditions of 1 atm CO pressure and CuCl_2 as the re-oxidant (Scheme 2.4) [1]. Furthermore in 1997 this work was expanded by the same group to include carbamates (Scheme 2.5) [2].

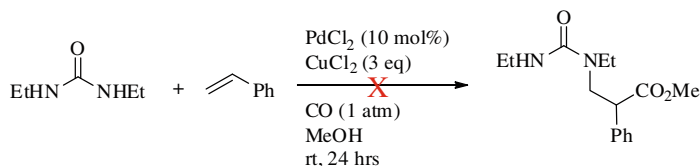
As of yet there is no general method for the intermolecular version of this reaction.

2.2 Results and Discussion

2.2.1 Attempted β -Amino Acid Synthesis

Initial reactions between 1,3-diethyl urea and styrene in methanol failed to yield any traces of product. CuCl_2 was employed as the re-oxidant and the optimal conditions of Tamaru [1] were followed, introducing an atmosphere of CO via a balloon (Scheme 2.6).

Tamaru reported large solvent effects between protic and non-protic media. CH_2Cl_2 and THF were slow and less efficient but a mixture of acetic acid and sodium acetate (3 eq) improved yields (up to 95 % from 79 % in methanol) and reduced the reaction times dramatically (from 3 days to <1 day). It was hoped a similar effect could be observed in the pursuit of β -amino acids. Increased solvation of the chloride ion from PdCl_2 through hydrogen bonding could expose the Pd(II) centre leading to better coordination to the alkene. Protonation of the urea

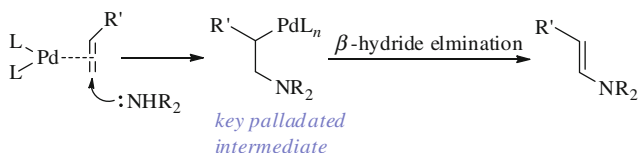


Scheme 2.6 Initial reaction screening

nitrogen should also lead to a weaker complexation to the palladium centre which has been known to shut down catalytic reactivity [3].

Unfortunately a comprehensive solvent screen (with or without the use of sodium acetate as an additive) did not furnish the expected product. Trace amounts of a Wacker oxidation product was observed by ^1H NMR but in an insignificant yield (approximately 3 %).

AA change in approach to conditions more familiar within the Booker-Milburn group was next adopted. The combination of $\text{Pd}(\text{MeCN})_2\text{Cl}_2$ with BQ as an oxidant has been successfully employed by Bar [4], and Elliott [5] in similar but non-carbonylative systems (Scheme 2.7).

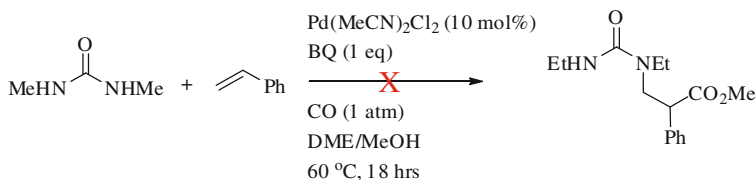


Scheme 2.7 Pd(II) mediated enamide formation

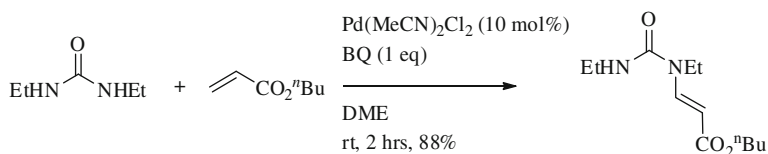
The palladated intermediate prior to β -hydride elimination is the key species which must undergo carbonylative insertion in order to form β -amino acids. With the knowledge that this intermediate forms under $\text{Pd}(\text{MeCN})_2\text{Cl}_2/\text{BQ}$ conditions, various attempts to intercept the β -hydride elimination pathway with CO were undertaken (Scheme 2.8).

With styrene as the alkene coupling partner, numerous experiments varying temperature, concentration, stoichiometries and solvents were trialled but to no avail.

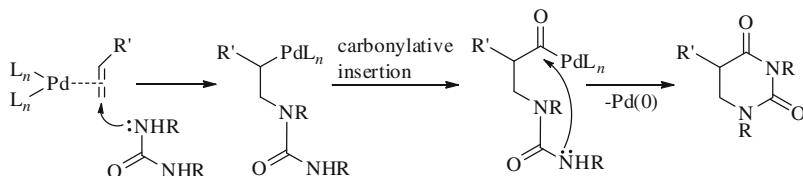
Bar reported a 45 % yield of enamide formation between the reaction of styrene and 1,3-diethylurea in the absence of CO [1]. [9], However in the author's hands, a maximum of 30 % was obtained. Despite this discrepancy, it is obvious that the intermediate described in Scheme 2.7 is not formed efficiently and the reaction is therefore impeded before the CO is even involved. It was therefore decided to investigate alternative alkenes. Elliott and Wigglesworth have demonstrated a range of acrylate derivatives undergoing 2,2 di-functionalisation via an aza-Wacker reaction [5], using *N*-tosylethanolamine derivatives as the nucleophile. During this study, urea nucleophiles were demonstrated to form enamides under facile conditions in excellent yields (Scheme 2.9).



Scheme 2.8 Pd(MeCN)₂Cl₂/BQ aminocarbonylation conditions



Scheme 2.9 Facile enamide formation with *n*butyl acrylate



Scheme 2.10 Pathway for the formation of pyrimidiones

Once again, this reaction proceeds via the key palladated intermediate prior to β -hydride elimination (Scheme 2.7). With the knowledge that this intermediate is formed efficiently, the reaction was repeated under an atmosphere of carbon monoxide. Only enamide was formed however, with CO seemingly having no effect (either detrimental or beneficial) to the efficiency or overall yield. β -Hydride elimination seems too facile in this particular case for the carbonylation to proceed. Alternative acrylate species were examined and discussed later (Sect. 2.2.2).

With no sign of CO incorporation in the initial screens, a simple lack of CO in solution may have been responsible. Performing the reactions at increased pressures therefore should negate this issue. Increased pressures may also aid in overcoming β -hydride elimination by forcing the CO ligand to migrate into the carbon-palladium bond.

Despite attempts at a variety of pressures (2, 5, 20 and 50 bar) and under different temperatures (rt, 50 °C and 70 °C) no products were detected with inactive palladium black appearing to form quickly.

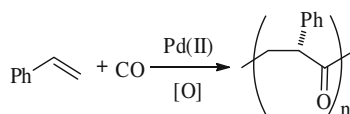
With little evidence of β -amino acid formation, it was hoped intramolecular attack from the second urea nitrogen on the desired acyl palladate would be more efficient. Pyrimidione formation was therefore investigated (Scheme 2.10).

2.2.2 Pyrimidione Formation

Initial screens were carried out using styrene and 1,3-diethylurea using the conditions described above. Both $\text{PdCl}_2/\text{CuCl}_2$ and $\text{Pd}(\text{MeCN})_2\text{Cl}_2/\text{BQ}$ systems were examined in the absence of methanol to effect the ring closure. A comprehensive solvent screen was also undertaken looking at a range of different properties. In particular, increased solubility of CO has been shown with fluorinated solvents [6] and within this series there is evidence trifluoroethanol [7] (TFE) can enhance the reactivity of many transition metal-based catalysis reactions. Due to these properties, dry and degassed TFE was used in the attempted cyclisation, once again this was to no avail. Alternative Pd(II) salts also proved ineffective as was a switch to 1,3-diethylurea.

All the main constituents are present for the much studied and industrially important copolymerisation of styrene (Scheme 2.11) [8]. Despite the apparent lack of polymer formation, the reaction was performed without the urea to ensure this was not a detrimental pathway.

Scheme 2.11 CO/vinyl polyketone synthesis



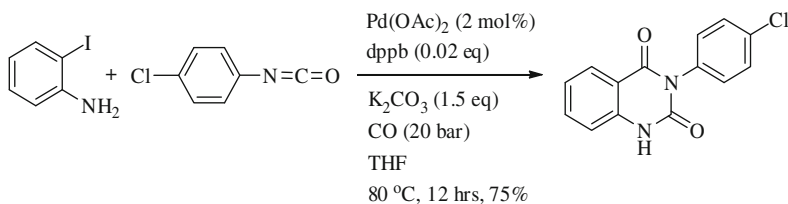
Only starting materials were isolated with an intact mass balance, so this potentially harmful pathway can be eliminated.

The fundamental problem of achieving carbonylative insertion still seemed to be impeding synthetic progress. Whether this was from lack of CO in solution or rapid β -hydride elimination was still unclear at this stage.

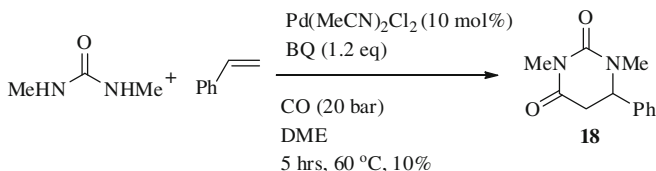
In efforts to resolve this situation, a reaction screen was performed under 20 bar of CO pressures. As mentioned previously, carbonylation occurs during a ligand migration process promoted by external ligands filling the vacant site left on the metal. With the added pressure there would be no uncertainty as to the CO being in solution and the insertion process itself would be given the best possible chance. If enamide **16** was still produced, the β -hydride elimination pathway would seem too efficient for the designed reaction to proceed. Precedent for this reaction with 20 bar of CO pressures came from the work by Alper [9], in which an in situ urea is produced from an *o*-iodoaniline and an isocyanate. Oxidative addition into the iodide bond followed by cyclocarbonylation completes the sequence (Scheme 2.12).

Operating under 20 bar of CO it was pleasing to observe (under standard conditions as described by Bar [18],) enamide formation no longer occurring and the desired pyrimidione was formed (Scheme 2.13).

Following on from this positive result it seemed the previous reactions at 1 atm suffered from a lack of CO in solution or decarbonylation rather than rapid β -hydride elimination. A further change in technique was adopted to determine whether the reaction could be facilitated at lower pressures. After charging the



Scheme 2.12 Palladium catalysed cyclocarbonylation of *o*-iodoanilines with heterocumulenes



Scheme 2.13 Successful pyrimidione formation

reaction with CO, the Schlenk tube was sealed but this time with the balloon (via a needle) inside the vessel, left fully open. It was hoped that this would provide enough positive pressure to enable the reaction to occur. Again the result was an encouraging one and with DME as the solvent, a 7 % yield of **18** was obtained.

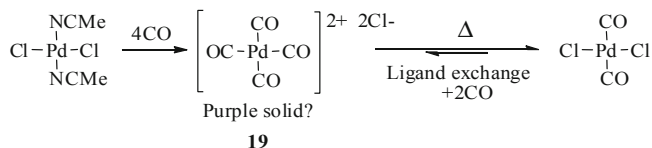
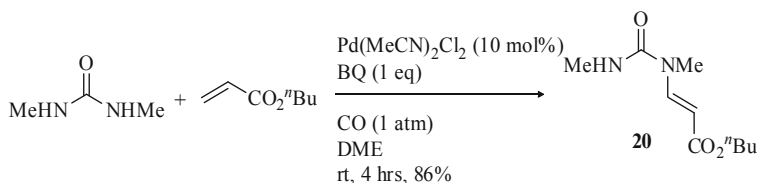
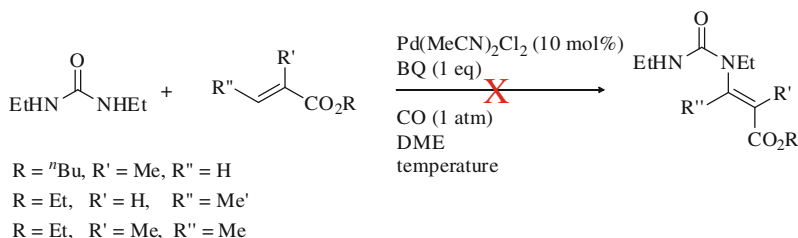
Having facilitated the reaction under milder conditions (using a balloon rather than 20 bar pressure) due to the technical advantages, experimental ease and wider possible applications, all subsequent attempts to increase the yield were performed using this method.

Reports by Stahl [47], have shown in similar Pd(II) catalysed systems, a first order dependence on the concentration of the alkene. Due to this, several experiments were carried out in order to ascertain if the yield could be improved. 0.6 M concentrations of styrene have been used up until this point; this was increased to 1.6 M and 3.3 M but with little effect.

A screen of catalysts was also performed in the hope that a change of electron density on the metal centre would increase the efficiency of the reaction. However $\text{Pd}(\text{MeCN})_2\text{Br}_2$, $\text{Pd}(\text{MeCN})_2\text{I}_2$, $\text{Pd}(\text{OAc})_2$ and $\text{Pd}(\text{TFA})_2$ were all ineffective.

During the process of charging the reaction mixture by bubbling CO into the solution, a purple precipitate was observed. Isolation and characterisation of this solid proved difficult, however it can be speculated to be a palladium complex, perhaps $[\text{Pd}(\text{CO})_4]^{2+}2\text{Cl}^-$ (**19**). This species is reportedly extremely unstable unless at low temperatures [11] matching the observation that the purple solid re-dissolved after gentle warming or continuous stirring. With rapid ligand exchange between the associate Cl^- counter ions it is easy to see how this process can occur (Scheme 2.14).

With the reaction appearing to be stoichiometric in palladium, investigations into the alkene source were undertaken. As mentioned in Sect. 2.2.2, styrene may not be the ideal reagent due to the modest reactivity shown in the formation of

**Scheme 2.14** Formation of a pre-catalyst?**Scheme 2.15** Enamide formation under a CO atmosphere**Scheme 2.16** Unsuccessful acrylate substrates

enamides via an aza-Wacker type reaction (Scheme 2.7). *n*Butyl acrylate was investigated in an effort to observe catalytic activity. Initial experiments with 1 atm of CO exclusively produced the enamide in an excellent yield (Scheme 2.15).

Surprised by the efficiency and rate of β -hydride elimination, the reaction was repeated at increased pressures of CO to try and overcome this. Disappointingly, enamide formation was still the predominant pathway up to pressures of 50 bar. Increased reaction temperatures and times, with or without the combination of pressure also failed to impede β -hydride elimination.

A switch to substituted acrylate species may retard enamide formation, changing conformations of intermediates and allowing time for carbonylative insertion. Of course substitution at the beta position would remove the hydrogens for the elimination step to occur. Combinations of acrylate derivatives were therefore screened (Scheme 2.16).

All substrates failed to yield either pyrimidione or even enamide under the conditions described. Removal of carbon monoxide from the system also produced the same result indicating change in substrate is responsible for the shutdown in reactivity. This is perhaps unsurprising as a lack of tolerance to substitution is a

well known limitation of many Pd(II) catalysed functionalisation of activated alkenes [1, 12]. Not only does the stability of an alkene-palladium complex decrease as alkene substitution increases but the approach of a nucleophile to the sterically crowded electrophilic centre can also be inhibited. Once again, increased temperatures and pressures of CO did not yield the title pyrimidione.

With extensive investigations proving unsuccessful, a change in direction towards the *ortho*-carbonylation of aryl ureas was initiated.

References

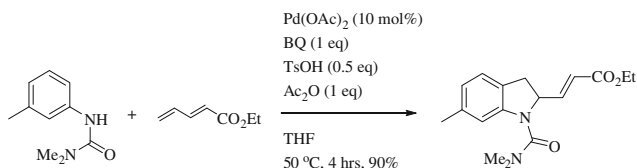
1. Tamaru Y, Hojo M, Higashimura H, Yoshida ZJ (1988) *Am Chem Soc* 110:3994–4002
2. Harayama H, Abe A, Sakado T, Kimura M, Fugami K, Tanaka S, Tamaru YJ (1997) *Org Chem* 62:2113–2122
3. Elliott L (2010) Unpublished Results
4. Bar GLJ, Lloyd-Jones GC, Booker-Milburn KIJ (2005) *Am Chem Soc* 127:7308–7309
5. Elliott LD, Wrigglesworth JW, Cox B, Lloyd-Jones GC, Booker-Milburn KI (2010) *Org Lett* 13:728–731
6. Deschamps J, Menz DH, Padia AAH, Costa-Gomes MFJ (2007) *Chem Thermodyn* 39: 847–854
7. Scarel A, Durand J, Franchi D, Zangrando E, Mestroni G, Milani B, Gladiali S, Carfagna C, Binotti B, Bronco S, Gragnoli TJ (2005) *Organomet Chem* 690:2106–2120
8. Coates GW, Hustad PD, Reinartz S (2002) *Angew Chem Int Ed* 41:2236–2257
9. Larksarp C, Alper HJ (2000) *Org Chem* 65:2773–2777
10. Kotov V, Scarborough CC, Stahl SS (2007) *Inorg Chem* 46:1910–1923
11. Shriver DF, Atkins PW, Langford CH (1992) *Inorganic chemistry*. Oxford Press, Langford
12. Hartley FR (1973) *The chemistry of platinum and palladium*. Wiley, New York

Chapter 3

Carbonylation of Aryl Ureas

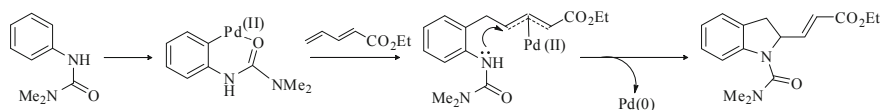
3.1 Background

In 2008 Booker-Milburn and Lloyd-Jones reported an intermolecular Pd(II)-catalysed 1,2-carboamidation of dienes (Scheme 3.1) [1].



Scheme 3.1 Intermolecular Pd(II)-catalysed 1,2-carboamidation of dienes

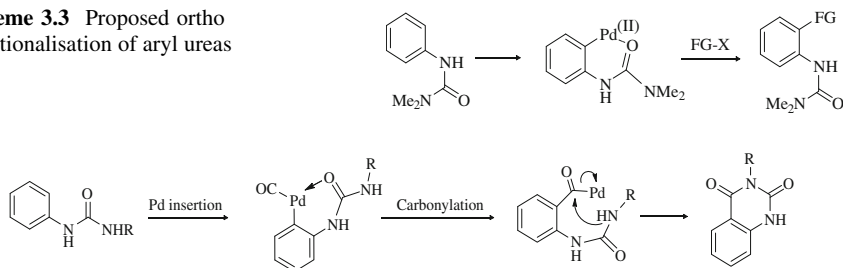
During this study Pd(OTs)₂(MeCN)₂ was found to be an efficient pre-catalyst. It could be used directly in the reaction with no appreciable decrease in yield. The reaction proceeded via an interrupted Heck-type process that evolves from a urea directed *ortho* C–H insertion by Pd(II). Carbopalladation followed by attack of the resultant palladate by the free urea nitrogen furnishes the indoline (Scheme 3.2).



Scheme 3.2 Suggested mechanism for indoline formation

It was proposed alternate functionality could be inserted into this activated *ortho* position via the intermediacy of the Ar–Pd bond (Scheme 3.3).

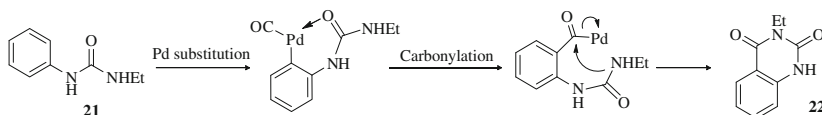
Insertion of CO could allow easy access into a variety of anthranilate derivatives. Mono-substitution at the alkyl urea nitrogen would hopefully allow cyclisation in situ to form quinazolinones (Scheme 3.4).

Scheme 3.3 Proposed *ortho* functionalisation of aryl ureas**Scheme 3.4** Carbonylative insertion followed by intramolecular cyclisation

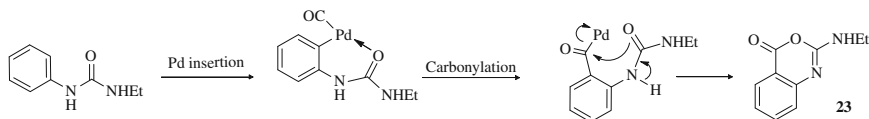
3.2 Results and Discussion

3.2.1 Stoichiometric Reactions

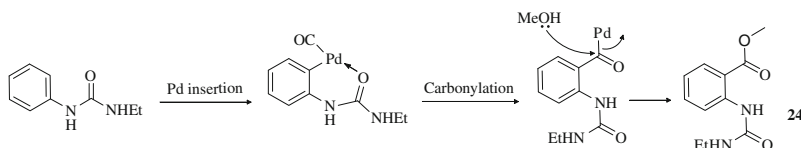
An initial reaction between 1-ethyl-3-phenylurea and 1 equivalent of $\text{Pd}(\text{OTf})_2$ (MeCN)₂ under 1 atm of CO in THF yielded a new species by tlc. The reaction immediately precipitated palladium black and was assumed to be complete. The product was expected to be quinazolinone **22** (Scheme 3.5).

**Scheme 3.5** Attempted quinazolinone synthesis

While mass spectrometry gave the correct mass for **22**, ¹H NMR did not match the literature values. After some investigation, cyclic imidate **23** was found to be the product formed (Scheme 3.6).

**Scheme 3.6** Cyclisation through the urea oxygen to produce cyclic imidates

Performing the above reaction in methanol instead of THF gave the corresponding *ortho* methyl ester (**24**) in a 60 % yield (Scheme 3.7).

**Scheme 3.7** Anthranilate ester formation

3.2.2 Catalytic Reactions: Ortho-Esterification

Despite the lack of quinazolinone formation, an optimisation study was undertaken to render the *ortho* esterification reaction catalytic.

Starting with 10 mol % of $\text{Pd}(\text{OTs})_2(\text{MeCN})_2$ in neat methanol, 1 equivalent of benzoquinone (as a reoxidant) was added to 1 equivalent of 1,1-dimethyl-3-phenylurea. The reaction was heated to 50 °C and put under an atmosphere of CO. The reaction was followed via tlc and upon consumption of BQ (2 h) the reaction was stopped. A 30 % yield of the anthranilate ester was obtained from this initial experiment. Showing promise, the following areas were investigated:

Water. Houlden has shown that trace amounts of water had a detrimental effect on the palladium tosylate pre-catalyst [1]. Following similar precautions (pre-drying the reaction mixture with Ac_2O /molecular sieves), yields remained unaffected. Bailey has shown that water is a good ligand for $\text{Pd}(\text{OTs})_2(\text{MeCN})_2$, [2] but CO should be a better ligand, perhaps preventing the water from ligating and causing catalyst poisoning.

Temperature. During stoichiometric studies (Sect. 3.2.1) the product was observed instantly and at room temperature. It was therefore pleasing to see the catalytic system succeed at these ambient conditions with little detriment to yield.

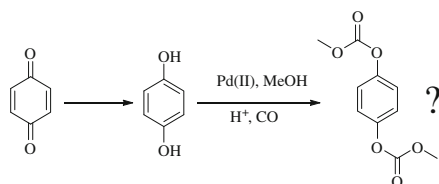
Ligands. Re-generation of the catalyst was initially problematic with only two or three turnovers per reaction. It was found that added tosylate ligands were required to keep the catalyst active and this was achieved with the addition of 0.5 equivalents of *p*-toluenesulfonic acid.

Re-oxidant. Complete consumption of BQ was observed after 2–3 h but yields remained between 40–50 %. An unidentified resinous material contaminated all reactions and this was proposed to be a polymeric by-product. Pd(II)/CO has been used in the manufacture of polymers from diols [3] and this unknown impurity could be a polycarbonate oligomer, formed from hydroquinone repeating units and methanol termini (Scheme 3.8).

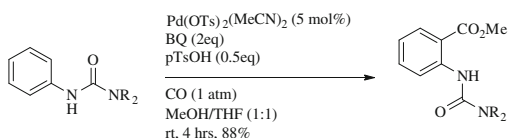
Mass spectrometry proved inconclusive while NMR experiments suggested a symmetrical molecule with a ratio of 4 aromatic protons to 3 alkyl protons. If palladium turnovers were expended in the formation of this by-product, more BQ could allow for an increased yield. Using 3 equivalents gave an improved 61 % of the target ester while five equivalents of BQ gave a yield of 81 %.

Solvent. Whilst five equivalents of BQ gave a good yield, this amount is synthetically undesirable. It was hoped reducing the concentration of methanol would lower the rate of by-product formation. Dilution with a co-solvent was found to improve yields and allowed for the reduction in levels of BQ (2 eq). Various ratios were trialled, with 1:1 methanol:co-solvent proving optimum. A wide range of solvents were tolerated, including THF, Et_2O , NMP, DMF, 1,4-Dioxane, EtOAc and Toluene. No reaction was observed with DMSO, most likely due to its coordinating ability. THF was selected for its availability and cost.

Scheme 3.8 Suggested formation of polymeric impurity



Scheme 3.9 Optimised conditions



Pressure. After optimising the reaction for 1 atmosphere of CO, different pressures were investigated. Both 3 bar and five bar of CO pressure gained little in yield. 1 atm presents the fewest technical issues so was used as standard.

Catalyst loading. After careful optimisation of the above factors, 10 mol % of Pd(OTs)₂(MeCN)₂ gave a 97 % yield of the *ortho*-ester (starting from 1,1-dimethyl-3-phenyl urea). Reduction of the catalyst loading to 5 mol % was only slightly detrimental to the yield (88 %). This was deemed an acceptably penalty for using half of the amount of catalyst and was therefore made standard (Scheme 3.9).

The above conditions were applied to a variety of aniline derivatives initially with substitution around the alkyl nitrogen (Table 3.1).

It can be seen that increased steric bulk gives an improved yield when the nitrogen is mono-substituted. This perhaps indicates a positive electron donating effect from the additional alkyl groups that in-turn increases electron density on the urea oxygen, allowing it to become a more efficient Lewis base for the vacant d-orbital on the metal. Conversely, yields decrease with additional steric bulk for the bis-substituted aryl nitrogen examples. This is perhaps simply accounting for an increase in difficulty for the approach of the incoming metal.

Substitution around the aromatic ring is also tolerated with some notable exceptions (Table 3.2).

Ureas substituted with strongly electron withdrawing groups are poorly tolerated under these conditions. *para*-CF₃ requires heating to 50 °C to give a modest yield of 30 % while *ortho*- and *meta*-CF₃ fail to react at all. *para*-NO₂ also fails to react at 50 °C. *ortho*-Vinyl substitution gave a complex mixture of side products, although this is perhaps unsurprising with the presence of Pd(II), CO and a strong acid. *para*-Nitrile was also unsuccessful, maybe due to its ability to coordinate to the metal centre (entry 14).

Interestingly naphthyl derivative (entry 15) failed to esterify, producing instead the equivalent cyclic imidate. Reasons for this lack of reactivity with methanol may be due to the strong aromatic stability of the imidate.

Table 3.1 Room temperature Pd(II) catalysed methoxycarbonylation

Entry	Urea	R	R'	Product	Yield (%)
1	25	Me	Me	34	88
2	26	Et	Et	35	76 ^a
3	27	<i>i</i> Pr	<i>i</i> Pr	36	55
4	28	Morpholine		37	75 ^a
5	29	Me	H	38	61
6	21	Et	H	24	81
7	31	<i>i</i> Pr	H	40	90 ^a
8	32	<i>t</i> Bu	H	41	88 ^a
9	33	Bn	H	42	85

^a Reaction conducted by Houlden**Table 3.2** Functionalisation of the aromatic ring

Entry	Urea	R	Product	Yield (%)
1	43	<i>o</i> -Me	58	88 ^b
2	44	<i>m</i> -Me	59	84
3	45	<i>p</i> -Me	60	78 ^b
4	46	<i>o</i> -MeO	61	15 (40) ^a
5	47	<i>m</i> -MeO	62	26 (40) ^a
6	48	<i>p</i> -MeO	63	31 (80) ^{a,b}
7	49	<i>p</i> -CF ₃	64	5 (30) ^a
8	50	<i>m</i> -Br	65	70 ^b
9	51	<i>p</i> -Br	66	40
10	52	<i>o,p</i> -Me	67	56 ^b
11	53	<i>p</i> -CO ₂ Me	68	36 (46) ^a
12	54	<i>p</i> -NO ₂	N/A	0
13	55	<i>p</i> -Vinyl	N/A	0
14	56	<i>p</i> -CN	N/A	0
15	57	2-naphthyl	N/A	0 ^{b,c}

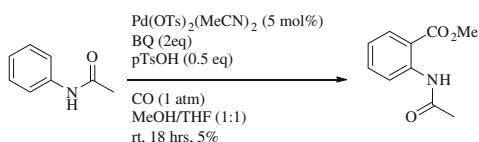
^a Reaction conducted at 50 °C^b Reaction conducted by Houlden^c Only cyclic imidate formed (Sect. 3.2.3)

Electron donating groups (i.e. methyl) returned excellent yields although the methoxy groups benefited from gentle heating (entries 4, 5 and 6). This may suggest the inductive effect of the electronegative oxygen playing a more important role than a mesomeric effect from the lone pair of electrons.

It was pleasing to see both bromo functionalised ureas giving moderate to good yields (entries 8 and 9). This allows for further functionalisation with classic Pd(0) chemistry.

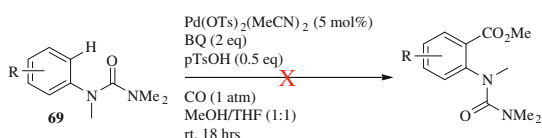
The powerful directing effect of ureas with this pre-catalyst was further highlighted by the poor yield when examining the reaction with acetanilide (Scheme 3.10).

Scheme 3.10 Failed reaction of acetanilide



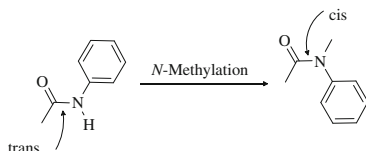
Methyl phenylcarbamate also failed to react as did substitution on the aryl urea nitrogen (also reported by de Vries) [4] (Scheme 3.11).

Scheme 3.11 Failed reaction of tetra-substituted ureas



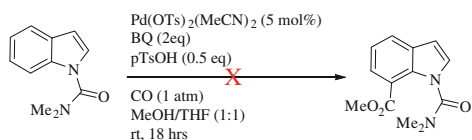
Yamasaki et. al. recently reported the conformational switching of phenyl acetamides [5]. The preferred *cis*-conformation of *N*-methylated phenyl acetamides, twists the directing carbonyl group away from the phenyl ring. If the same model applies to the analogous aryl ureas, this *cis*-conformation formed upon *N*-methylation does not allow the carbonyl oxygen to ‘trap’ the palladium (II) species in the *ortho* position (Scheme 3.12).

Scheme 3.12 *cis*-Conformational preference of *N*-methylated anilides



To probe this effect, indole was derivatised with dimethylcarbamoyl chloride and subjected to the carbonylation conditions. With the carbonyl group held in position, unable to twist away from the C–H bond, a positive result would support conformational reasoning. Disappointingly the substrate did not furnish the desired ester, suggesting a more subtle effect (Scheme 3.13).

Scheme 3.13 Failed indole substrate



Alternatively, substitution of the aryl nitrogen may disrupt the conformation of the urea, reducing the overlap between the nitrogen lone pair of electrons and the π -orbital of the carbonyl. This may have important implications, limiting the ability of the oxygen to coordinate with the metal. As this nitrogen also overlaps with the π -system of the phenyl ring, the whole conjugated system may be interrupted.

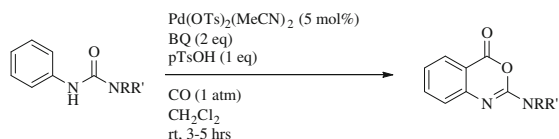
3.2.3 Cyclic Imidate Formation

Having developed a useful synthesis for the formation of anthranilate ester derivatives, attention now was focused on rendering cyclic imidate formation catalytic (Scheme 3.6).

Fortunately, optimal conditions did not vary greatly from those already developed. CH_2Cl_2 was found to be the most favourable solvent and the amount of required tosylate ligand increased to 1 equivalent (Scheme 3.14).

The cyclic imidates seemed sensitive to the reaction conditions as prolonged

Scheme 3.14 Optimised conditions for cyclic imidate formation



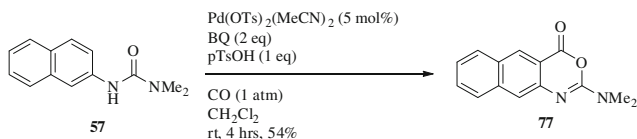
reaction times resulted in a reduction in yield. Isolation of the title products initially proved difficult with purification via column chromatography unsuccessful. Washing the reaction mixture with 1 M NaOH (aq) was found to be essential to release the protonated product at the end of the reaction. Table 3.3 details the successful substrates obtained from this study:

Table 3.3 Room temperature palladium (II) catalysed cyclic imidate formation

Entry	Urea	R	R'	Product	Yield (%)
1	25	Me	Me	70	67 ^a
2	26	Et	Et	71	50
3	27	<i>i</i> Pr	<i>i</i> Pr	72	40 ^a
4	28	Morpholine		73	49 ^a
5	29	Me	H	74	34
6	21	Et	H	23	40
7	31	<i>i</i> Pr	H	75	66 ^a
8	32	<i>t</i> Bu	H	76	85

^a Reaction conducted by Houlden

As discussed in Table 3.2, Entry 15, the naphthyl derivative failed to esterify, leading only to the cyclic imidate in a 54 % yield. This tri-cyclic system may have enhanced aromatic stability proving resistant to subsequent alcoholysis (Scheme 3.15).

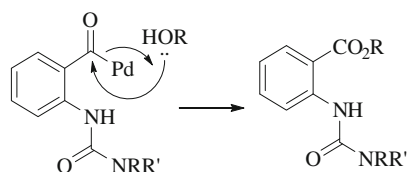


Scheme 3.15 Cyclic imidate formation from naphthyl derived urea **57**

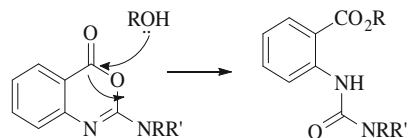
3.2.4 Mechanism of Action

When performing the reaction in methanol (Scheme 3.9), the transient formation of cyclic imidates was occasionally observed by tlc. This led to the question of whether ester formation proceeds via direct solvolysis of an acyl palladate (Scheme 3.16) or by a postcatalytic methanolysis of the imidate (Scheme 3.17).

Scheme 3.16 Solvolysis of an acyl palladate

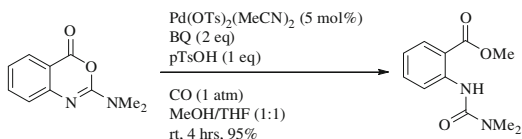


Scheme 3.17 Postcatalytic methanolysis of a cyclic imidate



A control experiment (Scheme 3.18) showed how labile cyclic imidates are to methanolysis under the carbonylation conditions. It is therefore suggested the reactions proceeds by a C–H insertion, carbonylation, cyclisation, and solvolytic ring-opening sequence.

Scheme 3.18 Ring opening of a cyclic imidate by methanol

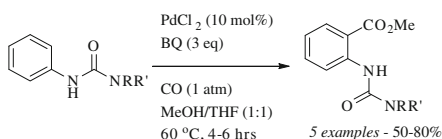


3.2.5 Alternative Conditions

Through the process of optimisation, various catalysts were explored. PdCl₂ was also found to be a successful catalyst, facilitating palladium insertion into the *ortho*-C–H bond, directed by the urea moiety. Initially this was stoichiometric in terms of palladium and efforts were directed to make this reaction catalytic.

After following similar optimisation efforts as before, an alternate synthesis for the formation of the anthranilate ester derivatives was developed (Scheme 3.19).

Scheme 3.19 Alternate ester synthesis utilising PdCl₂



The powerful nature of the Pd(OTs)₂(MeCN)₂ pre-catalyst is highlighted when comparing the two systems. The reaction utilising PdCl₂ does not proceed at room temperature and requires an additional equivalent of benzoquinone. Further to that, twice as much palladium is required and the yields are significantly lower (Table 3.4).

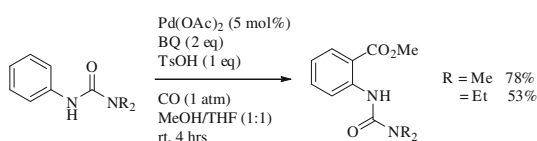
Table 3.4 PdCl₂ vs. Pd(OTs)₂(MeCN)₂ in the formation of anthranilate esters

Entry	Urea	R	R'	Product	PdCl ₂ (%) ^a	Pd(OTs) ₂ (MeCN) ₂ (%) ^b
1	25	Me	Me	34	60	88
2	29	Me	H	38	50	61
3	21	Et	H	24	69	81
4	31	<i>i</i> Pr	H	40	60	90
5	32	<i>t</i> Bu	H	41	80	88

^a PdCl₂ (10 mol %), BQ (3 eq), 60 °C; ^b Pd(OTs)₂(MeCN)₂ (5 mol %), BQ (2 eq), TsOH (0.5 eq), rt

Houlden and Bailey demonstrated the ability to form palladium tosylate in situ from Pd(OAc)₂ and *p*-TsOH.⁸³ This system was trialed, replacing Pd(OTs)₂(MeCN)₂ with Pd(OAc)₂, while keeping all other aspects the same. The results showed promise, however yields were generally lower compared to using the pre-made tosylate catalyst (Scheme 3.20).

Scheme 3.20 In-situ formation of palladium (II) tosylate

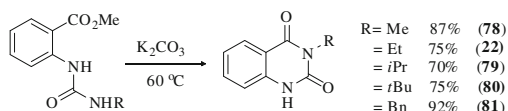


3.2.6 Quinazolinone Formation

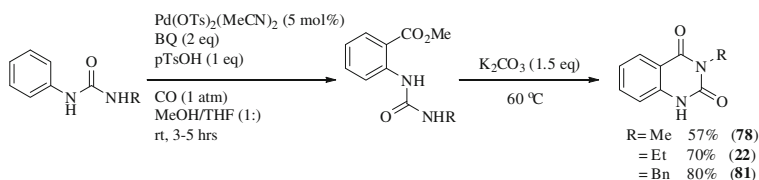
The synthetic utility of the urea anthranilates was further demonstrated by their cyclisation to form quinazolinones, a key pharmacophore in numerous drug compounds [6].

A short screen was first undertaken in order to determine the most appropriate base to ring cyclise, with both K_2CO_3 and $NaOtBu$ proving successful. The addition of K_2CO_3 to a sample of pure anthranilate ester (mono-substituted on the alkyl nitrogen), followed by heating ($60\text{ }^\circ\text{C}$) furnished the cyclised product in good yields (Scheme 3.21).

Scheme 3.21 Base induced cyclisation



Further development led to in situ addition of base, allowing quinazolinone formation in one-pot from the starting aryl urea (Scheme 3.22). After the full consumption of BQ is observed by tlc in the initial carbonylation reaction, 1.5 eq of K_2CO_3 is added, the reaction re-sealed and heated to $60\text{ }^\circ\text{C}$. Not all substrates were successful via this in situ method.



Scheme 3.22 One-pot formation of quinazolinones

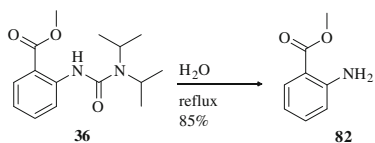
3.2.7 Urea Removal

Anthranilic acid (vitamin L) is a valuable amino acid and a precursor to tryptophan. It is used as an intermediate for the production of dyes and pigments. Ester derivatives are used in the production of perfumes (imitate jasmine and orange) and pharmaceuticals. Removal of the urea directing group, post esterification would allow direct access into these valuable compounds.

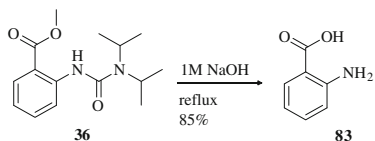
Although ureas are often thought of as inert to hydrolysis, often requiring high temperatures, acidic/basic [7, 8] conditions or metal catalysis [9–12] to remove/interconvert them, previous work within the group had observed 1,1-diisopropyl-3-phenylurea derivatives undergoing facile solvolysis in methanol under neutral conditions [13]. It was hoped that anthranilate ester **36** would be susceptible to a

similar process. Remarkably it was found that simply heating **36** in water gave methyl anthranilate **82** in an 85 % yield with no ester hydrolysis (Scheme 3.23).

Scheme 3.23 Unexpected, selective urea hydrolysis



Scheme 3.24 Anthranilic acid formation



Replacing water with 1 M NaOH (aq), hydrolysed the methyl ester as well as the urea, giving anthranilic acid (**83**) in an excellent yield (Scheme 3.24) [14].

References

- Houlden CE, Bailey CD, Ford JG, Gagné MR, Lloyd-Jones GC, Booker-Milburn KI (2008) *J Am Chem Soc* 130:10066–10067
- Bailey CD (2009) UoB, PhD Third Year Report
- Okamoto M, Sugiyama T, Yamamoto T (2008) *J Appl Polym Sci* 10:3902–3907
- Boele MDK, van Strijdonck GPF, de Vries AHM, Kamer PCJ, de Vries JG, van Leeuwen PWNM (2002) *J Am Chem Soc* 124:1586–1587
- Yamasaki R, Tanatani A, Azumaya I, Saito S, Yamaguchi K, Kagechika H (2003) *Org Lett* 5:1265–1267
- Larkarp C, Alper H (2000) *J Org Chem* 65:2773–2777
- Osborn HMI, Williams NAO (2004) *Org Lett* 6:3111–3113
- Clayden J, Dufour J, Grainger DM, Helliwell MJ (2007) *Am Chem Soc* 129:7488–7489
- Blakeley RL, Treston A, Andrews RK, Zerner BJ (1982) *Am Chem Soc* 104:612–614
- Kaminskaia NV, Kostic NM (1997) *Inorg Chem* 36:5917–5926
- Kaminskaia NV, Kostic NM (1998) *Inorg Chem* 37:4302–4312
- Wang J, Li Q, Dong W, Kang M, Wang X, Peng S (2004) *Appl Catal A-Gen* 261:191–197
- Houlden CE (2006) Unpublished results
- Houlden CE, Hutchby M, Bailey CD, Ford JG, Tyler SNG, Gagné MR, Lloyd-Jones GC, Booker-Milburn KI (2009) *Angew Chem Int Ed* 48:1830–1833

Chapter 4

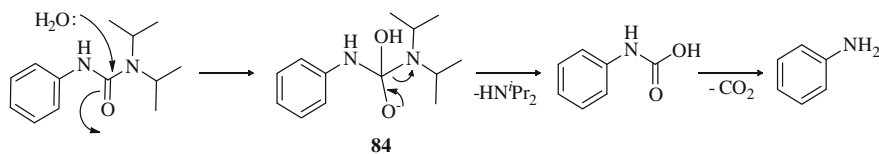
Urea Hydrolysis

4.1 Background

Following on from the remarkable hydrolysis of diisopropyl substituted aryl ureas, a thorough investigation was undertaken to understand this reactivity.

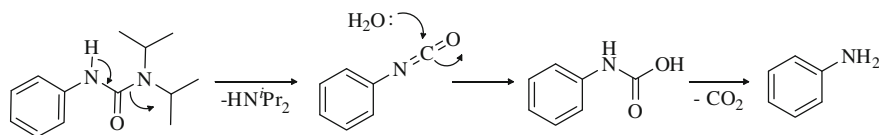
With dimethyl and diethyl analogues failing to show any sign of hydrolysis, the most obvious difference is the increased steric bulk afforded by the isopropyl groups.

Two reaction pathways are viable for this unprecedented hydrolysis. The first, nucleophilic attack at the carbonyl centre results in an unstable tetrahedral intermediate **84**, which subsequently breaks down expelling diisopropylamine (Scheme 4.1). This pathway seems to contradict the observed reactivity in which an increased steric bulk is necessary for the reaction to precede.



Scheme 4.1 Nucleophilic attack and subsequent breakdown of the tetrahedral intermediate

Capasso [1] and Clayden [2] both report hydrolysis of ureas to proceed through an isocyanate intermediate. Perhaps the increased steric compression around the carbonyl group facilitates isocyanate formation through the extrusion of the free amine (Scheme 4.2).



Scheme 4.2 Isocyanate formation and subsequent decarboxylation

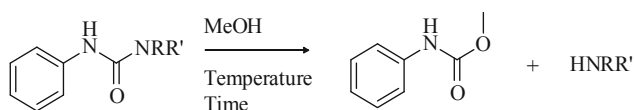
4.2 Results and Discussion

4.2.1 Mechanism

In order to ascertain which of these two models most accurately describes this unusual reactivity, a series of mechanistic studies was undertaken.

4.2.1.1 Structural Features

Initially, substrate control was investigated, determining the essential components required for a successful transformation. This was done by studying alcoholysis by methanol (Scheme 4.3); growth of the resultant methyl carbamate could easily be followed by ^1H NMR.



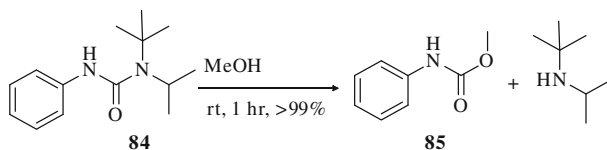
Scheme 4.3 Carbamate formation via methanolysis of aryl ureas

Whilst dimethyl and diethyl analogues failed to react under identical conditions, increasing the steric bulk to a *tert*-butyl-*iso*-propyl group (**84**) facilitated the transformation rapidly and in a quantitative yield. Further to this, **84** reacted quickly at room temperature (<1 h) to produce methyl phenyl carbamate (MPC) (**85**) in a > 99 % yield (Scheme 4.4).

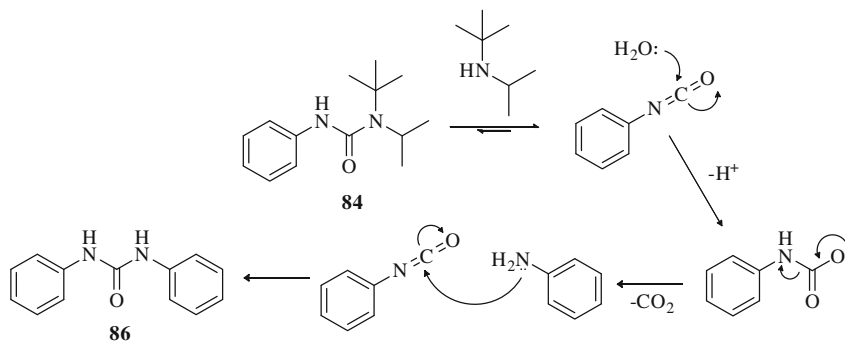
This extreme reactivity is also apparent when synthesising **84** from phenylisocyanate and *tert*-butyl-*iso*-propylamine. Despite numerous attempts, including slow addition, low temperatures ($-78\text{ }^\circ\text{C}$) and alternate orders of addition, urea formation was unusually complicated, forming many by-products. The compound can be purified by column chromatography, but as previously stated, quickly degrades in the solid state after a few days, leaving 1,3-diphenylurea (**86**) and a strong amine smell. Any water present in the atmosphere can act as a nucleophile, attacking phenylisocyanate. Decarboxylation forms aniline which subsequently attacks another phenylisocyanate molecule (Scheme 4.5).

An alternate urea was therefore sought after that could be synthetically useful, perhaps as a C–H directing group, but also would be susceptible to hydrolysis under mild/neutral conditions. 1,1-diisopropyl-3-phenylurea (**27**) was deemed too slow at elevated temperatures (81 % after 18 h at $70\text{ }^\circ\text{C}$) but **84** (for the above reasons) was too reactive/unstable. A urea presenting reactivity somewhere in the middle of these examples would provide an ideal platform to build upon.

As *mono*-substituted (on the alkyl urea nitrogen) examples were not susceptible to solvolysis, it was thought essential to have *bis*-substitution to provide the steric



Scheme 4.4 Rapid and quantitative methanolysis at room temperature



Scheme 4.5 Extreme reactivity of aryl urea derivative **26**

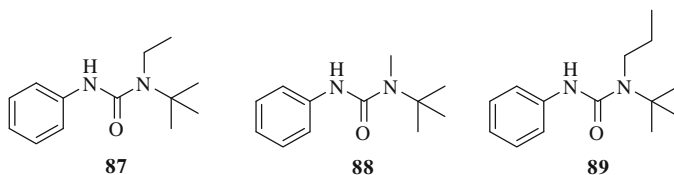
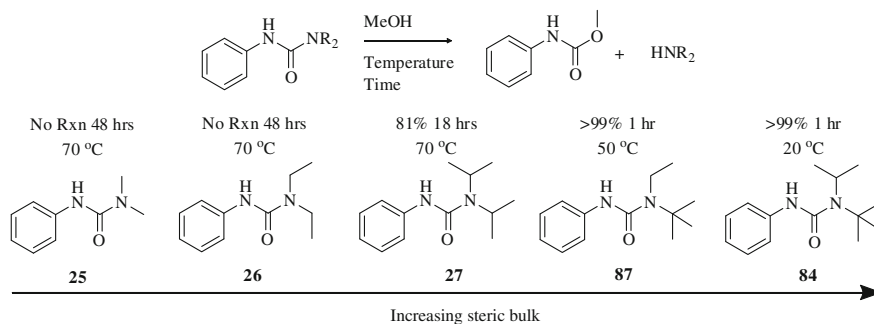


Fig. 4.1 Alternative hindered ureas

compression required around the urea carbonyl. Urea **87** was chosen as a target. It does not appear to be as sterically demanding as **84** but was hoped to be more bulky than **27**. As *tert*-butyl-ethylamine is not commercially available¹ it was made *in situ* from the reductive amination of *tert*-butylamine and acetaldehyde with NaCNBH₃ [4]. Addition of phenylisocyanate to the reaction furnished the urea. In parallel to this synthesis, ureas **88** and **89** were also prepared (Fig. 4.1).

When subjecting the above ureas to the standard hydrolysis conditions (methanol at 70 °C) it was pleasing to see all three rapidly formed MPC in a quantitative yield. Fearing reactivity akin to **84**, the reactions were repeated at room temperature. Carbamate formation this time was slower, taking 18 h to go to completion.

¹ The free amine can be synthesised and isolated following the procedure by Schmitt [3].



Scheme 4.6 Unusual reactivity trend in the methanolysis of tri-substituted ureas

Reactions performed at 50 °C were complete after 1 h. A full reactivity profile around the non-aryl nitrogen is shown in Scheme 4.6.

The increasing steric bulk from dimethyl < diethyl < diisopropyl < *tert*-butyl-*iso*-propyl under nucleophilic conditions should lead to a decrease in activity. Increasing steric crowding around the carbonyl centre should reduce the ability of the nucleophile to reach the site of attack. Rate of decomposition of the aryl urea to phenylisocyanate however, may be increased by increasing steric bulk. The leaving group ability of the amine is enhanced by the steric compression afforded by the alkyl groups. The larger the repulsions, the greater the steric compression and the greater the rate of isocyanate formation (Fig. 4.2).

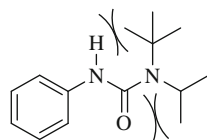
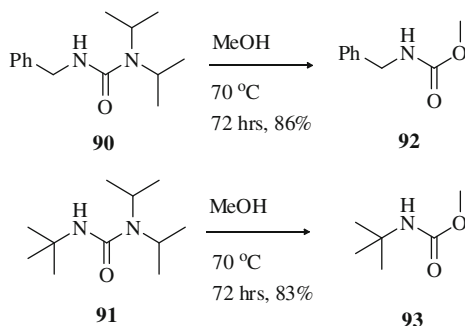
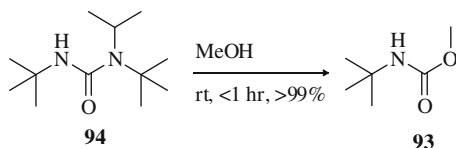
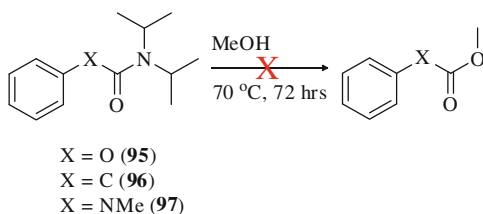
Expanding substrate scope further, alternatives to the phenyl group were investigated to determine whether this functionality is essential for reactivity. Ureas **90** and **91** were therefore synthesised from diisopropylamine and their respective isocyanates (commercially available).

Reacting in methanol at 70 °C, both gave encouraging results. After 72 h, the ureas had shown similar propensity towards methanolysis (Scheme 4.7).

Encouraged by these results, efforts were made to increase the rate of reaction. It was thought that the introduction of a bulkier alkyl group would have a similar rate increasing effect as it did for the parent phenyl system (i.e. going from diisopropyl to *tert*-butyl-*iso*-propyl).

Urea **94** was therefore synthesised and subjected to identical reaction conditions (as above) and was quantitatively converted to the methyl carbamate product within 5 min. Repeating at room temperature provided the same result after 1 h. (Scheme 4.8). This once again shows the exceptional reactivity imparted by the *tert*-butyl-*iso*-propyl moiety.

In order to probe the mechanistic differences between nucleophilic attack and isocyanate formation, a range of analogues were synthesised, all **without** the ability to form an isocyanate (**95**, **96**, **97**). Subjecting these derivatives to methanolysis at 70 °C did indeed result in a shutdown in reactivity (Scheme 4.9). As nucleophilic attack should not have been impeded with the change from nitrogen to oxygen, the pathway via an isocyanate seemed more likely.

Fig. 4.2 Steric compression**Scheme 4.7** Reactivity away from aryl anilides**Scheme 4.8** Rapid and quantitative conversion of a tri-alkyl urea**Scheme 4.9** Shutdown of reactivity by alteration of substrate

4.2.1.2 Physical Features

An examination of the physical properties was undertaken to identify any unusual characteristics which could explain this remarkable reactivity.

The IR carbonyl stretch may be significantly different between those ureas exhibiting mild solvolysis against those which do not. More double bond character (i.e. a higher wavenumber) may be expected for those that are reactive. The ease at which the C–N bond is broken may suggest a poor overlap of the nitrogen lone pair, possibly from a twisting effect due to the increase in steric bulk around the nitrogen. The carbonyl group for 1,1-dimethyl-3-phenylurea is observed at 1641 cm^{-1} whereas the stretch for 1,1-diisopropyl-3-phenylurea is at 1635 cm^{-1} . This stretch is well within the expected urea carbonyl region and is not significantly different from those that are inert to mild solvolysis.

An increase in reactivity may also relate to an increase in C–N bond length. Examination of the crystal structures shows an insignificant difference between dimethyl and diisopropyl urea derivatives (see Appendix) [5].

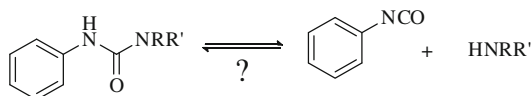
The ^{13}C NMR shift for the carbonyl groups of the **25** versus **84** was also examined. A downfield shift would indicate more of a positive charge on carbon and therefore more susceptibility to nucleophilic attack. Once again, there was no significant difference between the two (**25** = 155.8, **84** = 154.5).

4.2.1.3 Mechanistic Features

Phenylisocyanate is used to make the aryl ureas shown and its reaction with the appropriate amine is rapid at room temperature. It seemed therefore improbable to detect isocyanate formation via NMR studies during the reaction. This was found to be true with various high temperature (70 °C) NMR experiments yielding no further information.

It seemed probable that any forward competition reactions would be ineffective due to the rapid and strong dynamic equilibrium (Scheme 4.10). If the phenyl alkyl urea is in a rapid equilibrium with phenylisocyanate (and the amine), introduction of a more reactive phenylisocyanate derivative should compete for the amine and a mixture of ureas will be seen (Scheme 4.11).

Scheme 4.10 Equilibrium between phenylisocyanate/diisopropylamine and phenyl diisopropyl urea

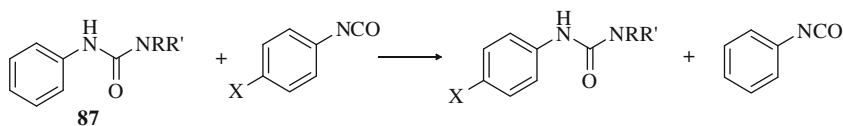


An NMR sample containing a solution of **87** (1 eq) and *para*-bromo phenylisocyanate (1 eq) in $[\text{D}_8]$ -toluene at 35 °C provided the key evidence for isocyanate formation. After 0.5 h, two sets of *t*butyl peaks were observed in the ^1H NMR spectrum. The new set was matched to 3-(4-bromophenyl)-1-(*tert*-butyl)-1-ethylurea (**98**) (which was independently synthesised from *para*-bromo phenylisocyanate and *tert*-butyl-ethylamine). The initial ratio (after 1 min) was 60:40 in favour of the *para*-bromo urea derivative. This was unchanged after 24 h of reaction time (Scheme 4.12).

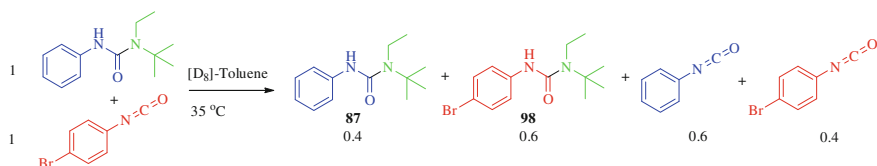
The formation of two species of urea provides clear evidence of isocyanate formation. As the parent urea is the only source of amine, there must be equilibrium between the two isocyanates.

Another specific result supporting the intermediacy of an isocyanate came from the reaction of **87** with a mixture of MeOH (1 M), EtOH (1 M) and *n*PrOH (1 M) in toluene at 35 °C. Within experimental error, the partitioning between carbamate products is identical to that generated by the reaction of a reference sample of phenyl isocyanate under the same conditions (Scheme 4.13).

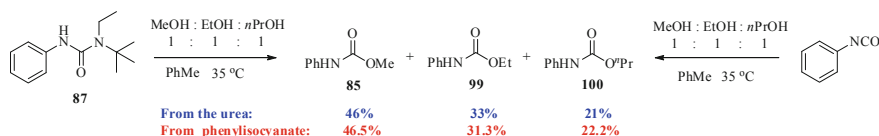
A control experiment confirmed there is no equilibrium under these conditions (Scheme 4.14).



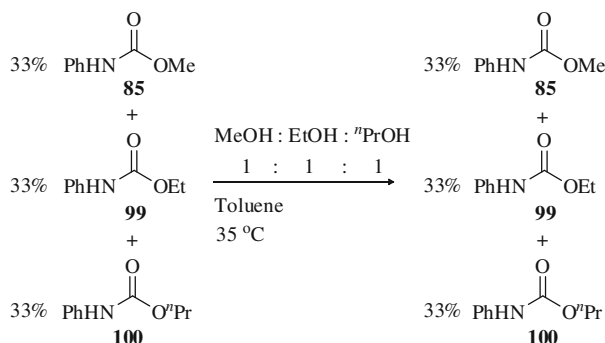
Scheme 4.11 Competition for alkylamine from alternate phenylisocyanates



Scheme 4.12 Crossover experiment proving the intermediacy of isocyanates



Scheme 4.13 Alcohol partitioning suggesting isocyanate intermediacy

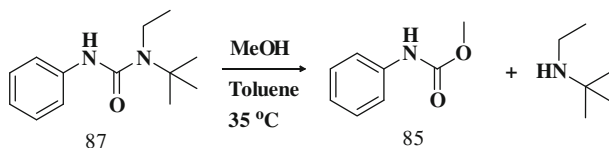


Scheme 4.14 No equilibrium between carbamates

The reaction was determined to be irreversible through subjection of MPC to the reaction conditions, and then under pseudo-first order conditions, a full kinetic profile for **87** at various concentrations of methanol was elucidated (Scheme 4.15).

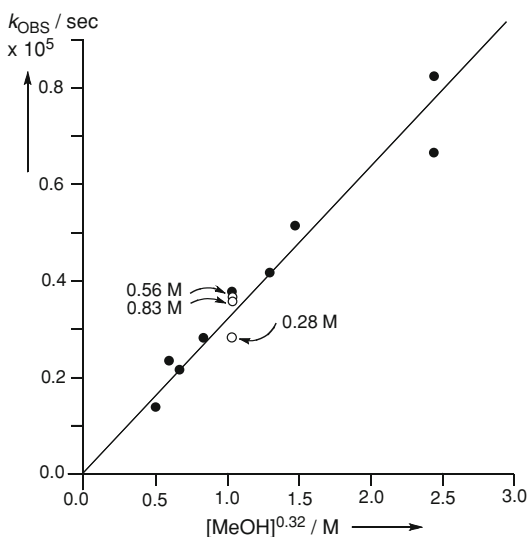
Plotting rate constants against $[\text{MeOH}]$, including those with added amine show a fractional dependence on $[\text{MeOH}]$, $-d[29]/dt = 3.2 \times 10^{-5}[29][\text{MeOH}]^{0.32}$ (Fig. 4.3). This fraction of 1/3 simply reflects the tendency of methanol to form trimers in hydrocarbon solvents such as toluene [6, 7].

The open circles show increased amounts of added *tert*-butyl-ethylamine and as described above, does not suppress the rate of reaction. This suggests amine attack



Scheme 4.15 Methanolysis of 29 in toluene

Fig. 4.3 Methanolysis of 1-*tert*-butyl, 1-ethyl, 3-phenyl urea in toluene at 35 °C



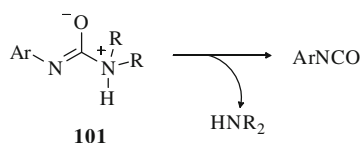
back onto phenylisocyanate is not rate limiting and it is the formation of the isocyanate that is.

4.2.1.4 Mechanistic Interpretation

With isocyanate formation established, a more detailed interpretation of the mechanism can be investigated.

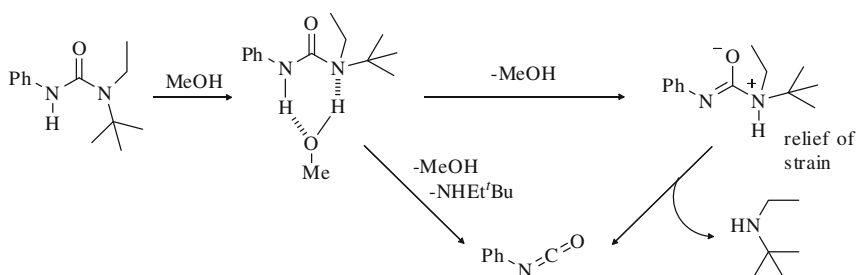
The hydrolysis mechanism of *N*-aryl ureas has been the subject of a number of detailed studies [1, 2, 8–12], with a general consensus that *N*-aryl isocyanates are generated as transient intermediates through the expulsion of HNR_2 from a zwitterionic species (**101**) (Scheme 4.16).

Scheme 4.16 Isocyanate liberation from a zwitterionic intermediate



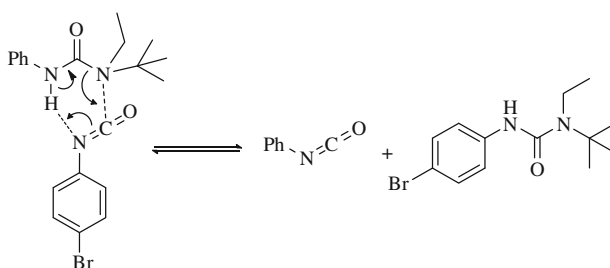
Pioneering work by O'Connor and co-workers led to the suggestion that water mediates a proton switch to generate this zwitterionic intermediate [13–15]. By simply adapting this proposal to the system presented here, we can envisage methanol mediating this proton switch, generating a highly strained zwitterion and it is the relief of the steric strain that drives the isocyanate formation (Scheme 4.17).

When examining the rate differences between the methanolysis as presented in Scheme 4.15 and the isocyanate/amine crossover experiment, there is a clear difference. Urea **87** takes several hours at room temperature to form MPC, whereas the equilibrium during the isocyanate competition is established within 1 min. The lack of an external proton switch during the amine crossover experiment also challenges the mechanistic interpretation presented in Scheme 4.17.



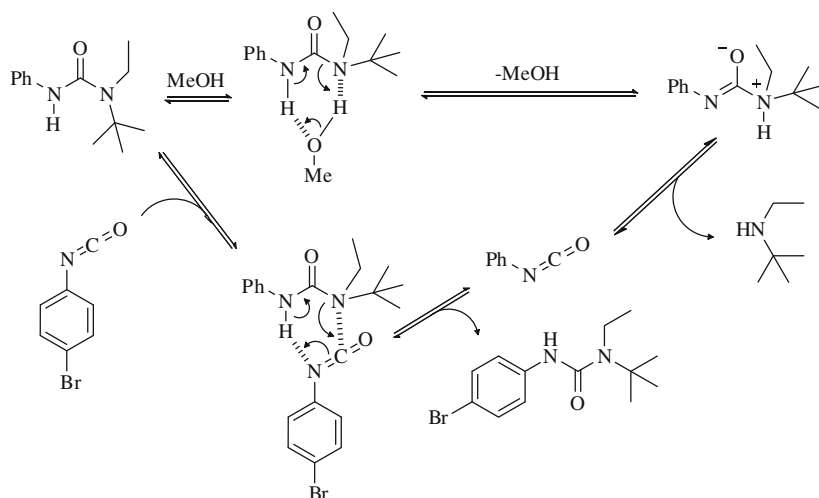
Scheme 4.17 Methanol mediated proton switch

An explanation for these differences may lie in the ability for an intra-molecular proton switch, generated from the interaction of urea and isocyanate (Scheme 4.18).



Scheme 4.18 Intra-molecular proton switch in the generation of alternate urea species

Combining both inter- and intra-molecular mechanisms leads to a complete picture of this unusual reactivity (Scheme 4.19).

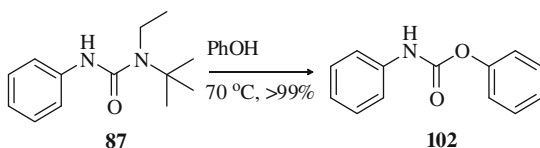


Scheme 4.19 Phenyl isocyanate liberation from inter- and intra-molecular proton transfer

4.2.2 Alternative Nucleophiles

To broaden the scope of this reaction, other nucleophiles were tested. Urea **87** was dissolved in a phenol melt (70 °C) which gratifyingly gave the desired phenolic carbamate **102** quantitatively after 1 h (Scheme 4.20).

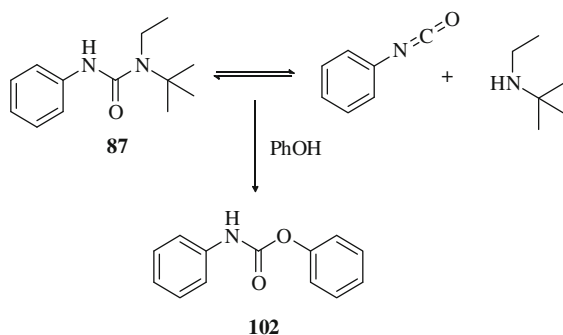
Scheme 4.20 Phenolic nucleophile



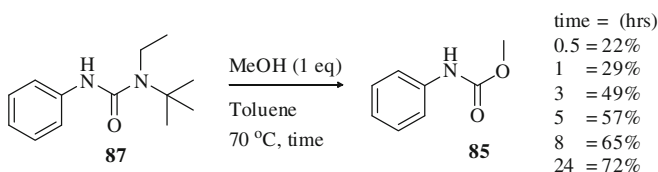
This is a complete reversal from the expected classical reactivity. The acidic phenol ($pK_a \sim 10$) would always be the leaving group if attacking as a nucleophile at the carbonyl centre in a $A_{AC}2$ mechanism (pK_a aniline ~ 27 , diisopropylamine ~ 36). However, it has been shown that ureas such as **87** are in constant equilibrium with the isocyanate and amine (in solution). When this labile C–N bond is replaced by a stronger C–O bond (upon formation of the carbamate) the equilibrium is pulled towards isocyanate formation (Scheme 4.21). This continues until all of the urea is consumed.

To render the reaction synthetically useful, efforts were undertaken to reduce the amount of nucleophile employed, from a large excess (solvent) to an equimolar level. This would also allow access to a much wider range of nucleophiles.

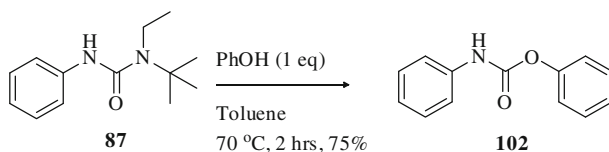
Due to its availability, ability to reach high temperatures and precedent during the mechanistic investigations, toluene was selected as solvent. Performing the reaction at 70 °C, 1 equivalent of methanol was reacted with **87**. MPC was formed

Scheme 4.21 Interception of the equilibrium by phenol

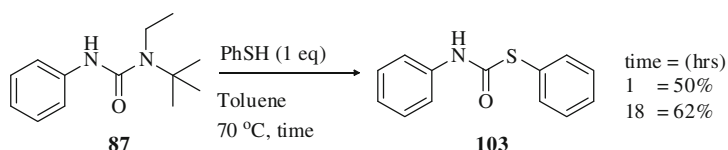
in a 22 % yield after 30 min. This reaction was followed over time by ^1H NMR reaching 65 % after 8 h. Leaving the reaction for 24 h gave a final conversion of 72 % (Scheme 4.22). 2 equivalents of methanol gave a similar result whereas 5 equivalents gave a quantitative yield after only 1 h.

**Scheme 4.22** Stoichiometric addition of methanol

Building on previous results, 1 equivalent of phenol was successfully utilised in an analogous reaction (Scheme 4.23).

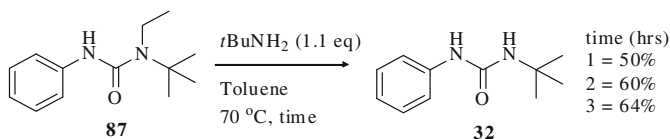
**Scheme 4.23** Stoichiometric addition of phenol

Thiophenol allows access to carbamothioates (**103**) and the reaction proceeds nicely with equimolar ratios (Scheme 4.24).

**Scheme 4.24** Stoichiometric addition of thiophenol

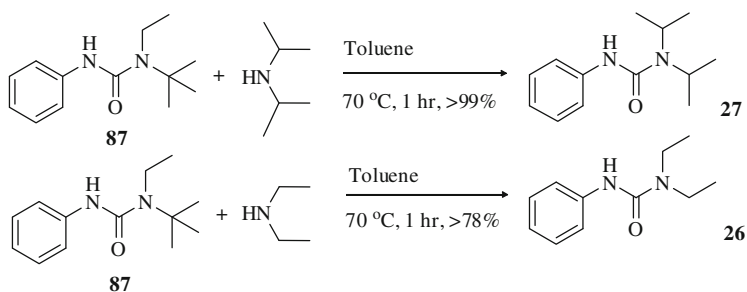
Stoichiometric reactions with water do not produce the expected aniline, but instead formed 1,3-diphenylurea **86** (see Scheme 4.5 for suggested mechanism). A low concentration of urea and a large excess of water is required to ensure aniline does not attack the phenylisocyanate generated.

Addition of a different amine would of course furnish the alternate urea species. This was initially accomplished with the addition of 2 equivalents of *tert*-butylamine to **87** in toluene at 70 °C (Scheme 4.25).



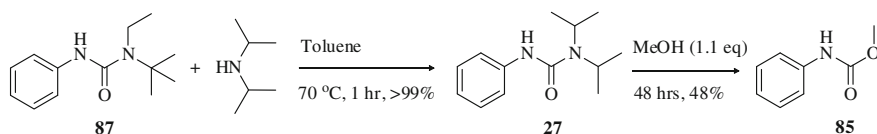
Scheme 4.25 Transamination

The introduction of any amine group which is less sterically demanding should produce the relevant urea. In separate experiments, diisopropylamine and diethylamine were reacted with **87** in equimolar ratios (Scheme 4.26), both providing rapid access to the urea derivatives.



Scheme 4.26 Ureas from ureas

Urea **27** has previously been shown to hydrolyse under neutral conditions and it was pleasing to be able to synthesis MPC from **87** via **27** in a one-pot, sequential reaction (Scheme 4.27).

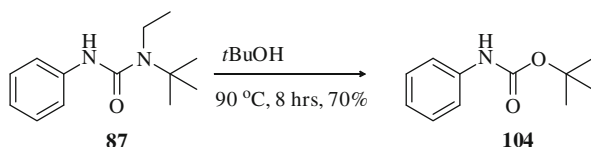


Scheme 4.27 Decreasing steric bulk allows for multiple transformations

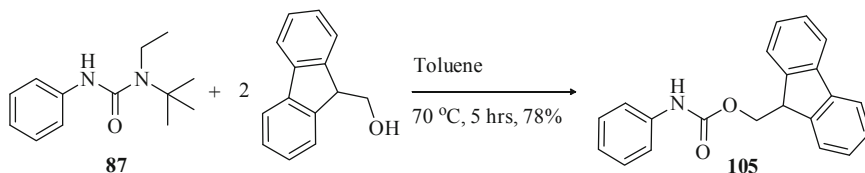
The ability to convert the urea moiety into other classical protecting groups was investigated. *tert*-Butyl esters (BOC), fluorenyloxycarbonyl (Fmoc) and carbobenzyloxy (Cbz) are all common and are all removed through a variety of different conditions (BOC = Acid, Fmoc = Base, Cbz = Hydrogenation). An ability to synthesise each of these carbamate protecting groups would be synthetically useful.

tert-Butanol would furnish the BOC protecting group but the hindered alcohol initially proved unreactive. Stoichiometric additions failed to yield the carbamate at 70 °C, whereas using the alcohol as solvent at the same temperature saw a slow rate of exchange—33 % after 24 h. Increasing the temperature to 90 °C produced the BOC aniline in a 70 % yield after 8 h (Scheme 4.28).

Scheme 4.28 The synthesis of BOC aniline

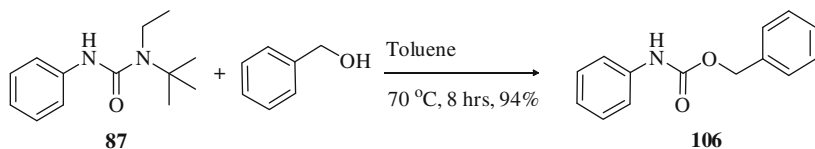


9-Fluorenyl methanol produces Fmoc-aniline in a 78 % yield after 5 h (Scheme 4.29). It was pleasing to see this reaction proceeding with stoichiometric amounts (2 equivalents) of the alcoholic reagent.



Scheme 4.29 The synthesis of Fmoc aniline

To complete the range of protecting groups, benzyl alcohol was also successfully reacted in an equimolar ratio with **29** (Scheme 4.30). The reaction was complete (>99 %) after 8 h.



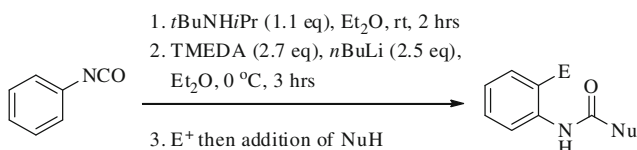
Scheme 4.30 The synthesis of Cbz-protected aniline

Encouraged by the ability to employ acidic nucleophiles, carbon nucleophiles were trialled. Unfortunately phenylmagnesium bromide resulted in a complicated

mixture of side products while acetophenone failed to react with or without a catalytic amount of lithium diisopropylamine. Dimethyl malonate also failed to react with varying amount of sodium methoxide base. Attempts at chlorination with LiCl failed, as did the attempted phenyl urea synthesis with NH_4Cl .

This facile and expedient solvolysis of hindered tri-substituted ureas was published as a communication in 2009 [16].

This methodology was further expanded by Houlden in the double lithiation of aniline derivatives, exploiting the transient nature of such labile ureas (Scheme 4.31) [17].



Scheme 4.31 One-pot *ortho*-derivatisation of isocyanates

In situ urea formation facilitated *ortho*-metalation upon the second equivalent of *n*BuLi. A range of electrophiles could then be added to this before invoking the proton switch mechanism via the addition of a nucleophile (e.g. ethanol). Performing this procedure in one-pot effectively enables the functionalisation of 2-lithiophenylisocyanate, a highly improbable intermediate.

References

- Salvestrini S, Di Cerbo P, Capasso S (2002) *J Chem Soc Perkin Trans 2*:1889–1893
- Clayden J, Hennecke U (2008) *Org Lett* 10:3567–3570
- Bottaro JC, Penwell PE, Schmitt RJ (1991) *J Org Chem* 56:1305–1307
- Pyun SY, Lee DC, Seung YJ, Cho BR (2005) *J Org Chem* 70:5327–5330
- Lewis RJ, Camilleri P, Kirby AJ, Marby CA, Slawin AA, Williams DJ (1991) *J Chem Soc Perkin Trans 2*:1625–1630
- Buck U, Huisken F (2000) *Chem Rev* 100:3863–3890
- Mandado M, Graña AM, Mosquera RA (2003) *Chem Phys Lett* 381:22–29
- Alexandrova AN, Jorgensen WL (2007) *J Phys Chem B* 111:720–730
- Callahan BP, Yuan Y, Wolfenden R (2005) *J Am Chem Soc* 127:10828–10829
- Williams A, Jencks WP (1974) *J Chem Soc Perkin Trans 2*:1753–1759
- Laudien R, Mitzner R (2001) *J Chem Soc Perkin Trans 2*:2226–2229
- Laudien R, Mitzner R (2001) *J Chem Soc Perkin Trans 2*:2230–2232
- Mollett KJ, O'Connor CJ (1976) *J Chem Soc Perkin Trans 2*:369–374
- Giffney CJ, O'Connor CJ (1976) *J Chem Soc Perkin Trans 2*:362–368
- O'Connor CJ, Barnett JW (1973) *J Chem Soc Perkin Trans 2*:1457–1461
- Hutchby M, Houlden CE, Ford JG, Tyler SNG, Gagné MR, Lloyd-Jones GC, Booker-Milburn KI (2009) *Angew Chem Int Ed* 48:8721–8724
- Houlden CE, Lloyd-Jones GC, Booker-Milburn KI (2010) *Org Lett* 12:3090–3092

Chapter 5

Amide Hydrolysis

5.1 Background

The solvolysis of hindered tri-substituted ureas (Sect. 4.2) was shown to proceed through an isocyanate intermediate, exploration of the analogous amide system led to the intriguing possibility of a novel ketene pathway (Scheme 5.1).

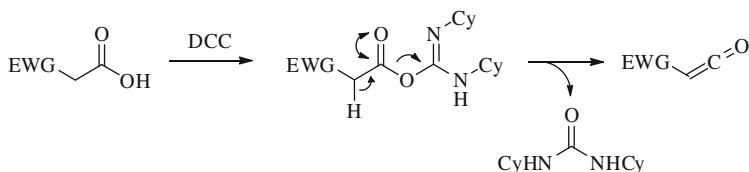
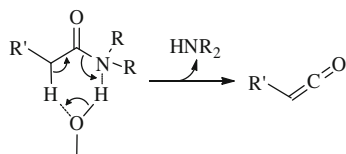
Not only would this enable the development of a new class of amide protecting group, with a mild, expedient method of removal but would lead to the exciting opportunity to merge this methodology with classic ketene cycloaddition reactions (Sect. 1.6).

Literature precedent suggests such a solvolysis reaction may be favourable, particularly when examining base catalysed hydrolysis of ester enolates [1, 2]. The reaction sees an enhancement in rate of ketene generation with increasingly bulky leaving groups.

Ketene formation from the dehydration of carboxylic acid derivatives containing electron withdrawing groups α to the carbonyl also provides encouragement [3]. Substrates used in this study show facile deprotonation by a weak base (DCC) and sufficiently stable ketenes to react further—attributes required to generate ketenes from hindered amides (Scheme 5.2).

Developments in this field may also contribute to the ongoing debate regarding the methods that nature can manipulate amide bonds. It has been hypothesised that enzyme driven twisting of an amide may be partially responsible for polypeptide lyase. [4, 5] To date all amides showing hyper-sensitivity towards hydrolysis have been constrained in lactams (Sect. 1.5).

Scheme 5.1 Ketene generation from an amide system



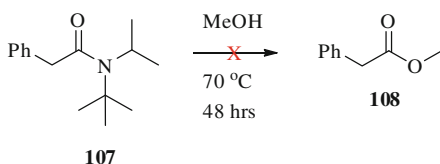
Scheme 5.2 Ketene generation from EWG containing carboxylic acid derivatives

5.2 Results and Discussion

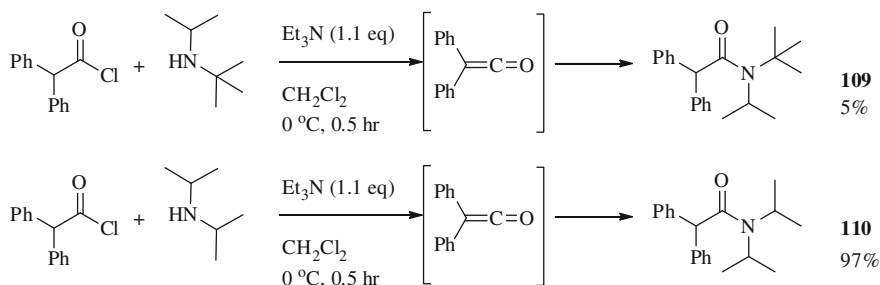
5.2.1 Substrate Exploration

Following on from the mild solvolysis of ureas, [6] the direct amide analogue was synthesised (**107**) and subjected to refluxing methanol. Disappointingly, only starting material was recovered after extended reaction times (up to 48 h) (Scheme 5.3).

Scheme 5.3 Unsuccessful amide methanolysis

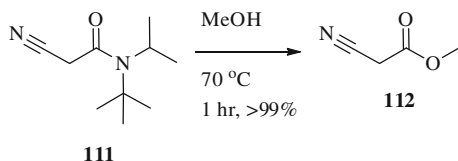


It seemed that the phenyl group failed to withdraw enough electron density from the CH_2 in order to allow for a facile proton switch to occur. *N-tert-butyl-N-isopropyl* diphenylacetamide (**109**) was also synthesised but once again failed to yield any methyl ester after 48 h in refluxing methanol. This result is perhaps more unexpected than the previous example as diphenylketene is well known and is particularly stable at room temperature for a prolonged period of time [7]. Interestingly, during the preparation of this hindered amide from diphenylacetyl chloride and triethylamine, a bright yellow solution was produced which was determined to be diphenylketene (solution phase IR $\text{C}=\text{O}$, 2100 cm^{-1}). Addition of the hindered amine to this solution did not consume the ketene and only a small amount of the amide was formed (<5%). With additions of diisopropylamine forming its respective amide (**110**) in an excellent yield, it can be assumed the bulky diphenylketene and hindered amine are unable to approach close enough to react (Scheme 5.4).



Scheme 5.4 Diphenylketene formation

Scheme 5.5 Rapid methanolysis of a hindered cyanoacetamide



This effect may also explain the lack of reactivity of **109**, with methanol unable to effect the proton switch due to the crowding and inaccessibility of the desired proton.

Undeterred by these results, amides with even more strongly electron withdrawing groups were targeted. *N-tert-butyl-N-isopropyl* cyanoacetamide (**111**) was synthesised and pleasingly produced the corresponding methyl ester in a quantitative yield after only 1 h in refluxing methanol (Scheme 5.5).

Encouraged by this result, a detailed steric profile was evaluated for the cyanoacetamide series (Table 5.1).

As seen with the urea study, steric hindrance around the amine leaving group plays a key role in facilitating the methanolysis reaction. Unlike that study however, the diisopropyl moiety is insufficiently bulky to provide enough steric relief of the strained zwitterionic intermediate to facilitate the reaction. It may also have an efficient overlap of the *N* lone pair with the $\text{C}=\text{O}$ π -system, leaving the nitrogen with little basic character needed to participate in the proton switch mechanism (Fig. 5.1).

Further examination of the steric influence on the reaction shows a significant trend as the amine portion of the molecule increases in size. This correlates nicely with the observations found in the analogous urea/isocyanate system. It was also pleasing to be able to synthesise, albeit in a low yield, an amide with the 2,2,6,6-tetramethylpiperidyl (TMP) motif (**115**). This member of the family was expected to provide the greatest steric resistance and thereby enhancing the reactivity beyond that of the *N-tert-butyl-N-isopropyl* analogue. The resulting reaction did indeed show remarkable propensity to form the methyl ester, requiring only 1 h at rt to fully esterify (Table 5.1, Entry 6). **115** is a stable white solid although the

Table 5.1 Cyanoacetamide methanolysis study

$$\text{N}\equiv\text{C}-\text{CH}_2-\text{C}(=\text{O})-\text{NR}_2 \xrightarrow[\text{Time, Temperature}]{\text{MeOH}} \text{N}\equiv\text{C}-\text{CH}_2-\text{C}(=\text{O})-\text{OCH}_3$$

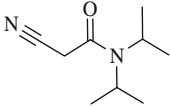
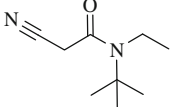
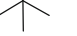
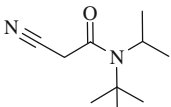
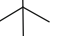
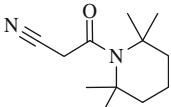
Entry	Amide	Cyanoacetamide	Temperature Time Yield
1	113		70 °C 48 h <1 %
2	114		50 °C 48 h 7 %
3			70 °C 48 h 33 %
4	111		50 °C 5 h >99 %
5			70 °C 1 h >99 %
6	115		rt 1 h >99 %

Fig. 5.1 Efficient overlap of the amide lone pair of electrons

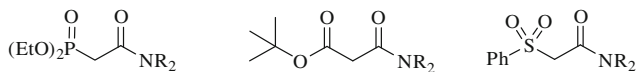
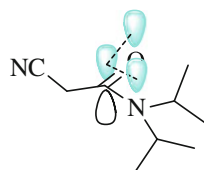


Fig. 5.2 Diethylphosphonate, malonate and phenylsulfonyl, derived amides

compound degrades over a period of days under atmospheric conditions (i.e. water mediated proton switch).

Having achieved proof of concept, it was clear only a certain type of substrate, one with a strongly electron withdrawing group at the α -position, would be susceptible to the neutral, mild and rapid methanolysis shown. Taking inspiration from the substrates Melman et al. [8] exploited in the ketene generation from DCC

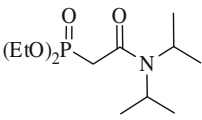
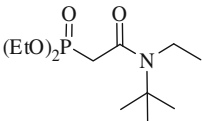
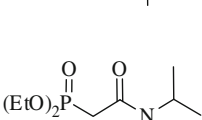
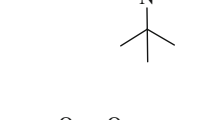
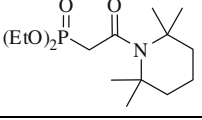

(Sect. 1.6.2, Scheme 46), diethylphosphonate, malonate and phenylsulfonyl derived amides were all synthesised (Fig. 5.2).

A complete profile was compiled examining the effects of steric bulk for all substrates and will be discussed in turn.

5.2.1.1 Diethylaminophosphonates

Once again the diisopropyl-derived amide (**117**) was unreactive and returned mainly starting material after 48 h. Increasing the bulk with an *N-tert*-butyl-*N*-ethyl group saw an increase in esterification at 70 °C but poor esterification at 50 °C suggesting an activation barrier between these two temperatures (Entries 2 and 3). The TMP-derived amide (**120**) again allowed for a reduction in reaction temperatures and time required (Entry 6) (Table 5.2).

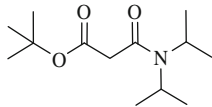
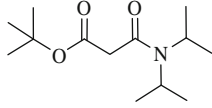
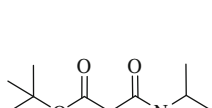
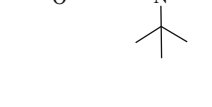
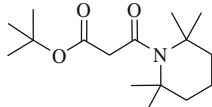

Table 5.2 Diethylaminophosphonate methanolysis study

Entry	Amide	Diethylaminophosphonate	Temperature	Time	Yield
1	117		70 °C	48 h	3 %
2	118		50 °C	48 h	11 %
3			70 °C	48 h	86 %
4	119		50 °C	9 h	60 %
5			70 °C	8 h	90 %
6	120		rt	1 h	>99 %

5.2.1.2 *tert*-Butyl Malonate Amides

Pleasingly the malonate substrates also showed the same trend as previous examples with the diisopropyl derived substrate (**122**) essentially unreactive and the TMP derivative (**125**) showing full conversion to the methyl ester at rt after 18 h (Table 5.3).

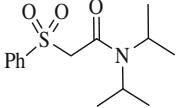
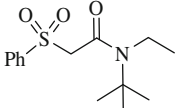
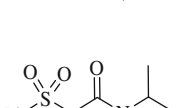
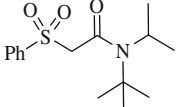
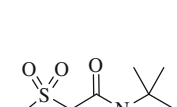
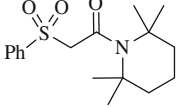
Table 5.3 *tert*-Butyl malonate amide methanolysis study

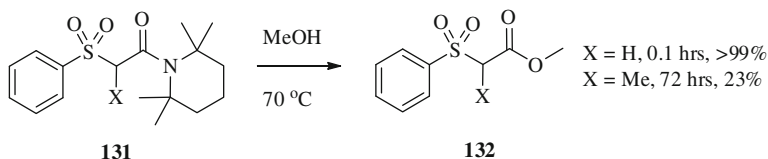
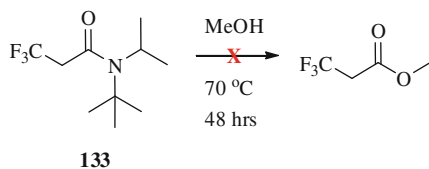
Entry	Amide	<i>tert</i> -Butyl malonate amide	Temperature Time Yield
1	122		70 °C 48 h <1 %
2	123		50 °C 48 h 33 %
3			70 °C 48 h 40 %
4	124		50 °C 18 h >99 %
5			70 °C 9 h 96 %
6	125		rt 18 h >99 %

5.2.1.3 Phenylsulfonylacetamides

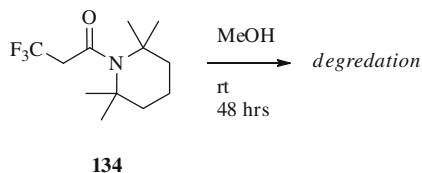
During the examination of this series, the more hindered amides **129** and **130** exhibited remarkable features at odds with the reactivity observed. They were stable, white crystalline solids that remained pure for an indefinite amount of time (**130** remained unchanged for 6 months) when stored on the bench. **130** also exhibits almost instantaneous reaction with methanol at rt, the fastest rate observed to date (Table 5.4, Entry 6).

Table 5.4 Phenylsulfonylacetylamine methanolysis study

Entry	Amide	Phenylsulfonylacetylamine	Temperature Time Yield
1	127		70 °C 48 h <1 %
2	128		50 °C 48 h 11 %
3			70 °C 48 h 52 %
4	129		50 °C 5 h >99 %
5			70 °C 1 h >99 %
6	130		rt 10 min >99 %

**Scheme 5.6** Examination of substitution effects**Scheme 5.7** Methanolysis resistant trifluoropropionamide derivative

Scheme 5.8 Uncontrolled reactivity of **134**



Exploring the limitations of **130**, a methyl group was installed in the α -position to determine the tolerance to substitution. No methyl ester was formed at rt and only when heating the reaction to reflux for a prolonged time was product observed (Scheme 5.6).

The drop in reactivity is substantial, with several mechanistic implications possible. Perhaps the electron donating methyl group does not allow for facile deprotonation, or the methyl group may facilitate a change in conformation of the molecule disrupting any twisting effect, necessary for the reactivity shown.

Following this successful study, alternative electron withdrawing groups were investigated. Interestingly trifluoropropionamides failed to yield any methyl ester when the *N*-*tert*-butyl-*iso*-propyl (**133**) was employed (Scheme 5.7).

Reactivity was only observed with the TMP-derivatised trifluoropropionamide (**134**). Physically the compound appeared to degrade from clear oil to a brown gum within a matter of hours at room temperature with several new species appearing on tlc. Unfortunately reacting this substrate with methanol (at rt or refluxing) led to a complicated mixture of products, none of which could be identified as the expected methyl ester (Scheme 5.8). Despite the lack of control, this result is still an encouraging one with reactivity observed in the presence of an electron withdrawing group and only with a large degree of steric influence.

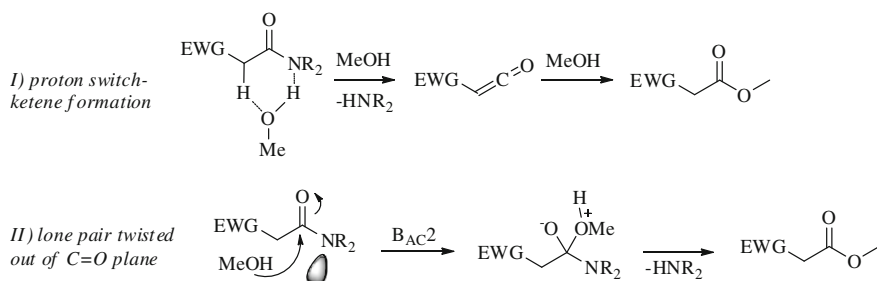
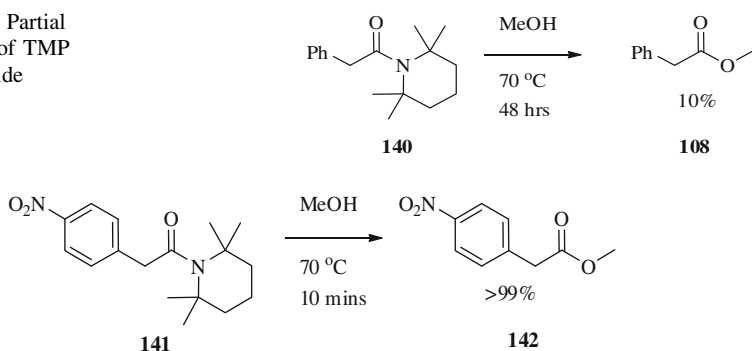
Following from this, a wider range of alternative TMP derived amides was synthesised in order to probe the limitations of the reaction and provide insights into the mechanism. The substrates presented in Table 5.5 failed to yield any of the corresponding esters.

There are two possible mechanisms which may facilitate the methanolysis seen so far. The previously discussed proton switch-ketene pathway (Scheme 5.9—I) or a classic $B_{AC}2$ resulting from a twisted amide bond (Scheme 5.9—II). Both of these mechanisms would benefit from greater steric bulk around the nitrogen and the presence of a strongly electron withdrawing group.

Amides **135** and **136** have no protons in the α -position and were model substrates to distinguish between the two available mechanisms. If a simple twist of the amide bond allowed for facile nucleophilic attack, then methanolysis should still occur for substrates **135** and **136**. As these substrates failed to react, the $B_{AC}2$ mechanism looks unlikely and the proton switch mechanism can still be invoked. It is perhaps unsurprising that **137** failed to undergo facile methanolysis due to its mesomeric electron donating nature and the failure of **138** and **139** was perhaps also expected due to the observations made with double substitution of the α -position (Scheme 5.7).

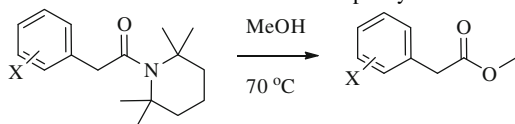
Table 5.5 Failed TMP derived amides

Entry	135	136	137	138	139
EWG					

**Scheme 5.9** Possible mechanistic pathways**Scheme 5.10** Partial methanolysis of TMP phenylacetamide**Scheme 5.11** Expedient and complete methanolysis of NO₂ phenylacetamide derivative

With the knowledge that TMP derivatisation can severely increase the rate of methanolysis, the previously unreactive phenylacetamide series was re-examined. After 48 h in refluxing methanol, 10 % of the target methyl ester was returned (Scheme 5.10).

This modest increase in methanolysis product showed potential but an unsubstituted phenyl ring still seemed insufficiently electron deficient to enable a facile proton switch. By placing electron withdrawing groups around the ring, it was hoped this problem would be negated and reactivity would be increased. Pleasingly

Table 5.6 Substituted TMP derived phenylacetamides

Entry	Amide	X	Time (h)	Ester	Yield (%)
1	141	<i>p</i> -NO ₂	0.2	142	>99
2	143	3,5-CF ₃	1	157	>99
3	144	<i>p</i> -SO ₂ Me	1	158	>99
4	145	<i>p</i> -CN	1.5	159	>99
5	146	<i>m</i> -NO ₂	2	160	>99
6	147	<i>o</i> -NO ₂	18	161	>99
7	148	<i>p</i> -CF ₃	32	162	>99
8	149	<i>m</i> -CF ₃	48	163	87
9	150	<i>o</i> -CF ₃	48	164	85
10	151	<i>p</i> -Br	48	165	88
11	152	<i>m</i> -Br	48	166	84
12	153	2-naphthyl	48	167	22
13	154	H	48	108	10
14	155	<i>m</i> -MeO	48	168	12
15	156	<i>p</i> -MeO	48	169	7

this was the case with the *p*-NO₂ substrate (**141**) fully converting to the methyl ester in only 10 min in refluxing methanol and in only 1.5 h at rt (Scheme 5.11).

Buoyed by this result, a series of amides was synthesised, each based around the TMP motif and each with an electronically derivatised phenyl ring. The results of their methanolysis are presented in Table 5.6.

A large variety of electron withdrawing substituents were found to effect the reaction with many showing complete esterification after only 2 h (Entries 1–5). *Ortho*, *meta* and *para* substituents were all tolerated (Entries 1, 5 and 6) and both mesomeric and inductive electron withdrawing groups facilitated the reaction (Entries 2–3). Satisfyingly bromo derivatives **151** and **152** gave excellent yields after prolonged reaction times allowing for further functionalisation of this useful handle. The electron releasing *p*-MeO (Entry 15) gave a predictably poor yield as the oxygen lone pair can resonate through the ring, however it was hoped that methoxy in the *meta* position (which is unable to resonate this way) may actually increase reactivity through the electronegative oxygen removing electron density through the σ – framework. This was not found to be the case however and the yield remained low.

5.2.2 Mechanistic Studies

X-Ray crystallography has played a key role in many previous twisted amide studies. Fortunately the phenylsulfonylacetamide series were crystalline solids and

crystal structures were obtained. As expected **127** which shows no propensity to esterify has a perfectly planar amide bond with the lone pair of electrons on the nitrogen able to fully overlap with the π -bond of the carbonyl bond (Fig. 5.3).

Interestingly the crystal structure of the TMP derivative **130** shows a twist of the bond with the nitrogen slightly pyramidalised and the lone pair not only twisted out of the plane but also pointing away from the carbonyl π -bond (Figs. 5.4 and 5.5).

Fig. 5.3 X-Ray crystal structure of **127**

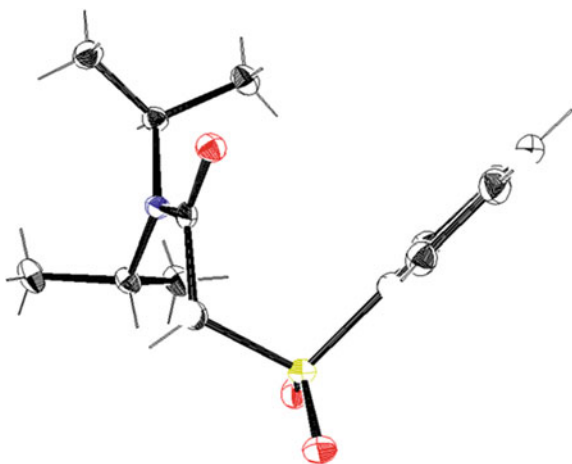
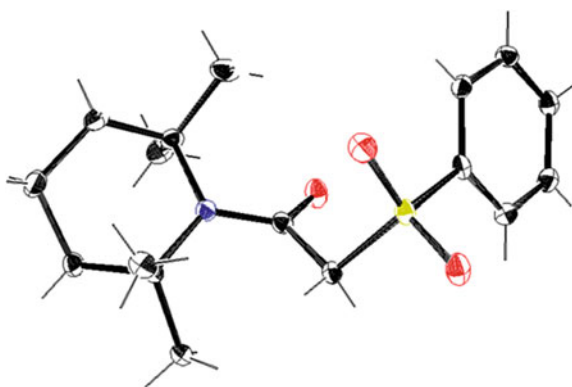


Fig. 5.4 X-Ray crystal structure of **130**



130 has a twist angle of 27.4° and **127** has an insignificant, almost planar angle of 2.1° . Whilst these values are for a solid state packing of a crystal and may not truly represent the conformation in solution, they perhaps reveal an insight into the low barrier of rotation and hence the facile solvolysis that can occur. Bond lengths do not show unusual deviation from standard amide values however there is a lengthening as steric bulk increases (**127** = 1.344 \AA –**130** = 1.366 \AA). This would be expected with an increasingly poor overlap between nitrogen lone pair and the $\text{C} = \text{O}$ π -bond.

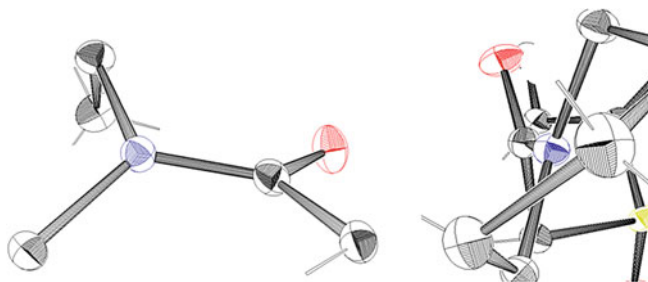


Fig. 5.5 Alternative amide bond perspectives of **130**

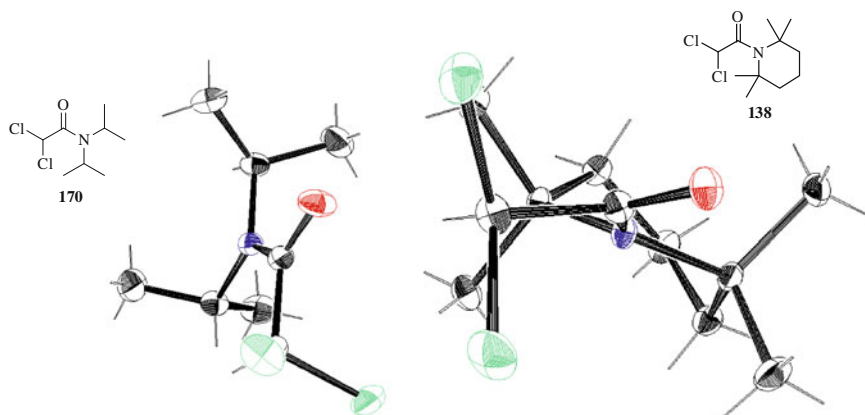


Fig. 5.6 Dichloroacetamide X-Ray crystal structures—diisopropyl (*left*), TMP (*right*)

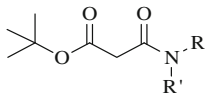
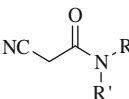
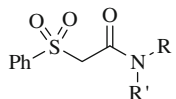
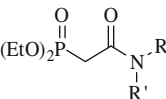
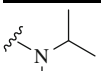
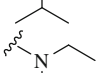
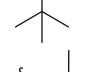
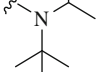
The remaining two substrates in this sulfonamide series (**128** and **129**) have increasing amounts of twisting according to the steric bulk, which in turn corresponds with increasing levels of reactivity.

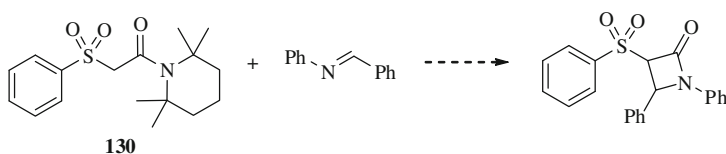
The unreactive, doubly substituted dichloroacetamides were also crystalline solids and crystals structures were obtained (Fig. 5.6).

Once again, the diisopropyl derivative (**170**) shows almost perfect planarity in the amide bond and the TMP derivative (**138**) shows a substantial twist, analogous to the phenylsulfonylacetamide series. The disparity between a reactive substrate and an unreactive one is therefore not just about the degree of twisting but also other factors, electronic and conformational.

Despite the obvious and pronounced distortion of the reactive amide bonds, examination of the structural features provided little extra information. For all the substrates examined the IR carbonyl stretch is around $1625\text{--}1640\text{ cm}^{-1}$, values expected for a standard amide and far removed from the ketone-like stretches ($\sim 1700\text{ cm}^{-1}$) observed for previous twisted amides (Sect. 1.5). ^{13}C NMR carbonyl signals also reveal very amide-like values (160–170 ppm) however a trend

Table 5.7 ^{13}C NMR shifts

^{13}C NMR C = O				
	167.2	159.9	159.8	163.1
	167.5	161.9	161.5	165.0
	168.1	163.1	163.3	167.3
	169.8	164.7	164.5	168.4

**Scheme 5.12** β -Lactam formation via a [2 + 2] cycloaddition with an imine

is observed when examining the differences within the phenyl sulfone series of sterically derivatised amides (Table 5.7).

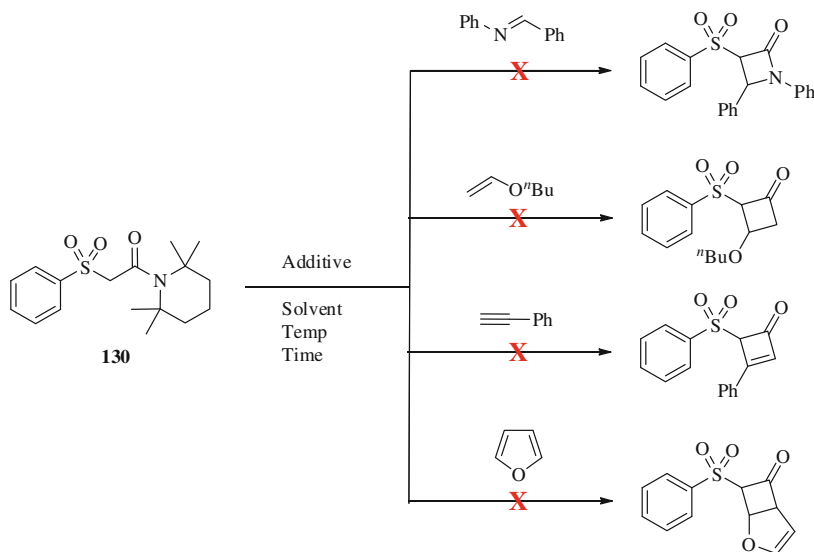
Moving down the table from diisopropyl to TMP, there is a small but significant shift downfield with the carbon becoming more electron deficient. This deficiency suggests a poorer overlap with the lone pair of electrons of the nitrogen, an effect that supports the twisting of the bond as observed in the X-Ray structure. There is no analogous pattern in the IR stretches.

In order to distinguish between straight nucleophilic attack of a twisted amide and the proton switch mechanism via a ketene intermediate, various cycloaddition reactions were attempted.

Classic keteneophiles under a variety of cycloaddition conditions were trialled with the most stable yet reactive hindered amide **130**.

β -Lactam formation with *N*-benzylideneaniline would be synthetically attractive, generating a new route into this important class of molecule (Scheme 5.12).

Despite numerous attempts however, the desired product was not formed with a range of solvents and temperatures proving ineffective. If the proton switch mechanism is indeed in operation then the ketene would need to be 'released'



Additive: TMP, NEt₃, MeOH *Solvent:* PhCH₃, CH₂Cl₂, MeCN, DMF, THF, EtOAc, Et₂O *Temp:* rt, reflux

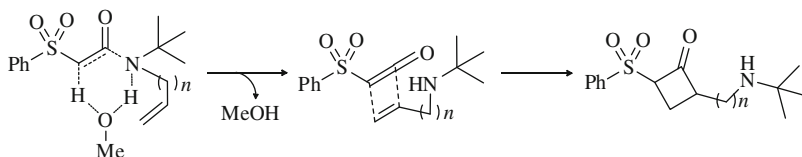
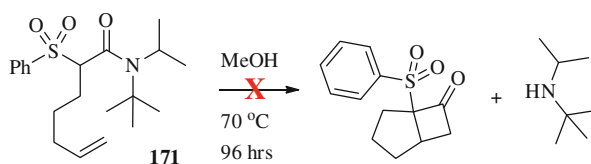
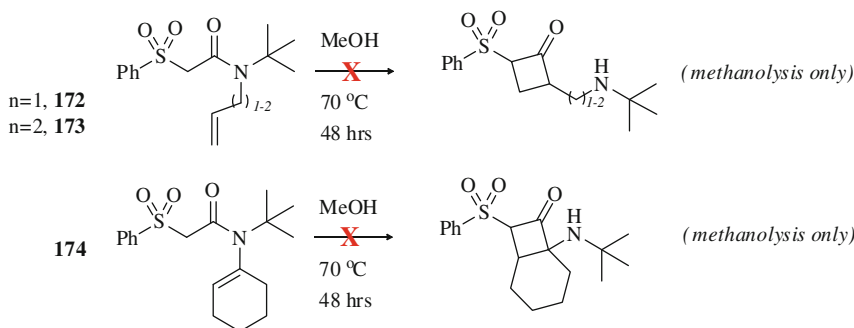
Scheme 5.13 Unsuccessful [2 + 2] cycloadditions

through this pathway before it could undergo a cycloaddition. Unfortunately methanol and any other neutral protic source can also act as a nucleophile and subsequently trap the ketene generated. A large excess of keteneophile was employed throughout and various additives such as triethylamine and catalytic amounts of methanol (1–5 %) were employed. Again, these reactions also proved ineffective, as did the use of various amounts of the TMP amine.

Alternative cycloaddition partners, including phenyl acetylene and butylvinyl ether, also failed to produce the desired products under a variety of conditions as described above. The use of furan as reaction solvent with or without catalytic amounts of methanol also failed to yield the cycloadduct (Scheme 5.13).

With intermolecular cycloadditions proving unsuccessful, various substrates for the intramolecular reaction were designed. Initially a pendent alkene was tethered to the α -position in the hope of a [2 + 2] cyclisation (**171**). As previously observed, substitution of this carbon results in a severe retardation of the reaction, the efficiency is inconsequential however as any yield of a cycloadduct would provide excellent evidence of a ketene intermediate. Unfortunately no cyclobutanone was observed, only a small trace of the methyl ester ($\sim 3\%$ by ¹H NMR) (Scheme 5.14).

Following this disappointing result, an alternative strategy of substituting the amine portion of the molecule was adopted. The procedure developed by Schmitt [9] enabled a variety of secondary amides to be synthesised, each sufficiently bulky to undergo mild solvolysis but also with an alkene present to trap the resultant intermediate. It was hoped that as the amine was ejected from the substrate it would be close enough to then immediately react with the ketene (Scheme 5.15).

Scheme 5.14 Unsuccessful intramolecular [2 + 2] cycloaddition**Scheme 5.15** Pseudo-intramolecular keteneophile**Scheme 5.16** Unsuccessful [2 + 2] cycloadditions

Despite several variations of the nitrogen leaving group, all attempts to furnish the [2 + 2] products were unsuccessful (Scheme 5.16).

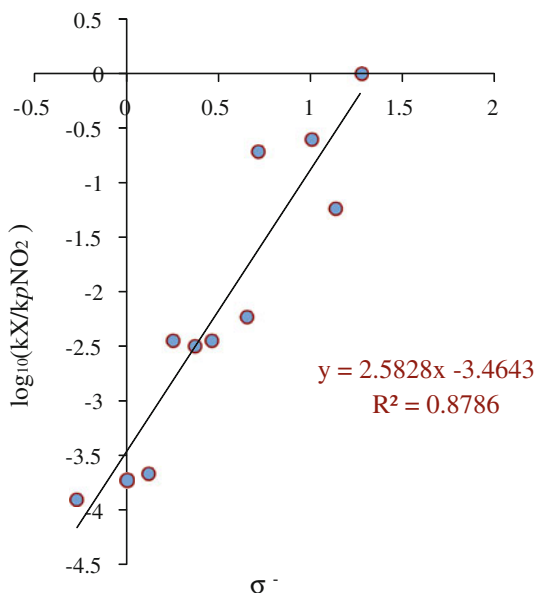
In all cases only the methyl ester was obtained suggesting the dominance of nucleophilic attack over any possible cycloaddition. This may be due to inherent reactivity, the vast excess of nucleophile or simply the proximity of methanol during the proton switch pathway.

Disappointed by the inability to directly implicate ketene formation, alternative mechanistic studies were undertaken.

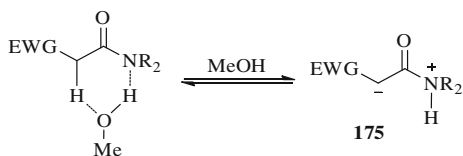
Utilising the arylacetamide series (**141**, **143–154**), a Hammett study was performed to determine the nature of charge build up in the rate determining step (Fig. 5.7).

A ρ^- value of 2.6 indicates a negative charge build up on the α -carbon during the reaction. This correlates with the proposed mechanism of zwitterion formation (**175**) prior to amine expulsion and ketene release (Scheme 5.17). The requirement for an electron withdrawing group can also be explained by this resonance stabilisation of the partial negative charge.

Fig. 5.7 Hammett analysis of aryl acetamide series ($\rho^- = 2.6$)



Scheme 5.17 Zwitterion formation



The rate of deuterium incorporation at the α -position was also examined for the sulfonyl series **127–130** in methanol d_4 . With **130**, the rate of reaction and D incorporation was over in a matter of minutes at rt; spectra were therefore run at 3 °C to slow the reaction down enough to achieve sufficient data points. The D incorporation rates for amides **127–129** were obtained at rt, allowing the activation energy (ΔG^\ddagger) for H/D exchange to be established (Fig. 5.8).

As steric bulk around nitrogen increases and the N-CO torsion energy drops, the increase in ΔG^\ddagger for H/D exchange implicates an increase in rate of the proton-switch. In conjunction with the Hammett findings (Fig. 5.7) a complete mechanistic picture can be established (Scheme 5.18).

5.2.3 Synthetic Uses

As with the analogous urea study (Sect. 4.2.2) a wide range of nucleophiles were employed in the synthesis of esters, thioesters and amides. All the reactions occurred at rt and produced high yields after short reaction times. Pleasingly

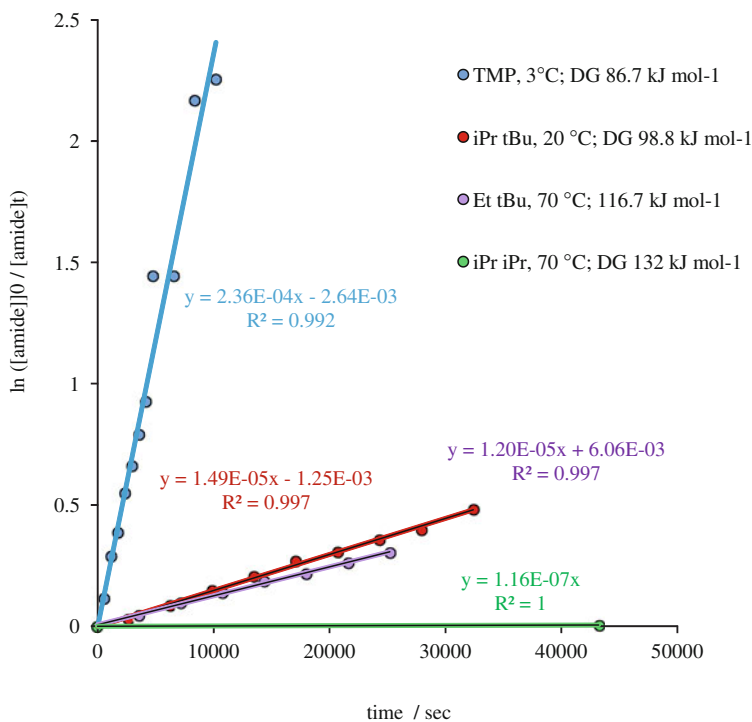
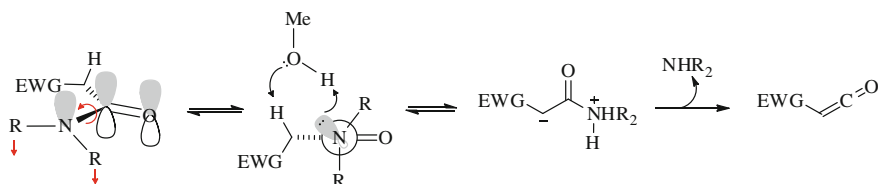


Fig. 5.8 Analysis of pseudo first order kinetics for α -CH/D exchange, giving $k_{\text{DBS}}^{\text{D}}$

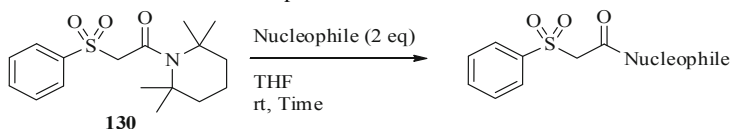


Scheme 5.18 Full mechanistic picture of ketene release

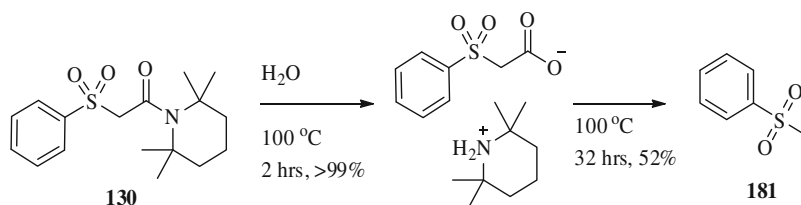
stoichiometric amounts of the nucleophile can be used rendering the reaction more attractive to synthetic chemists (Table 5.8).

Both phenol and thiophenol efficiently form the ester (**179**) and thioester (**180**) respectively and highlight the counterintuitive nature of the reaction. Under the classic nucleophilic attack mechanism, the breakdown of the tetrahedral intermediate would result in the expulsion of the best leaving group, nominally phenol or thiophenol ($\text{p}K_{\text{a}}$; $\text{PhSH} = 6.6$, $\text{PhOH} = 10$) and not the amine ($\text{p}K_{\text{a}} > 30$).

When water was used as the nucleophile it forms the carboxylic acid which in turn is deprotonated by extruded amine to form the salt. A simple 1 M HCl wash furnishes the free acid. With water as solvent (at 100 °C due to solubility issues),

Table 5.8 Alternative nucleophile addition

Entry	Nucleophile	Product	Time (h)	Yield (%)
1	H ₂ O	176	24	94
2	MeOH	108	6	95
3	<i>t</i> BuOH	177	24	89
4	<i>t</i> BuNH ₂	178	4	97
5	PhOH	179	6	93
6	PhSH	180	2	97

**Scheme 5.19** Methyl sulfone formation via decarboxylation of an acid intermediate

the reaction is complete within 2 h and if this is left for extended times, decarboxylation can occur furnishing the methyl sulfone (**181**) (Scheme 5.19).

In summary, hindered amides possessing an electron withdrawing group have shown to undergo mild solvolysis under neutral conditions. A low activation barrier to rotation of the C–N bond allows the more basic amide nitrogen to participate in proton switch to generate a ketene intermediate which is subsequently attacked by a nucleophile.

References

- Inoue M, Bruice TC (1983) *J Org Chem* 48:3559–3561
- Inoue M, Bruice TC (1986) *J Org Chem* 51:959–963
- Shelkov R, Nahmany M, Melman A (2002) *J Org Chem* 67:8975–8982
- Albers MW, Walsh CT, Schreiber SL (1990) *J Org Chem* 55:4984–4986
- Romanelli A, Shekhtman A, Cowburn D, Muir TW (2004) *Proc Natl Acad Sci U S A* 101:6397–6402
- Hutchby M, Houlden CE, Ford JG, Tyler SNG, Gagné MR, Lloyd-Jones GC, Booker-Milburn KI (2009) *Angew Chem Int Ed* 48:8721–8724
- Machiguchi T, Hasegawa T, Ishiwata A, Terashima S, Yamabe S, Minato T (1999) *J Am Chem Soc* 121:4771–4786
- Nahmany M, Melman A (2001) *Org Lett* 3:3733–3735
- Bottaro JC, Penwell PE, Schmitt RJ (1991) *J Org Chem* 56:1305–1307

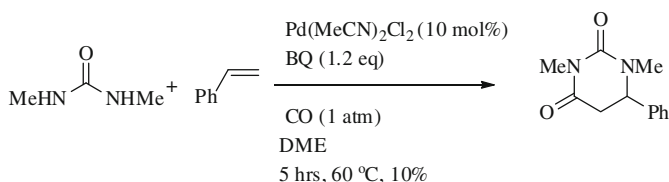
Chapter 6

Conclusions and Future Work

6.1 Conclusions

6.1.1 Pd(II) Catalysed Aminocarbonylations of Alkenes

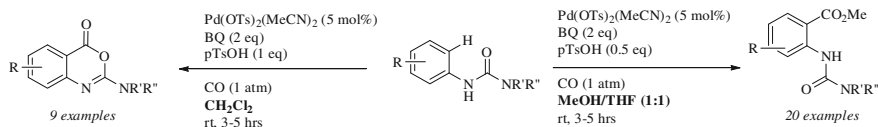
During attempted investigations into the Pd(II) catalysed aminocarbonylations of alkenes (Chap. 2) conditions were found to form pyrimidiones in low yields. The reaction is stoichiometric with respect to the palladium. Unfortunately efforts to render the reaction catalytic were unsuccessful. The reaction is substrate specific with rates of β -hydride elimination of the palladated intermediate critical to reactivity. Unfortunately the analogous reaction with methanol failed to furnish β -amino acid derivatives (Scheme 6.1).



Scheme 6.1 Pyrimidione formation

6.1.2 Carbonylation of Aryl Ureas

Aryl ureas have been shown to *ortho* carbonylate whereby a range of heterocycles and esters were formed at room temperature in less than 5 h. Pd(OTs)₂(MeCN)₂ can be used in the reaction with the metal directed to the *ortho* position by the oxygen of the urea. Mono and bis substitution of the alkyl nitrogen was tolerated as was a wide range of functionality on the aromatic ring. Methylation of the aryl nitrogen resulted in a shutdown of the reaction, while strongly electron withdrawing groups in the aromatic ring returned poor yields (Scheme 6.2).

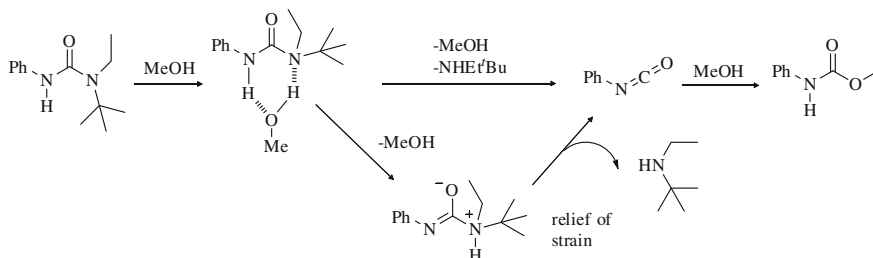


Scheme 6.2 *Ortho* functionalisation of aryl ureas

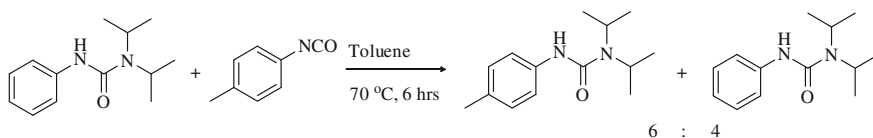
6.1.3 Urea Hydrolysis

Chapter 4 described the unusual solvolysis of hindered tri-substituted ureas. The rate of methanolysis was found to dramatically increase with an increase in steric bulk, a counterintuitive observation based on classical $B_{AC}2/A_{AC}2$ solvolysis. A detailed mechanistic study found substantial evidence of an isocyanate intermediate generated from a proton switch mechanism (Scheme 6.3).

Generation of this intermediate was explicitly implicated through a crossover experiment where urea formation could only occur via the generation of an isocyanate (Scheme 6.4).



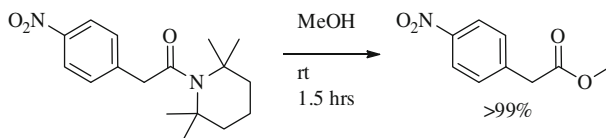
Scheme 6.3 Facile methanolysis of hindered tri-substituted ureas



Scheme 6.4 Amine partitioning between isocyanates

6.1.4 Amide Hydrolysis

Finally hindered amides possessing an electron withdrawing group have been shown to undergo facile solvolysis in an analogous system to that of the ureas. Sterically bulky groups generate a low barrier to rotation of the C–N bond rendering the nitrogen more basic and enabling to participate in the proton shift mechanism. It is proposed that these compounds are a new class of amides



Scheme 6.5 Facile methanolysis of hindered amides

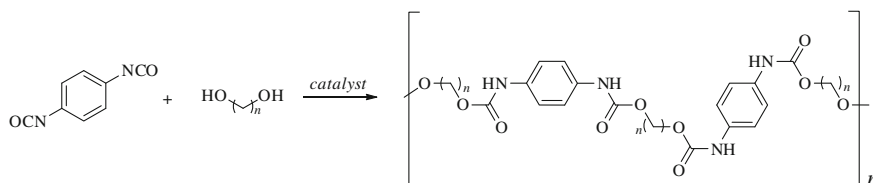
(‘rotamides’) exhibiting physical and spectral characteristics of standard amides but the reactivity of conformationally locked ‘twisted amides’. These compounds may have a significant impact in the understanding of peptide hydrolysis and the method by which nature is able to easily manipulate this robust moiety (Scheme 6.5).

The reaction is thought to proceed via a ketene intermediate but all efforts to directly observe this species through a cycloaddition reaction were unsuccessful. Indirect implications through a Hammett study and deuterium incorporation rates suggest a proton switch mechanism, thereby corroborating the hypothesised intermediacy of a ketene.

6.2 Future Work

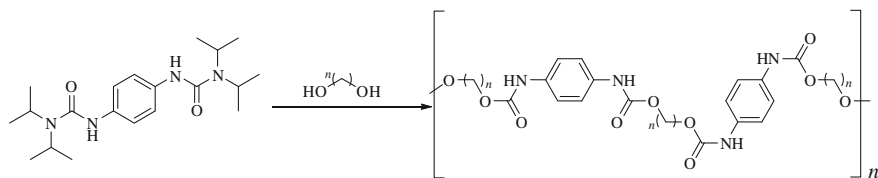
6.2.1 Polymerisation of Hindered Tri-Substituted Ureas

Polyurethanes are polymers consisting of organic units joined by a carbamate (urethane) linker. They can be found in a wide variety of products ranging from flexible foam seating, foam insulation panels, foam seals, gaskets, elastomeric wheels and tyres, adhesives, surface coatings and even carpet underlay. Many of these materials are formed through the polymerisation of a monomer containing at least two isocyanate functional groups with another monomer containing at least two hydroxyl groups [1] (Scheme 6.6).



Scheme 6.6 Urethane synthesis

In order to facilitate a polymerisation, catalysts are normally required which can either be tertiary amine based or organometallic [1]. The latter include mercury, lead, tin, bismuth and zinc based compounds, many of which are highly toxic. Isocyanates can also be difficult to handle, unstable and toxic molecules [2].



Scheme 6.7 Possible urethane synthesis from hindered tri-substituted ureas

With strong evidence that hindered tri-substituted ureas undergo a proton switch mechanism to yield isocyanates, [3] it should be feasible to generate polyurethanes from doubly substituted ureas and a polyol (Scheme 6.7).

The benefits of such a development include the removal of the need for a catalyst and the enhanced stability and ease of handling when compared to an isocyanate. Polymerisation reactions would also be highly controllable. By selecting an appropriate level of steric hindrance the reaction could be tailored around temperature and time all having an impact on the degree and type of polymer formed.

6.2.2 Amide Hydrolysis: Direct Evidence of Ketene Formation

With intramolecular cycloaddition reactions failing to provide significant evidence of ketene intermediate, malonate derivatives may be more successful.

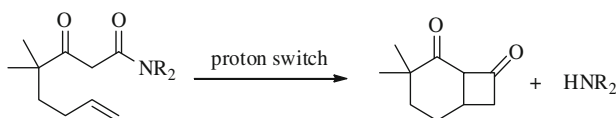
By appending a keteneophile to the terminal end of such molecules, the α -position would remain available to engage in the proton switch mechanism, allowing the ketene to be released (Scheme 6.8).

Such a route would be highly dependent on the orientation of the keteneophile trap and its proximity to the ketene as it is generated. As before the source of protons may be critical with methanol perhaps too small and nucleophilic to allow the [2 + 2] cycloaddition. Alternative proton switches could also be investigated with phenol and *t*BuOH prime candidates.

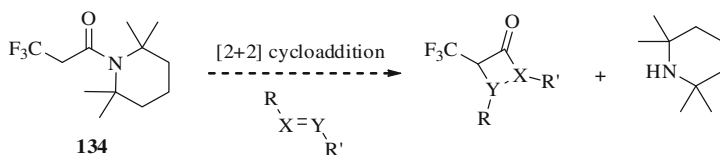
In addition to this, the uncontrolled reactivity of **134** could perhaps be exploited. The substrate appeared to undergo a reaction in the presence of methanol but did not furnish the expected methyl ester. This perhaps presents an opportunity to intercept any potential ketene generated with classical [2 + 2] cycloadditions as described in Sect. 5.2.2 (Scheme 6.9).

6.2.3 Amide Hydrolysis: Manipulations of Reactivity

During the Hammett investigations into the electronic influences on amide hydrolysis, an anomalous reading from the *p*-CF₃ derived substrate led to an

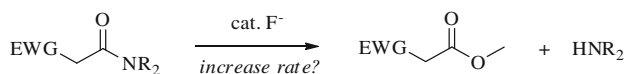


Scheme 6.8 Possible intramolecular ketene trap



Scheme 6.9 Exploitation of 134

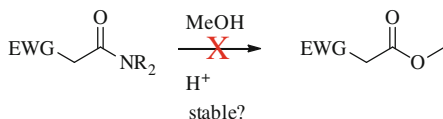
observed rate many times faster than expected. After re-synthesising the substrate, the rate returned to the expected level indicating a contaminant in the original batch that was enhancing reactivity. It would be prudent to investigate potential impurities with fluoride a potential source. F^- could act as a base, assisting in the de-protonation/enolisation of the amide thereby increasing the rate of solvolysis. Catalytic sources of fluoride (KF, TBAF etc.) may provide an easy and convenient additive to enhance reactivity of those with slow rates (Scheme 6.10).



Scheme 6.10 Fluoride catalysed rate enhancement

In contrast to the effect of added base, an investigation into the addition of acid may provide details into the stability of *rotamides*. It is noticeable that these compounds, in particular the most reactive amides are stable to aqueous acidic workups and column chromatography (performed in reagent grade solvent) despite their propensity to hydrolyse with only a few equivalents of water at room temperature. Slightly acidic silica used in chromatography may be responsible for this effect and development of an H^+ based stabiliser may render these molecules indefinitely stable allowing for easier storage and increasing their synthetic value (Scheme 6.11).

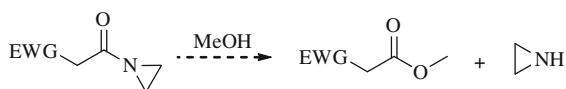
Scheme 6.11 Acid catalysed inhibition



6.2.4 Alternative Rotamides

Amides possessing an aziridine moiety have been shown to develop a high degree of pyramidalisation leading to a poorer overlap of the nitrogen lone pair of electrons with the carbonyl π -bond and as consequence a rapid rate of hydrolysis [3]. A full and comprehensive literature search yields no substrates that contain both this aziridine headgroup and an electron withdrawing unit at the α -position. An examination of such molecules therefore may lead to easily solvolysed amides which are not reliant on steric bulk (Scheme 6.12).

Scheme 6.12 Aziridine based 'rotamides'



References

1. Seymour SB, Kauffman GBJ (1992) Chem Ed 69:909
2. Centers for Disease Control and Prevention (2011). Available at <http://www.cdc.gov/niosh/topics/isocyanates/>
3. Hutchby M, Houlden CE, Ford JG, Tyler SNG, Gagné MR, Lloyd-Jones GC, Booker-Milburn KI (2009) Angew Chem Int Ed 48:8721–8724
4. Slebocka-Tilk H, Brown RSJ (1987) Org Chem 52:805–808

Chapter 7

Experimental

7.1 General Experimental Detail

For rapid screening of conditions and substrates, reactions were frequently carried out using a Radley's 12 port reaction carousel with reduced volume tubes. However results were identical when repeated using standard Schlenk techniques. All glassware was washed in acid (conc. HNO_3) and base baths (*i*PrOH/KOH) before being rinsed (H_2O /acetone) and oven-dried at 150 °C for at least 18 h. Dry solvents were purchased (*Aldrich, Fluka, Alfa Aesar*) and distilled or obtained by passage through an *Anhydrous Engineering* drying column. Solvents for extraction and chromatography were technical grade. Carbon monoxide was purchased from BOC. Purchased chemicals (*Aldrich, Acros, Fluka, Alfa Aesar*) were used as received, unless otherwise stated. Reagents requiring purification were done so according to Purification of Laboratory Chemicals [1]. Benzoquinone was sublimed before use.

Melting points were conducted with a *Stuart Scientific* melting point apparatus. IR spectra were obtained with *Perkin-Elmer Spectrum One* apparatus; peaks are reported in cm^{-1} with the following intensities: s (strong, 70–100 %), m (medium, 30–70 %), w (weak, 1–30 %). NMR spectra were obtained from *Jeol Eclipse 400, Lambda 300, Varian 400* or *Varian 500* instruments. ^1H and ^{13}C NMR chemical shifts δ (ppm) are reported relative to residual solvent non-deuterated. Multiplicities are indicated as s (singlet), d (doublet), t (triplet), q (quartet), sept (septet), br (broadened), app (apparent) or m (multiplet, when multiplicity is complex). Coupling constants, *J*, are reported in Hz. MS (EI, CI, ESI, LRMS, HRMS) were conducted by the University of Bristol Mass Spectrometry Service using *Fisons Autospec* instruments. Flash chromatography was conducted using *Fluorochem* silica gel 60 (0.040–0.063). Eluting solvent used as indicated in the text. Thin Layer Chromatography (TLC) was conducted with 0.25 mm *Merck* silica gel 60 F254 on aluminium plates, developed with the indicated solvent systems (PE = 40/60 petroleum ether, EtOAc = ethyl acetate), visualising at 254 nm or developed with KMnO_4 .

7.2 Pd(II) Catalysed Aminocarbonylation of Alkenes

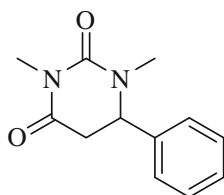
Procedure 1: Reactions performed at atmospheric pressure

$\text{Pd}(\text{MeCN})_2\text{Cl}_2$ (26 mg, 0.1 mmol, 0.1 eq), benzoquinone (120 mg, 1.1 mmol, 1.1 eq) and *N,N'*-dialkylurea (1 mmol, 1 eq) were added to a Schlenk tube. The reagents were dissolved in the relevant dry and degassed solvent (1 mL) to leave a homogeneous orange solution. CO was bubbled through the solution from a balloon via a needle for 5 min, in which time a purple solid precipitated. The tube was sealed with a suba seal, maintaining a positive pressure of CO by leaving the needle and balloon open. The vessel was heated at 60 °C for 20 min during which time the solid re-dissolved to leave a yellow solution. The alkene (2 mmol, 2 eq) was then added via a syringe into the vessel. The reaction was stirred at 60 °C for the appropriate amount of time (typically 6–18 h). The reaction was then cooled to room temperature and solvent removed *in vacuo*. The resulting residue was washed with DCM (2×5 mL) and the resulting solids (palladium metal and hydroquinone) removed via gravity filtration. The filtrate was concentrated *in vacuo* and the resulting brown oil purified by column chromatography, the appropriate eluent being indicated by TLC (nominally 100 % Et_2O or 1:1 EtOAc : PE).

Procedure 2: Reactions performed at increased pressure

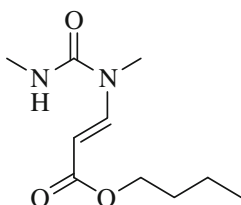
$\text{Pd}(\text{MeCN})_2\text{Cl}_2$ (26 mg, 0.1 mmol, 0.1 eq), benzoquinone (120 mg, 1.1 mmol, 1.1 eq) and *N,N'*-dialkylurea (1 mmol, 1 eq) were added to a 28 mL capacity vial. The reagents were dissolved in the relevant dry and degassed solvent (1 mL) to leave a homogeneous orange solution. The alkene (2 mmol, 2 eq) was added to the reaction mixture before the vial was fitted with screw lid pierced with a 2 mm diameter hole. The vessel was placed inside a 120 bar Parr autoclave which was subsequently sealed and flushed with 3×1 atm CO. The reaction was then placed under the relevant pressure of CO and heated to 60 °C for the appropriate amount of time (typically 4–16 h). Upon completion, the reaction was allowed to cool to room temperature and the reaction solvent removed *in vacuo*. The resulting residue was washed with DCM (2×5 mL) and the resulting solids (palladium metal and hydroquinone) removed via vacuum filtration. The filtrate was concentrated *in vacuo* and the resulting brown oil purified by column chromatography, the most appropriate eluent being indicated by TLC (nominally 100 % Et_2O or 1:1 Petrol: EtOAc).

1,3-Dimethyl-6-phenyldihydropyrimidine-2,4(1H,3H)-dione (18)



Aminocarbonylation procedure 2 was followed at a pressure of 20 bar using *N,N'*-dimethyl urea and styrene. The reaction mixture was purified by column chromatography (100 % Et₂O) to give the title pyrimidione (22 mg, 10 %) as a pale brown oil; *R_f* 0.28 (100 % Et₂O); ¹H NMR (400 MHz, CDCl₃): δ = 7.30–7.41 (m, 3H, ArH), 7.13–7.10 (m, 2H, ArH), 4.55 (dd, *J* = 7.0, 3.5 Hz, 1H, CH), 3.24 (s, 3H, CH₃NCOCO), 3.19 (dd, *J* = 16.5, 7.0 Hz, 1H, CHH), 3.03 (s, 3H, CH₃NCH), 2.88 (dd, *J* = 16.5, 3.5 Hz, 1H, CHH); ¹³C NMR (100 MHz, CDCl₃): δ = 168.1 (C), 154.1 (C), 138.4 (C), 129.4 (CH), 129.1 (CH), 128.6 (CH), 128.1 (CH), 125.8 (CH), 57.3 (CH), 39.1 (CH₂), 35.2 (CH₃), 27.7 (CH₃); IR (cm⁻¹) 1,677 (s), 1,643 (s); HRMS; *m/z* (CI), calculated for C₁₂H₁₅N₂O₂, 219.1133 [M + H]⁺, found 219.1131 [M + H]⁺.

(E)-Butyl 3-(1,3-dimethylureido)acrylate (20)



Aminocarbonylation procedure 1 was followed using *N,N'*-dimethyl urea and *n*butyl acrylate (*Note* Procedure 2 under CO pressures of up to 50 bar produced identical results). The reaction mixture was purified by column chromatography (1:1 EtOAc: PE) to give the title enamide (173 mg, 81 %) as a white solid; *R_f* 0.20 (1:1 EtOAc: PE); mp 95–98 °C; ¹H NMR (400 MHz, CDCl₃): δ = 8.20 (d, *J* = 14.0 Hz, 1H, NCH = CHCO), 5.72 (br. s, 1H, NH), 5.07 (d, *J* = 14.0 Hz, 1H, NCH = CHCO), 4.08 (t, *J* = 7.0 Hz, 2H, OCH₂CH₂), 3.07 (s, 3H, CH₃NH), 2.86 (d, *J* = 4.5 Hz, 3H, CH₃NCH = CH), 1.57–1.64 (m, 2H, OCH₂CH₂CH₂), 1.32–1.42 (m, 2H, CH₂CH₂CH₂CH₃), 0.91 (t, *J* = 7.0 Hz, 3H, CH₂CH₂CH₃); ¹³C NMR (100 MHz, CDCl₃): δ = 168.3 (C), 155.6 (C), 143.1 (CH), 95.7 (CH), 63.8 (CH₂), 31.2 (CH₃), 30.8 (CH₂), 27.8 (CH₃), 19.1 (CH₂), 13.7 (CH₃); IR (cm⁻¹) 3,379 (m), 2,962 (w), 1,707 (s), 1,660 (s), 1,627 (s), 1,530 (m); HRMS: *m/z* (CI), calculated for C₁₀H₁₉N₂O₃, 215.1401 [M + H]⁺, found 215.1396 [M + H]⁺.

7.3 Carbonylation of Aryl Ureas

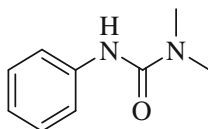
7.3.1 Preparation of Ureas

The preparation of non-commercial ureas was performed using the appropriate isocyanate and amine. For those which were volatile, amines were free-based from their hydrochloride salt using triethylamine at 0 °C, prior to the addition of

isocyanate. A representative example for the formation of 1,1-dimethyl-3-phenylurea is as follows:

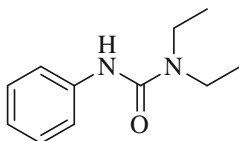
To a suspension of dimethylamine hydrochloride (3.26 g, 40 mmol, 1 eq) in dry dichloromethane (150 mL), triethylamine (5.46 mL, 40 mmol, 1 eq) was added and the reaction allowed to stir for 10 min at 0 °C. To this, phenyl isocyanate (3.69 mL, 34 mmol, 0.85 eq) was added slowly and the solution allowed to stir at room temperature for up to 16 h. The solution was washed using 2 M HCl (3 × 50 mL) and extracted into DCM (150 mL), dried over MgSO₄, filtered and the solvent removed *in vacuo*. The resulting white solid was recrystallised from toluene to yield pure urea (5.13 g, 92 %). (*Note* No triethylamine is required for a free amine source and in many cases the ureas were recovered by simple recrystallisation (from toluene) of the crude reaction mixture.)

1,1-Dimethyl-3-phenylurea (25)

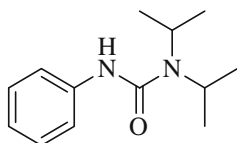


92 %; R_f 0.40 (100 % EtOAc); mp 134–135 °C (Ref: 132–134 °C); ¹H NMR (300 MHz, CDCl₃), δ = 7.35–7.39 (m, 2H, ArH), 7.24–7.30 (m, 2H, ArH), 6.98–7.04 (m, 1H, ArH), 6.37 (br. s, 1H, NH), 3.01 (s, 6H, N(CH₃)₂); ¹³C NMR (75 MHz, CDCl₃), δ = 155.8 (C), 139.3 (C), 129.0 (CH), 123.0 (CH), 119.9 (CH), 36.5 (CH₃); IR (cm⁻¹), 3,345 (w), 1,641 (s), 1,594 (s), 1,526 (s); HRMS: m/z (CI), calculated for C₉H₁₃N₂O, 165.1028 [M]⁺, found 165.1023 [M]⁺ [2].

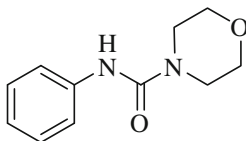
1,1-Diethyl-3-phenylurea (26)



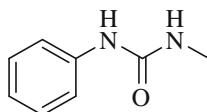
97 %; R_f 0.40 (1:1 EtOAc: PE); mp 90 °C (Ref: 86–88 °C); ¹H NMR (400 MHz, DMSO-*d*₆), δ = 8.12 (br. s, 1H, NH), 7.45–7.50 (m, 2H, ArH), 7.18–7.24 (m, 2H, ArH), 6.89–6.94 (m, 1H, ArH), 3.33 (q, J = 7.0 Hz, 4H, N(CH₂CH₃)₂), 1.08 (t, J = 7.0 Hz, 6H, N(CH₂CH₃)₂); ¹³C NMR (100 MHz, DMSO-*d*₆), δ = 154.4 (C), 140.7 (C), 128.1 (CH), 121.5 (CH), 120.0 (CH), 40.5 (CH₂), 13.9 (CH₃); IR (cm⁻¹) 3,297 (w), 2,974 (w), 2,932 (w), 1,635 (s), 1,593 (s), 1,526 (s); HRMS: m/z (CI), calculated for C₁₁H₁₇N₂O, 193.1341 [M + H]⁺, found 193.1347 [M + H]⁺ [3].

1,1-Diisopropyl-3-phenylurea (27)

71 %; R_f 0.59 (1:1 EtOAc: PE); mp 123–124 °C (Ref: 121–123 °C); ^1H NMR (400 MHz, CDCl_3), δ = 7.22–7.39 (m, 4H, ArH), 6.95–7.03 (m, 1H, ArH), 6.17 (br. s, 1H, NH), 3.98 (sept, J = 7.0 Hz, 2H, 2CH), 1.32 (d, J = 7.0 Hz, 12H, 4(CH₃)); ^{13}C NMR (100 MHz, CDCl_3), δ = 154.5 (C), 139.3 (C), 128.6 (CH), 122.4 (CH), 119.6 (CH), 45.4 (CH), 21.3 (CH₃); IR (cm^{-1}) 3,289 (w), 2,968 (w), 1,635 (s), 1,594 (s), 1,522 (s), 1,445 (s), 1,333 (s); HRMS: m/z (CI), calculated for $\text{C}_{13}\text{H}_{21}\text{N}_2\text{O}$, 221.1654 [$\text{M} + \text{H}$]⁺, found 221.1664 [$\text{M} + \text{H}$]⁺ [4].

1-Morpholine-3-phenylurea (28)

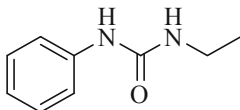
90 %; R_f 0.37 (100 % EtOAc); mp 158–160 °C (Ref: 156–159 °C); ^1H NMR (300 MHz, CDCl_3), δ = 7.26–7.36 (m, 4H, ArH), 7.02–7.07 (m, 1H, ArH), 6.41 (s, 1H, NH), 3.71–3.74 (m, 4H, OCH₂), 3.45–3.48 (m, 4H, NCH₂); ^{13}C NMR (75 MHz, CDCl_3), δ = 155.2 (C), 138.8 (C), 129.0 (CH), 123.5 (CH), 120.2 (CH), 66.6 (CH₂), 44.3 (CH₂); IR (cm^{-1}), 3,252 (w), 2,858 (w), 1,631 (s), 1,594 (s), 1,528 (s), 1,499 (s), 1,441 (s), 1,406 (s); HRMS: m/z (CI), calculated for $\text{C}_{11}\text{H}_{15}\text{N}_2\text{O}_2$, 207.1134 [$\text{M} + \text{H}$]⁺, found 207.1136 [$\text{M} + \text{H}$]⁺ [5].

1-Methyl-3-phenylurea (29)

56 %; R_f 0.08 (1:1 EtOAc: PE); mp 150–152 °C (Ref: 148–150 °C); ^1H NMR (300 MHz, $\text{DMSO}-d_6$), δ = 8.47 (br. s, 1H, ArNH), 7.39 (br. d, J = 8.0 Hz, 2H, ArH), 7.20 (br. t, J = 8.0 Hz, 2H, ArH), 6.87 (br. t, J = 8.0 Hz, 1H, ArH), 5.99 (br. q, J = 4.5 Hz, 1H, NHCH₃), 2.63 (d, J = 4.5 Hz, 3H, CH₃); ^{13}C NMR (75 MHz, $\text{DMSO}-d_6$), δ = 155.9 (C), 140.6 (C), 128.6 (CH), 121.0 (CH), 117.7 (CH), 26.3 (CH₃); IR (cm^{-1}), 3,290 (w), 2,975 (w), 2,933 (w), 1,635 (s), 1,592 (s),

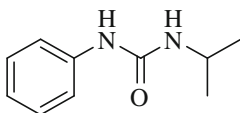
1,528 (s), 1,442 (s); HRMS: m/z (CI), calculated for $C_8H_{11}N_2O$, 151.0871 $[M + H]^+$, found 151.0867 $[M + H]^+$ [6].

1-Ethyl-3-phenylurea (21)



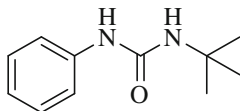
94 %; R_f 0.50 (100 % EtOAc); mp 100–101 °C (Ref: 92–95 °C); 1H NMR (270 MHz, $DMSO-d_6$), δ = 8.39 (s, 1H, ArNH), 7.35–7.39 (m, 2H, ArH), 7.17–7.24 (m, 2H, ArH), 6.84–6.90 (m, 1H, ArH), 6.07 (t, J = 6.0 Hz, 1H, CH_2NH), 3.10 (dq, J = 7.0, 6.0 Hz, 2H NCH_2), 1.05 (t, J = 7.0 Hz, 3H, CH_2CH_3); ^{13}C NMR (68 MHz, $DMSO-d_6$), δ = 155.7 (C), 141.2 (C), 129.2 (CH), 121.4 (CH), 118.2 (CH), 34.5 (CH_2), 16.0 (CH_3); IR (cm^{-1}), 3,308 (w), 1,643 (s), 1,603 (s), 1,544 (s); HRMS: m/z (CI), calculated for $C_9H_{12}N_2O$, 164.0949 $[M + H]^+$, found 164.0944 $[M + H]^+$ [7].

1-isoPropyl-3-phenylurea (31)



89 %; R_f 0.38 (1:1 EtOAc: PE); mp 157–158 °C (Ref: 155–156 °C); 1H NMR (300 MHz, $DMSO-d_6$), δ = 8.27 (br. s, 1H, ArNH), 7.37 (m, 2H, ArH), 7.20 (m, 2H, ArH), 6.87 (m, 1H, ArH), 5.98 (br. d, J = 7.0 Hz, 1H, NHCH), 3.76 (d of sept, J = 7.0, 6.5 Hz, 1H, CH), 1.08 (d, J = 6.5 Hz, 6H, 2(CH_3)); ^{13}C NMR (75 MHz, $DMSO-d_6$), δ = 154.5 (C), 140.6 (C), 128.6 (CH), 120.9 (CH), 117.5 (CH), 40.9 (CH), 23.0 (CH_3); IR (cm^{-1}), 3,340 (w), 2,977 (w), 2,965 (w), 1,636 (s), 1,595 (s); HRMS: m/z (CI), calculated for $C_{10}H_{15}N_2O$, 179.1184 $[M + H]^+$, found 179.1188 $[M + H]^+$ [8].

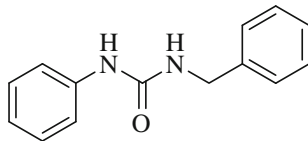
1-(tert-Butyl)-3-phenylurea (32)



68 %; R_f 0.57 (1:1 EtOAc: PE); mp 170–171 °C; 1H NMR (400 MHz, $DMSO-d_6$), δ = 8.21 (br. s, 1H, ArNH), 7.31–7.35 (m, 2H, ArH), 7.16–7.22 (m, 2H, ArH), 6.86 (m, 1H, ArH), 5.97 (br. s, 1H, NHC(CH_3)₃), 1.28 (s, 9H, C(CH_3)₃); ^{13}C NMR (100 MHz, $DMSO-d_6$), δ = 154.4 (C), 140.6 (C), 128.6 (CH), 120.7

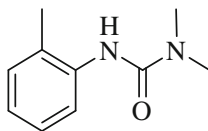
(CH), 117.3 (CH), 49.4 (C), 29.0 (CH₃); IR (cm⁻¹), 3,297 (w), 2,971 (w), 1,646 (s), 1,594 (s), 1,540 (s), 1,498 (s); HRMS: *m/z* (CI), calculated for C₁₁H₁₇N₂O, 193.1341 [M + H]⁺, found 193.1348 [M + H]⁺.

1-Benzyl-3-phenylurea (33)



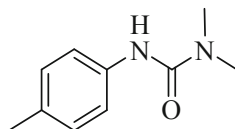
81 %; R_f 0.47 (1:1 EtOAc: PE); mp 173–174 °C (Ref: 169–171 °C); ¹H NMR (400 MHz, DMSO-*d*₆), δ = 8.55 (br. s, 1H, ArNH), 7.19–7.42 (m, 9H, ArH), 6.89 (br. t, *J* = 7.0 Hz, 1H, ArH), 6.60 (br. t, *J* = 7.0 Hz, 1H, NHCH₂), 4.30 (d, *J* = 7.0 Hz, 2H, CH₂); ¹³C NMR (100 MHz, DMSO-*d*₆), δ = 155.2 (C), 140.5 (C), 140.4 (C), 128.7 (CH), 128.3 (CH), 127.1 (CH), 126.7 (CH), 121.1 (CH) 117.7 (CH), 42.7 (CH₂); IR (cm⁻¹), 3,304 (w), 3,029 (w), 1,685 (w), 1,630 (s); HRMS: *m/z* (CI), calculated for C₁₄H₁₅N₂O, 227.1184 [M + H]⁺, found 227.1177 [M + H]⁺ [9].

1,1-Dimethyl-3-(*o*-tolyl)urea (43)



94 %; R_f 0.35 (100 % EtOAc); mp 143–144 °C; ¹H NMR (300 MHz, CDCl₃), δ = 7.69–7.72 (m, 1H, ArH), 7.13–7.20 (m, 2H, ArH), 6.97–7.02 (m, 1H, ArH), 6.12 (br. s, 1H, NH), 3.03 (s, 6H, N(CH₃)₂), 2.24 (s, 3H, ArCH₃); ¹³C NMR (75 MHz, CDCl₃), δ = 156.0 (C), 137.3 (C), 130.3 (CH), 128.3 (C), 126.8 (CH), 123.8 (CH), 122.5 (CH), 36.5 (CH₃), 17.9 (CH₃); IR (cm⁻¹), 3,264 (w), 1,635 (s), 1,482 (s); HRMS: *m/z* (CI), calculated for C₁₀H₁₅N₂O, 179.1176 [M + H]⁺, found 179.1184 [M + H]⁺.

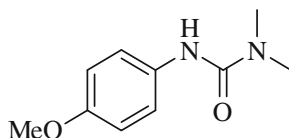
1,1-Dimethyl-3-(*p*-tolyl)urea (45)



97 %; R_f 0.37 (100 % EtOAc); mp 137–138 °C (Ref: 152–153 °C); ¹H NMR (270 MHz, CDCl₃), δ = 7.22–7.25 (m, 2H, ArH), 7.04–7.07 (m, 2H, ArH), 6.30

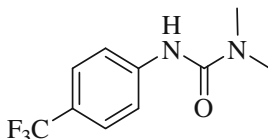
(br. s, 1H, **NH**), 2.99 (s, 6H, $\text{N}(\text{CH}_3)_2$), 2.27 (s, 3H, ArCH_3); ^{13}C NMR (68 MHz, CDCl_3), $\delta = 156.0$ (C), 136.6 (C), 132.6 (C), 129.4 (CH), 120.2 (CH), 36.5 (CH_3), 20.8 (CH_3); IR (cm^{-1}), 3,277 (w), 1,640 (s), 1,531 (s); HRMS: m/z (CI), calculated for $\text{C}_{10}\text{H}_{15}\text{N}_2\text{O}$, 179.1180 $[\text{M} + \text{H}]^+$, found 179.1184 $[\text{M} + \text{H}]^+$ [5].

3-(4-Methoxyphenyl)-1,1-dimethylurea (48)



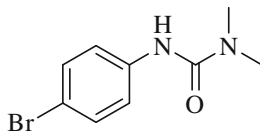
66 %; R_f 0.32 (100 % EtOAc); mp 131–132 °C (Ref: 130–132 °C); ^1H NMR (270 MHz, CDCl_3), $\delta = 7.23$ – 7.27 (m, 2H, **ArH**), 6.80–6.83 (m, 2H, **ArH**), 6.19 (br. s, 1H, **NH**), 3.76 (s, 3H, OCH_3), 3.00 (s, 6H, $\text{N}(\text{CH}_3)_2$); ^{13}C NMR (100 MHz, CDCl_3), $\delta = 155.9$ (C), 132.3 (C), 122.3 (CH), 114.2 (CH), 55.6 (CH_3), 36.6 (CH_3); IR (cm^{-1}), 3,299 (w), 1,638 (s), 1,509 (s); HRMS: m/z (CI), calculated for $\text{C}_{10}\text{H}_{15}\text{N}_2\text{O}_2$, 195.1130 $[\text{M} + \text{H}]^+$, found 195.1134 $[\text{M} + \text{H}]^+$ [5].

1,1-Dimethyl-3-(4-(trifluoromethyl)phenyl)urea (49)



43 %; R_f 0.11 (1:2 EtOAc: PE); mp 193–194 °C; ^1H NMR (400 MHz, CDCl_3), $\delta = 7.54$ (app. d, $J = 7.0$ Hz, 4H, **ArH**), 6.52 (br. s, 1H, **NH**), 3.07 (s, 6H, $\text{N}(\text{CH}_3)_2$); ^{13}C NMR (100 MHz, CDCl_3), $\delta = 155.2$ (C), 142.5 (C), 126.2 (q, $J = 3.6$ Hz, CH), 119.0 (CH), 36.6 (CH_3), quaternary CF_3 and C-CF_3 not observed; IR (cm^{-1}), 3,321 (w), 1,652 (s), 1,601 (m), 1,525, (s); HRMS: m/z (CI), calculated for $\text{C}_{10}\text{H}_{12}\text{N}_2\text{OF}_3$, 233.0902 $[\text{M} + \text{H}]^+$, found 233.0899 $[\text{M} + \text{H}]^+$.

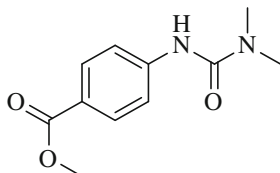
3-(4-Bromophenyl)-1,1-dimethylurea (51)



87 %; R_f 0.21 (1:1 EtOAc: PE); mp 163 °C (Ref: 169 °C); ^1H NMR (400 MHz, $\text{DMSO-}d_6$), $\delta = 8.40$ (br. s, 1H, **NH**), 7.43–7.48 (m, 2H, **ArH**), 7.36–7.41 (m, 2H, **ArH**), 2.91 (s, 6H, $\text{N}(\text{CH}_3)_2$); ^{13}C NMR (100 MHz, $\text{DMSO-}d_6$), $\delta = 155.5$ (C),

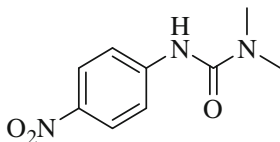
140.2 (C), 131.0 (CH), 121.4 (CH), 113.0 (C), 36.2 (CH₃); IR (cm⁻¹) 3,299 (w), 2,932 (w), 1,642 (s), 1,588 (s); HRMS: *m/z* (CI), calculated for C₉H₁₂N₂O⁷⁹Br, 243.0134 [M + H]⁺, found 243.0133 [M + H]⁺ [10].

Methyl 4-(3,3-dimethylureido)benzoate (53)



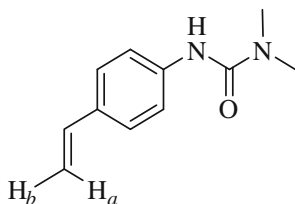
65 %; R_f 0.10 (1:1 EtOAc: PE); mp 174–175 °C (Ref: 168–170 °C); ¹H NMR (300 MHz, CDCl₃), δ = 7.91 (br. d, *J* = 8.5 Hz, 2H, ArH), 7.47 (br. d, *J* = 8.5 Hz, 2H, ArH), 6.88 (br. s, 1H, NH), 3.86 (s, 3H, OCH₃), 3.00 (s, 6H, N(CH₃)₂); ¹³C NMR (100 MHz, CDCl₃), δ = 166.8 (C), 155.0 (C), 143.7 (C), 130.7 (CH), 124.0 (C), 118.3 (CH), 51.8 (CH₃), 36.5 (CH₃); IR (cm⁻¹) 3,361 (w), 3,285 (w), 2,950 (w), 1,708 (s), 1,649 (s), 1,594 (s), 1,526 (s); HRMS: *m/z* (CI), calculated for C₁₁H₁₅N₂O₃, 223.1083 [M + H]⁺, found 223.1081 [M + H]⁺ [11].

1,1-Dimethyl-3-(4-nitrophenyl)urea (54)



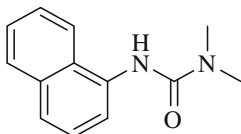
34 %; R_f 0.16 (1:1 EtOAc: PE); mp 224–225 °C; ¹H NMR (400 MHz, DMSO-*d*₆), δ = 9.01 (br. s, 1H, NH), 8.12–8.17 (m, 2H, ArH), 7.72–7.77 (m, 2H, ArH), 2.96 (s, 6H, N(CH₃)₂); ¹³C NMR (100 MHz, DMSO-*d*₆), δ = 154.9 (C), 147.6 (C), 140.7 (C), 124.7 (CH), 118.3 (CH), 36.3 (CH₃); IR (cm⁻¹) 3,344 (m), 2,929 (w), 1,655 (s), 1,608 (s), 1,596 (s); HRMS: *m/z* (CI), calculated for C₉H₁₂N₃O₃, 210.0879 [M + H]⁺, found 210.0885 [M + H]⁺.

1,1-Dimethyl-3-(4-vinylphenyl)urea (55)



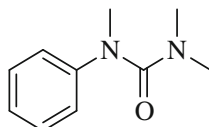
56 %; R_f 0.08 (1:1 EtOAc: PE); mp 130–132 °C; ^1H NMR (400 MHz, CDCl_3), $\delta = 7.26\text{--}7.27$ (m, 4H, ArH), 6.58 (dd, $J = 17.5, 11.0$ Hz, 1H, CH = CH₂), 5.33 (dd, $J = 17.5, 1.0$ Hz, 1H, CH = CHH_a), 5.07 (dd, $J = 11.0, 1.0$ Hz, 1H, CH = CH_bH), 2.95 (s, 6H, N(CH₃)₂); ^{13}C NMR (100 MHz, CDCl_3), $\delta = 155.5$ (C), 138.8 (C), 136.3 (C), 132.29 (CH), 126.7 (CH), 119.6 (CH), 112.1 (CH₂), 36.4 (CH₃); IR (cm^{-1}) 3,288 (w), 2,927 (w), 1,638 (s), 1,511 (s); HRMS: m/z (CI), calculated for C₁₁H₁₅N₂O, 191.118 [M + H]⁺, found 191.1175 [M + H]⁺.

1,1-Dimethyl-3-(naphthalen-1-yl)urea (57)



73 %; R_f 0.12 (1:1 EtOAc: PE); mp 174–175 °C (Ref: 170–171 °C); ^1H NMR (400 MHz, DMSO- d_6), $\delta = 8.37$ (br. s, 1H, NH), 7.87–7.97 (m, 2H, ArH), 7.71 (d, $J = 8.0$ Hz, 1H, ArH), 7.40–7.53 (m, 4H, ArH), 3.01 (s, 6H, N(CH₃)₂); ^{13}C NMR (100 MHz, DMSO- d_6), $\delta = 156.9$ (C), 135.8 (C), 133.8 (C), 129.5 (C), 127.9 (CH), 125.7 (CH), 125.5 (CH), 125.4 (CH), 124.8 (CH), 123.6 (CH), 122.8 (CH), 36.4 (CH₃); IR (cm^{-1}) 3261 (w), 3,052 (w), 2,936 (w), 1,636 (s), 1,597 (s), 1,528 (s); HRMS: m/z (CI), calculated for C₁₃H₁₅N₂O, 215.1184 [M + H]⁺, found 215.1187 [M + H]⁺ [12].

1,1,3-Trimethyl-3-phenylurea (69)



N,N,N'-Trimethyl-*N*-phenyl urea **69** was synthesised by refluxing methyl aniline (1.08 mL, 10 mmol, 1 eq), dimethyl carbamyl chloride (0.92 mL, 10 mmol, 1 eq) and 4-(dimethylamino)pyridine (122 mg, 1 mmol, 0.1 eq) in dichloromethane (50 mL). After 18 h the reaction mixture was allowed to cool and washed several times with HCl (1 M) and then water. The organic layer was dried with MgSO₄, filtered and concentrated *in vacuo* to a colourless oil. 400 mg (22 %). R_f 0.25 (1:1 EtOAc: PE); oil; ^1H NMR (400 MHz, CDCl_3), $\delta = 7.25\text{--}7.31$ (m, 2H, ArH), 7.00–7.08 (m, 3H, ArH), 3.18 (s, 3H, ArNCH₃), 2.65 (s, 6H, N(CH₃)₂); ^{13}C NMR (100 MHz, CDCl_3), $\delta = 161.7$ (C), 146.7 (C), 129.2 (CH), 124.0 (CH), 123.4 (CH), 39.4 (CH₃), 37.7 (CH₃); IR (cm^{-1}) 2,933 (w), 1,644 (s), 1,595 (s), 1,490 (s); HRMS: m/z (CI), calculated for C₁₀H₁₅N₂O, 179.1184 [M + H]⁺, found 179.1192 [M + H]⁺.

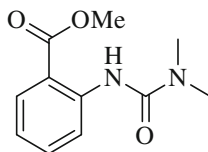
7.3.2 Preparation of $\text{Pd}(\text{OTs})_2(\text{MeCN})_2$

$\text{Pd}(\text{OTs})_2(\text{MeCN})_2$ was prepared using a variation of the procedure reported by Drent et al. [13] $\text{Pd}(\text{OAc})_2$ (2.65 g, 11.7 mmol, 1 eq) was dissolved in stirring dry acetonitrile (230 mL). *p*-Toluenesulfonic acid monohydrate (12 g, 63.2 mmol, 5.4 eq) in dry acetonitrile (150 mL) was added slowly over 10 min effecting a colour change to yellow. After complete addition, the solution was cooled to 0 °C and Et_2O (280 mL) was added slowly over 30 min affecting a precipitation of the title compound towards the end of the addition. The resulting slurry was filtered and dried *in vacuo* to yield $\text{Pd}(\text{OTs})_2(\text{MeCN})_2$ as a yellow powder. *Note* Up to an extra 20 % yield can be obtained if the filtrate is placed in a freezer for 18 h and re-filtered. All analytical data matches that reported in the literature [13].

7.3.3 Procedure for the Preparation of Ortho-Ester Aryl Ureas

The desired urea (1 mmol, 1 eq), benzoquinone (216 mg, 2 mmol, 2 eq), palladium ditosylate bisacetonitrile (26 mg, 5 mol %, 0.05 eq) and tosic acid monohydrate (95 mg, 0.5 mmol, 0.5 eq) were loaded into a reaction vessel equipped with a stirring bead. THF (0.5 mL) and methanol (0.5 mL) were then added and the mixture stirred at room temperature. The reaction vessel was then briefly put under vacuum followed by charging with CO. This procedure was repeated several times to ensure a headspace flushed with 1 atm. CO. Reaction progress was monitored by TLC. On completion (2–5 h), the reaction mixture was concentrated *in vacuo*, the residue dissolved in DCM and washed with HCl (1 M). The organic layer was then washed with water, dried over MgSO_4 , filtered and concentrated *in vacuo*. Purification by flash chromatography (10–40 % EtOAc/PE afforded the pure products. (*Note* The main purpose of this workup is to remove hydroquinone, if the product is easily separable from hydroquinone by column chromatography then the reaction mixture can be loaded directly onto the silica column).

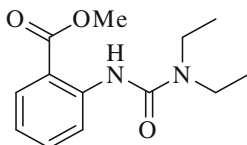
Methyl 2-(3,3-dimethylureido)benzoate (34)



88 %; R_f 0.36 (1:1 EtOAc: PE); mp 90–92 °C (Ref: 88–89 °C); ^1H NMR (300 MHz, $\text{DMSO}-d_6$), δ = 10.39 (br. s, 1H, **NH**), 8.45 (dd, J = 8.5, 1.0 Hz, 1H, **ArH**), 7.93 (dd, J = 8.5, 1.0 Hz, 1H, **ArH**), 7.54 (ddd, J = 8.5, 7.0, 1.0 Hz, 1H,

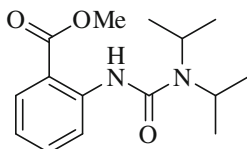
ArH), 7.02 (ddd, $J = 8.5, 7.0, 1.0$ Hz, 1H, ArH), 3.87 (s, 3H, OCH₃), 2.98 (s, 6H, N(CH₃)₂); ¹³C NMR (76 MHz, DMSO-*d*₆), $\delta = 168.5$ (C), 154.6 (C), 142.9 (C), 134.3 (CH), 130.5 (CH), 120.6 (CH), 118.9 (CH), 113.9 (C), 52.4 (CH₃), 35.8 (CH₃); IR (cm⁻¹), 3,262 (w), 2,950 (w), 1,693 (s), 1,665 (s); HRMS: m/z (CI), calculated for C₁₁H₁₅N₂O₃, 223.1083 [M + H]⁺, found 223.1078 [M + H]⁺ [14].

Methyl 2-(3,3-diethylureido)benzoate (35)

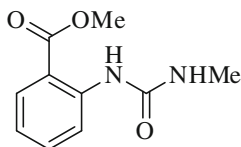


76 %; R_f 0.51 (1:1 EtOAc: PE); oil; ¹H NMR (400 MHz, CDCl₃), $\delta = 10.59$ (br. s, 1H, NH), 8.59 (app. d, $J = 8.5$ Hz, 1H, ArH), 7.97 (dd, $J = 8.5, 2.0$ Hz, 1H, ArH), 7.47 (ddd, $J = 8.5, 7.0, 2.0$ Hz, 1H, ArH), 6.89–6.96 (m, 1H, ArH), 3.89 (s, 3H, OCH₃), 3.42 (q, $J = 7.0$ Hz, 4H, N(CH₂CH₃)₂), 1.24 (t, $J = 7.0$ Hz, 6H, N(CH₂CH₃)₂); ¹³C NMR (100 MHz, CDCl₃), $\delta = 169.2$ (C), 154.5 (C), 143.8 (C), 134.5 (CH), 130.6 (CH), 120.3 (CH), 119.4 (CH), 113.7 (C), 52.1 (CH₃) 41.5 (CH₂), 13.7 (CH₃); IR (cm⁻¹), 3,313 (w), 2,975 (w), 1,666 (s), 1,588 (s), 1,528 (s); HRMS: m/z (CI), calculated for C₁₃H₁₉N₂O₃, 251.1396 [M + H]⁺, found 251.1384 [M + H]⁺.

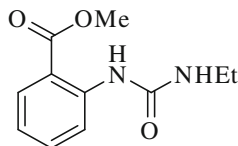
Methyl 2-(3,3-diisopropylureido)benzoate (36)



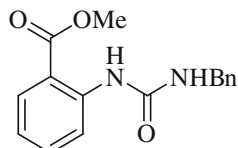
55 %; R_f 0.65 (1:1 EtOAc: PE); oil; ¹H NMR (400 MHz, DMSO-*d*₆), $\delta = 10.11$ (br. s, 1H, NH), 8.30 (dd, $J = 8.5, 1.5$ Hz, 1H, ArH), 7.91 (dd, $J = 8.5, 1.5$ Hz, 1H, ArH), 7.50 (ddd, $J = 8.5, 7.0, 1.5$ Hz, 1H, ArH), 6.98 (ddd, $J = 8.5, 7.0, 1.5$ Hz, 1H, ArH) 3.87 (sept, $J = 6.5$ Hz, 2H, 2CH), 3.85 (s, 3H, OCH₃), 1.27 (d, $J = 6.5$ Hz, 12H, 4(CH₃)); ¹³C NMR (76 MHz, DMSO-*d*₆), $\delta = 168.5$ (C), 153.2 (C), 143.2 (C), 134.2 (CH), 130.5 (CH), 120.4 (CH), 119.7 (CH), 114.0 (C), 52.5 (CH₃) 45.8 (CH), 20.8 (CH₃); IR (cm⁻¹), 3,316 (w), 2,970 (w), 1,664 (s), 1,587 (s); HRMS: m/z (CI), calculated for C₁₅H₂₃N₂O₃, 279.1709 [M + H]⁺, found 279.1704 [M + H]⁺.

Methyl 2-(3-methylureido)benzoate (38)

61 %; R_f 0.32 (1:1 EtOAc: PE); mp 117–120 °C (Ref: 113 °C); ^1H NMR (400 MHz, CDCl_3), δ = 10.37 (br. s, 1H, ArNH), 8.54 (dd, J = 8.5, 1.0 Hz, 1H, ArH), 7.98 (dd, J = 8.5, 1.0 Hz, 1H, ArH), 7.47–7.54 (m, 1H, ArH), 6.93–7.00 (m, 1H, ArH) 4.76 (br. s, 1H, NHCH₃), 3.90 (s, 3H, OCH₃), 2.91 (d, J = 5.0 Hz, 3H, NHCH₃); ^{13}C NMR (100 MHz, CDCl_3), δ = 169.2 (C), 155.7 (C), 143.3 (C), 134.6 (CH), 130.7 (CH), 120.6 (CH), 119.4 (CH), 113.6 (C), 52.1 (CH₃), 27.2 (CH₃); IR (cm^{-1}), 3,310 (w), 2,946 (w), 1,706 (s), 1,654 (s), 1,560 (s); HRMS: m/z (CI), calculated for $\text{C}_{10}\text{H}_{13}\text{N}_2\text{O}_3$, 209.0926 [M + H]⁺, found 209.0929 [M + H]⁺ [14].

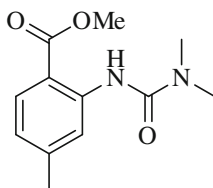
Methyl 2-(3-ethylureido)benzoate (24)

81 %; R_f 0.36 (1:1 EtOAc: PE); mp 125–128 °C; ^1H NMR (300 MHz, CDCl_3), δ = 10.31 (br. s, 1H, ArNH), 8.53 (dd, J = 8.5, 1.0 Hz, 1H, ArH), 7.96 (dd, J = 8.5, 1.0 Hz, 1H, ArH), 7.44–7.52 (m, 1H, ArH), 6.91–6.98 (m, 1H, ArH) 4.92 (br. s, 1H, NHCH₂), 3.88 (s, 3H, OCH₃), 3.33 (qd, J = 7.5, 5.5 Hz, 2H, CH₂), 1.20 (d, J = 7.5 Hz, 3H, CH₂CH₃); ^{13}C NMR (100 MHz, CDCl_3), δ = 169.1 (C), 155.0 (C), 143.3 (C), 134.5 (CH), 130.6 (CH), 120.5 (CH), 119.4 (CH), 113.6 (C), 52.1 (CH₃), 35.3 (CH₂), 15.1 (CH₃); IR (cm^{-1}), 3,308 (w), 2,967 (w), 2,948 (w), 1,710 (s), 1,648 (s); HRMS: m/z (CI), calculated for $\text{C}_{11}\text{H}_{15}\text{N}_2\text{O}_3$, 223.1083 [M + H]⁺, found 223.1089 [M + H]⁺.

Methyl 2-(3-benzylureido)benzoate (42)

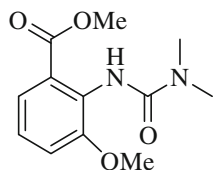
85 %; R_f 0.59 (1:1 EtOAc: PE); mp 139–140 °C; $^1\text{H NMR}$ (400 MHz, $\text{DMSO-}d_6$), δ = 9.86 (br. s, 1H, ArNH), 8.39 (br. d, J = 8.5 Hz, 1H, ArH), 8.05 (br. t, J = 5.5 Hz, 1H, NHCH₂), 7.90 (dd, J = 8.5, 1.5 Hz, 1H, ArH), 7.51 (ddd, J = 8.0, 7.0, 1.5 Hz, 1H, ArH), 7.21–7.36 (m, 5H, CH₂C₆H₅), 6.96–7.02 (m, 1H, ArH), 4.30 (d, J = 6.0 Hz, 2H, CH₂), 3.85 (s, 3H, OCH₃); $^{13}\text{C NMR}$ (100 MHz, $\text{DMSO-}d_6$), δ = 167.8 (C), 154.7 (C), 142.7 (C), 140.1 (CH), 134.0 (CH), 130.5 (CH), 128.3 (CH), 127.3 (CH), 126.8 (CH), 120.4 (CH), 119.6 (CH), 114.2 (C), 52.2 (CH₃), 42.9 (CH₂); IR (cm⁻¹), 3,288 (w), 2,968 (w), 2,927 (w), 1,634 (s), 1,593 (s), 1,522 (s); HRMS: m/z (CI), calculated for C₁₆H₁₇N₂O₃, 285.1239 [M + H]⁺, found 285.1237 [M + H]⁺.

Methyl 2-(3,3-dimethylureido)-4-methylbenzoate (59)

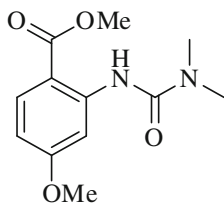


85 %; R_f 0.53 (1:1 EtOAc: PE); mp 73–74 °C; $^1\text{H NMR}$ (400 MHz, CDCl_3), δ = 10.63 (br. s, 1H, NH), 8.43 (br. s, 1H, ArH), 7.87 (d, J = 8.0 Hz, 1H, ArH), 6.77 (dd, J = 8.0, 1.0 Hz, 1H, ArH), 3.88 (s, 3H, OCH₃), 3.08 (s, 6H, N(CH₃)₂), 2.36 (s, 3H, ArCH₃); $^{13}\text{C NMR}$ (100 MHz, CDCl_3), δ = 169.3 (C), 155.7 (C), 145.7 (C), 143.5 (C), 130.5 (CH), 121.7 (CH), 119.6 (CH), 111.2 (C), 52.0 (CH₃), 36.3 (CH₃), 22.1 (CH₃); IR (cm⁻¹), 3,246 (w), 2,953 (w), 1,664 (s), 1,616 (s); HRMS: m/z (CI), calculated for C₁₂H₁₇N₂O₃, 237.1239 [M + H]⁺, found 237.1231 [M + H]⁺.

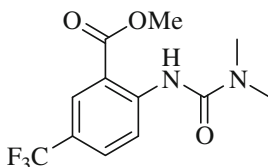
Methyl 2-(3,3-dimethylureido)-3-methoxybenzoate (61)



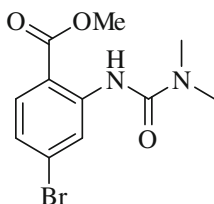
15 %; R_f 0.33 (1:1 EtOAc: PE); mp 116–118 °C; $^1\text{H NMR}$ (300 MHz, CDCl_3), δ = 8.00 (br. s, 1H, NH), 7.44 (dd, J = 7.0, 2.5 Hz, 1H, ArH), 7.01–7.12 (m, 2H, ArH), 3.86 (s, 3H, OCH₃), 3.85 (s, 3H, OCH₃), 3.05 (s, 6H, N(CH₃)₂); $^{13}\text{C NMR}$ (76 MHz, CDCl_3), δ = 169.1 (C), 164.5 (C), 155.6 (C), 145.9 (C), 132.1 (CH), 108.7 (CH), 106.2 (C), 101.9 (CH), 55.3 (CH₃), 51.8 (CH₃), 36.3 (CH₃); IR (cm⁻¹), 3,248 (w), 2,950 (w), 1,660 (s), 1,614 (s), 1,590 (s); HRMS: m/z (CI), calculated for C₁₂H₁₇N₂O₄, 253.2664 [M + H]⁺, found 253.2668 [M + H]⁺.

Methyl 2-(3,3-dimethylureido)-4-methoxybenzoate (62)

26 %; R_f 0.44 (1:1 EtOAc: PE); mp 98–99 °C; ^1H NMR (300 MHz, CDCl_3), δ = 10.88 (br. s, 1H, NH), 8.31 (d, J = 2.5 Hz, 1H, ArH), 7.90 (d, J = 9.0 Hz, 1H, ArH), 6.49 (dd, J = 9.0, 2.5 Hz, 1H, ArH), 3.87 (s, 3H, OCH_3), 3.86 (s, 3H, OCH_3), 3.09 (s, 6H, $\text{N}(\text{CH}_3)_2$); ^{13}C NMR (100 MHz, CDCl_3), δ = 169.1 (C), 164.5 (C), 155.6 (C), 145.9 (C), 132.1 (CH), 108.7 (CH), 106.2 (C), 101.9 (CH), 55.3 (CH_3), 51.8 (CH_3), 36.3 (CH_3); IR (cm^{-1}), 3,304 (w), 3,261 (w), 2,937 (w), 1,656 (s), 1,615 (s); HRMS: m/z (CI), calculated for $\text{C}_{12}\text{H}_{17}\text{N}_2\text{O}_4$, 253.1188 $[\text{M} + \text{H}]^+$, found 253.1183 $[\text{M} + \text{H}]^+$.

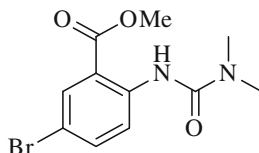
Methyl 2-(3,3-dimethylureido)-5-(trifluoromethyl)benzoate (64)

5 %; R_f 0.45 (1:1 EtOAc: PE); mp 173–174 °C; ^1H NMR (400 MHz, CDCl_3), δ = 10.85 (br. s, 1H, NH), 8.77 (d, J = 9.0 Hz, 1H, ArH), 8.27 (d, J = 2.0 Hz, 1H, ArH), 7.71 (dd, J = 9.0, 2.0 Hz, 1H, ArH), 3.96 (s, 3H, OCH_3), 3.11 (s, 6H, $\text{N}(\text{CH}_3)_2$); ^{13}C NMR (75 MHz, CDCl_3), δ = 168.4 (C), 155.1 (C), 146.3 (C), 131.0 (q, J = 3.9, CH), 128.1 (q, J = 4.4 Hz, CH), 122.4 (q, J = 33.5 Hz, C), 119.5 (CH), 113.2 (C), 52.6 (CH_3), 36.4 (CH_3), (CF_3 not observed); IR (cm^{-1}), 3,253 (w), 3,212 (w), 2,955 (w), 1,702 (s), 1,676 (s), 1,604 (s); HRMS: m/z (CI), calculated for $\text{C}_{12}\text{H}_{14}\text{N}_2\text{O}_3\text{F}_3$, 291.0957 $[\text{M} + \text{H}]^+$, found 291.0954 $[\text{M} + \text{H}]^+$.

Methyl 4-bromo-2-(3,3-dimethylureido)benzoate (65)

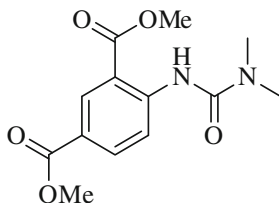
70 %; R_f 0.56 (1:1 EtOAc: PE); oil; $^1\text{H NMR}$ (400 MHz, CDCl_3), $\delta = 10.63$ (br. s, 1H, NH), 8.85 (d, $J = 2.0$ Hz, 1H, ArH), 7.76 (d, $J = 8.5$ Hz, 1H, ArH), 7.02 (dd, $J = 8.5, 2.0$ Hz, 1H, ArH), 3.86 (s, 3H, OCH_3), 3.03 (s, 6H, $\text{N}(\text{CH}_3)_2$); $^{13}\text{C NMR}$ (100 MHz, CDCl_3), $\delta = 168.6$ (C), 154.9 (C), 144.3 (C), 131.6 (CH), 129.5 (C), 123.5 (CH), 121.9 (CH), 112.1 (C), 52.2 (CH_3), 36.1 (CH_3); IR (cm^{-1}), 3,079 (w), 1,674 (s), 1,595 (s), 1,581 (s); HRMS: m/z (CI), calculated for $\text{C}_{11}\text{H}_{14}\text{N}_2\text{O}_3^{\text{Br}}$, 301.1365 $[\text{M} + \text{H}]^+$, found 301.1368 $[\text{M} + \text{H}]^+$.

Methyl 5-bromo-2-(3,3-dimethylureido)benzoate (66)



40 %; R_f 0.26 (1:1 EtOAc: PE); mp 140 °C; $^1\text{H NMR}$ (400 MHz, CDCl_3), $\delta = 10.6$ (br. s, 1H, NH), 8.51 (d, $J = 9.0$ Hz, 1H, ArH), 8.11 (d, $J = 2.5$ Hz, 1H, ArH), 7.57 (dd, $J = 9.0, 2.5$ Hz, 1H, ArH), 3.92 (s, 3H, OCH_3), 3.08 (s, 6H, $\text{N}(\text{CH}_3)_2$); $^{13}\text{C NMR}$ (100 MHz, CDCl_3), $\delta = 168.2$ (C), 153.9 (C), 142.6 (C), 137.2 (CH), 133.0 (CH), 121.2 (CH), 116.0 (C), 112.7 (C), 52.5 (CH_3), 36.3 (CH_3); IR (cm^{-1}), 3,244 (w), 2,953 (w), 1,700 (m), 1,670 (s), 1,592 (s); HRMS: m/z (CI), calculated for $\text{C}_{11}\text{H}_{14}\text{N}_2\text{O}_3^{\text{Br}}$, 301.1365 $[\text{M} + \text{H}]^+$, found 301.1363 $[\text{M} + \text{H}]^+$.

Dimethyl 4-(3,3-dimethylureido)isophthalate (68)

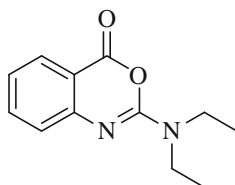


36 %; R_f 0.40 (1:1 EtOAc: PE); mp 137 °C; $^1\text{H NMR}$ (400 MHz, CDCl_3), $\delta = 10.91$ (br. s, 1H, NH), 8.65–8.69 (m, 2H, ArH), 8.1 (dd, $J = 9.0, 2.0$ Hz, 1H, ArH), 3.92 (s, 3H, OCH_3), 3.88 (s, 3H, OCH_3), 3.08 (s, 6H, $\text{N}(\text{CH}_3)_2$); $^{13}\text{C NMR}$ (100 MHz, CDCl_3), $\delta = 168.7$ (C), 166.0 (C), 154.9 (C), 147.2 (C), 135.3 (CH), 132.8 (CH), 121.9 (C), 118.6 (CH), 113.1 (C), 52.4 (CH_3), 52.0 (CH_3), 36.3 (CH_3); IR (cm^{-1}), 3,251 (w), 2,952 (w), 1,717 (m), 1,694 (m), 1,672 (s), 1,591 (s), 1,433 (s); HRMS: m/z (CI), calculated for $\text{C}_{13}\text{H}_{17}\text{N}_2\text{O}_5$, 281.1059 $[\text{M} + \text{H}]^+$, found 281.1062 $[\text{M} + \text{H}]^+$.

7.3.4 Procedure for the Preparation of Cyclic Imidates

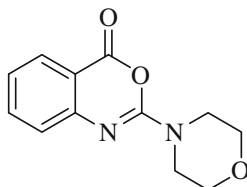
The desired urea (1 mmol, 1 eq), benzoquinone (216 mg, 2 mmol, 2 eq), Pd(OTs)₂(MeCN)₂ (52 mg, 10 mol %, 0.1 eq) and *p*-toluenesulfonic acid monohydrate (190 mg, 1 mmol, 1 eq) were loaded into the reaction vessel containing a stirring bead. The reaction vessel was then briefly put under vacuum followed by charging with CO. This procedure was repeated several times to ensure a head-space flushed with CO (1 atm). DCM (1 mL) was then added and the mixture stirred at room temperature. The reaction was followed by TLC. Reaction time was between 2–5 h. On completion the mixture was diluted with DCM and washed with Na₂CO₃ (sat sol.). The DCM layer was extracted and set to one side. The aqueous layer was then washed with EtOAc (3 × 20 mL) and the organic layer collected. Both organic fractions were then combined and concentrated *in vacuo* onto silica. Purification by column chromatography (PE/EtOAc) afforded the pure product. (*Note* these compounds decompose at elevated temperatures and over time. Care should be taken when removing the solvent and with storage).

2-(Diethylamino)-4H-benzo[d][1,3]oxazin-4-one (71)



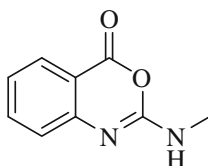
50 %; R_f 0.65 (1:1 EtOAc: PE); oil; ¹H NMR (400 MHz, CDCl₃), δ = 7.98 (m, 1H, ArH), 7.58 (m, 1H, ArH), 7.21 (m, 1H, ArH), 7.08 (m, 1H, ArH), 3.55 (q, *J* = 7.0 Hz, 4H, N(CH₂CH₃)₂), 1.25 (t, *J* = 7.0 Hz, 6H, N(CH₂CH₃)₂); ¹³C NMR (100 MHz, CDCl₃), δ = 160.3 (C), 153.4 (C), 151.4 (C), 136.4 (CH), 128.5 (CH), 124.0 (CH), 122.6 (CH), 112.1 (C), 42.1 (CH₂), 13.3 (CH₂); IR (cm⁻¹), 2,976 (w), 2,935 (w), 1,753 (s), 1,618 (m), 1,588 (s), 1,566 (s); HRMS: *m/z* (CI), calculated for C₁₂H₁₅N₂O₂, 219.1134 [M + H]⁺, found 219.1127 [M + H]⁺.

2-Morpholino-4H-benzo[d][1,3]oxazin-4-one (73)



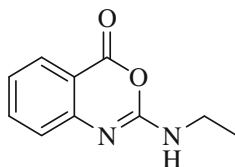
49 %; R_f 0.53 (1:1 EtOAc: PE); mp 156–158 °C (Ref: 157 °C); ^1H NMR (400 MHz, CDCl_3), δ = 8.01 (dd, J = 8.0, 1.5 Hz, 1H, ArH), 7.62 (m, 1H, ArH), 7.24 (br. d, J = 8.0 Hz, 1H, ArH), 7.13–7.19 (m, 1H, ArH), 3.72–3.80 (m, 8H, $\text{N}(\text{CH}_2\text{CH}_2)_2\text{O}$); ^{13}C NMR (100 MHz, CDCl_3), δ = 159.6 (C), 153.2 (C), 150.4 (C), 136.7 (CH), 128.7 (CH), 124.3 (CH), 123.6 (CH), 112.5 (C), 66.3 (CH_2), 44.3 (CH_2); IR (cm^{-1}), 2,922 (w), 2,872 (w), 1,764 (s), 1,598 (s), 1,568 (s), 1,474 (s); HRMS: m/z (CI), calculated for $\text{C}_{12}\text{H}_{13}\text{N}_2\text{O}_3$, 233.0926 $[\text{M} + \text{H}]^+$, found 233.0930 $[\text{M} + \text{H}]^+$ [15].

2-(Methylamino)-4H-benzo[d][1,3]oxazin-4-one (74)

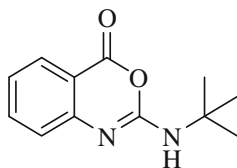


34 %; R_f 0.38 (1:1 EtOAc: PE); mp 198–200 °C (Ref: 202–203 °C); ^1H NMR (400 MHz, $\text{DMSO}-d_6$), δ = 7.89 (app. q, J = 5.0 Hz, 1H, NH), 7.87 (m, 1H, ArH), 7.66 (m, 1H, ArH), 7.21 (br. d, J = 8.0 Hz, 1H, ArH), 7.15 (m, 1H, ArH), 2.81 (d, J = 5.0 Hz, 3H, CH_3); ^{13}C NMR (100 MHz, $\text{DMSO}-d_6$), δ = 159.7 (C), 154.8 (C), 151.4 (C), 136.9 (CH), 128.2 (CH), 123.9 (CH), 123.1 (CH), 110.9 (C), 27.7 (CH_3); IR (cm^{-1}), 3,298 (w), 1,739 (s), 1,627 (s), 1,596 (s), 1,473 (s); HRMS: m/z (CI), calculated for $\text{C}_9\text{H}_9\text{N}_2\text{O}_2$, 177.0664 $[\text{M} + \text{H}]^+$, found 177.0656 $[\text{M} + \text{H}]^+$ [15].

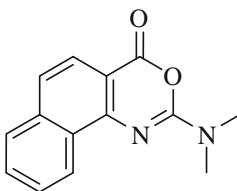
2-(Ethylamino)-4H-benzo[d][1,3]oxazin-4-one (23)



R_f 0.50 (1:1 EtOAc: PE); 177–178 °C (Ref: 169–171 °C); ^1H NMR (400 MHz, CDCl_3), δ = 8.03 (m, 1H, ArH), 7.64 (m, 1H, ArH), 7.28 (br. d, J = 8.0 Hz, 1H, ArH), 7.18 (m, 1H, ArH), 4.90 (br. s, 1H, NH), 3.50 (qd, J = 7.5, 7.0 Hz, 2H, CH_2), 1.29 (t, J = 7.0 Hz, 3H, CH_3); ^{13}C NMR (75 MHz, $\text{DMSO}-d_6/\text{CDCl}_3$), δ = 159.4 (C), 153.8 (C), 150.7 (C), 136.0 (CH), 127.8 (CH), 123.6 (CH), 122.3 (CH), 112.4 (C), 35.5 (CH_2), 14.0 (CH_3); IR (cm^{-1}), 3,297 (s), 2,982 (w), 1,735 (s), 1,627 (s), 1,598 (s), 1,473 (s); HRMS: m/z (CI), calculated for $\text{C}_{10}\text{H}_{11}\text{N}_2\text{O}_2$, 191 $[\text{M} + \text{H}]^+$, found 191 $[\text{M} + \text{H}]^+$ [15].

2-(*tert*-Butylamino)-4H-benzo[d][1,3]oxazin-4-one (76)

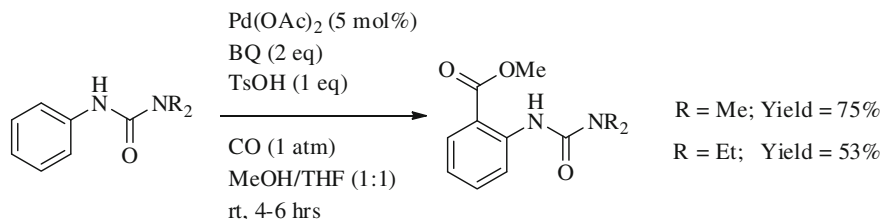
85 %; R_f 0.70 (1:1 EtOAc: PE); mp 127–128 °C; ^1H NMR (400 MHz, CDCl_3), δ = 8.02 (m, 1H, ArH), 7.62 (m, 1H, ArH), 7.27 (br. d, J = 7.5 Hz, 1H, ArH), 7.16 (m, 1H, ArH), 4.82 (br. s, 1H, NH), 1.49 (s, 9H, $\text{C}(\text{CH}_3)_3$); ^{13}C NMR (100 MHz, CDCl_3), δ = 160.2 (C), 152.0 (C), 150.4 (C), 136.5 (CH), 128.6 (CH), 124.5 (CH), 123.5 (CH), 113.3 (C), 51.9 (CH), 28.8 (CH_3); IR (cm^{-1}), 3296 (m), 2973 (w), 1,737 (s), 1,627 (s), 1,605 (s), 1,569 (s), 1,474 (s); HRMS: m/z (CI), calculated for $\text{C}_{12}\text{H}_{15}\text{N}_2\text{O}_2$, 219.1134 $[\text{M} + \text{H}]^+$, found 219.1142 $[\text{M} + \text{H}]^+$.

2-(Dimethylamino)-4H-naphtho[1,2-d][1,3]oxazin-4-one (77)

54 %; R_f 0.48 (1:1 EtOAc: PE); 183–184 °C; ^1H NMR (400 MHz, CDCl_3), δ = 8.77 (m, 1H, ArH), 7.90 (d, J = 8.5 Hz, 1H, ArH), 7.81 (m, 1H, ArH), 7.67 (ddd, J = 8.5, 7.0, 1.5 Hz, 1H, ArH), 7.59 (ddd, J = 8.5, 7.0, 1.5 Hz, 1H, ArH), 7.49 (d, J = 8.5 Hz, 1H, ArH), 3.30 (br. s, 6H, $\text{N}(\text{CH}_3)_2$); ^{13}C NMR (100 MHz, CDCl_3), δ = 160.4 (C), 155.4 (C), 151.1 (C), 137.5 (C), 129.8 (CH), 128.3 (C), 127.8 (CH), 126.1 (CH), 125.4 (CH), 122.9 (CH), 122.6 (CH), 113.2 (C), 33.2 (CH_3); IR (cm^{-1}) 3,261 (w), 2,927 (w), 1,733 (s), 1,609 (s), 1,598 (s), 1,564 (s); HRMS: m/z (CI), calculated for $\text{C}_{14}\text{H}_{13}\text{N}_2\text{O}_2$, 241.0977 $[\text{M} + \text{H}]^+$, found 241.0973 $[\text{M} + \text{H}]^+$.

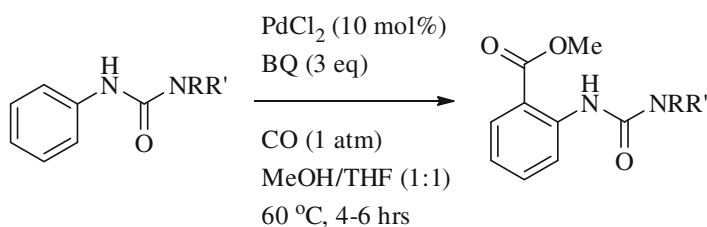
7.3.5 Use of $\text{Pd}(\text{OAc})_2$

Same as Sect. 7.3.3 except $\text{Pd}(\text{OAc})_2$ (11 mg, 5 mol %) used instead of palladium ditosylate bisacetonitrile and the amount of tosic acid monohydrate raised to 1 mmol (190 mg).



7.3.6 Use of PdCl_2

The desired urea (1 mmol, 1 eq), benzoquinone (324 mg, 3 mmol, 3 eq) and palladium dichloride (17 mg, 10 mol %, 0.1 eq) were loaded into a reaction vessel equipped with a stirring bead. Methanol (1 mL) was then added and the mixture stirred at room temperature. The reaction vessel was then briefly put under vacuum followed by charging with CO. This procedure was repeated several times to ensure a headspace flushed with 1 atm CO. The reaction was then heated to 60 °C. Reaction progress was monitored by TLC. On completion (4–6 h), the reaction mixture was concentrated *in vacuo*, the residue dissolved in DCM and washed with HCl (1 M). The organic layer was then washed with water, dried over MgSO_4 , filtered and concentrated *in vacuo*. Purification by flash chromatography (10–40 % EtOAc/PE) afforded the pure products. (*Note* The main purpose of this workup is to remove hydroquinone, if the product is easily separable from hydroquinone by column chromatography then the reaction mixture can be loaded directly onto the silica column).



R	R'	Yield (%)
Me	Me	60
Me	H	50
Et	H	69

(continued)

(continued)

R	R'	Yield (%)
<i>i</i> Pr	H	60
<i>t</i> Bu	H	80

7.3.7 Procedure for the Preparation of Quinazolidiones

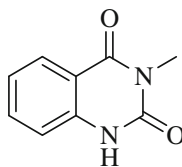
Procedure 1: 2-step cyclisation

Ortho-esterification of the desired aryl is performed (as Sect. 7.3.3). The pure, isolated ester (1 mmol) and K₂CO₃ (268 mg, 2 mmol, 2 eq) are loaded into a reaction vessel equipped with a stirring bead. THF (1 mL) is added and the reaction is heated to 60 °C. Consumption of the ester is followed by TLC. On completion (~2 h), the reaction mixture was concentrated *in vacuo*, the residue dissolved in DCM and washed with HCl (1 M). The organic layer was then washed with water, dried over MgSO₄, filtered and concentrated *in vacuo*. Purification by column chromatography (10–40 % EtOAc/PE) afforded the pure products.

Procedure 2: In situ formation

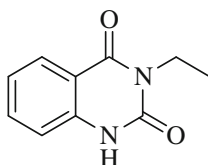
The desired urea (1 mmol, 1 eq), benzoquinone (216 mg, 2 mmol, 2 eq), palladium ditosylate bisacetonitrile (26 mg, 5 mol %, 0.05 eq) and *p*-toluenesulfonic acid monohydrate (95 mg, 0.5 mmol, 0.5 eq) were loaded into a reaction vessel equipped with a stirring bead. THF (0.5 mL) and the methanol (0.5 mL) were then added and the mixture stirred at room temperature. The reaction vessel was then briefly put under vacuum followed by charging with CO. This procedure was repeated several times to ensure a headspace flushed with 1 atm. CO. Reaction progress was monitored by TLC. Once the reaction was complete (~2–5 h), K₂CO₃ (268 mg, 2 mmol, 2 eq) was added and the reaction temperature raised to 60 °C. Consumption of the ester product was followed by TLC. On completion (~2 h), the reaction mixture was concentrated *in vacuo*, the residue dissolved in DCM and washed with HCl (1 M). The organic layer was then washed with water, dried over MgSO₄, filtered and concentrated *in vacuo*. Purification by column chromatography (10–40 % EtOAc/PE) afforded the pure products.

3-Methylquinazoline-2,4(1H,3H)-dione (78)



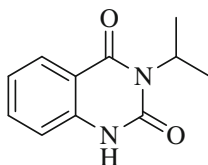
Procedure 1 (87 %) or 2 (57 %): R_f 0.14 (1:1 EtOAc: PE); mp 234–236 °C (Ref: 248–250 °C); ^1H NMR (400 MHz, DMSO- d_6), δ = 11.42 (br. s, 1H, **NH**), 7.92 (dd, J = 8.0, 1.0 Hz, 1H, **ArH**), 7.61–7.67 (m, 1H, **ArH**), 7.15–7.22 (m, 2H, **ArH**), 3.25 (s, 3H, **CH**₃); ^{13}C NMR (100 MHz, DMSO- d_6), δ = 162.1 (C), 150.3 (C), 139.3 (C), 134.8 (CH), 127.2 (CH), 122.4 (CH), 115.0 (CH), 113.7 (C), 27.0 (CH₃); IR (cm⁻¹), 3,312 (w), 2,932 (w), 1,698 (s), 1,646 (s), 1,592 (s), 1,541 (s); HRMS: m/z (CI), calculated for C₉H₉N₂O₂, 177.0664 [M + H]⁺, found 177.0662 [M + H]⁺ [16].

3-Ethylquinazoline-2,4(1H,3H)-dione (22)

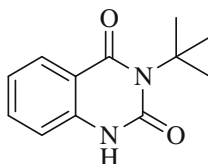


Procedure 1 (75 %) or 2 (70 %): R_f 0.34 (1:1 EtOAc: PE); mp 196–198 °C (Ref: 194–196 °C); ^1H NMR (400 MHz, DMSO- d_6), δ = 11.4 (br. s, 1H, **NH**), 7.93 (ddd, J = 8.0, 1.5, 0.5 Hz, 1H, **ArH**), 7.65 (ddd, J = 8.0, 7.0, 1.5 Hz, 1H, **ArH**), 7.14–7.23 (m, 2H, **ArH**), 3.92 (q, J = 7.0 Hz, 2H, **CH**₂), 1.14 (t, J = 7.0 Hz, 3H, **CH**₃); ^{13}C NMR (100 MHz, DMSO- d_6), δ = 161.7 (C), 150.0 (C), 139.4 (C), 135.0 (CH), 127.3 (CH), 122.5 (CH), 115.1 (CH), 113.8 (C), 35.1 (CH₂), 13.0 (CH₃); IR (cm⁻¹), 3,049 (w), 2,976 (w), 2,935 (w), 1,709 (s), 1,651 (s), 1,622 (s), 1,493 (s), 1,448 (s), 1,448 (s), 1,275 (s); HRMS: m/z (CI), calculated for C₁₀H₁₁N₂O₂, 191.0821 [M + H]⁺, found 191.0824[M + H]⁺ [17].

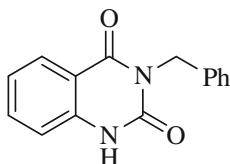
3-Isopropylquinazoline-2,4(1H,3H)-dione (79)



Procedure 1 (70 %): R_f 0.47 (1:1 EtOAc: PE); mp 183–184 °C (Ref: 188 °C); ^1H NMR (400 MHz, DMSO- d_6), δ = 11.28 (br. s, 1H **NH**), 7.84 (dd, J = 7.5, 1.5 Hz, 1H, **ArH**), 7.56–7.64 (m, 1H, **ArH**), 7.10–7.19 (m, 2H, **ArH**), 5.14 (sept, J = 7.0 Hz, 1H, **CH**), 1.42 (d, J = 7.0 Hz, 6H, 2(**CH**₃)); ^{13}C NMR (100 MHz, DMSO- d_6), δ = 162.3 (C), 150.2 (C), 139.5 (C), 134.8 (CH), 127.4 (CH), 122.3 (CH), 114.8 (CH), 114.2 (C), 44.4 (CH), 19.3 (CH₃); IR (cm⁻¹), 3,195 (w); HRMS: m/z (CI), calculated for C₁₁H₁₃N₂O₂, 205.0977 [M + H]⁺, found 205.0976 [M + H]⁺ [18].

3-(*tert*-Butyl)quinazoline-2,4(1H,3H)-dione (80)

Procedure 1 (75 %): R_f 0.51 (1:1 EtOAc: PE); mp 168–169 °C; ^1H NMR (400 MHz, CDCl_3), δ = 10.14 (br. s, 1H, **NH**), 7.94 (br. d, J = 8.0 Hz, 1H, **ArH**), 7.47 (ddd, J = 8.0, 7.5, 1.5 Hz, 1H, **ArH**), 7.09 (ddd, J = 8.0, 7.5, 1.5 Hz, 1H, **ArH**), 6.93 (dd, J = 8.0, 1.5 Hz, 1H, **ArH**), 1.73 (s, 9H, $\text{C}(\text{CH}_3)_3$); ^{13}C NMR (100 MHz, $\text{DMSO}-d_6$), δ = 164.3 (C), 153.2 (C), 138.1 (C), 134.3 (CH), 128.1 (CH), 122.8 (CH), 117.0 (CH), 114.0 (C), 62.1 (C), 30.0 (CH_3); IR (cm^{-1}), 3,123 (w), 1709 (s), 1,651 (s), 1,620 (s), 1,490 (s); HRMS: m/z (CI), calculated for $\text{C}_{12}\text{H}_{15}\text{N}_2\text{O}_2$, 219.1134 [$\text{M} + \text{H}$] $^+$, found 219.1139 [$\text{M} + \text{H}$] $^+$.

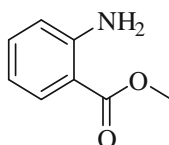
3-Benzylquinazoline-2,4(1H,3H)-dione (81)

Procedure 1 (92 %) or 2 (80 %): R_f 0.40 (1:1 EtOAc: PE); mp 219–221 °C (Ref: 227 °C); ^1H NMR (400 MHz, $\text{DMSO}-d_6$), δ = 11.54 (br. s, 1H, **NH**), 7.94 (dd, J = 8.0, 1.0 Hz, 1H, **ArH**), 7.65–7.70 (m, 1H, **ArH**), 7.19–7.32 (m, 7H, **ArH**), 5.09 (s, 2H, CH_2); ^{13}C NMR (100 MHz, CDCl_3), δ = 162.0 (C), 150.2 (C), 139.5 (C), 137.4 (C), 136.6 (C), 135.1 (CH), 128.3 (CH), 127.5 (CH), 127.1 (CH), 122.6 (CH), 115.2 (CH), 113.7 (CH), 43.2 (CH_2); IR (cm^{-1}), 3,346 (w), 2,903 (w), 1,710 (s), 1,648 (s), 1,491 (s); HRMS: m/z (CI), calculated for $\text{C}_{15}\text{H}_{13}\text{N}_2\text{O}_2$, 253.0977 [$\text{M} + \text{H}$] $^+$, found 253.0983 [$\text{M} + \text{H}$] $^+$ [18].

7.3.8 Procedure for the Preparation of Methyl 2-aminobenzoate

Methyl 2-(3,3-diisopropylureido)benzoate (168 mg, 0.6 mmol) was refluxed in water (15 mL) for 18 h. Consumption of starting material was followed by TLC. Once reaction was complete, the mixture was cooled to room temperature, extracted into DCM and concentrated *in vacuo*. The residue was suspended in chloroform and filtered, the filtrite was collected as a white solid (80 %).

Methyl 2-aminobenzoate (82)

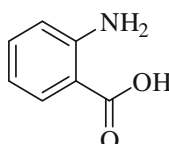


All data consistent with commercially available methyl anthranilate (CAS 134-20-3).

7.3.9 Procedure for the Preparation of 2-Aminobenzoic Acid

Methyl 2-(3,3-diisopropylureido)benzoate (168 mg, 0.6 mmol) was refluxed in NaOH (1 M, 15 mL) for 18 h. Consumption of starting material was followed by TLC. The reaction was cooled, acidified with HCl (Conc.) to pH 2 and concentrated *in vacuo* to a white solid. EtOAc (100 mL) was added and the suspension sonicated, water (5 mL) was then added, followed by further sonication. The organic layer was then collected and concentrated *in vacuo* to a mustard coloured solid (90 %).

2-Aminobenzoic acid (83)



All data consistent with commercially available anthranilic acid (CAS 118-92-3)

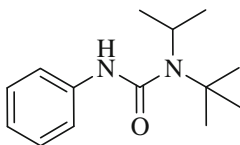
7.4 Urea Hydrolysis

7.4.1 Preparation of Ureas

The preparation of non-commercial ureas was performed using the appropriate isocyanate and amine as detailed in Sect. 7.3.1. Non-commercial amines were synthesised by a modification of the procedure by Schmitt [19] Alkyl bromide (1 mmol, 1 eq) was mixed with *tert*-butylamine (314 mL, 3 mmol, 3 eq) at 0 °C. The reaction was allowed to warm to room temperature over 5 h and allowed to

stir for a further 18 h. 10 M NaOH (500 mL) was added to the reaction and the amine layer separated. Purification via distillation yielded the title amine (55–91 %).

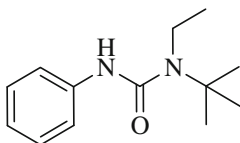
1-*tert*-Butyl-1-isopropyl-3-phenylurea* (84)



55 %; R_f 0.72 (1:1 EtOAc: PE); oil; $^1\text{H NMR}$ (400 MHz, CDCl_3), $\delta = 7.22$ – 7.35 (m, 4H, ArH), 6.93–6.99 (app. t, $J = 7.0$ Hz, 1H, ArH), 6.46 (br. s, 1H, NH), 3.70 (sept, $J = 7.0$ Hz, 1H, NCH), 1.36 (s, 9H, $\text{C}(\text{CH}_3)_3$), 1.33 (d, $J = 7.0$ Hz, 6H, 2(CH_3)); $^{13}\text{C NMR}$ (100.6 MHz, CDCl_3), $\delta = 158.0$ (C), 138.9 (C), 128.9 (CH), 122.6 (CH), 118.9 (CH), 56.3 (C), 46.4 (CH), 28.7 (CH_3), 23.5 (CH_3); IR (cm^{-1}) 3,291 (w), 2,970 (w), 1,641 (s), 1,594 (s); HRMS: m/z (CI), calculated for $\text{C}_{14}\text{H}_{23}\text{N}_2\text{O}$, 235.1810 $[\text{M} + \text{H}]^+$, found 235.1807 $[\text{M} + \text{H}]^+$.

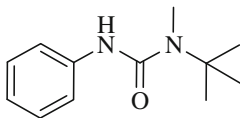
*Care required when handling and storing, sensitive to moisture and prolonged exposure to the atmosphere.

1-*tert*-Butyl-1-ethyl-3-phenylurea (87)



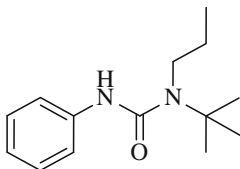
69 %; R_f 0.68 (1:1 EtOAc: PE); mp 75–77 °C; $^1\text{H NMR}$ (400 MHz, CDCl_3), $\delta = 7.23$ – 7.35 (m, 4H, ArH), 6.97–7.00 (app. t, $J = 7.0$ Hz, 1H, ArH), 6.33 (br. s, 1H, NH), 3.39 (q, $J = 7.0$ Hz, 2H, CH_2), 1.48 (s, 9H, $\text{C}(\text{CH}_3)_3$), 1.28 (t, $J = 7.0$ Hz, 3H, CH_2CH_3); $^{13}\text{C NMR}$ (100 MHz, CDCl_3), $\delta = 156.0$ (C), 139.4 (C), 129.0 (CH), 122.8 (CH), 120.0 (CH), 56.4 (C), 39.5 (CH_2), 29.4 (CH_3), 16.9 (CH_3); IR (cm^{-1}) 3,326 (w), 2,972 (w), 1,634 (s), 1,593 (s), 1,534 (s); HRMS: m/z (CI), calculated for $\text{C}_{13}\text{H}_{21}\text{N}_2\text{O}$, 221.1654 $[\text{M} + \text{H}]^+$, found 221.1647 $[\text{M} + \text{H}]^+$.

1-*tert*-Butyl-1-methyl-3-phenylurea (88)



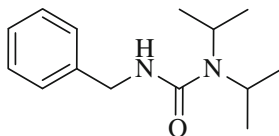
45 %; R_f 0.60 (1:1 EtOAc: PE); mp 111–112 °C (Ref: 127–128 °C); ^1H NMR (400 MHz, CDCl_3), $\delta = 7.23\text{--}7.32$ (m, 4H, ArH), 6.96–7.06 (m, 1H, ArH), 6.19 (br. s, 1H, NH), 2.96 (s, 3H, NCH_3), 1.44 (s, 9H, $\text{C}(\text{CH}_3)_3$); ^{13}C NMR (100 MHz, CDCl_3), $\delta = 156.7$ (C), 139.4 (C), 128.8 (CH), 122.8 (CH), 119.7 (CH), 55.9 (C), 32.5 (CH_3), 28.6 (CH_3); IR (cm^{-1}) 3,233 (w), 2,960 (w), 1,643 (s), 1,595 (s), 1,533 (s); HRMS: m/z (CI), calculated for $\text{C}_{12}\text{H}_{18}\text{N}_2\text{O}$, 207.1494 $[\text{M} + \text{H}]^+$, found 207.1497 $[\text{M} + \text{H}]^+$ [20].

1-*tert*-Butyl-3-phenyl-1-propylurea (89)

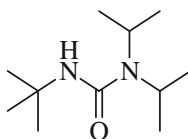


28 %; R_f 0.71 (1:1 EtOAc: PE); mp 63–64 °C; ^1H NMR (400 MHz, CDCl_3), $\delta = 7.21\text{--}7.33$ (m, 4H, ArH), 6.94–6.99 (app. t, $J = 6.5$ Hz, 1H, ArH), 6.45 (br. s, 1H, NH), 3.17–3.23 (m, 2H, NCH_2), 1.58–1.71 (app. sext, $J = 7.5$ Hz, 2H, CH_2CH_3), 1.45 (s, 9H, $\text{C}(\text{CH}_3)_3$), 0.95 (t, $J = 7.5$ Hz, 3H, CH_2CH_3); ^{13}C NMR (100 MHz, CDCl_3), $\delta = 156.2$ (C), 139.4 (C), 128.8 (CH), 122.6 (CH), 119.9 (CH), 56.3 (C), 47.3 (CH_2), 29.4 (CH_3), 24.9 (CH_2), 11.4 (CH_3); IR (cm^{-1}), 3,273 (w), 2,967 (w), 1,631 (s), 1,594 (s), 1,535 (s); HRMS: m/z (CI), calculated for $\text{C}_{14}\text{H}_{23}\text{N}_2\text{O}$, 235.1810 $[\text{M} + \text{H}]^+$, found 235.1813 $[\text{M} + \text{H}]^+$.

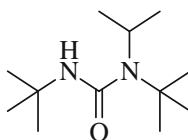
3-Benzyl-1,1-diisopropylurea (90)



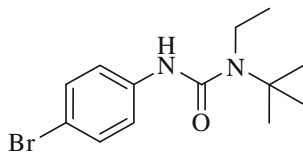
84 %; R_f 0.49 (1:1 EtOAc: PE); mp 81–83 °C; ^1H NMR (400 MHz, CDCl_3), $\delta = 7.24$ (m, 5H, ArH), 4.44 (m, 2H, CH_2), 3.89 (sept, $J = 6.5$ Hz, 2H, 2CH), 1.24 (d, $J = 6.5$ Hz, 12H, 4(CH_3)); ^{13}C NMR (100 MHz, CDCl_3), $\delta = 157.0$ (C), 139.8 (C), 128.5 (CH), 127.5 (CH), 127.0 (CH), 45.1 (CH), 44.7 (CH_2), 21.4 (CH_3); IR (cm^{-1}) 3,328 (w), 2,965 (w), 1,616 (s), 1,530 (s); HRMS: m/z (CI), calculated for $\text{C}_{14}\text{H}_{23}\text{N}_2\text{O}$, 235.1810 $[\text{M} + \text{H}]^+$, found 235.1812 $[\text{M} + \text{H}]^+$.

3-*tert*-Butyl-1,1-diisopropylurea (91)

63 %; R_f 0.58 (1:1 EtOAc: PE); oil; ^1H NMR (400 MHz, CDCl_3), $\delta = 4.14$ (br. s, 1H, NH), 3.89–3.99 (sept, $J = 7.0$ Hz, 2H, 2CH), 1.37 (s, 9H, $\text{C}(\text{CH}_3)_3$), 1.22 (d, $J = 7.0$ Hz, 12H, 4(CH_3)); ^{13}C NMR (100 MHz, CDCl_3), $\delta = 50.6$ (C), 44.3 (CH), 29.7 (CH_3), 21.5 (CH_3), (Note Carbonyl (C) is not observed); IR (cm^{-1}) 3,374 (w), 2,964 (w), 1,637 (s), 1,508 (s); HRMS: m/z (CI), calculated for $\text{C}_{11}\text{H}_{25}\text{N}_2\text{O}$, 201.2000 $[\text{M} + \text{H}]^+$, found 201.1922 $[\text{M} + \text{H}]^+$.

1,3-Di-*tert*-butyl-1-isopropylurea (94)

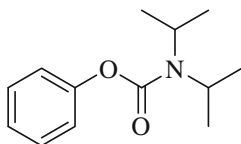
41 %; R_f 0.79 (1:1 EtOAc: PE); oil; ^1H NMR (400 MHz, CDCl_3), $\delta = 4.55$ (br. s, 1H, NH), 3.55 (sept, $J = 7.0$ Hz, 1H, CH), 1.33 (s, 9H, $\text{NHC}(\text{CH}_3)_3$), 1.28 (s, 9H, $\text{NC}(\text{CH}_3)_3$), 1.24 (d, $J = 7.0$ Hz, 6H, $\text{CH}(\text{CH}_3)_2$); ^{13}C NMR (100 MHz, CDCl_3), $\delta = 160.0$ (C), 55.3 (C), 50.2 (C), 45.5 (CH), 29.2 (CH_3), 28.7 (CH_3), 23.6 (CH_3); IR (cm^{-1}) 3,462 (w), 2,966 (w), 1,667 (s), 1,493 (s); HRMS: m/z (CI), calculated for $\text{C}_{12}\text{H}_{27}\text{N}_2\text{O}$, 215.2123 $[\text{M} + \text{H}]^+$, found 215.2129 $[\text{M} + \text{H}]^+$.

3-(4-Bromophenyl)-1-*tert*-butyl-1-ethylurea (98)

57 %; R_f 0.69 (1:1 EtOAc: PE); oil; ^1H NMR (400 MHz, Toluene- d_8), $\delta = 7.17$ –7.19 (m, 2H, ArH), 7.07–7.09 (m, 2H, ArH), 5.81 (br. s, 1H, NH), 2.78 (q, $J = 7.5$ Hz, 2H, CH_2), 1.34 (s, 9H, $\text{C}(\text{CH}_3)_3$), 0.80 (t, $J = 7.5$ Hz, 3H, CH_2CH_3); ^{13}C NMR (100 MHz, Toluene- d_8), $\delta = 155.3$ (C), 139.6 (C), 131.8 (CH), 121.1 (CH), 114.8 (C), 56.3 (C), 39.3 (CH_2), 29.3 (CH_3), 16.8 (CH_3); HRMS: m/z (CI), calculated for $\text{C}_{13}\text{H}_{20}^{79}\text{BrN}_2\text{O}$, 299.0759 $[\text{M} + \text{H}]^+$, found 299.0762 $[\text{M} + \text{H}]^+$.

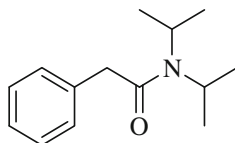
7.4.2 Preparation of Unreactive Analogues

Phenyl diisopropylcarbamate (95)



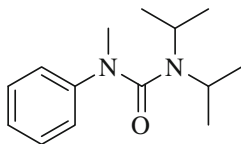
Phenol (0.94 g, 10 mmol, 1 eq) and diisopropyl carbamoyl chloride (1.63 g, 10 mmol, 1 eq) were heated in pyridine (10 mL) at 100 °C. After 18 h the reaction mixture was allowed to cool, extracted into diethyl ether, washed twice with HCl (1 M) and then twice with NaOH (1 M). The organic layer was dried (MgSO₄), filtered and concentrated *in vacuo* to a colourless oil. 1.92 g (87 %). R_f 0.31(1:1 EtOAc: PE); ¹H NMR (500 MHz, Toluene-*d*₈, 75 °C), δ = 7.05–7.11 (m, 4H, ArH), 6.89–6.91 (app. t, *J* = 7.0 Hz, 1H, ArH), 3.82 (app. qu, *J* = 6.5 Hz, 2H, 2CH), 1.13–1.14 (d, *J* = 6.5 Hz, 12H, 4(CH₃)); ¹³C NMR (100 MHz, CDCl₃), δ = 153.8 (C), 151.3 (C), 129.1 (CH), 124.8 (CH), 121.7 (CH), 46.8 (CH), 21.5 (CH₃). *Note* Variable temperature NMR studies required to resolve rotameric effects. Further data agrees with that presented in the literature [21].

1, 1-Diisopropyl-2-phenylacetamide (96)



A solution of phenylacetyl chloride (1.32 mL, 10 mmol, 1 eq) and diisopropylamine (2.80 mL, 20 mmol, 2 eq) in dry DCM (20 mL) was stirred at room temperature. After 1 h the reaction mixture was washed with HCl (1 M) and then water. The organic layer was dried with MgSO₄, filtered and concentrated *in vacuo* to a white solid. 2.03 g (93 %). All data consistent with that presented in the literature [22].

1,1-Diisopropyl-3-methyl-3-phenylurea (97)

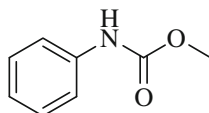


Methyl aniline (2.16 mL, 20 mmol, 2 eq), diisopropyl carbamoyl chloride (1.63 g, 10 mmol, 1 eq) were dissolved in THF (15 mL). The reaction was heated to reflux for 18 h and then allowed to cool, upon which white crystals precipitated. The mixture was filtered under vacuum and the filtrate purified via column chromatography (5 % EtOAc in PE) to yield a colourless oil. 1.47 g (63 %). R_f 0.67 (1:1 EtOAc: PE); oil; $^1\text{H NMR}$ (400 MHz, CDCl_3), $\delta = 7.27\text{--}7.33$ (m, 2H, ArH), 7.04–7.12 (m, 3H, ArH), 3.61 (app. qu, $J = 6.5$ Hz, 2H, 2CH), 3.05 (s, 3H, NCH_3), 1.07 (d, $J = 6.5$ Hz, 12H, 4(CH_3)); $^{13}\text{C NMR}$ (100 MHz, CDCl_3), $\delta = 161.5$ (C), 148.3 (C), 129.3 (CH), 124.5 (CH), 118.8 (CH), 47.5 (CH_3), 40.1 (CH_2), 20.6 (CH_3); IR (cm^{-1}), 2,965 (w), 1,646 (s), 1,596 (s), 1,494 (s); HRMS: m/z (CI), calculated for $\text{C}_{14}\text{H}_{23}\text{N}_2\text{O}$, 235.1810 [$\text{M} + \text{H}$] $^+$, found 235.1800 [$\text{M} + \text{H}$] $^+$.

7.4.3 Procedure for the Methanolysis of Hindered Tri-Substituted Ureas

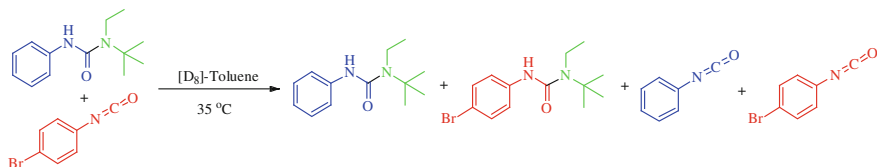
The desired urea (0.33 mmol) was dissolved in methanol (1 mL) and then heated to the stated temperature. Aliquots were taken periodically (solvent and amine removed *in vacuo*) and the reaction followed by $^1\text{H NMR}$ until complete. Upon completion all volatiles were removed under vacuum. The residue was weighed then dissolved in CDCl_3 with yield/purity determined by $^1\text{H NMR}$.

Methyl *N*-phenylcarbamate (85)



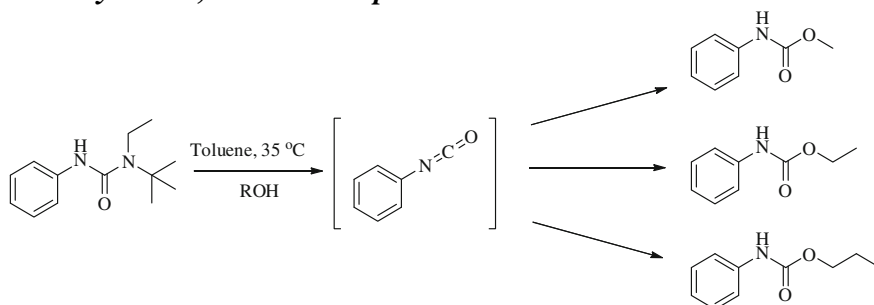
$^1\text{H NMR}$ (400 MHz, CDCl_3), $\delta = 7.29\text{--}7.42$ (m, 4H, ArH), 7.07 (app. t, 7.5 Hz, 1H, ArH), 6.83 (br. s, 1H, NH), 3.79 (s, 3H, OCH_3); $^{13}\text{C NMR}$ (100 MHz, CDCl_3), $\delta = 154.1$ (C), 137.8 (C), 129.0 (CH), 123.4 (CH), 118.7 (CH), 52.3 (CH_3). Further data agrees with that presented in the literature [23].

7.4.4 Procedure for Isocyanate Crossover Experiment



[D₈]-toluene (0.8 ml) was distilled from 3 Å molecular sieves before immediate addition to a sample vial containing **87** (10 mg, 0.045 mmol, 1 eq). To this was added *p*-bromophenyl isocyanate (9 mg, 0.045 mmol, 1 eq) and the mixture transferred to an NMR tube. The sample was run on a 500 MHz Varian spectrometer set at 35 °C and spectra recorded at regular intervals.

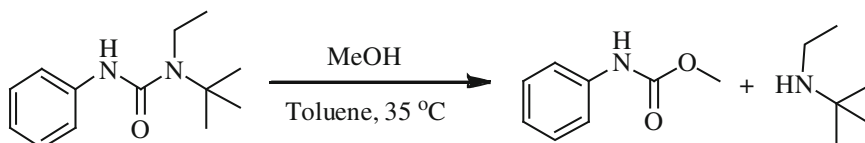
7.4.5 Partitioning of In Situ Generated *N*-Phenylisocyanate by Meoh, Etoh and Nproh



Reaction from phenyl isocyanate. Methanol (100 μL, 2.5 mmol, 1 eq), ethanol (145 μL, 2.5 mmol, 1 eq) and *n*-propanol (187 μL, 2.5 mmol, 1 eq) were dissolved in toluene (1.6 mL) and heated to 35 °C with vigorous stirring. To this was added a solution of phenyl isocyanate (27 μL, 0.25 mmol, 0.1 eq) dissolved in toluene (1 mL) dropwise (over 1 min) into the centre of the vortex of the alcoholic solvent mixture. After 10 min the volatiles were removed under vacuum. The residue was dissolved in CDCl₃ and the ratios of carbamates analysed by ¹H NMR.

Reaction from urea derivative **87.** Methanol (130 μL, 3 mmol, 1 eq), ethanol (190 μL, 3 mmol, 1 eq) and *n*-propanol (246 μL, 3 mmol, 1 eq) were dissolved in toluene (2.4 mL) and heated to 35 °C. To this was added urea **87** (66 mg, 0.3 mmol, 0.1 eq). The reaction was stirred at this temperature for 18 h after which all volatiles were removed under vacuum. The residue was dissolved in CDCl₃ and analysed by ¹H NMR as above.

7.4.6 Kinetics of the Methanolysis of Hindered Tri-Substituted Ureas



General procedure for kinetic experiments: Methanalysis were run in sealed “reduced volume” Radley’s tubes in an isoelectric water bath maintained at 35 °C. Urea **87** (73 mg, 0.33 mmol, 1 eq) was weighed into the tube and allowed to reach temperature in the water bath over 5 min. Separately, the required amount of anhydrous methanol was measured into a 3 mL volumetric flask via a Hamilton gastight syringe. Anhydrous toluene was then added to dilute the methanol to a total volume of 3 mL. This solution was then placed in the water bath and allowed to reach temperature (5 min) before being added to the tube charged with **87**. The urea dissolved rapidly (less than 5 s). 50 μ L volume samples were removed at regular intervals via gastight syringe, rapidly transferred to a sample vial, cooled in ice, and the volatiles removed under vacuum. The residue was dissolved in CDCl_3 and the ratio of **87/85** analysed by ^1H NMR. A control experiment in which **87/85** were dissolved in *N*-ethyl *N*-*tert*-butylamine confirmed the inertness of **85** towards regeneration of **87** (Fig. 7.1).

Entry	Initial [MeOH] (M)	Pseudo first order rate constant (s^{-1})
A	0.11	1.38E-05
B	0.28	2.15E-05
C	0.19	2.34E-05
D	0.55	2.81E-05
E	1.11	3.77E-05
F	2.22	4.18E-05
G	15.99	5.14E-05
H	16.52	8.22E-05
I	16.52	6.63E-05

General procedure for kinetic experiments with added amine: As for general kinetic procedures but with addition of *N*-ethyl *N*-*tert*-butylamine once the solvent was added to the urea. Samples were taken at regular intervals and analysed as detailed above.

A consolidated plot of $\ln(A(0)/A(t))$ versus time (s) at $[\text{MeOH}] = 1.11 \text{ M}$ with various amounts of added *N*-*tert*-butyl, *N*-ethylamine where $A = [\mathbf{87}]$ (Fig. 7.2).

Entry	Initial [Amine] (M)	Pseudo first order rate constant (s^{-1})
A	0.28	2.85E-05
B	0.83	3.69E-05
C	0.56	3.63E-05
D	0.0	3.77E-05

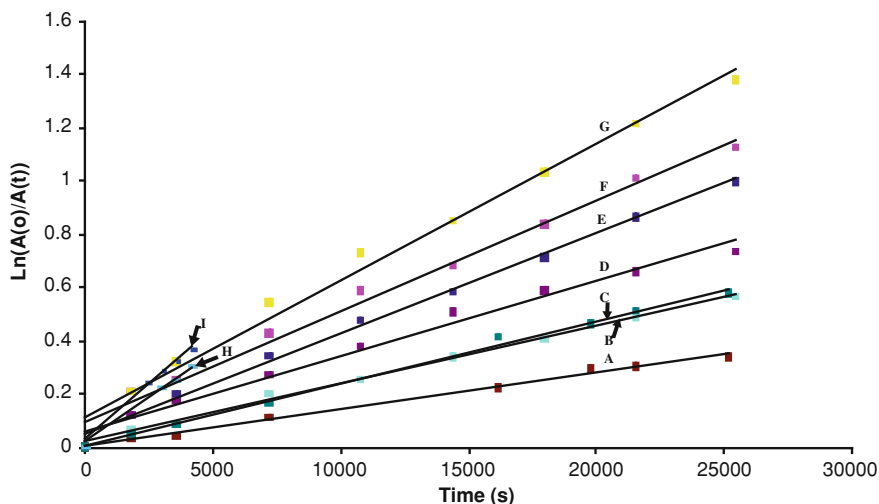


Fig. 7.1 Consolidated plot of $\ln(A(0)/A(t))$ versus time (s) at various concentrations of MeOH ($A = [87]$)

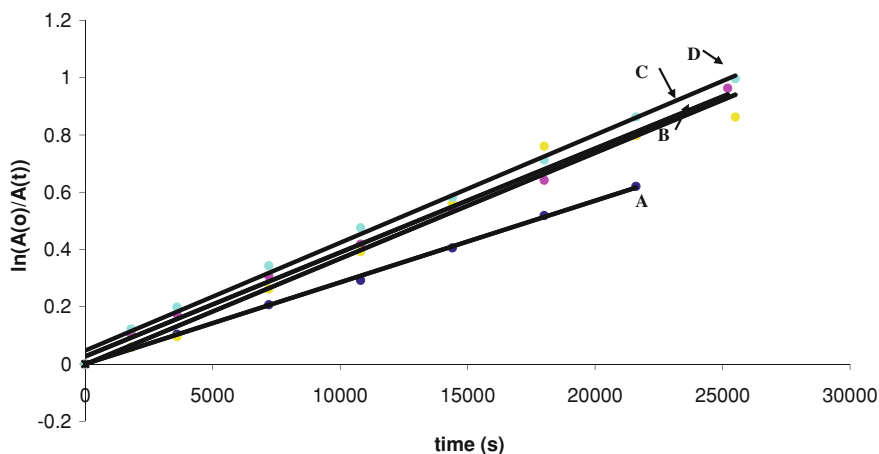


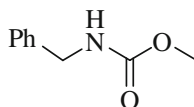
Fig. 7.2 A consolidated plot of $\ln(A(0)/A(t))$ versus time (s) at $[MeOH] = 1.11$ M with various amounts of added *N-tert-butyl*, *N-ethylamine* ($A = [87]$)

7.4.7 Procedure for the Preparation of Carbamate Derivatives

1-*tert-butyl*-1-ethyl-3-phenylurea (**87**) (1 mmol) was suspended in toluene (1 mL). The appropriate amount of nucleophile was then added and the mixture heated to the desired temperature. Aliquots were taken periodically (solvent and amine removed *in vacuo*) and the reaction followed by 1H NMR until complete. For those

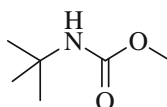
reactions not going to completion, the reaction was concentrated *in vacuo* and purified via column chromatography (10–50 % EtOAc in PE).

Methyl *N*-benzylcarbamate (**92**)



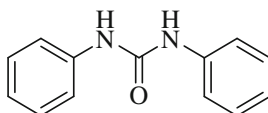
^1H NMR (400 MHz, CDCl_3), $\delta = 7.24\text{--}7.36$ (m, 5H, ArH), 5.09 (br. s, 1H, NH), 4.36 (d, $J = 6.0$ Hz, 2H, CH_2), 3.69 (s, 3H, OCH_3); ^{13}C NMR (100 MHz, CDCl_3), $\delta = 157.1$ (C), 138.5 (C), 128.6 (CH), 127.4 (CH), 118.3 (CH), 52.7 (CH_3), 45.0 (CH_2). Further data agrees with that presented in the literature [24].

Methyl *N*-*tert*-butylcarbamate (**93**)



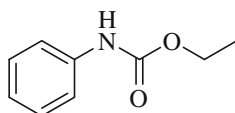
^1H NMR (400 MHz, CDCl_3), $\delta = 4.74$ (br. s, 1H, NH), 3.64 (s, 3H, CH_3), 1.34 (s, 9H, $\text{C}(\text{CH}_3)_3$); ^{13}C NMR (100 MHz, CDCl_3), $\delta = 155.5$ (C), 51.2 (C), 28.9 (CH_3), 25.5 (CH_3). Further data agrees with that presented in the literature [25].

1,3-Diphenylurea (**86**)

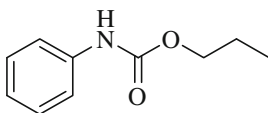


All data consistent with commercially available 1,3-diphenylurea (CAS: 3112-85-4).

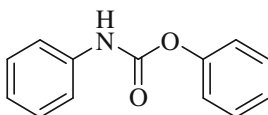
Ethyl phenylcarbamate (**99**)



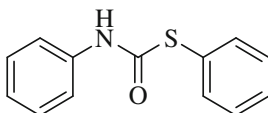
All data consistent with commercially available ethyl phenylcarbamate (CAS: 101-99-5).

Propyl phenylcarbamate (100)

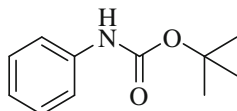
All data consistent with that in the literature [26].

1,3-Diphenylcarbamate (102)

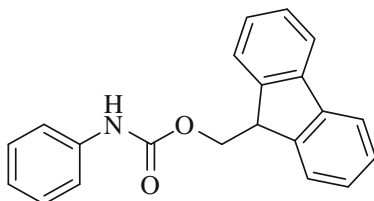
^1H NMR (400 MHz, CDCl_3), $\delta = 7.08\text{--}7.38$ (m, 9H, ArH), 7.00 (app. t, $J = 7.5$ Hz, 1H, ArH), 6.96 (br. s, 1H, NH); ^{13}C NMR (100 MHz, CDCl_3), $\delta = 151.8$ (C), 150.5 (C), 137.3 (C), 129.4 (CH), 129.1 (CH), 125.7 (CH), 123.8 (CH), 121.6 (CH), 118.7 (CH). IR (cm^{-1}) 3,312 (m), 1,711 (s), 1,597 (m), 1,530 (s); LRMS: $\text{C}_{13}\text{H}_{11}\text{NO}_2$, m/z (CI), 94.1 (93 %), 120.1 (31 %), 214.0 (100 %) $[\text{M} + \text{H}]^+$. Further data agrees with that presented in the literature [27].

1,3-Diphenylcarbamothioate (103)

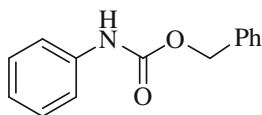
^1H NMR (400 MHz, CDCl_3), $\delta = 7.21\text{--}7.63$ (m, 9H, ArH), 7.09 (app. t, $J = 7.5$ Hz, 1H, ArH); ^{13}C NMR (100 MHz, CDCl_3), $\delta = 179.8$ (C), 137.5 (C), 135.5 (C), 129.9 (CH), 129.4 (CH), 129.0 (CH), 128.0 (CH), 127.8 (CH), 124.6 (CH); IR (cm^{-1}) 3,250 (m), 1,659 (m), 1,596 (m), 1,532 (s); LRMS: $\text{C}_{13}\text{H}_{11}\text{NOS}$, m/z (CI), 91.1 (13 %), 111.0 (94 %), 120.1 (100 %), 230.1 (77 %) $[\text{M} + \text{H}]^+$. Further data agrees with that presented in the literature [9].

***N*-Boc-aniline (104)**

All data consistent with commercially available *N*-Boc-aniline (CAS: 3422-01-3)

(9H-Fluoren-9-yl)methyl phenylcarbamate (105)

^1H NMR (400 MHz, $\text{DMSO-}d_6$), $\delta = 9.70$ (br. s, 1H, **NH**), 7.90 (d, $J = 7.5$ Hz, 2H, **ArH**), 7.75 (d, $J = 7.5$ Hz, 2H, **ArH**), 7.23–7.45 (m, 8H, **ArH**₂) 6.98 (app. t, $J = 7.5$ Hz, 1H, **ArH**), 4.48 (d, $J = 6.5$ Hz, 2H, **CH**₂), 4.30 (t, $J = 6.5$ Hz, 1H, **CH**); ^{13}C NMR (100 MHz, $\text{DMSO-}d_6$), $\delta = 153.6$ (C), 143.9 (C), 141.0 (C), 139.1 (C), 129.1 (C), 128.9 (CH), 127.5 (CH), 127.3 (CH), 125.3 (CH), 122.7 (CH), 121.5 (CH), 120.3 (CH), 120.2 (CH), 118.5 (CH), 114.1 (C), 65.7 (CH₂), 47.8 (CH). Further data agrees with that presented in the literature [28].

Benzyl N-phenylcarbamate (106)

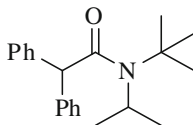
^1H NMR (400 MHz, CDCl_3), $\delta = 7.28$ –7.42 (m, 9H, **ArH**), 7.09 (app. t, $J = 7.5$ Hz, 1H, **ArH**), 6.81 (br. s, 1H, **NH**), 5.22 (s, 2H, **CH**₂); ^{13}C NMR (100 MHz, CDCl_3), $\delta = 153.3$ (C), 137.7 (C), 136.0 (C), 129.0 (CH), 128.6 (CH), 128.3 (CH), 125.6 (CH), 123.5 (CH), 118.7 (CH), 66.9 (CH₂). Further data agrees with that presented in the literature [26].

7.5 Amide Hydrolysis**7.5.1 Procedure for the Preparation of Diphenylacetamides**

A solution of diphenylacetyl chloride [29] (1.15 g, 5 mmol, 1 eq) in anhydrous DCM (20 mL) was cooled in an ice bath for 15 min. To this was added triethylamine (525 mg, 5.2 mmol, 1.04 eq) dropwise upon which the solution became bright yellow. The appropriate amine (10 mmol, 2 eq) was then added dropwise and the reaction allowed to warm to room temperature and stir overnight. The reaction was then quenched with 1 M HCl (20 mL) and the organic layer subsequently washed with water (50 mL) and then brine (50 mL), dried with MgSO_4

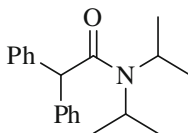
and then concentrated *in vacuo*. The resulting residue was then purified via column chromatography to yield the desired amide.

***N*-(*tert*-Butyl)-*N*-isopropyl-2,2-diphenylacetamide (109)**



5 %; R_f 0.61 (1:1 EtOAc: PE); oil; ^1H NMR (400 MHz, CDCl_3), δ = 7.39–7.45 (m, 10H, ArH), 5.25 (s, 1H, CHCO), 4.09 (br. s, 1H, CH(CH₃)₂), 1.46 (s, 9H, C(CH₃)₃), 1.41 (d, J = 7.0 Hz, 6H, CH(CH₃)₂); ^{13}C NMR (100 MHz, CDCl_3), δ = 174.3 (C), 141.0 (C), 129.0 (CH), 128.2 (CH), 126.5 (CH), 58.8 (C), 58.0 (CH), 47.0 (CH) 29.6 (CH₃), 24.2 (CH₃); IR (cm^{-1}) 2,975 (w), 1,635 (s), 1,433 (m), 1,333 (m); HRMS: m/z (CI), calculated for C₂₁H₂₈NO, 310.2164 [M + H]⁺, found 310.2171 [M + H]⁺.

***N,N*-Diisopropyl-2,2-diphenylacetamide (110)**



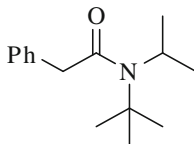
97 %; R_f 0.59 (1:1 EtOAc: PE); oil; ^1H NMR (400 MHz, CDCl_3), δ = 7.14–7.25 (m, 10H, ArH), 5.05 (s, 1H, CHCO), 4.02 (sept, J = 6.5 Hz, 1H, CH(CH₃)₂), 3.32 (br. s, 1H, CH(CH₃)₂), 1.36 (d, J = 6.5 Hz, 6H, CH(CH₃)₂), 0.91 (d, J = 6.5 Hz, 6H, CH(CH₃)₂); ^{13}C NMR (100 MHz, CDCl_3), δ = 170.2 (C), 140.2 (C), 129.1 (CH), 128.4 (CH), 126.7 (CH), 56.4 (CH), 46.1 (CH), 21.1 (CH₃), 20.5 (CH₃); IR (cm^{-1}) 2,971 (w) 1,637 (s), 1,434 (m), 1,330 (m); HRMS: m/z (CI), calculated for C₂₀H₂₆NO, 296.2023 [M + H]⁺, found 296.1014 [M + H]⁺.

7.5.2 Procedure for the Preparation of Hindered Amides

To a solution/suspension of the appropriate carboxylic acid (3 mmol, 1 eq) in anhydrous DCM (20 mL) was added 2-chloro-1-methylpyridinium iodide (Mukaiyama's reagent) (1.15 g, 4.5 mmol, 1.5 eq). The resulting suspension was stirred under an inert atmosphere for 15 min at which time the desired amine (9 mmol, 3 eq) was added dropwise. The reaction was allowed to stir for 1 h at room temperature before being quenched with 1 M HCl (20 mL). The organic layer was subsequently washed with water (50 mL) and then brine (50 mL), dried with

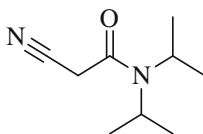
MgSO₄ and then concentrated *in vacuo*. The resulting residue was then purified via column chromatography to yield the desired amide.

***N*-(*tert*-Butyl)-*N*-isopropyl-2-phenylacetamide (107)**



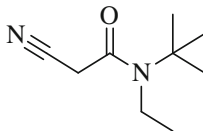
49 %; R_f 0.63 (1:1 EtOAc: PE); oil; ¹H NMR (400 MHz, CDCl₃), δ = 7.25–7.39 (m, 5H, ArH), 4.10 (sept, *J* = 7.0 Hz, 1H, CH), 3.77 (s, 2H, CH₂CO), 1.52 (s, 9H, C(CH₃)₃), 1.44 (d, *J* = 7.0 Hz, 6H, CH(CH₃)₂); ¹³C NMR (100 MHz, CDCl₃), δ = 173.4 (C), 136.8 (C), 128.3 (CH), 128.4 (CH), 126.3 (CH), 58.6 (C), 46.0 (CH), 45.1 (CH₂), 29.6 (CH₃), 23.6 (CH₃); IR (cm⁻¹) 2,968 (w) 1,634 (s), 1,200 (m); HRMS: *m/z* (CI), calculated for C₁₅H₂₄NO, 234.1858 [M + H]⁺, found 234.1850 [M + H]⁺.

2-Cyano-*N,N*-diisopropylacetamide (113)



99 %; R_f 0.51 (1:1 EtOAc: PE); mp 53–54 °C (Ref: 50–51 °C); ¹H NMR (400 MHz, CDCl₃), δ = 3.79 (sept, *J* = 6.5 Hz, 1H, CH), 3.49 (sept, *J* = 6.5 Hz, 1H, CH), 3.45 (s, 2H, CH₂CO), 1.38 (d, *J* = 6.5 Hz, 6H, CH(CH₃)₂), 1.25 (d, *J* = 6.5 Hz, 6H, CH(CH₃)₂); ¹³C NMR (100 MHz, CDCl₃), δ = 159.9 (C), 114.4 (C), 50.2 (CH), 46.7 (CH), 27.0 (CH₂), 20.7 (CH₃), 20.2 (CH₃); IR (cm⁻¹) 2,973 (w), 2,251 (w), 1,638 (s), 1,445 (m), 1,345 (s); HRMS: *m/z* (CI), calculated for C₉H₁₇N₂O, 169.1341 [M + H]⁺, found 169.1336 [M + H]⁺ [30].

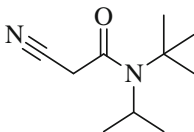
***N*-(*tert*-Butyl)-2-cyano-*N*-ethylacetamide (114)**



96 %; R_f 0.52 (1:1 EtOAc: PE); oil; ¹H NMR (400 MHz, CDCl₃), δ = 3.53 (s, 2H, CH₂CO), 3.34 (q, *J* = 7.0 Hz, 2H, NCH₂CH₃), 1.46 (s, 9H, C(CH₃)₃), 1.24 (t, *J* = 7.0 Hz, 3H, NCH₂CH₃); ¹³C NMR (100 MHz, CDCl₃), δ = 161.9 (C), 114.7 (C), 58.1 (C), 40.2 (CH₂), 28.4 (CH₃), 27.4 (CH₂) 16.6 (CH₃); IR (cm⁻¹) 2,970

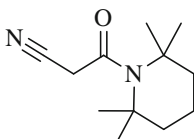
(w), 2,930 (w), 2,258 (w), 1,648 (s); HRMS: m/z (CI), calculated for $C_9H_{17}N_2O$, 169.1346 $[M + H]^+$, found 169.1341 $[M + H]^+$.

***N*-(*tert*-Butyl)-2-cyano-*N*-isopropylacetamide (111)**



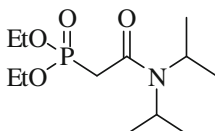
98 %; R_f 0.55 (1:1 EtOAc: PE); oil; 1H NMR (400 MHz, $CDCl_3$), δ = 3.97 (sept, J = 7.0 Hz, 1H, CH), 3.52 (s, 2H, CH_2CO), 1.45 (s, 9H, $C(CH_3)_3$), 1.39 (d, J = 7.0 Hz, 6H, $NCH(CH_3)_2$); ^{13}C NMR (100 MHz, $CDCl_3$), δ = 163.1 (C), 115.0 (C), 59.7 (C), 46.9 (CH), 29.3 (CH_2), 28.9 (CH_3), 23.1 (CH_3); IR (cm^{-1}) 2,972 (w), 2,257 (w), 1,642 (s), 1,334 (m); HRMS: m/z (CI), calculated for $C_{10}H_{19}N_2O$, 183.1497 $[M + H]^+$, found 183.1504 $[M + H]^+$.

3-Oxo-3-(2,2,6,6-tetramethylpiperidin-1-yl)propanenitrile (115)



30 %; R_f 0.70 (1:1 EtOAc: PE); mp 65 °C; 1H NMR (400 MHz, $CDCl_3$), δ = 3.50 (s, 2H, CH_2CO), 1.74 (m, 6H, $(CH_2)_3$), 1.45 (s, 12H, $4(CH_3)$); ^{13}C NMR (100 MHz, $CDCl_3$), δ = 164.7 (C), 115.3 (C), 56.8 (C), 36.4 (CH_2), 30.3 (CH_2), 29.8 (CH_3), 14.1 (CH_2); IR (cm^{-1}) 2,978 (w), 2,915 (w), 2,244 (w), 1,633 (s), 1,466 (m); HRMS: m/z (CI), calculated for $C_{12}H_{21}N_2O$, 209.1654 $[M + H]^+$, found 209.1646 $[M + H]^+$.

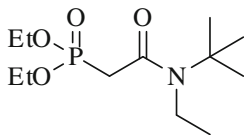
Diethyl (2-(diisopropylamino)-2-oxoethyl)phosphonate (117)



78 %; R_f 0.16 (1:1 EtOAc: PE); oil; 1H NMR (400 MHz, $DMSO-d_6$), δ = 3.97–4.10 (m, 5H, $CH(CH_3)_2$ & $P(OCH_2CH_3)_2$), 3.44 (br. sept, J = 6.5 Hz, 1H, $CH(CH_3)_2$), 3.06 (d, J = 22.0 Hz, 2H, CH_2CO), 1.28 (d, J = 6.5 Hz, 6H, $CH(CH_3)_2$), 1.22 (t, J = 7.0 Hz, 6H, $P(OCH_2CH_3)_2$), 1.13 (d, J = 6.5 Hz, 6H, $CH(CH_3)_2$); ^{13}C NMR (100 MHz, $DMSO-d_6$), δ = 163.0 (d, J = 5.4 Hz, C), 61.5 (d, J = 6.0 Hz, CH_2), 49.7 (CH), 45.0 (CH), 34.6 (d, J = 130.5 Hz, CH_2), 20.4

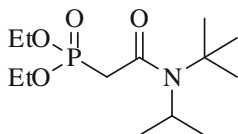
(CH₃) 20.3 (CH₃), 16.1 (d, $J = 6.0$ Hz, CH₃); IR (cm⁻¹) 3,475 (w), 2,969 (w), 1,636 (m), 1,444 (w), 1,335 (m), 1,250 (m), 1,110 (s); HRMS: m/z (CI), calculated for C₁₂H₂₇N₂O₄P, 280.1678 [M + H]⁺, found 280.1686 [M + H]⁺.

Diethyl (2-(*tert*-butyl(ethyl)amino)-2-oxoethyl)phosphonate (118)



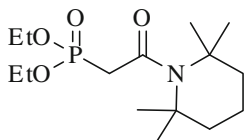
89 %; R_f 0.16 (1:1 EtOAc: PE); oil; ¹H NMR (400 MHz, DMSO-*d*₆), $\delta = 4.00$ (qd, $J = 8.0, 7.0$ Hz, 4H, P(OCH₂CH₃)₂), 3.41 (q, $J = 7.0$ Hz, 2H, NCH₂CH₃), 3.03 (d, $J = 22.0$ Hz, 2H, CH₂CO), 1.37 (s, 9H, C(CH₃)₂), 1.22 (t, $J = 7.0$ Hz, 6H, P(OCH₂CH₃)₂), 1.11 (t, $J = 7.0$ Hz, 3H, NCH₂CH₃); ¹³C NMR (100 MHz, DMSO-*d*₆), $\delta = 164.9$ (d, $J = 4.5$ Hz, C), 61.5 (d, $J = 6.0$ Hz, CH₂), 56.7 (C), 39.5 (CH₂), 35.2 (d, $J = 133.0$ Hz, CH₂), 28.5 (CH₃), 16.8 (CH₃), 16.2 (d, $J = 6.0$ Hz, CH₃); IR (cm⁻¹) 3,469 (w), 2,978 (w), 2,930 (w), 1,640 (s), 1,392 (m), 1,248 (m); HRMS: m/z (CI), calculated for C₁₂H₂₇NO₄P, 280.1668 [M + H]⁺, found 280.1678 [M + H]⁺.

Diethyl (2-(*tert*-butyl(isopropyl)amino)-2-oxoethyl)phosphonate (119)



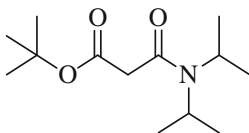
68 %; R_f 0.18 (1:1 EtOAc: PE); oil; ¹H NMR (400 MHz, DMSO-*d*₆), $\delta = 4.02$ (qd, $J = 8.0, 7.0$ Hz, 4H, P(OCH₂CH₃)₂), 4.00 (br. s, 1H, CH(CH₃)₂), 3.05 (d, $J = 22.0$ Hz, 2H, CH₂CO), 1.37 (s, 9H, C(CH₃)₃), 1.30 (d, $J = 7.0$ Hz, 6H, CH(CH₃)₂), 1.22 (t, $J = 7.0$ Hz, 6H, P(OCH₂CH₃)₂); ¹³C NMR (100 MHz, CDCl₃), $\delta = 166.7$ (d, $J = 5.5$ Hz, C), 62.1 (d, $J = 7.0$ Hz, CH₂), 58.9 (C), 46.9 (CH), 38.0 (d, $J = 137.5$ Hz, CH₂), 29.3 (CH₃), 23.4 (CH₃), 16.2 (d, $J = 6.0$ Hz, CH₃); IR (cm⁻¹) 3,446 (w), 2,976 (w), 1,637 (s); HRMS: m/z (CI), calculated for C₁₃H₂₉NO₄P, 294.1834 [M + H]⁺, found 294.1830 [M + H]⁺.

Diethyl (2-oxo-2-(2,2,6,6-tetramethylpiperidin-1-yl)ethyl)phosphonate (120)



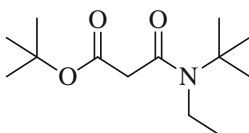
21 %; R_f 0.52 (1:1 MeCN:DCM); oil; ^1H NMR (400 MHz, CDCl_3), δ = 4.15–4.23 (m, 4H, $(\text{OCH}_2\text{CH}_3)_2$), 3.11 (d, J = 22.0 Hz, 2H, CH_2CO), 1.73–1.76 (m, 6H, $(\text{CH}_2)_3$), 1.46 (s, 12H, 4 (CH_3)), 1.33 (t, J = 7.0 Hz, 6H, $(\text{OCH}_2\text{CH}_3)_2$); ^{13}C NMR (100 MHz, CDCl_3), δ = 168.5 (d, J = 6.0 Hz, C), 62.2 (d, J = 6.0 Hz, CH_2), 56.2 (C), 39.7 (d, J = 136.0 Hz, CH_2), 36.3 (CH_2), 30.0 (CH_3), 16.4 (d, J = 6.0 Hz, CH_3), 14.3 (CH_2); IR (cm^{-1}) 3,479 (w), 2,974 (w), 1,634 (s), 1,367 (m), 1,344 (m), 1,252 (m), 1,022 (s), 960 (m); HRMS: m/z (CI), calculated for $\text{C}_{15}\text{H}_{31}\text{NO}_4$, 320.1991 $[\text{M} + \text{H}]^+$, found 320.1985 $[\text{M} + \text{H}]^+$.

***tert*-Butyl 3-(diisopropylamino)-3-oxopropanoate (122)**



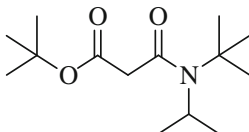
93 %; R_f 0.45 (3:7 EtOAc: PE); oil; ^1H NMR (400 MHz, CDCl_3), δ = 3.82 (sept, J = 7.0 Hz, 1H, $\text{CH}(\text{CH}_3)_2$), 3.41–3.54 (br. m, 1H, $\text{CH}(\text{CH}_3)_2$), 3.32 (s, 2H, CH_2CO), 1.48 (s, 9H, $\text{C}(\text{CH}_3)_3$), 1.41 (d, J = 7.0 Hz, 6H, $\text{CH}(\text{CH}_3)_2$), 1.21 (d, J = 7.0 Hz, 6H, $\text{CH}(\text{CH}_3)_2$); ^{13}C NMR (100 MHz, CDCl_3), δ = 167.2 (C), 164.9 (C), 81.5 (C), 49.7 (CH), 45.8 (CH), 44.7 (CH_2), 28.0 (CH_3), 20.7 (CH_3), 20.3 (CH_3); IR (cm^{-1}) 2,970 (w), 2,933 (w), 1,729 (s), 1,640 (s), 1,443 (m), 1,339 (m), 1,146 (s); HRMS: m/z (CI), calculated for $\text{C}_{13}\text{H}_{26}\text{NO}_3$, 244.1913 $[\text{M} + \text{H}]^+$, found 244.1922 $[\text{M} + \text{H}]^+$.

***tert*-Butyl 3-(*tert*-butyl(ethyl)amino)-3-oxopropanoate (123)**



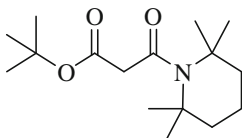
89 %; R_f 0.51 (3:7 EtOAc: PE); oil; ^1H NMR (400 MHz, CDCl_3), δ = 3.34 (s, 2H, CH_2CO), 3.33 (q, J = 7.0 Hz, 2H, NCH_2CH_3), 1.48 (s, 9H, $\text{OC}(\text{CH}_3)_3$), 1.46 (s, 9H, $\text{NC}(\text{CH}_3)_3$), 1.19 (t, J = 7.0 Hz, 3H, NCH_2CH_3); ^{13}C NMR (100 MHz, CDCl_3), δ = 167.5 (C), 166.8 (C), 81.5 (C), 57.3 (C), 45.0 (CH_2), 40.2 (CH_2), 28.9 (CH_3), 28.0 (CH_3), 17.1 (CH_3); IR (cm^{-1}) 2,975 (w), 1,731 (s), 1,646 (s), 1,395 (m); HRMS: m/z (CI), calculated for $\text{C}_{13}\text{H}_{26}\text{NO}_3$, 244.1913 $[\text{M} + \text{H}]^+$, found 244.1904 $[\text{M} + \text{H}]^+$.

***tert*-Butyl 3-(*tert*-butyl(isopropyl)amino)-3-oxopropanoate (124)**



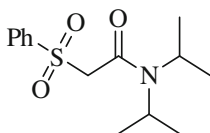
56 %; R_f 0.58 (3:7 EtOAc: PE); oil; $^1\text{H NMR}$ (400 MHz, CDCl_3), $\delta = 3.96$ (sept, $J = 7.0$ Hz, 1H, $\text{CH}(\text{CH}_3)_2$), 3.38 (s, 2H, CH_2CO), 1.48 (s, 9H, $\text{OC}(\text{CH}_3)_3$), 1.47 (s, 9H, $\text{NC}(\text{CH}_3)_3$), 1.38 (d, $J = 7.0$ Hz, 6H, $\text{CH}(\text{CH}_3)_2$); $^{13}\text{C NMR}$ (100 MHz, CDCl_3), $\delta = 168.1$ (C), 167.5 (C), 81.1 (C), 58.7 (C), 46.7 (CH_2), 46.5 (CH), 29.5 (CH_3), 27.9 (CH_3), 23.2 (CH_3); IR (cm^{-1}) 2,975 (w), 1,733 (s), 1,639 (s), 1,367 (m), 1,146 (s); HRMS: m/z (CI), calculated for $\text{C}_{14}\text{H}_{28}\text{NO}_3$, 258.2069 [$\text{M} + \text{H}$] $^+$, found 258.2071 [$\text{M} + \text{H}$] $^+$.

***tert*-Butyl 3-oxo-3-(2,2,6,6-tetramethylpiperidin-1-yl)propanoate (125)**



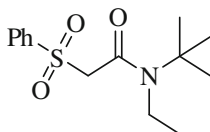
15 %; R_f 0.62 (1:1 EtOAc: PE); oil; $^1\text{H NMR}$ (400 MHz, CDCl_3), $\delta = 3.39$ (s, 2H, CH_2CO), 1.75–1.79 (m, 6H, $(\text{CH}_2)_3$), 1.47 (s, 21H, $\text{C}(\text{CH}_3)_3$ & $4(\text{CH}_3)$); $^{13}\text{C NMR}$ (100 MHz, CDCl_3), $\delta = 169.8$ (C), 167.4 (C), 81.0 (C), 56.1 (C), 48.3 (CH_2), 36.8 (CH_2), 29.9 (CH_3), 28.0 (CH_3), 14.5 (CH_2); IR (cm^{-1}) 2,973 (w), 1,736 (s), 1,636 (s), 1,368 (m), 1,257 (m), 1,143 (s); HRMS: m/z (ESI), calculated for $\text{C}_{16}\text{H}_{29}\text{NO}_3\text{Na}$, 306.2040 [$\text{M} + \text{Na}$] $^+$, found 306.2045 [$\text{M} + \text{Na}$] $^+$.

***N,N*-Diisopropyl-2-(phenylsulfonyl)acetamide (127)**



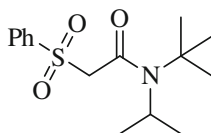
97 %; R_f 0.38 (1:1 EtOAc: PE); mp 144–146 °C (Ref: 144–145 °C); $^1\text{H NMR}$ (400 MHz, CDCl_3), $\delta = 7.91$ –7.93 (m, 2H, ArH), 7.64–7.70 (m, 1H, ArH), 7.53–7.59 (m, 2H, ArH), 4.21 (s, 2H, CH_2CO), 4.17–4.25 (m, 1H, $\text{CH}(\text{CH}_3)_2$), 3.48 (sept, $J = 6.5$ Hz, 1H, $\text{CH}(\text{CH}_3)_2$); 1.31 (d, $J = 6.5$ Hz, 6H, $\text{CH}(\text{CH}_3)_2$), 1.27 (d, $J = 6.5$ Hz, 6H, $\text{CH}(\text{CH}_3)_2$); $^{13}\text{C NMR}$ (100 MHz, CDCl_3), $\delta = 159.8$ (C), 138.8 (C), 134.1 (CH), 129.0 (CH), 128.5 (CH), 61.7 (CH_2), 50.9 (CH), 46.5 (CH), 20.8 (CH_3), 20.0 (CH_3); IR (cm^{-1}) 2,935 (w), 1,635 (s), 1,449 (m), 1,307 (s), 1,156 (s), 1,141 (s); HRMS: m/z (CI), calculated for $\text{C}_{14}\text{H}_{22}\text{NO}_3\text{S}$, 284.1314 [$\text{M} + \text{H}$] $^+$, found 284.1320 [$\text{M} + \text{H}$] $^+$ [31].

***N*-(*tert*-Butyl)-*N*-ethyl-2-(phenylsulfonyl)acetamide (128)**



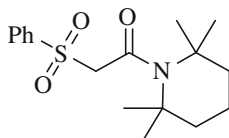
98 %; R_f 0.40 (1:1 EtOAc: PE); mp 108–110 °C; ^1H NMR (400 MHz, CDCl_3), $\delta = 7.88\text{--}7.94$ (m, 2H, ArH), 7.65 (app. tt, $J = 7.5, 2.0$ Hz, 1H, ArH), 7.51–7.58 (m, 2H, ArH), 4.21 (s, 2H, CH_2CO), 3.54 (q, $J = 7.0$ Hz, 2H, NCH_2CH_3), 1.38 (s, 9H, $\text{C}(\text{CH}_3)_3$), 1.18 (t, $J = 7.0$ Hz, 3H, NCH_2CH_3); ^{13}C NMR (100 MHz, CDCl_3), $\delta = 161.5$ (C), 138.8 (C), 133.9 (CH), 128.9 (CH), 128.6 (CH), 62.1 (CH_2), 58.1 (C), 40.4 (CH_2), 28.5 (CH_3), 17.0 (CH_3); IR (cm^{-1}) 2,972 (w), 1,640 (s), 1,306 (s), 1,151 (s), 1,079 (s); HRMS: m/z (CI), calculated for $\text{C}_{14}\text{H}_{22}\text{NO}_3\text{S}$, 284.1320 $[\text{M} + \text{H}]^+$, found 284.1311 $[\text{M} + \text{H}]^+$.

***N*-(*tert*-Butyl)-*N*-isopropyl-2-(phenylsulfonyl)acetamide (129)**

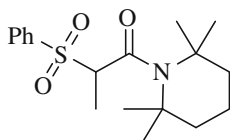


96 %; R_f 0.44 (1:1 EtOAc: PE); mp 88–90 °C; ^1H NMR (400 MHz, CDCl_3), $\delta = 7.93\text{--}7.95$ (m, 2H, ArH), 7.65 (app. tt, $J = 7.5, 2.0$ Hz, 1H, ArH), 7.53–7.57 (m, 2H, ArH), 4.25 (s, 2H, CH_2CO), 4.00 (br. s, 1H, $\text{CH}(\text{CH}_3)_2$), 1.40 (s, 9H, $\text{C}(\text{CH}_3)_3$), 1.39 (d, $J = 7.5$ Hz, 6H, $\text{CH}(\text{CH}_3)_2$); ^{13}C NMR (100 MHz, CDCl_3), $\delta = 163.3$ (C), 139.6 (C), 133.6 (CH), 128.7 (CH), 128.7 (CH), 63.8 (CH_2), 59.4 (C), 48.6 (CH), 29.1 (CH_3), 23.7 (CH_3); IR (cm^{-1}) 2,959 (w), 1,641 (s), 1,446 (m), 1,305 (s), 1,290 (m), 1,155 (s), 1,084 (m); HRMS: m/z (CI), calculated for $\text{C}_{15}\text{H}_{24}\text{NO}_3\text{S}$, 298.1477 $[\text{M} + \text{H}]^+$, found 298.1488 $[\text{M} + \text{H}]^+$.

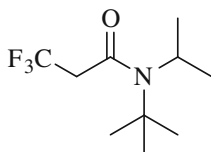
2-(Phenylsulfonyl)-1-(2,2,6,6-tetramethylpiperidin-1-yl)ethanone (130)



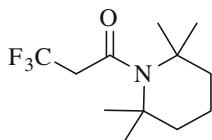
39 %; R_f 0.50 (1:1 EtOAc: PE); mp 133–134 °C; ^1H NMR (400 MHz, CDCl_3), $\delta = 7.89\text{--}7.94$ (m, 2H, ArH), 7.61 (app. tt, $J = 7.5, 2.5$ Hz, 1H, ArH), 7.49–7.55 (m, 2H, ArH), 4.27 (s, 2H, CH_2CO), 1.72 (s, 6H, $(\text{CH}_2)_3$), 1.40 (s, 12H, 4 (CH_3)); ^{13}C NMR (100 MHz, CDCl_3), $\delta = 164.5$ (C), 139.7 (C), 133.4 (CH), 128.7 (CH), 128.6 (CH), 64.9 (CH_2), 56.4 (C), 35.8 (CH_2), 29.7 (CH_3), 14.0 (CH_2); IR (cm^{-1}) 2,954 (w), 1,638 (s), 1,370 (m), 1,304 (s), 1,154 (s); HRMS: m/z (CI), calculated for $\text{C}_{17}\text{H}_{26}\text{NO}_3\text{S}$, 324.1633 $[\text{M} + \text{H}]^+$, found 324.1646 $[\text{M} + \text{H}]^+$.

2-(Phenylsulfonyl)-1-(2,2,6,6-tetramethylpiperidin-1-yl)propan-1-one (131)

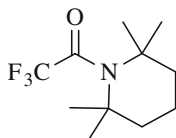
NaH (60 % in mineral oil) (40 mg, 1 mmol, 1 eq) was suspended in anhydrous THF (5 mL) cooled in an ice bath. To this was added 2-(phenylsulfonyl)-1-(2,2,6,6-tetramethylpiperidin-1-yl)ethanone (323 mg, 1 mmol, 1 eq). After stirring at 0 °C for 1 h, methyl iodide (62 μ L, 1 mmol, 1 eq) was added dropwise and the reaction was allowed warm to room temperature and stir overnight. The reaction was carefully quenched with sequential addition of EtOAc (25 mL), ethanol (5 mL) then water (20 mL). The organic fractions were combined, dried over MgSO_4 and concentrated *in vacuo*. The residue was purified via column chromatography (1:4 EtOAc: PE) to yield the title compound as a clear oil (71 mg, 21 %). R_f 0.57 (1:1 EtOAc: PE); oil; ^1H NMR (400 MHz, CDCl_3 , 50 °C), δ = 7.86–7.91 (m, 2H, ArH), 7.62–7.68 (m, 1H, ArH), 7.51–7.57 (m, 2H, ArH), 4.41 (q, J = 6.5 Hz, 1H, CHCO), 2.02–2.10 (m, 2H, CH_2), 1.75–1.82 (m, 2H, CH_2), 1.57 (br. s, 6H, $\text{C}(\text{CH}_3)_2$), 1.56–1.64 (m, 2H, CH_2), 1.51 (br. s, 6H, $\text{C}(\text{CH}_3)_2$), 1.47 (d, J = 6.5 Hz, 3H, CHCH_3); ^{13}C NMR (100 MHz, CDCl_3 , 50 °C), δ = 169.3 (C), 137.0 (C), 133.6 (CH), 130.5 (CH), 128.4 (CH), 68.4 (CH), 56.6 (C), 36.3 (CH_2), 32.4 (CH_3), 28.0 (CH_3) 14.2 (CH_2), 14.2 (CH_3); IR (cm^{-1}) 2,941 (w), 1,634 (m), 1,446 (w), 1,376 (m), 1,298 (m), 1,130 (m); HRMS: m/z (CI), calculated for $\text{C}_{18}\text{H}_{28}\text{NO}_3\text{S}$, 338.1790 [$\text{M} + \text{H}$] $^+$, found 338.1787 [$\text{M} + \text{H}$] $^+$.

***N*-(*tert*-Butyl)-3,3,3-trifluoro-*N*-isopropylpropanamide (133)**

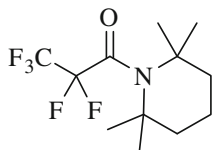
55 %; R_f 0.25 (1:9 Et_2O : PE); oil; ^1H NMR (400 MHz, CDCl_3), δ = 3.94 (sept, J = 7.0 Hz, 1H, $\text{CH}(\text{CH}_3)_2$), 3.18 (q, J = 10.0 Hz, 2H, CH_2CO), 1.42 (s, 9H, $\text{C}(\text{CH}_3)_4$), 1.35 (d, J = 7.0 Hz, 6H, $\text{CH}(\text{CH}_3)_2$); ^{13}C NMR (100 MHz, CDCl_3), δ = 165.4 (C), 124.2 (q, J = 276.5 Hz, CF_3), 59.3 (C), 46.3 (CH), 42.3 (q, J = 28.0 Hz, CH_2), 29.3 (CH_3), 22.4 (CH_3); ^{19}F NMR (376 MHz, CDCl_3), δ = -65.6; IR (cm^{-1}) 2,974 (w), 1,651 (s), 1,361 (s), 1,272 (m), 1,114 (m); HRMS: m/z (CI), calculated for $\text{C}_{10}\text{H}_{19}\text{NOF}_3$, 226.1419 [$\text{M} + \text{H}$] $^+$, found 226.1425 [$\text{M} + \text{H}$] $^+$

3,3,3-Trifluoro-1-(2,2,6,6-tetramethylpiperidin-1-yl)propan-1-one (134)

11 %; R_f 0.30 (1:9 Et₂O: PE); oil; ¹H NMR (400 MHz, CDCl₃), δ = 3.23 (q, J = 10.0 Hz, 2H, CH₂CO), 1.74–1.78 (m, 6H, (CH₂)₃), 1.45 (s, 12H, 4(CH₃)); ¹³C NMR (100 MHz, CDCl₃), δ = 166.9 (C), 124.4 (q, J = 278.0 Hz, CF₃), 56.4 (C), 43.8 (q, J = 27.5 Hz, CH₂), 36.3 (CH₂), 29.8 (CH₃), 14.2 (CH₂); ¹⁹F NMR (376 MHz, CDCl₃), δ = -61.9; IR (cm⁻¹) 1,637 (s), 1,389 (s), 1,233 (m), 1,118 (m); HRMS: m/z (CI), calculated for C₁₂H₂₁NOF₃, 252.1575 [M + H]⁺, found 252.1886 [M + H]⁺.

2,2,2-Trifluoro-1-(2,2,6,6-tetramethylpiperidin-1-yl)ethanone (135)

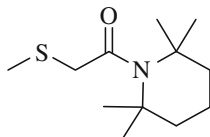
70 %; R_f 0.81 (1:1 EtOAc: PE); mp 57–58 °C (Ref: 45–47 °C); ¹H NMR (400 MHz, CDCl₃), δ = 1.77–1.79 (m, 6H, (CH₂)₃), 1.47 (s, 12H, 4(CH₃)); ¹³C NMR (100 MHz, CDCl₃), δ = 162.3 (q, J = 37.0 Hz, C), 116.2 (q, J = 289.0 Hz, CH), 58.6 (C), 35.7 (CH₂), 28.9 (CH₃), 14.1 (CH₂); ¹⁹F NMR (376 MHz, CDCl₃), δ = -68.2; IR (cm⁻¹) 2,979 (w), 1,673 (s), 147.2 (w), 1,222 (m), 1,127 (m), 1,177 (m), 1,146 (m), 1,029 (m); HRMS: m/z (ESI), calculated for C₁₁H₁₈F₃NO, 236.13 [M-H]⁺, found 236.10 [M-H]⁺ [32].

2,2,3,3,3-Pentafluoro-1-(2,2,6,6-tetramethylpiperidin-1-yl)propan-1-one (136)

20 %; R_f 0.22 (1:1 MeCN:DCM); mp 150–160 °C; ¹H NMR (400 MHz, CDCl₃), δ = 1.66–1.67 (m, 6H, (CH₂)₃), 1.50 (s, 12H, 4(CH₃)); ¹³C NMR (100 MHz, CDCl₃), δ = 161.5 (t, J = 24.5 Hz, C), 118.9 (tq, J = 285.5, 35.0 Hz, CF₃), 107.7 (qt, J = 285.5, 35.0 Hz, CF₂), 56.2 (C), 34.4 (CH₂), 27.1 (CH₃), 16.4 (CH₂); ¹⁹F NMR (376 MHz, CDCl₃), δ = -82.7, -120.5; IR (cm⁻¹) 2,943 (w),

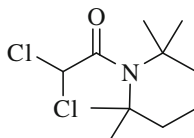
1,682 (s), 1,203 (m), 1,156 (m), 1,026 (m); LRMS: $C_{12}H_{18}F_5NO$, m/z (CI), 126.1 (100 %), 142.2 (68 %) 165.0 (32 %) 288 (6 %) $[M + H]^+$.

2-(Methylthio)-1-(2,2,6,6-tetramethylpiperidin-1-yl)ethanone (137)



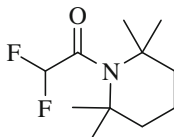
34 %; R_f 0.20 (1:4 Et_2O : PE); oil; 1H NMR (400 MHz, $CDCl_3$), δ = 3.31 (s, 2H, CH_2CO), 2.24 (s, 3H, SCH_3), 1.72 (s, 6H, $(CH_2)_3$), 1.42 (s, 12H, 4(CH_3)); ^{13}C NMR (100 MHz, $CDCl_3$), δ = 174.0 (C), 55.8 (C), 41.0 (CH_2), 36.3 (CH_2), 29.9 (CH_3), 16.7 (CH_3), 14.3 (CH_2); IR (cm^{-1}) 2,944 (w), 1,632 (s), 1,464 (m), 1,365 (m), 1,338 (m); HRMS: m/z (CI), calculated for $C_{12}H_{24}NOS$, 230.1579 $[M + H]^+$, found 230.1590 $[M + H]^+$.

2,2-Dichloro-1-(2,2,6,6-tetramethylpiperidin-1-yl)ethanone (138)



13 %; R_f 0.42 (1:4 Et_2O : PE); mp 83 °C; 1H NMR (400 MHz, $CDCl_3$), δ = 6.34 (s, 1H, $CHCO$), 1.80 (s, 6H, $(CH_2)_3$), 1.47 (s, 12H, 4(CH_3)); ^{13}C NMR (100 MHz, $CDCl_3$), δ = 168.1 (C), 67.9 (CH), 56.5 (C), 35.4 (CH_2), 29.7 (CH_3), 14.0 (CH_2); IR (cm^{-1}) 2,952 (w), 1,654 (s), 1,472 (w), 1,372 (m), 1,348 (m); HRMS: m/z (CI), calculated for $C_{11}H_{20}NOCl_2$, 252.0922 $[M + H]^+$, found 252.0918 $[M + H]^+$.

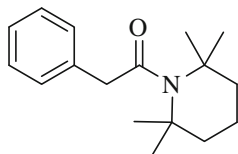
2,2-Difluoro-1-(2,2,6,6-tetramethylpiperidin-1-yl)ethanone (139)



17 %; R_f 0.44 (1:4 Et_2O : PE); oil; 1H NMR (400 MHz, $CDCl_3$), δ = 6.19 (t, J = 54.5 Hz, 1H, $CHCO$), 1.77 (s, 6H, $(CH_2)_3$), 1.46 (s, 12H, 4(CH_3)); ^{13}C NMR (100 MHz, $CDCl_3$), δ = 166.5 (t, J = 26.5 Hz, C), 106.4 (t, J = 243.5 Hz, CH), 56.7 (C), 35.8 (CH_2), 29.8 (CH_3), 14.0 (CH_2); ^{19}F NMR (376 MHz, $CDCl_3$), δ = -121.6, -121.8; IR (cm^{-1}) 2,949 (w), 1,666 (s), 1,309 (m), 1,127 (m);

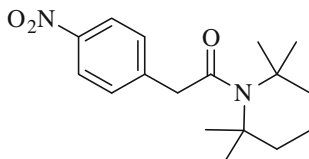
HRMS: m/z (CI), calculated for $C_{11}H_{20}NOF_2$, 220.1513 $[M + H]^+$, found 220.1511 $[M + H]^+$.

2-Phenyl-1-(2,2,6,6-tetramethylpiperidin-1-yl)ethanone (140)



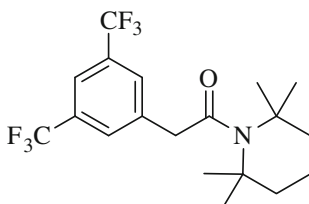
18 %; R_f 0.20 (1:4 Et₂O: PE); oil; ¹H NMR (400 MHz, CDCl₃), δ = 7.19–7.34 (m, 5H, ArH), 3.73 (s, 2H, CH₂CO), 1.79 (s, 6H, (CH₂)₃), 1.46 (s, 12H, 4(CH₃)); ¹³C NMR (100 MHz, CDCl₃), δ = 175.3 (C), 137.1 (C), 129.1 (CH), 128.2 (CH), 126.2 (CH), 55.8 (C), 46.3 (CH₂), 36.5 (CH₂), 30.1 (CH₃), 14.4 (CH₂); IR (cm⁻¹) 2,944 (w), 1,634 (s), 1,454 (w), 1,367 (m); HRMS: m/z (CI), calculated for $C_{17}H_{26}NO$, 260.2014 $[M + H]^+$, found 260.2025 $[M + H]^+$.

2-(4-Nitrophenyl)-1-(2,2,6,6-tetramethylpiperidin-1-yl)ethanone (141)



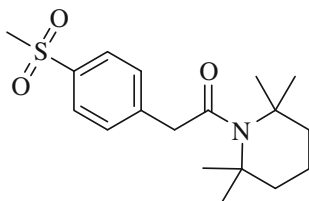
22 %; R_f 0.25 (1:1 Et₂O: PE); mp 68–70 °C; ¹H NMR (400 MHz, CDCl₃), δ = 8.13 (dd, J = 9.0, 2.0 Hz, 2H, ArH), 7.46 (dd, J = 9.0, 2.0 Hz, 2H, ArH), 3.81 (s, 2H, CH₂CO), 1.77–1.79 (m, 6H, (CH₂)₃), 1.46 (s, 12H, 4(CH₃)); ¹³C NMR (100 MHz, CDCl₃), δ = 173.5 (C), 146.6 (C), 144.7 (C), 130.0 (CH), 123.3 (CH), 56.1 (C), 46.0 (CH₂), 36.4 (CH₂), 30.1 (CH₃), 14.3 (CH₂); IR (cm⁻¹) 2,970 (w), 1,626 (s), 1,608 (m), 1,518 (s), 1,368 (m), 1,337 (s), 727 (s); HRMS: m/z (CI), calculated for $C_{17}H_{25}N_2O_3$, 306.1943 $[M + H]^+$, found 306.1923 $[M + H]^+$.

2-(3,5-Bis(trifluoromethyl)phenyl)-1-(2,2,6,6-tetramethylpiperidin-1-yl)ethanone (143)



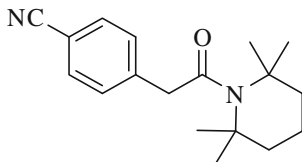
33 %; R_f 0.40 (1:1 EtOAc: PE); mp 94 °C; ^1H NMR (400 MHz, CDCl_3), $\delta = 7.77$ (s, 2H, ArH), 7.75 (s, 1H, ArH), 3.84 (s, 2H, CH_2CO), 1.81 (s, 6H, $(\text{CH}_2)_3$), 1.49 (s, 12H, 4(CH_3)); ^{13}C NMR (100 MHz, CDCl_3), $\delta = 173.4$ (C), 139.5 (C), 131.4 (q, $J = 33.0$ Hz, C), 129.5 (CH), 129.4 (CH), 123.4 (q, $J = 273.5$ Hz, CF_3), 120.5 (sept, $J = 4.0$ Hz, CH) 56.3 (C), 45.8 (CH_2), 36.5 (CH_2), 30.2 (CH_3), 14.4 (CH_2); IR (cm^{-1}) 2,953 (w), 1,629 (m), 1,371 (m), 1,274 (s); HRMS: m/z (CI), calculated for $\text{C}_{19}\text{H}_{24}\text{NOF}_6$, 396.1762 $[\text{M} + \text{H}]^+$, found 396.1,760 $[\text{M} + \text{H}]^+$.

2-(4-(Methylsulfonyl)phenyl)-1-(2,2,6,6-tetramethylpiperidin-1-yl)ethanone (144)

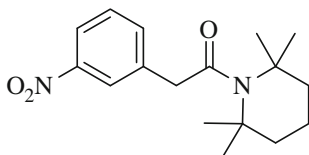


43 %; R_f 0.30 (100 % Et_2O); mp 135–136 °C; ^1H NMR (400 MHz, CDCl_3), $\delta = 7.87$ (dd, $J = 8.5, 2.0$ Hz, 2H, ArH), 7.50 (dd, $J = 8.5, 2.0$ Hz, 2H, ArH), 3.81 (s, 2H, CH_2CO), 3.03 (s, 3H, SO_2CH_3), 1.80 (s, 6H, $(\text{CH}_2)_3$), 1.48 (s, 12H, 4(CH_3)); ^{13}C NMR (100 MHz, CDCl_3), $\delta = 173.8$ (C), 143.6 (C), 138.5 (C), 130.2 (CH), 127.6 (CH), 56.2 (C), 46.1 (CH_2), 44.5 (CH_3), 36.5 (CH_2), 30.2 (CH_3), 14.3 (CH_2); IR (cm^{-1}) 2,929 (w), 1,736 (w), 1,625 (s), 1,370 (m), 1,348 (m), 1,287 (s), 1,141 (s), 1,090 (m); HRMS: m/z (CI), calculated for $\text{C}_{18}\text{H}_{28}\text{NO}_3\text{S}$, 338.1790 $[\text{M} + \text{H}]^+$, found 338.1796 $[\text{M} + \text{H}]^+$.

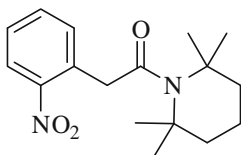
4-(2-Oxo-2-(2,2,6,6-tetramethylpiperidin-1-yl)ethyl)benzonitrile (145)



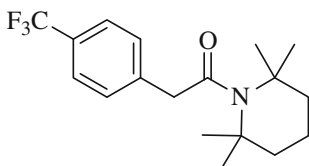
14 %; R_f 0.35 (1:1 Et_2O : PE); mp 93–94 °C; ^1H NMR (400 MHz, CDCl_3), $\delta = 7.60$ (dd, $J = 8.5, 2.0$ Hz, 2H, ArH), 7.43 (dd, $J = 8.5, 2.0$ Hz, 2H, ArH), 3.78 (s, 2H, CH_2CO), 1.80 (s, 6H, $(\text{CH}_2)_3$), 1.48 (s, 12H, 4(CH_3)); ^{13}C NMR (100 MHz, CDCl_3), $\delta = 173.7$ (C), 142.6 (C), 132.0 (CH), 130.0 (CH), 119.0 (C), 110.3 (C), 56.1 (C), 46.3 (CH_2), 36.4 (CH_2), 30.2 (CH_3), 14.3 (CH_2); IR (cm^{-1}) 2,935 (w), 2,230 (m), 1,737 (w), 1,624 (s), 1,345 (m), 1,132 (m); HRMS: m/z (CI), calculated for $\text{C}_{18}\text{H}_{25}\text{N}_2\text{O}$, 285.1967 $[\text{M} + \text{H}]^+$, found 285.1964 $[\text{M} + \text{H}]^+$.

2-(3-Nitrophenyl)-1-(2,2,6,6-tetramethylpiperidin-1-yl)ethanone (146)

25 %; R_f 0.31 (1:1 Et₂O: PE); mp 80–81 °C; ¹H NMR (400 MHz, CDCl₃), δ = 8.14–8.16 (m, 1H, ArH), 8.08–8.11 (m, 1H, ArH), 7.69 (app. d, J = 6.5 Hz, 1H, ArH), 7.48 (app. t, J = 8.0 Hz, 1H, ArH), 3.83 (s, 2H, CH₂CO), 1.79–1.81 (m, 6H, (CH₂)₃), 1.50 (s, 12H, 4(CH₃)); ¹³C NMR (100 MHz, CDCl₃), δ = 173.8 (C), 148.1 (C), 139.1 (C), 135.7 (CH), 129.1 (CH), 124.1 (CH), 121.6 (CH), 56.2 (C), 45.8 (CH₂), 36.5 (CH₂), 30.2 (CH₃), 14.6 (CH₂); IR (cm⁻¹) 2,964 (w), 1,624 (s), 1,611 (m), 1,526 (s), 1,346 (s), 1,157 (m), 734 (s); HRMS: m/z (CI), calculated for C₁₇H₂₅N₂O₃, 305.1865 [M + H]⁺, found 305.1877[M + H]⁺.

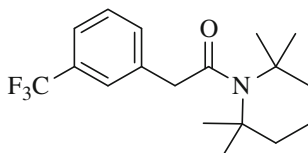
2-(2-Nitrophenyl)-1-(2,2,6,6-tetramethylpiperidin-1-yl)ethanone (147)

30 %; R_f 0.29 (1:1 Et₂O: PE); mp 118–119 °C; ¹H NMR (400 MHz, CDCl₃), δ = 8.02 (dd, J = 8.0, 1.5 Hz, 1H, ArH), 7.55 (app. dt, J = 8.0, 1.5 Hz, 1H, ArH), 7.36–7.43 (m, 2H, ArH), 4.11 (s, 2H, CH₂CO), 1.72–1.86 (m, 6H, (CH₂)₃), 1.51 (s, 12H, 4(CH₃)); ¹³C NMR (100 MHz, CDCl₃), δ = 172.4 (C), 148.7 (C), 138.6 (C), 133.8 (CH), 133.0 (CH), 127.6 (CH), 124.9 (CH), 56.7 (C), 45.1 (CH₂), 37.4 (CH₂), 29.9 (CH₃), 14.7 (CH₂); IR (cm⁻¹) 2,952 (w), 1,619 (s), 1,520 (s), 1,371 (m), 1,350 (s), 720 (s); HRMS: m/z (CI), calculated for C₁₇H₂₅N₂O₃, 305.1865 [M + H]⁺, found 305.1860 [M + H]⁺.

1-(2,2,6,6-Tetramethylpiperidin-1-yl)-2-(4-(trifluoromethyl)phenyl)ethanone (148)

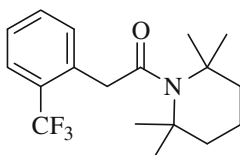
22 %; R_f 0.41 (1:1 Et₂O: PE); mp 57 °C; ¹H NMR (400 MHz, CDCl₃), δ = 7.55 (app. d, J = 8.5 Hz, 2H, ArH), 7.43 (app. d, J = 8.5 Hz, 2H, ArH), 3.77 (s, 2H, CH₂CO), 1.77–1.80 (m, 6H, (CH₂)₃), 1.48 (s, 12H, 4(CH₃)); ¹³C NMR (100 MHz, CDCl₃), δ = 174.3 (C), 141.2 (C), 129.5 (CH), 128.6 (q, J = 32.5 Hz, C), 125.1 (q, J = 4.0 Hz, CH), 124.3 (q, J = 271.5 Hz, CF₃), 56.0 (C), 46.1 (CH₂), 36.5 (CH₂), 30.1 (CH₃), 14.4 (CH₂); IR (cm⁻¹) 2,948 (w), 1,637 (s), 1,369 (m), 1,321 (s); HRMS: m/z (CI), calculated for C₁₈H₂₅NOF₃, 328.1888 [M + H]⁺, found 328.1893 [M + H]⁺.

1-(2,2,6,6-Tetramethylpiperidin-1-yl)-2-(3-(trifluoromethyl)phenyl)ethanone (149)

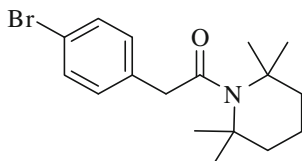


29 %; R_f 0.46 (1:1 Et₂O: PE); mp 49–50 °C; ¹H NMR (400 MHz, CDCl₃), δ = 7.47–7.56 (m, 3H, ArH), 7.40–7.45 (m, 1H, ArH), 3.78 (s, 2H, CH₂CO), 1.78–1.82 (m, 6H, (CH₂)₃), 1.49 (s, 12H, 4(CH₃)); ¹³C NMR (100 MHz, CDCl₃), δ = 174.4 (C), 138.1 (C), 132.8 (CH), 130.5 (q, J = 32.5 Hz, C), 128.7 (CH), 125.8 (q, J = 4.0 Hz, CH), 124.2 (q, J = 272.0 Hz, CF₃), 123.3 (q, J = 4.0 Hz, CH), 56.1 (C), 46.1 (CH₂), 36.5 (CH₂), 30.2 (CH₃), 14.4 (CH₂); IR (cm⁻¹) 2,949 (w), 1,636 (s); HRMS: m/z (CI), calculated for C₁₈H₂₅NOF₃, 328.1888 [M + H]⁺, found 328.1880 [M + H]⁺.

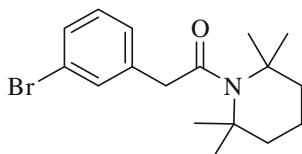
1-(2,2,6,6-Tetramethylpiperidin-1-yl)-2-(2-(trifluoromethyl)phenyl)ethanone (150)



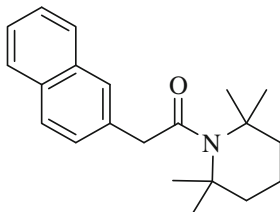
27 %; R_f 0.66 (1:1 Et₂O: PE); mp 75–76 °C; ¹H NMR (400 MHz, CDCl₃), δ = 7.63 (app. d, J = 8.0 Hz, 1H, ArH), 7.44–7.53 (m, 2H, ArH), 7.33 (app. t, J = 8.0 Hz, 1H, ArH), 3.91 (s, 2H, CH₂CO), 1.76–1.85 (m, 6H, (CH₂)₃), 1.50 (s, 12H, 4(CH₃)); ¹³C NMR (100 MHz, CDCl₃), δ = 173.1 (C), 135.5 (q, J = 1.5 Hz, C), 132.8 (CH), 131.5 (CH), 128.2 (q, J = 29.5 Hz, C), 126.4 (CH), 125.7 (q, J = 5.5 Hz, CH), 124.5 (q, J = 274.0 Hz, CF₃), 56.4 (C), 43.1 (q, J = 1.5 Hz, CH₂), 37.5 (CH₂), 29.9 (CH₃), 14.6 (CH₂); IR (cm⁻¹) 2,937 (w), 1,626 (s), 1,368 (m); HRMS: m/z (CI), calculated for C₁₈H₂₅NOF₃, 328.1888 [M + H]⁺, found 328.1872 [M + H]⁺.

2-(4-Bromophenyl)-1-(2,2,6,6-tetramethylpiperidin-1-yl)ethanone (151)

16 %; R_f 0.41 (1:1 Et₂O: PE); mp 75–76 °C; ¹H NMR (400 MHz, CDCl₃), δ = 7.42 (dd, J = 8.5, 2.0 Hz, 2H, ArH), 7.20 (dd, J = 8.5, 2.0 Hz, 2H, ArH), 3.66 (s, 2H, CH₂CO), 1.77–1.79 (m, 6H, (CH₂)₃), 1.47 (s, 12H, 4(CH₃)); ¹³C NMR (100 MHz, CDCl₃), δ = 174.7 (C), 136.1 (C), 131.3 (CH), 130.9 (CH), 120.3 (C), 56.0 (C), 45.7 (CH₂), 36.5 (CH₂), 30.2 (CH₃) 14.4 (CH₂); IR (cm⁻¹) 2,963 (w), 1,641 (s), 1,487 (m), 1,364 (s), 1,338 (s), 1,145 (m), 1,068 (m), 797 (s); HRMS: m/z (CI), calculated for C₁₇H₂₅NO⁷⁹Br, 338.1120 [M + H]⁺, found 338.1120 [M + H]⁺.

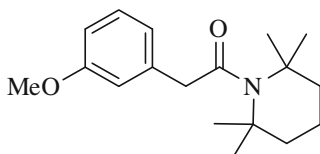
2-(3-Bromophenyl)-1-(2,2,6,6-tetramethylpiperidin-1-yl)ethanone (152)

17 %; R_f 0.41 (1:1 Et₂O: PE); mp 83–85 °C; ¹H NMR (400 MHz, CDCl₃), δ = 7.46 (app. t, J = 2.0 Hz, 1H, ArH), 7.35 (app. dt, J = 8.0, 2.0 Hz, 1H, ArH), 7.26 (m, 1H, ArH), 7.17 (app. t, J = 8.0 Hz, 1H, ArH), 3.69 (s, 2H, CH₂CO), 1.78–1.80 (m, 6H, (CH₂)₃), 1.48 (s, 12H, 4(CH₃)); ¹³C NMR (100 MHz, CDCl₃), δ = 174.5 (C), 139.3 (C), 138.2, (C) 132.1 (CH), 129.7 (CH), 129.5 (CH), 122.2 (CH), 56.0 (C), 45.8 (CH₂), 36.5 (CH₂), 30.2 (CH₃) 14.4 (CH₂); IR (cm⁻¹) 2,951 (w), 1,625 (s), 1,472 (m), 1,367 (m); HRMS: m/z (CI), calculated for C₁₇H₂₅NO⁷⁹Br, 338.1120 [M + H]⁺, found 338.1117 [M + H]⁺.

2-(Naphthalen-2-yl)-1-(2,2,6,6-tetramethylpiperidin-1-yl)ethanone (153)

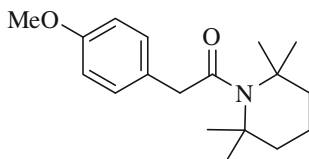
23 %; R_f 0.38 (1:1 Et₂O: PE); mp 66–67 °C; ¹H NMR (400 MHz, CDCl₃), δ = 7.78–7.84 (m, 4H, ArH), 7.43–7.52 (m, 3H, ArH), 3.91 (s, 2H, CH₂CO), 1.80–1.83 (m, 6H, (CH₂)₃), 1.53 (s, 12H, 4(CH₃)); ¹³C NMR (100 MHz, CDCl₃), δ = 175.3 (C), 134.7 (C), 133.5 (C), 132.2 (C), 127.8 (CH), 127.7 (CH), 127.6 (CH), 127.5 (CH), 126.2 (CH), 125.7 (CH), 125.3 (CH), 55.9 (C), 46.5 (CH₂), 36.6 (CH₂), 30.2 (CH₃) 14.5 (CH₂); IR (cm⁻¹) 2,942 (w), 1,621 (s), 1,365 (m), 1,343 (m), 1,271 (m), 1,162 (m); HRMS: m/z (CI), calculated for C₂₁H₂₈NO, 310.2171 [M + H]⁺, found 310.2176 [M + H]⁺.

2-(3-Methoxyphenyl)-1-(2,2,6,6-tetramethylpiperidin-1-yl)ethanone (155)

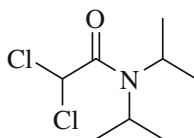


11 %; R_f 0.31 (100 % Et₂O); oil; ¹H NMR (400 MHz, CDCl₃), δ = 7.21 (app. t, J = 8.0 Hz, 1H, ArH), 6.89 (m, 2H, ArH), 6.77 (ddd, J = 8.0, 2.5, 1.0 Hz, 1H, ArH), 3.80 (s, 3H, OCH₃), 3.70 (s, 2H, CH₂CO), 1.77–1.79 (m, 6H, (CH₂)₃), 1.49 (s, 12H, 4(CH₃)); ¹³C NMR (100 MHz, CDCl₃), δ = 175.2 (C), 159.5 (C), 138.7 (C), 129.1 (CH), 121.6 (CH), 114.9 (CH), 111.8 (CH), 55.9 (C), 55.1 (CH₃), 46.4 (CH₂), 36.6 (CH₂), 30.2 (CH₃) 14.4 (CH₂); IR (cm⁻¹) 2,941 (w), 1,635 (s), 1,367 (m), 1,342 (m); HRMS: m/z (CI), calculated for C₁₈H₂₈NO₂, 290.2120 [M + H]⁺, found 290.2127 [M + H]⁺.

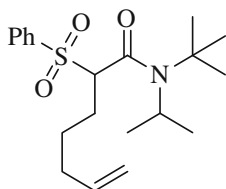
2-(4-Methoxyphenyl)-1-(2,2,6,6-tetramethylpiperidin-1-yl)ethanone (156)



9 %; R_f 0.31 (1:1 Et₂O: PE); oil; ¹H NMR (400 MHz, CDCl₃), δ = 7.24 (dd, J = 8.5, 2.0 Hz, 2H, ArH), 6.76 (dd, J = 8.5, 2.0 Hz, 2H, ArH), 3.70 (s, 3H, OCH₃), 3.57 (s, 2H, CH₂CO), 1.70 (s, 6H, (CH₂)₃), 1.40 (s, 12H, 4(CH₃)); ¹³C NMR (100 MHz, CDCl₃), δ = 175.8 (C), 158.1 (C), 130.4 (C), 130.1 (CH), 129.3 (CH), 114.1 (CH), 113.7 (CH), 55.8 (C), 55.2 (CH₃), 45.4 (CH₂), 36.5 (CH₂), 30.2 (CH₃) 14.4 (CH₂); IR (cm⁻¹) 2,938 (w), 1,635 (s), 1,510 (s), 1,367 (m), 1,244 (s); HRMS: m/z (CI), calculated for C₁₈H₂₈NO₂, 290.2120 [M + H]⁺, found 290.2116 [M + H]⁺.

2,2-dichloro-*N,N*-diisopropylacetamide (170)

R_f 0.45 (1:4 Et₂O: PE); mp 62 °C; ¹H NMR (400 MHz, CDCl₃), δ = 6.13 (s, 1H, CHCO), 4.34 (sept, J = 6.5 Hz, 1H, CH(CH₃)₂), 3.49 (br. sept, J = 6.5 Hz, 1H, CH(CH₃)₂), 1.40 (d, J = 6.5 Hz, 6H, CH(CH₃)₂), 1.28 (d, J = 6.5 Hz, 6H, CH(CH₃)₂); ¹³C NMR (100 MHz, CDCl₃), δ = 162.0 (C), 67.3 (CH), 49.4 (CH), 47.0 (CH), 20.3 (CH₃), 19.9 (CH₃); IR (cm⁻¹) 2,972 (w), 1,659 (s), 1,441 (m), 1,332 (m); HRMS: m/z (CI), calculated for C₈H₁₆NOCl₂, 212.0609 [M + H]⁺, found 212.0608 [M + H]⁺.

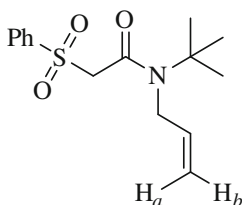
***N*-(*tert*-Butyl)-*N*-isopropyl-2-(phenylsulfonyl)hept-6-enamide (171)**

NaH (60 % in mineral oil) (80 mg, 2 mmol, 1 eq) was suspended in anhydrous THF (10 mL) cooled in an ice bath. To this was added *N*-(*tert*-butyl)-*N*-isopropyl-2-(phenylsulfonyl)acetamide (594 mg, 2 mmol, 1 eq). After stirring at 0 °C for 1 h, 5-bromo-1-pentene (237 μ L, 2 mmol, 1 eq) was added dropwise and the reaction was allowed to warm to room temperature and stir overnight. The reaction was carefully quenched with sequential addition of EtOAc (25 mL), ethanol (5 mL) then water (20 mL). The organic fractions were combined, dried over MgSO₄ and concentrated *in vacuo*. The residue was purified via column chromatography (1:4 EtOAc: PE) to yield the title compound as a clear oil (220 mg, 30 %). R_f 0.63 (1:1 EtOAc: PE); oil; ¹H NMR (400 MHz, CDCl₃, 50 °C), δ = 7.84–7.91 (m, 2H, ArH), 7.58–7.65 (m, 1H, ArH), 7.48–7.54 (m, 2H, ArH), 5.70 (ddt, J = 17.0, 10.5, 6.5 Hz, 1H, CH = CH₂), 4.90–4.98 (m, 2H, CH = CH₂), 4.32 (br. s, 1H, CHCO), 4.11 (br. s, 1H, CH(CH₃)₂), 1.97–2.03 (br. m, 2H, CH₂CH = CH₂), 1.72–1.99 (br. m, 2H, CH₂), 1.30–1.65 (br. m, 8H, CH₂ & CH(CH₃)₂) 1.47 (br. s, 9H, C(CH₃)₃); ¹³C NMR (100 MHz, CDCl₃), δ = 167.7 (C), 137.0 (C), 133.8 (CH), 130.4 (CH), 128.4 (CH), 115.2 (CH₂), 71.7 (CH), 69.4 (CH), 60.1 (C), 50.1 (CH₃), 45.9 (CH), 33.6 (CH₂), 29.5 (CH₃), 29.1 (CH₂), 25.4 (CH₂); IR (cm⁻¹) 3,070 (w), 2,928 (w), 1,638 (m), 1,447 (m), 1,306 (m); HRMS: m/z (CI), calculated for C₂₀H₃₂NO₃S, 366.2103 [M + H]⁺, found 366.2113 [M + H]⁺.

7.5.3 Procedure for the Preparation of Amides 172–174

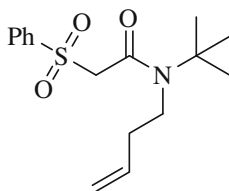
Amides **172–174** were synthesised using procedure 7.5.2. Non-commercial *tert*-butyl amines were synthesised using the procedure described in Sect. 7.4.1.

N-Allyl-*N*-(*tert*-butyl)-2-(phenylsulfonyl)acetamide (**172**)

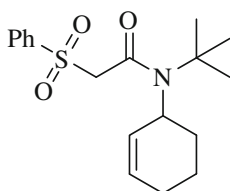


R_f 0.50 (1:1 EtOAc: PE); mp 90–92 °C; ^1H NMR (400 MHz, CDCl_3), $\delta = 7.89\text{--}7.93$ (m, 2H, ArH), 7.64–7.68 (m, 1H, ArH), 7.53–7.58 (m, 2H, ArH), 5.88 (ddt, $J = 17.0, 10.5, 4.0$ Hz, 1H, CH = CH_b), 5.26 (dtd, $J = 10.5, 2.0, 1.0$ Hz, 1H, CH = CH_bH), 5.16 (dtd, $J = 17.0, 2.0, 1.0$ Hz, 1H, CH = CH_a), 4.20 (app. dt, $J = 4.0, 2.0$ Hz, 2H, NCH₂CH = CH₂), 4.14 (s, 2H, CH₂CO), 1.39 (s, 9H, C(CH₃)₃); ^{13}C NMR (100 MHz, CDCl_3), $\delta = 162.3$ (C), 138.9 (C), 135.1 (CH), 134.0 (CH), 128.9 (CH), 128.6 (CH), 116.4 (CH₂), 62.2 (CH₂), 58.3 (C), 47.5 (CH₂), 28.2 (CH₃); IR (cm^{-1}) 2,958 (w), 1,637 (s), 1,405 (m), 1,391 (m), 1,315 (s), 1,305 (s); HRMS: m/z (CI), calculated for $\text{C}_{15}\text{H}_{22}\text{NO}_3\text{S}$, 296.1310 $[\text{M} + \text{H}]^+$, found 296.1320 $[\text{M} + \text{H}]^+$.

N-(But-3-en-1-yl)-*N*-(*tert*-butyl)-2-(phenylsulfonyl)acetamide (**173**)



R_f 0.50 (1:1 EtOAc: PE); oil; ^1H NMR (400 MHz, CDCl_3), $\delta = 7.86\text{--}7.91$ (m, 2H, ArH), 7.60–7.66 (m, 1H, ArH), 7.49–7.56 (m, 2H, ArH), 5.71 (ddt, $J = 17.0, 10.5, 7.0$ Hz, 1H, CH₂CH = CH₂), 5.05–5.13 (m, 2H, CH₂CH = CH₂), 4.20 (s, 2H, CH₂CO), 3.50 (t, $J = 8.0$ Hz, 2H, NCH₂CH₂), 2.23–2.31 (m, 2H, CH₂CH₂CH), 1.36 (s, 9H, C(CH₃)₃); ^{13}C NMR (100 MHz, CDCl_3), $\delta = 161.5$ (C), 138.7 (C), 133.9 (CH), 133.4 (CH), 128.8 (CH), 128.4 (CH), 117.7 (CH₂), 62.2 (CH₂), 58.0 (C), 45.2 (CH₂), 35.8 (CH₂), 28.4 (CH₃); IR (cm^{-1}) 2,976 (w), 1,644 (s), 1,447 (w); HRMS: m/z (CI), calculated for $\text{C}_{16}\text{H}_{24}\text{NO}_3\text{S}$, 310.1481 $[\text{M} + \text{H}]^+$, found 310.1477 $[\text{M} + \text{H}]^+$.

***N*-(*tert*-Butyl)-*N*-(cyclohex-2-en-1-yl)-2-(phenylsulfonyl)acetamide (174)**

R_f 0.52 (1:1 EtOAc: PE); oil; ^1H NMR (400 MHz, CDCl_3), δ = 7.89–7.93 (m, 2H, ArH), 7.59–7.65 (m, 1H, ArH), 7.49–7.56 (m, 2H, ArH), 5.81 (m, 1H, CHCH = CHCH₂), 5.56 (m, 1H, CHCH = CHCH₂), 4.24–4.27 (m, 3H, CH₂CO & NCH), 1.85–2.10 (m, 4H, (CH₂)₂), 1.59–1.79 (m, 2H, CH₂), 1.39 (s, 9H, C(CH₃)₃); ^{13}C NMR (100 MHz, CDCl_3), δ = 163.7 (C), 139.9 (C), 133.5 (CH), 131.7 (CH), 129.3 (CH), 128.6 (CH), 128.7 (CH), 63.0 (CH₂), 59.4 (C), 52.7 (CH), 32.1 (CH₂), 28.8 (CH₃), 24.0 (CH₂), 22.5 (CH₂); IR (cm^{-1}) 2,937 (w), 1,641 (s), 1,447 (m), 1,318 (m); HRMS: m/z (CI), calculated for C₁₈H₂₆NO₃S, 336.1638 [M + H]⁺, found 336.1633 [M + H]⁺.

7.5.4 Linear Free Energy Relationship for Methanolysis of Arylacetamides

Methanolyses were run in sealed “reduced volume” *Radleys* tubes in a *Radleys* 12-port reaction carousel at 70 °C. The appropriate amide (0.5 mmol) and methanol (1 mL) were added to separate tubes and allowed to reach temperature in the carousel over 5 min. On transfer of the MeOH, the amide dissolved rapidly (less than 5 s). Samples (50 μL) were removed at regular intervals via gas-tight syringe, rapidly transferred to a sample vial, cooled in ice, and the volatiles removed under vacuum. The residue was dissolved in CDCl_3 and the amide/ester ratio analysed by ^1H NMR. All of the reactions were devoid of side products (by ^1H NMR analysis) and standard linear logarithmic analysis based on pseudo first order kinetics gave good correlations in all cases.

Entry	Entry X	k_{obs}	σ^-	$\log_{10}(kX/kp\text{NO}_2)$
1	<i>p</i> -NO ₂	0.19802857	1.27	0.0
2	<i>p</i> -CN	0.04950714	1.0	-0.60204119
3	<i>m</i> -NO ₂	0.03850556	0.71	-0.71118566
4	<i>p</i> -MeSO ₂	0.01155167	1.13	-1.23406441
5	<i>p</i> -CF ₃	0.00119089	0.65	-2.22083614
6	<i>m</i> -CF ₃	0.00072198	0.46	-2.43818439
7	<i>p</i> -Br	0.00072198	0.25	-2.43818439

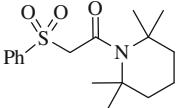
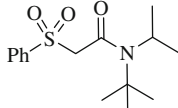
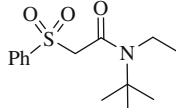
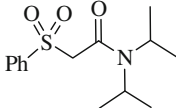
(continued)

(continued)

Entry	Entry X	k_{obs}	σ^-	$\log_{10}(kX/kp\text{NO}_2)$
8	<i>m</i> -Br	0.00064176	0.37	-2.48933691
9	<i>m</i> -MeO	4.3756E-05	0.12	-3.65566833
10	H	3.7025E-05	0.0	-3.728219
11	<i>p</i> -MeO	2.5333E-05	-0.27	-3.89302925

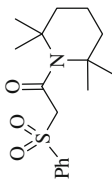
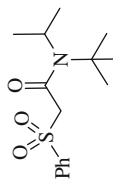
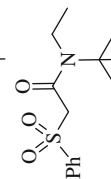
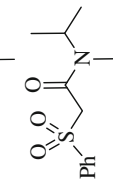
7.5.5 Kinetics of α -CH/D Exchange

For the H/D exchange, reactions were run analogously to that detailed above (7.5.4), but in CH_3OD in NMR tubes, with thermal pre-equilibration in the NMR probe. For fast exchange, spectra were acquired with a single FID. Analysis of the mol-fraction of α - CH_2 residual in the amide was made by integration against reference signals from the amide "R" group(s), with the α -CHD being well resolved through isotope shift. All of the reactions were devoid of side products (by ^1H NMR analysis) and standard linear logarithmic analysis based on pseudo first order kinetics gave good correlations in all cases. Linear regression, without weighting for heteroscedasticity, afforded k_{OBS} values for α -CH/D exchange ($k_{\text{OBS}}^{\text{D}}$). For **127** a single time point (0.5 % conversion, 12 h, 70 °C) was employed to estimate reactivity in methanolysis.

							
Time (s)	\log^a	Time (s)	\log^a	Time (s)	\log^a	Time (s)	\log^a
0	5.3999E-05	0	0.0	0	2.19998E-05	0	0.0
600	0.11528926	2,700	0.029558802	3,600	0.045692037	43,200	0.00501254
1,200	0.28964265	6,300	0.086177696	7,200	0.09787779		
1,800	0.38754686	9,900	0.148420005	10,800	0.139377521		
2,400	0.54980669	13,500	0.207014169	14,400	0.18700557		
3,000	0.66219094	17,100	0.270027137	18,000	0.217542294		
3,600	0.79128336	20,700	0.3074847	21,600	0.261667098		
4,200	0.92697505	24,300	0.357674444	25,200	0.303926908		
4,800	1.44202136	27,900	0.39877612				
6,600	1.44202136	32,400	0.482426149				
8,400	2.16539307						
10,200	2.25255037						

^a $\ln([\text{amide}]_0/[\text{amide}]_t)$

Empirical rate constants were also converted to empirical free energy of activation: $\Delta G_{\ddagger, \text{OBS}}^{\ddagger} = -RT \ln(k_{\text{obs}}h/k_{\text{B}}T)$.

Amide	k	T (°C)	T (K)	h/kbT	$\ln(k \times h/kbT)$	-RT	DG	DG kJ mol ⁻¹
	2.36E-04	3	276	2E-13	-37.7977	-2,294.66	86,733.0853	86.7330853
	1.49E-05	20	293	2E-13	-40.5571	-2,436	98,797.2347	98.7972347
	1.20E-05	70	343	1E-13	-40.9324	-2,851.7	116,672.022	116.727022
	1.16E-07	70	343	1E-13	-46.364	-2,851.7	132,216.252	132.216252

h 6.626068 × 10⁻³⁴

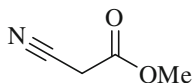
kb 1.3806503 × 10⁻²³

DG = -RTln(k × h/kbT)

7.5.6 Procedure for the Preparation of Methyl Ester Derivatives

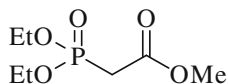
The desired amide (1 mmol) was dissolved in methanol (2 mL) and the solution was heated to the desired temperature. Aliquots were taken periodically (solvent and amine removed *in vacuo*) and the reaction followed by ^1H NMR until complete. For those reactions not going to completion, the reaction was concentrated *in vacuo* and purified via column chromatography (10–50 % EtOAc in PE).

Methyl 2-cyanoacetate (112)



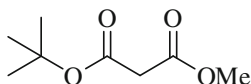
^1H NMR (400 MHz, CDCl_3), $\delta = 3.80$ (s, 3H, OCH_3), 3.48 (s, 2H, CH_2CO); ^{13}C NMR (100 MHz, CDCl_3), $\delta = 163.4$ (C), 113.0 (C), 53.4 (CH_3), 24.4 (CH_2). All further data consistent with the commercially available ester. CAS: 105-34-0.

Methyl 2-(diethoxyphosphoryl)acetate (116)

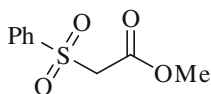


^1H NMR (400 MHz, CDCl_3), $\delta = 4.17$ (qd, $J = 7.5, 1.0$ Hz, 4H, $\text{P}(\text{OCH}_2\text{CH}_3)_2$), 3.75 (s, 3H, OCH_3), 2.96 (d, $J = 21.5$ Hz, 2H, CH_2CO), 1.33 (td, $J = 7.5, 1.0$ Hz, 6H, $\text{P}(\text{OCH}_2\text{CH}_3)_2$); ^{13}C NMR (100 MHz, CDCl_3), $\delta = 166.2$ (d, $J = 5.5$ Hz, C), 62.5 (d, $J = 6.0$ Hz, CH_2), 52.4 (CH_3), 34.0 (d, $J = 135.5$ Hz, CH_2), 16.2 (d, $J = 6.0$ Hz, CH_3). All further data consistent with the commercially available ester. CAS: 1067-74-9.

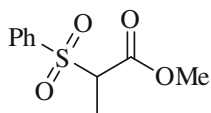
tert-Butyl methyl malonate (121)



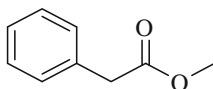
^1H NMR (400 MHz, CDCl_3), $\delta = 3.75$ (s, 3H, OCH_3), 3.31 (s, 2H, CH_2CO), 1.48 (s, 9H, $\text{C}(\text{CH}_3)_3$). ^{13}C NMR (100 MHz, CDCl_3), $\delta = 167.3$ (C), 165.7 (C), 82.1 (C), 52.3 (CH_3), 42.6 (CH_2), 27.9 (CH_3). All further data consistent with the commercially available ester. CAS: 42726-73-8.

Methyl 2-(phenylsulfonyl)acetate (126)

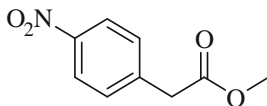
^1H NMR (400 MHz, CDCl_3), $\delta = 7.95\text{--}7.98$ (m, 2H, ArH), 7.69–7.73 (m, 1H, ArH), 7.58–7.63 (m, 2H, ArH), 4.14 (s, 2H, CH_2CO), 3.72 (s, 3H, OCH_3); ^{13}C NMR (100 MHz, CDCl_3), $\delta = 162.7$ (C), 138.5 (C), 134.2 (CH), 129.1 (CH), 128.3 (CH), 60.6 (CH_2), 52.9 (CH_3). All further data consistent with the commercially available ester. CAS: 34097-60-4.

Methyl 2-(phenylsulfonyl)propanoate (132)

R_f 0.28 (1:1 EtOAc: PE); oil; ^1H NMR (400 MHz, CDCl_3), $\delta = 7.86\text{--}7.89$ (m, 2H, ArH), 7.66–7.71 (m, 1H, ArH), 7.75–7.60 (m, 2H, ArH), 4.06 (q, $J = 7.1$ Hz, 1H, CHCO), 3.66 (s, 3H, OCH_3), 1.55 (d, $J = 7.3$ Hz, 3H, CHCH_3); ^{13}C NMR (100 MHz, CDCl_3), $\delta = 166.6$ (C), 136.8 (C), 134.2 (CH), 129.2 (CH), 129.0 (CH), 65.3 (CH), 52.9 (CH_3), 11.8 (CH_3); IR (cm^{-1}) 2,954 (w), 1,739 (s), 1,447 (m), 1,320 (m), 1,309 (s), 1,146 (s), 1,083 (m); HRMS: m/z (CI), calculated for $\text{C}_{10}\text{H}_{13}\text{O}_4\text{S}$, 229.0535 [$\text{M} + \text{H}$] $^+$, found 229.0526 [$\text{M} + \text{H}$] $^+$.

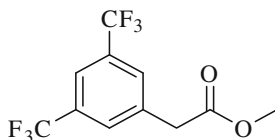
Methyl 2-phenylacetate (108)

^1H NMR (400 MHz, CDCl_3), $\delta = 7.30\text{--}7.37$ (m, 5H, ArH), 3.72 (s, 3H, OCH_3), 3.66 (s, 2H, CH_2CO); ^{13}C NMR (100 MHz, CDCl_3), $\delta = 171.8$ (C), 133.9 (C), 129.1 (CH), 128.5 (CH), 127.0 (CH), 51.9 (CH_3), 41.1 (CH_2). All further data consistent with the commercially available ester. CAS: 101-41-7.

Methyl 2-(4-nitrophenyl)acetate (142)

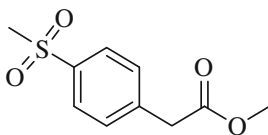
^1H NMR (400 MHz, CDCl_3), $\delta = 8.21$ (dd, $J = 8.5, 2.0$ Hz, 2H, ArH), 7.47 (dd, $J = 8.5, 2.0$ Hz, 2H, ArH), 3.75 (s, 2H, CH_2CO), 3.74 (s, 3H, OCH_3); ^{13}C NMR (100 MHz, CDCl_3), $\delta = 170.5$ (C), 147.1 (C), 141.2 (C), 130.2 (CH), 123.6 (CH), 52.3 (CH_3), 40.6 (CH_2). All further data consistent with the commercially available ester. CAS: 2945-08-6.

Methyl 2-(3,5-bis(trifluoromethyl)phenyl)acetate (157)



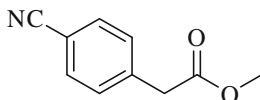
R_f 0.51 (1:1 Et_2O : PE); oil; ^1H NMR (400 MHz, CDCl_3), $\delta = 7.81$ (s, 1H, ArH), 7.77 (s, 2H, ArH), 3.77 (s, 2H, CH_2CO), 3.75 (s, 3H, OCH_3); ^{13}C NMR (100 MHz, CDCl_3), $\delta = 170.4$ (C), 136.3 (C), 131.8 (q, $J = 33.5$ Hz, C), 129.7 (q, $J = 4.5$ Hz, CH), 123.1 (q, $J = 272.5$ Hz, CF_3), 121.3 (sept, $J = 4.5$ Hz, CH), 52.4 (CH_3) 40.4 (CH_2); IR (cm^{-1}) 2,960 (w), 1,740 (s), 1,380 (m), 1,275 (s), 1,167 (s), 1,124 (s); HRMS: m/z (CI), calculated for $\text{C}_{11}\text{H}_9\text{O}_2\text{F}_6$, 287.0507 [$\text{M} + \text{H}$] $^+$, found 287.0515 [$\text{M} + \text{H}$] $^+$.

Methyl 2-(4-(methylsulfonyl)phenyl)acetate (158)



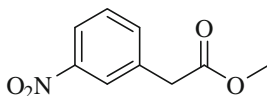
R_f 0.08 (1:1 Et_2O : PE); mp 84–85 °C; ^1H NMR (400 MHz, CDCl_3), $\delta = 7.92$ (dd, $J = 8.5, 2.0$ Hz, 2H, ArH), 7.50 (dd, $J = 8.5, 2.0$ Hz, 2H, ArH), 3.74 (s, 2H, CH_2CO), 3.74 (s, 3H, OCH_3), 3.06 (s, 3H, SO_2CH_3); ^{13}C NMR (100 MHz, CDCl_3), $\delta = 170.8$ (C), 140.2 (C), 139.4 (C), 130.3 (CH), 127.7 (CH), 52.8 (CH_3), 44.5 (CH_3), 40.9 (CH_2); IR (cm^{-1}) 1,731 (s), 1,302 (m), 1,219 (m), 1,168 (s), 1,147 (s), 1,091 (s), 959 (s); HRMS: m/z (CI), calculated for $\text{C}_{10}\text{H}_{13}\text{O}_4\text{S}$, 229.0535 [$\text{M} + \text{H}$] $^+$, found 229.0544 [$\text{M} + \text{H}$] $^+$.

Methyl 2-(4-cyanophenyl)acetate (159)



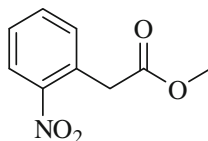
^1H NMR (400 MHz, CDCl_3), $\delta = 7.59$ (dd, $J = 8.5, 2.0$ Hz, 2H, ArH), 7.38 (dd, $J = 8.5, 2.0$ Hz, 2H, ArH), 3.69 (s, 3H, OCH_3), 3.68 (s, 2H, CH_2CO); ^{13}C NMR (100 MHz, CDCl_3), $\delta = 170.6$ (C), 139.1 (C), 132.1 (CH), 130.0 (CH), 118.5 (C), 111.0 (C), 52.1 (CH_3), 40.8 (CH_2). All further data consistent with that presented in the literature [33].

Methyl 2-(3-nitrophenyl)acetate (160)



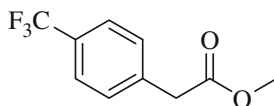
^1H NMR (400 MHz, CDCl_3), $\delta = 8.15$ – 8.19 (m, 1H, ArH), 7.64 (ddd, $J = 7.5, 2.0, 0.5$ Hz, 2H, ArH), 7.52 (app. t, $J = 8.0$ Hz, 1H, ArH), 3.76 (s, 2H, CH_2CO), 3.74 (s, 3H, OCH_3); ^{13}C NMR (100 MHz, CDCl_3), $\delta = 170.7$ (C), 148.3 (C), 135.8 (C), 135.6 (CH), 129.4 (CH), 124.4 (CH), 122.3 (CH), 52.4 (CH_3), 40.5 (CH_2). All further data consistent with that presented in the literature [34].

Methyl 2-(2-nitrophenyl)acetate (161)

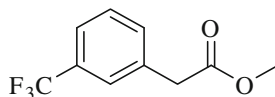


^1H NMR (400 MHz, CDCl_3), $\delta = 8.07$ (dd, $J = 7.0, 1.5$ Hz, 1H, ArH), 7.57 (app. dt, $J = 7.0, 1.5$ Hz, 1H, ArH), 7.45 (app. dt, $J = 7.0, 1.5$ Hz, 1H, ArH), 7.34 (dd, $J = 7.0, 1.5$ Hz, 1H, ArH), 4.00 (s, 2H, CH_2CO), 3.68 (s, 3H, OCH_3). ^{13}C NMR (100.6 MHz, CDCl_3), $\delta = 170.2$ (C), 148.6 (C), 133.5 (C), 133.2 (CH), 129.5 (CH), 125.5 (CH), 125.0 (CH), 52.0 (CH_3), 39.3 (CH_2). All further data consistent with that presented in the literature [35].

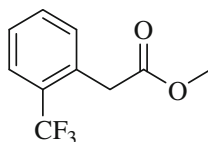
Methyl 2-(4-(trifluoromethyl)phenyl)acetate (162)



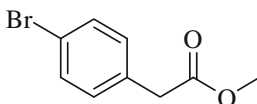
^1H NMR (400 MHz, CDCl_3), $\delta = 7.60$ (d, $J = 8.0$ Hz, 2H, ArH), 7.41 (dd, $J = 8.0, 1.0$ Hz, 2H, ArH), 3.72 (s, 3H, OCH_3), 3.70 (s, 2H, CH_2CO). ^{13}C NMR (100 MHz, CDCl_3), $\delta = 171.1$ (C), 137.9 (C), 129.6 (CH), 129.4 (q, $J = 32.5$ Hz, C), 125.4 (q, $J = 3.0$ Hz, CH), 124.2 (q, $J = 271.5$ Hz, CF_3), 52.1 (CH_3), 40.8 (CH_2). All further data consistent with that presented in the literature [36].

Methyl 2-(3-(trifluoromethyl)phenyl)acetate (163)

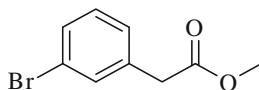
^1H NMR (400 MHz, CDCl_3), $\delta = 7.53\text{--}7.57$ (m, 2H, ArH), 7.45–7.51 (m, 2H, ArH), 3.73 (s, 3H, OCH_3), 3.70 (s, 2H, CH_2CO); ^{13}C NMR (100 MHz, CDCl_3), $\delta = 171.2$ (C), 134.8 (C), 132.7 (CH), 130.8 (q, $J = 32.0$ Hz, C), 129.0 (CH), 126.1 (q, $J = 4.0$ Hz, CH), 124.0 (q, $J = 272.5$ Hz, CF_3), 124.0 (q, $J = 4.0$ Hz, CH), 52.1 (CH_3), 40.7 (CH_2). All further data consistent with that presented in the literature [37].

Methyl 2-(3-(trifluoromethyl)phenyl)acetate (164)

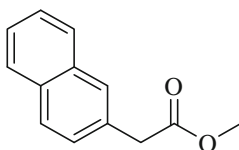
R_f 0.46 (1:1 Et_2O : PE); oil; ^1H NMR (400 MHz, CDCl_3), $\delta = 7.67$ (app. d, $J = 7.5$ Hz, 1H, ArH), 7.51–7.55 (m, 1H, ArH), 7.37–7.41 (m, 2H, ArH), 3.85 (s, 2H, CH_2CO), 3.71 (s, 3H, OCH_3); ^{13}C NMR (100 MHz, CDCl_3), $\delta = 171.1$ (C), 132.5 (CH), 132.4 (q, $J = 1.5$ Hz, C), 131.9 (CH), 128.9 (q, $J = 30.5$ Hz, C), 127.4 (CH), 126.0 (q, $J = 5.5$ Hz, CH), 124.3 (q, $J = 273.5$ Hz, CF_3), 52.1 (CH_3), 38.0 (CH_3); IR (cm^{-1}) 2,956 (w), 1,740 (s), 1,313 (s), 1,160 (m), 1,107 (s), 1,037 (s); HRMS: m/z (CI), calculated for $\text{C}_{10}\text{H}_{10}\text{O}_2\text{F}_3$, 219.0633 [$\text{M} + \text{H}$] $^+$, found 219.0625 [$\text{M} + \text{H}$] $^+$.

Methyl 2-(4-bromophenyl)acetate (165)

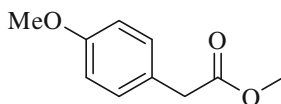
^1H NMR (400 MHz, CDCl_3), $\delta = 7.45$ (dd, $J = 8.0, 2.0$ Hz, 2H, ArH), 7.16 (dd, $J = 8.0, 2.0$ Hz, 2H ArH), 3.69 (s, 3H, OCH_3), 3.58 (s, 2H, CH_2CO); ^{13}C NMR (100 MHz, CDCl_3), $\delta = 171.3$ (C), 132.8 (C), 131.6 (CH), 130.9 (CH), 121.1 (C), 52.0 (CH_3), 40.4 (CH_2). All further data consistent with that presented in the literature [38].

Methyl 2-(3-bromophenyl)acetate (166)

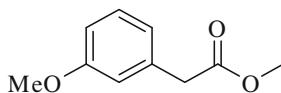
^1H NMR (400 MHz, CDCl_3), $\delta = 7.44\text{--}7.46$ (m, 1H, ArH), 7.41 (app. td, $J = 6.5, 2.0$ Hz, 1H, ArH), 7.18–7.23 (m, 2H, ArH), 3.71 (s, 3H, OCH_3), 3.60 (s, 2H, CH_2CO); ^{13}C NMR (100 MHz, CDCl_3), $\delta = 171.2$ (C), 136.0 (C), 132.2 (CH), 130.2 (CH), 130.0 (CH), 127.9 (CH), 122.4 (C), 52.1 (CH_3), 40.6 (CH_2). All further data consistent with that presented in the literature [38].

Methyl 2-(naphthalen-2-yl)acetate (167)

^1H NMR (400 MHz, CDCl_3), $\delta = 7.83\text{--}7.87$ (m, 3H, ArH), 7.77 (s, 1H, ArH), 7.45–7.53 (m, 3H, ArH), 3.83 (s, 2H, CH_2CO), 3.74 (s, 3H, OCH_3); ^{13}C NMR (100 MHz, CDCl_3), $\delta = 171.9$ (C), 133.4 (C), 132.4 (C), 131.4 (C), 128.2 (CH), 127.9 (CH), 127.6 (CH), 127.6 (CH), 127.3 (CH), 126.1 (CH), 125.7 (CH), 52.0 (CH_3), 41.3 (CH_2). All further data consistent with that presented in the literature [39].

Methyl 2-(4-methoxyphenyl)acetate (168)

^1H NMR (400 MHz, CDCl_3), $\delta = 7.21$ (dd, $J = 9.0, 2.0$ Hz, 2H, ArH), 6.68 (dd, $J = 9.0, 2.0$ Hz, 2H, ArH), 3.80 (s, 3H, OCH_3), 3.69 (s, 3H, OCH_3), 3.58 (s, 2H, CH_2CO); ^{13}C NMR (100 MHz, CDCl_3), $\delta = 172.2$ (C), 158.6 (C), 130.2 (CH), 125.9 (C), 113.9 (CH), 55.1 (CH_3), 51.8 (CH_3), 40.1 (CH_2). All further data consistent with the commercially available ester. CAS: 23786-14-3

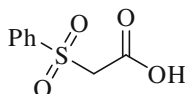
Methyl 2-(3-methoxyphenyl)acetate (169)

^1H NMR (400 MHz, CDCl_3), $\delta = 7.25$ (app. t, $J = 7.5$ Hz, 1H, ArH), 6.81–6.89 (m, 3H, ArH), 3.81 (s, 3H, OCH_3), 3.71 (s, 3H, OCH_3), 3.62 (s, 2H, CH_2CO); ^{13}C NMR (100 MHz, CDCl_3), $\delta = 171.8$ (C), 159.6 (C), 135.3 (CH), 129.5 (C), 121.5 (CH), 114.8 (CH), 112.5 (CH), 55.1 (CH_3), 52.0 (CH_3), 41.1 (CH_2). All further data consistent with the commercially available ester. CAS: 18927-05-4.

7.5.7 Procedure for the Preparation of Carboxylic Acid Derivatives

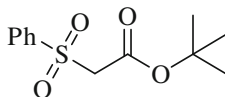
2-(phenylsulfonyl)-1-(2,2,6,6-tetramethylpiperidin-1-yl)ethanone (**130**) (1 mmol) was dissolved in toluene (2 mL). The appropriate amount of nucleophile was then added and the mixture heated to the desired temperature if necessary. The reaction was followed by TLC. Upon consumption of the amide the reaction was concentrated *in vacuo* and purified by column chromatography (10–50 % EtOAc in PE).

2-(Phenylsulfonyl)acetic acid (**176**)

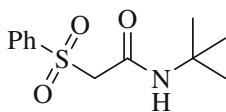


^1H NMR (400 MHz, CDCl_3), $\delta = 7.94$ – 8.00 (m, 2H, ArH), 7.67–7.72 (m, 1H, ArH), 7.56–7.62 (m, 2H, ArH), 5.30 (br. s 1H, OH), 4.17 (s, 2H, CH_2CO); ^{13}C NMR (100 MHz, CDCl_3), $\delta = 165.7$ (C), 138.4 (C), 134.6 (CH), 129.4 (CH), 128.5 (CH), 60.5 (CH_2). All further data consistent with the commercially available acid. CAS: 3959-23-7.

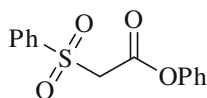
tert-Butyl 2-(phenylsulfonyl)acetate (**177**)



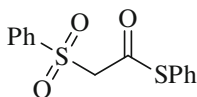
R_f 0.58 (1:1 EtOAc: PE); oil; ^1H NMR (400 MHz, CDCl_3), $\delta = 7.92$ – 7.97 (m, 2H, ArH), 7.69 (app. tt, $J = 7.5, 1.0$ Hz, 1H, ArH), 7.55–7.61 (m, 2H, ArH), 4.04 (s, 2H, CH_2CO), 1.35 (s, 9H, $\text{C}(\text{CH}_3)_3$); ^{13}C NMR (100 MHz, CDCl_3), $\delta = 161.2$ (C), 138.9 (C), 134.1 (CH), 129.1 (CH), 128.5 (CH), 83.6 (C), 62.0 (CH_2), 27.6 (CH_3); IR (cm^{-1}) 2,980 (w), 1,728 (s), 1,324 (s), 1,143 (s), 1,083 (s); HRMS: m/z (CI), calculated for $\text{C}_{12}\text{H}_{16}\text{O}_4\text{S}$, 257.0759 [$\text{M} + \text{H}$] $^+$, found 257.0762 [$\text{M} + \text{H}$] $^+$.

***N*-(*tert*-Butyl)-2-(phenylsulfonyl)acetamide (178)**

R_f 0.32 (1:1 EtOAc: PE); oil; ^1H NMR (400 MHz, CDCl_3), δ = 7.91–7.93 (m, 2H, ArH), 7.69 (app. tt, J = 7.5 Hz, 2.0 Hz, 1H, ArH), 7.57–7.60 (m, 2H, ArH), 6.46 (br. s, 1H NH), 3.93 (s, 2H, CH_2CO), 1.33 (s, 9H, $\text{C}(\text{CH}_3)_3$); ^{13}C NMR (100 MHz, CDCl_3), δ = 159.3 (C), 138.1 (C), 134.4 (CH), 129.3 (CH), 128.1 (CH), 62.8 (CH_2), 52.1 (C), 28.1 (CH_3); IR (cm^{-1}) 3,362 (w), 2,970 (w), 1,659 (s), 1,539 (m), 1,308 (s), 1,151 (s), 1,084 (m); HRMS: m/z (CI), calculated for $\text{C}_{12}\text{H}_{18}\text{NO}_3\text{S}$, 256.1007 [$\text{M} + \text{H}$] $^+$, found 256.1008 [$\text{M} + \text{H}$] $^+$.

Phenyl 2-(phenylsulfonyl)acetate (179)

R_f 0.45 (1:1 EtOAc: PE); mp 80–82 °C; ^1H NMR (400 MHz, CDCl_3), δ = 8.01–8.04 (m, 2H, ArH), 7.72 (app. tt, J = 7.5, 2.0 Hz, 1H, ArH), 7.59–7.63 (m, 2H, ArH), 7.36–7.39 (m, 2H, ArH), 7.24–7.27 (m, 1H, ArH), 7.00–7.03 (m, 2H, ArH), 4.36 (s, 2H, CH_2CO); ^{13}C NMR (100 MHz, CDCl_3), δ = 161.0 (C), 150.0 (C), 138.6 (C), 134.5 (CH), 129.6 (CH), 129.4 (CH), 128.6 (CH), 126.5 (CH), 121.0 (CH), 61.1 (CH_2); IR (cm^{-1}) 2,944 (w), 1,756 (s), 1,325 (m), 1,190 (s), 1,147 (s), 1,081 (s); HRMS: m/z (CI), calculated for $\text{C}_{14}\text{H}_{13}\text{O}_4\text{S}$, 277.0535 [$\text{M} + \text{H}$] $^+$, found 277.0538 [$\text{M} + \text{H}$] $^+$.

***S*-Phenyl 2-(phenylsulfonyl)ethanethioate (180)**

R_f 0.53 (1:1 EtOAc: PE); mp 90–92 °C; ^1H NMR (400 MHz, CDCl_3), δ = 7.95–7.98 (m, 2H, ArH), 7.70 (app. tt, J = 7.5, 1.0 Hz, 1H, ArH), 7.59 (app. tt, J = 7.5, 1.0 Hz, 2H, ArH), 7.40–7.44 (m, 3H, ArH), 7.32–7.34 (m, 2H, ArH), 4.36 (s, 2H, CH_2CO); ^{13}C NMR (100 MHz, CDCl_3), δ = 185.5 (C), 138.4 (C), 134.4 (CH), 134.2 (CH), 130.2 (CH), 129.5 (CH), 129.3 (CH), 128.8 (CH), 126.0 (C), 66.7 (CH_2); IR (cm^{-1}) 2,983 (w), 2,923 (w), 1,677 (s), 1,310 (s), 1,244 (m), 1,152 (s), 995 (s); HRMS: m/z (CI), calculated for $\text{C}_{14}\text{H}_{13}\text{O}_3\text{S}_2$, 293.0306 [$\text{M} + \text{H}$] $^+$, found 293.0307 [$\text{M} + \text{H}$] $^+$.

(Methylsulfonyl)benzene (181)

R_f 0.43 (1:1 EtOAc: PE); oil; ¹H NMR (400 MHz, CDCl₃), δ = 7.95–7.98 (m, 2H, ArH), 7.65–7.70 (m, 1H, ArH), 7.56–7.62 (m, 2H, ArH), 3.06 (s, 3H, CH₃); ¹³C NMR (100 MHz, CDCl₃), δ = 140.5 (C), 133.7 (CH), 129.3 (CH), 127.3 (CH), 44.3 (CH₃); IR (cm⁻¹) 1,447 (m), 1,294 (s), 1,143 (s), 1,086 (m); LRMS: C₇H₈O₂S, *m/z* (CI), 91.1 (13 %), 100.2 (7 %) 157.1 (100 %) [M + H]⁺. All further data consistent with the commercially available (methylsulfonyl)benzene. CAS: 102-07-8.

References

1. Perrin DD, Armarego WLF (1988) Purification of laboratory chemicals, 3rd edn. Butterworth Heinemann, Oxford
2. Wagar R, Brown JM (2008) *Angew Chem Int Ed* 47:4228–4230
3. Iwakura Y, Izawa S-IJ (1964) *Org Chem* 29:379–382
4. Azad S, Kumamoto K, Uegaki K, Ichikawa Y, Kotsuki H (2006) *Tetrahedron Lett* 47:587–590
5. Franz RA et al (1962) *J Org Chem* 27:4341–4346
6. Synder JK, Stock LMJ (1980) *Org Chem* 45:886–891
7. Lengyei I, Stephani RA, Patel H (2007) *J Heterocycles* 73:349–375
8. Fikes LE, Shechter HJ (1979) *Org Chem* 44:741–744
9. Oh HK, Park JE, Sung DD, Lee IJ (2004) *Org Chem* 69:3150–3153
10. Mukiyama T et al (1967) *J Org Chem* 32:3475–3477
11. Thavonekham B (1997) *Synthesis* 10:1189–1194
12. Kurth TL, Lewis FDJ (2003) *Am Chem Soc* 45:13760–13767
13. Drent E, Broekhoven JAM, Doyle MJJ (1991) *Organomet Chem* 417:235–240
14. Hegarty AF, Bruice TCJ (1970) *Am Chem Soc* 92:6575–6588
15. Krantz A, Spencer RW, Tam TF, Liak T-J, Copp LJ, Thomas EM, Rafferty SPJ (1990) *Med Chem* 33:464–479
16. Molina P, Alajarin M, Vidal A (1989) *Tetrahedron* 31:4263–4286
17. Sheehan JC, Davies GDJ (1964) *Org Chem* 29:3599–3601
18. Staiger RP, Wanger ECJ (1959) *Org Chem* 18:1427–1439
19. Bottaro JC, Penwell PE, Schmitt RJ (1991) *J Org Chem* 56:1305–1307
20. Bortnick NB, Lusk LS, Hurwitz MD, Craig WE, Mirza JJ (1956) *Am Chem Soc* 78:4039–4042
21. Clayden J, Helliwell M, McCarthy C, Westlund NJ (2000) *Chem Soc Perkin Trans* 1:3232–3249
22. Song B, Wang S, Sun C, Deng H, Xu B (2007) *Tetrahedron Lett* 48:8982–8986
23. Moriarty RM, Chany CJ, Vaid RK, Prakash O, Tuladhar SMJ (1993) *Org Chem* 58:2478–2482
24. Selva M, Tundo P, Perosa A, Dall'Acqua FJ (2005) *Org Chem* 70:2771–2777
25. Pirkle WH, Simmons KA, Boeder CWJ (1979) *Org Chem* 44:4891–4896

26. Bratt MO, Taylor PCJ (2003) *Org Chem* 68:5439–5444
27. Aresta M, Berloco C, Quaranta E (1995) *Tetrahedron* 51:8073–8088
28. Sumiyoshi H, Shimizu T, Katoh M, Baba Y, Sodeoka M (2002) *Org Lett* 4:3923–3926
29. De Risi C, Ferraro L, Pollini GP, Tanganelli S, Valente F, Veronese AC (2008) *Bioorganic Med Chem* 16:9904–9910
30. Manikowski A, Kolarska Z (2009) *Synth Commun* 39:3621–3638
31. Lozanova AV, Ugurchieva TM, Veselovsky VV (2008) *Russ Chem B* 57:1753–1755
32. Creary XJ (1980) *Org Chem* 45:2419–2425
33. Bodnar BS, Vogt PFJ (2009) *Org Chem* 74:2598–2600
34. Bell IM, Abell C, Leeper FJJ (1994) *Chem Soc Perkin Trans 1*:1997–2006
35. Salerno CP, Magde D, Patron APJ (2000) *Org Chem* 65:3971–3981
36. Durandetti M, Gosmini C, Périchon J (2007) *Tetrahedron* 63:1146–1153
37. Li JH, Liang Y, Wang DP, Liu WJ, Xie YX, Yin DL (2005) *J Org Chem* 70:2832–2834
38. Chen Q-H, Rao PNP, Knaus EE (2005) *Bioorganic Med Chem* 13:4694–4703
39. Pei T, Wang X, Widenhofer RA (2002) *J Am Chem Soc* 125:648–649

Appendix

X-Ray Crystal Structures Publications

A.1 General Procedure

Crystallisation was achieved using a diffusion method at room temperature after 2 days. Crystals appear as small white coloured cubes. EtOAc was used as solvent and hexanes as antisolvent. The solvents used were anhydrous. The saturated EtOAc-substrate solution was filtered before being placed in the crystallisation vial.

X-ray diffraction experiments were carried out at 100K on a Bruker APEX II diffractometer using Mo-K α radiation ($\lambda = 0.71073 \text{ \AA}$). Data collections were performed using a CCD area detector from a single crystal mounted on a glass fibre. Intensities were integrated [1] from several series of exposures measuring 0.5° in ω or ϕ . Absorption corrections were based on equivalent reflections using SADABS [2]. The structures were solved using SHELXS and refined against all F_o^2 data with hydrogen atoms riding in calculated positions using SHELXL [3].

A.2 Amides

A.2.1 Phenylsulfonyl Derivatives 127–130

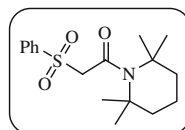
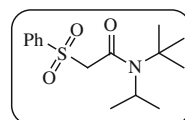
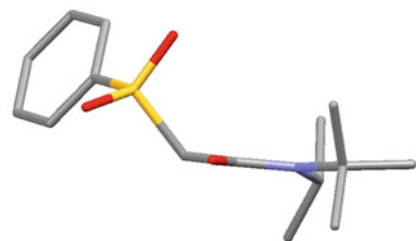
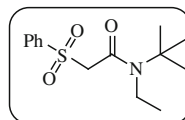
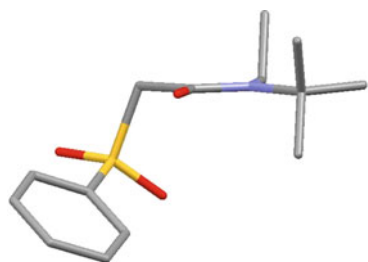
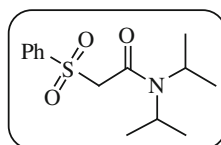
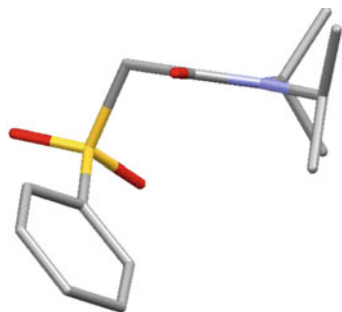
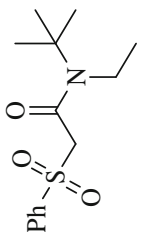
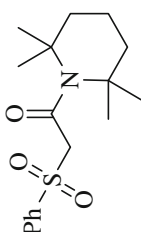
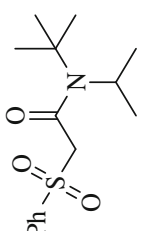
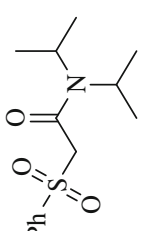


Table 1

Compound				
Colour, habit	colourless rod	colourless block	colourless block	colourless block
Size/mm	$0.35 \times 0.08 \times 0.08$	$0.35 \times 0.180.16$	$0.45 \times 0.16 \times 0.16$	$0.49 \times 0.35 \times 0.30$
Empirical Formula	$C_{14}H_{21}NO_3S$	$C_{17}H_{23}NO_3S$	$C_{15}H_{23}NO_3S$	$C_{14}H_{21}NO_3S$
M	283.38	323.44	297.40	283.38
Crystal system	monoclinic	orthorhombic	monoclinic	orthorhombic
Space group	$P2_1/c$	$P2_12_12_1$	$P2_1/n$	$P2_12_12_1$
<i>a</i> /Å	5.76110(10)	5.92450(10)	8.91880(10)	5.8678(2)
<i>b</i> /Å	13.2333(2)	14.6890(2)	15.8358(2)	14.0582(5)
<i>c</i> /Å	19.6067(3)	19.0746(3)	12.02010(10)	17.5020(6)
α /°	90.00	90.00	90.00	90.00
β /°	95.6350(10)	90.00	111.4630(10)	90.00
γ /°	90.00	90.00	90.00	90.00
<i>V</i> /Å ³	1487.56(4)	1659.97(4)	1579.95(3)	1443.75(9)
Z	4	4	4	4
μ /mm ⁻¹	0.221	0.207	0.212	0.228
T/K	100	100	100	100
$\theta_{\text{min,max}}$	1.86,27.51	1.75,27.57	2.23,27.55	1.86,27.54
Completeness	1.000 to $\theta = 27.51^\circ$	0.998 to $\theta = 27.57^\circ$	0.998 to $\theta = 27.55^\circ$	0.999 to $\theta = 27.54^\circ$
Reflections:	25867/3439	14900/3829	28765/3650	11795/3330
total/independent				
R_{int}	0.0240	0.0341	0.0295	0.0356
Final <i>R</i> 1 and <i>wR</i> 2	0.0316, 0.0846	0.0309, 0.0775	0.0379, 0.1002	0.0306, 0.0739
Largest peak, hole/eÅ ⁻³	0.400, -0.344	0.328, -0.300	0.833, -0.345	0.272, -0.248
ρ_{calc} /g cm ⁻³	1.265	1.294	1.250	1.304
Flack parameter	n/a	-0.02(6)	n/a	0.00(6)
Twist angle	2.1(1)	27.4(1)	9.3(1)	2.7(1)

A.2.2 Dichloroacetamide Derivatives 138 and 170

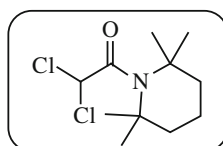
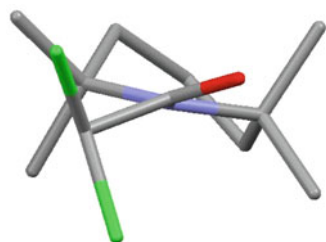
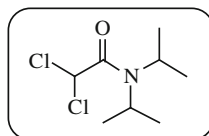
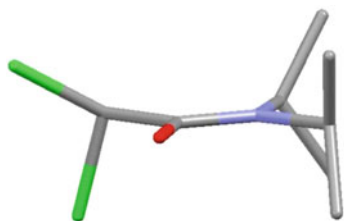
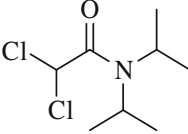
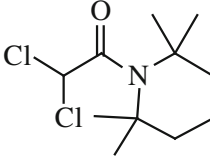


Table 2

Compound

Compound		
Colour, habit	colourless plate	colourless block
Size/mm	0.33 × 0.24 × 0.04	0.45 × 0.21 × 0.20
Empirical Formula	C ₈ H ₁₅ Cl ₂ NO	C ₁₁ H ₁₉ Cl ₂ NO
M	212.11	252.17
Crystal system	orthorhombic	monoclinic
Space group	<i>P</i> 2 ₁ 2 ₁ 2 ₁	<i>P</i> 2 ₁ / <i>c</i>
<i>a</i> /Å	8.4561(6)	11.7466(4)
<i>b</i> /Å	10.7401(6)	7.2919(2)
<i>c</i> /Å	11.9971(7)	15.6929(5)
<i>α</i> /°	90.00	90.00
<i>β</i> /°	90.00	110.626(2)
<i>γ</i> /°	90.00	90.00

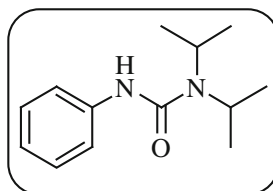
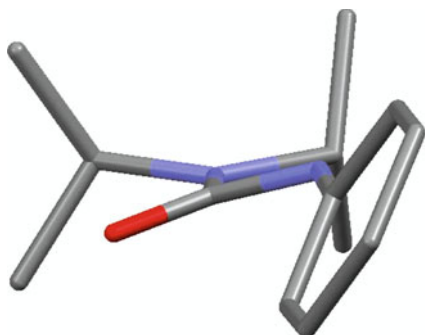
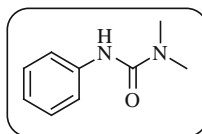
(continued)

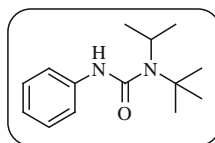
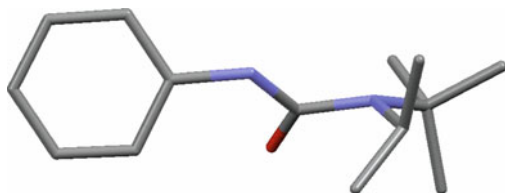
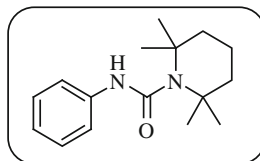
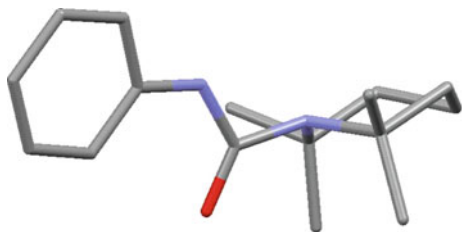
Table 2 (continued)

Compound		
$V/\text{\AA}^3$	1089.57(12)	1258.01(7)
Z	4	4
μ/mm^{-1}	0.554	0.492
T/K	100	100
$\theta_{\text{min,max}}$	2.55,27.48	1.85,33.01
Completeness	1.000 to $\theta = 27.48^\circ$	1.000 to $\theta = 27.50^\circ$
Reflections: total/independent	9100/2475	39760/4422
R_{int}	0.0211	0.0281
Final $R1$ and $wR2$	0.0267, 0.0630	0.0322, 0.0858
Largest peak, hole/ $e\text{\AA}^{-3}$	0.249, -0.203	0.744, -0.472
$\rho_{\text{calc}}/\text{g cm}^{-3}$	1.293	1.331
Flack parameter	0.02(6)	n/a

A.3 Ureas

All urea structures obtained by Houlden and are available on the Cambridge Crystallography Data Centre (CCDC).





References

1. Bruker-AXS SAINT V7.68A, Madison, Wisconsin.
2. G. M. Sheldrick, SADABS V2008/1, University of Göttingen, Germany.
3. G. M. Sheldrick, *Acta Cryst.* **A64**, 112 (2008).